

DEVELOPMENT OF INSTRUMENTAL ANALYTICAL  
METHODS FOR THE INVESTIGATION OF OMEGA-3 FATTY  
ACID INDUCED EFFECTS ON THE FATTY ACID AND  
OXYLIPIN PATTERN

---

**Dissertation**

to obtain the academic degree

Doctor rerum naturalium

(Dr. rer. nat.)

Faculty of Mathematics and Natural Sciences

of the

Bergische Universität Wuppertal

by

**Annika I. Ostermann**

Vechta

- 2017 -

Die Dissertation kann wie folgt zitiert werden:

urn:nbn:de:hbz:468-20170518-112000-5

[<http://nbn-resolving.de/urn/resolver.pl?urn=urn%3Anbn%3Ade%3Ahbz%3A468-20170518-112000-5>]

Erster Gutachter: ..... Prof. Dr. Nils Helge Schebb

Zweiter Gutachter: ..... Prof. Dr. Pablo Steinberg

Tag der mündlichen Prüfung: ..... \_\_\_\_\_. \_\_\_\_\_. 2017

Tag der Promotion: ..... \_\_\_\_\_. \_\_\_\_\_. 2017

*Für meine Eltern*



# Table of Contents

<b>Chapter 1</b>	<b>Introduction and Scope .....</b>	<b>1</b>
1.1	References.....	3
<b>Chapter 2</b>	<b>Effects of Omega-3 Fatty Acid Supplementation on the Pattern of Oxylipins – A Short Review About the Modu- lation of Hydroxy-, Dihydroxy-, and Epoxy-Fatty Acids.....</b>	<b>5</b>
2.1	Introduction .....	6
2.2	Dose, intervention period and study population .....	8
2.3	Methods for the quantitative comparison of results .....	12
2.4	Modulation of the n6- and n3-oxylipin pattern following n3-PUFA supplementation.....	13
2.5	Dose and time dependent responses in the oxylipin pattern to dietary n3-PUFA supplementation .....	18
2.6	Inter-individual variations in responses to n3-PUFA supplementation.....	21
2.7	Modulation of oxylipins by n3-supplementation in (the onset of) diseases .....	23
2.8	Conclusion .....	24
2.9	References.....	26
<b>Chapter 3</b>	<b>Determining the Fatty Acid Composition in Plasma and Tissues as Fatty Acid Methyl Esters Using Gas Chromato- graphy – A Comparison of Different Derivatization and Extraction Procedures .....</b>	<b>31</b>
3.1	Introduction .....	32

3.2	Experimental .....	33
3.2.1	Chemicals and biological material.....	33
3.2.2	GC-FID analysis.....	34
3.2.3	Sample preparation.....	35
3.3	Results .....	37
3.3.1	Derivatization efficacy for different lipid classes.....	37
3.3.2	Derivatization of lipid extracts from plasma.....	38
3.3.3	Efficacies of the Bligh and Dyer versus the MTBE/MeOH extraction .....	41
3.3.4	Saponification of tissue samples prior extraction .....	41
3.4	Discussion.....	43
3.5	References.....	47

**Chapter 4 Comparison of Sample Preparation Methods for the  
Quantitative Analysis of Eicosanoids and other Oxylipins  
in Plasma by Means of LC-MS/MS ..... 51**

4.1	Introduction .....	52
4.2	Experimental .....	54
4.2.1	Chemicals and biological materials.....	54
4.2.2	Oxylipin extraction.....	55
4.2.3	LC-MS analysis.....	57
4.3	Results .....	58
4.3.1	Recoveries of internal standards.....	58
4.3.2	Extraction of oxylipins from plasma.....	62
4.3.3	Cartridge size.....	64
4.3.4	Calculated concentrations.....	65
4.4	Discussion.....	67
4.5	Conclusion .....	72
4.6	References.....	73

<b>Chapter 5</b>	<b>Development of an Online-SPE-LC-MS/MS Method for 26 Hydroxylated Polyunsaturated Fatty Acids as Rapid Targeted Metabolomics Approach for the LOX, CYP and Autoxidation Pathways of the Arachidonic Acid Cascade ....</b>	<b>75</b>
5.1	Introduction .....	76
5.2	Experimental .....	78
5.2.1	Chemicals and Biological Materials.....	78
5.2.2	LC-MS analysis .....	79
5.2.3	Sample preparation.....	82
5.2.4	Cell culture .....	82
5.3	Results and Discussion .....	83
5.3.1	Online-SPE-LC-MS .....	83
5.3.2	Analysis of OH-FA pattern in cell culture.....	92
5.4	Conclusion .....	98
5.5	References.....	99
<b>Chapter 6</b>	<b>Modulation of the Endogenous Omega-3 Fatty Acid and Oxylipin Profile <i>in vivo</i> – A Comparison of the fat-1 Transgenic Mouse with C57BL/6 Wildtype Mice on an Omega-3 Fatty Acid Enriched Diet.....</b>	<b>103</b>
6.1	Introduction .....	104
6.2	Experimental .....	107
6.2.1	Chemicals .....	107
6.2.2	Feeding experiment .....	107
6.2.3	Fatty acid analysis .....	108
6.2.4	Oxylipin analysis .....	109
6.3	Results .....	110
6.3.1	Behaviour and bodyweight.....	110
6.3.2	Fatty acid profile.....	110
6.3.3	Oxylipin pattern .....	116
6.4	Discussion.....	122

6.5	References.....	130
<b>Chapter 7</b>	<b>A Diet Rich in Omega-3 Fatty Acids Enhances Expression of Soluble Epoxide Hydrolase in Murine Brain.....</b>	<b>135</b>
7.1	Introduction .....	136
7.2	Experimental .....	138
7.2.1	Chemicals .....	138
7.2.2	Feeding experiment .....	138
7.2.3	Fatty acid and oxylipin analysis.....	139
7.2.4	Transcription analysis by quantitative real-time PCR (qRT-PCR) .....	140
7.3	Results and Discussion .....	141
7.4	References.....	153
<b>Chapter 8</b>	<b>Future Perspectives .....</b>	<b>157</b>
<b>Summary</b>	<b>.....</b>	<b>159</b>
<b>Appendix</b>	<b>.....</b>	<b>163</b>
<b>Abbreviations</b>	<b>.....</b>	<b>213</b>
<b>Acknowledgement.....</b>	<b>.....</b>	<b>217</b>
<b>Curriculum Vitae.....</b>	<b>.....</b>	<b>219</b>
<b>List of Publications</b>	<b>.....</b>	<b>221</b>



# Chapter 1

## Introduction and Scope

In the late 1970 Dyerberg and Bang associated high endogenous levels of omega-3 fatty acids (n3-PUFA) in Greenland Inuit with a low risk of myocardial infarction [1]. Since then, dietary intake of omega-3 fatty acids has not only been correlated with beneficial effects on atherosclerosis and related diseases, such as coronary heart disease, but also on inflammatory diseases [2, 3].

On a molecular level, biological effects of n3-PUFA are diverse: For instance, the membrane composition and fluidity is altered and the transcription of pro-inflammatory genes is reduced, e.g. by inhibition of NF- $\kappa$ B translocation to the nucleus [2, 3]. A relevant part of n3-PUFA related effects has been attributed to their oxidative metabolites – oxylipins – which are formed by enzymes of the arachidonic acid cascade or via autoxidation [4]. However, the power of dietary n3-PUFA to modulate the endogenous oxylipin profile and details on changes in individual enzyme pathways is not completely understood. Current knowledge about the modification of the oxylipin pattern by n3-PUFA is summarized in chapter 2 of this thesis.

Today, the effectivity of n3-PUFA is discussed controversially and many questions regarding clinical importance of n3-PUFA related effects or mechanisms of action of individual n3-PUFA (and their oxylipins) remain unanswered [2, 3, 5]. Interpretation of the observed effects is further impeded by high inter-individual variations in the response to dietary n3-PUFA (chapter 2).

In order to investigate biological effects of n3-PUFA and their role in pathophysiology, analytical methods are required allowing a quantification of fatty acids and their oxidative metabolites in biological samples, such as plasma and tissues. For this purpose, in chapter 3 extraction and derivatization strategies for lipids from small biological samples (plasma and liver) are compared in order to find the most suitable one for the analysis of total fatty acids. In chapter 4 and 5 analytical tools for the investigation of oxylipins in plasma and cell culture medium are established. While the aim in chapter 4 is to find the extraction procedure most suitable to extract free oxylipins from all groups in plasma, chapter 5 deals with the optimization of a fast, liquid chromatography-mass spectrometry (LC-MS) method for the quantification of hydroxy fatty acids in cell culture medium and plasma samples.

For the investigation of n3-PUFA related effects in animal models, two strategies are dominantly used: i.) feeding of diets enriched with n3-PUFA and ii.) the use of transgenic *fat-1* mice which can biosynthesize n3- from n6-PUFA. In chapter 6, for the first time these approaches are comprehensively compared regarding their power to modulate the endogenous fatty acid and oxylipin profile.

An interesting observation is described in chapter 6 was the modulation of the cerebral oxylipin pattern upon rather short dietary feeding with n3-PUFA (30 days). In chapter 7, this finding is therefore investigated in more detail, utilizing two independent feeding experiments and transcription analysis. Based on the changes in epoxy-PUFA to dihydroxy-PUFA ratios, it was found that n3-PUFA elevate the expression of the soluble epoxide hydrolase.

Overall, this thesis contributes to a better understanding of n3-PUFA biology by providing detailed data on the modulation of oxylipins, including several potent lipid mediators, following elevation of endogenous n3-PUFA level. This information is important for the interpretation of changes in the oxylipin pattern in the context of n3-PUFA related effects on (patho)physiology.

## 1.1 References

1. Dyerberg J, Bang HO. Dietary fat and thrombosis. *Lancet*. 1978;1(8056):152.
2. Calder PC. Marine omega-3 fatty acids and inflammatory processes: Effects, mechanisms and clinical relevance. *Biochim Biophys Acta*. 2015;1851(4):469-484.
3. Mozaffarian D, Wu JH. Omega-3 fatty acids and cardiovascular disease: effects on risk factors, molecular pathways, and clinical events. *J Am Coll Cardiol*. 2011;58(20):2047-2067.
4. Gabbs M, Leng S, Devassy JG, Monirujjaman M, Aukema HM. Advances in Our Understanding of Oxylipins Derived from Dietary PUFAs. *Advances in Nutrition*. 2015;6(5):513-540.
5. Weylandt KH, Serini S, Chen YQ, Su HM, Lim K, Cittadini A, Calviello G. Omega-3 Polyunsaturated Fatty Acids: The Way Forward in Times of Mixed Evidence. *Biomed Res Int*. 2015;2015:143109.



# Chapter 2

## Effects of Omega-3 Fatty Acid Supplementation on the Pattern of Oxylipins – A Short Review About the Modulation of Hydroxy-, Dihydroxy-, and Epoxy-Fatty Acids\*

*A growing body of evidence suggests that intake of the long chain omega-3 polyunsaturated fatty acids (n3-PUFA) eicosapentaenoic acid (C20:5 n3, EPA) and docosahexaenoic acid (C22:6 n3, DHA) is linked to beneficial health effects, particularly in the prevention of cardiovascular and inflammatory diseases. Though the molecular mode of action of n3-PUFA is still not fully understood, it is not controversial that a significant portion of the (patho)-physiological effects of PUFA are mediated by their oxidative metabolites, i.e. eicosanoids and other oxylipins. Quantitative targeted oxylipin methods allow to comprehensively monitor changes in the pattern of oxylipins. In this short review, results from intervention studies are summarized analyzing >30 oxylipins from different PUFA in response to n3-PUFA supplementation. The results are not only qualitatively compared with respect to the study design, n3-PUFA dose and trends in the lipid mediators, but the induced changes are also quantitatively compared based on the relative change in oxylipin level induced by n3-PUFA. The evaluation of the data from these studies shows that the change in hydroxy-, epoxy- and dihydroxy-PUFA generally corresponds to the observed changes in their precursor PUFA. Thus, the lower the individual n3-status is at baseline, the higher the increase in EPA and DHA derived oxylipins. Strongest relative increases were found in EPA derived oxylipins, while changes ARA derived eicosanoids were heterogeneous. After 3-12 weeks of supplementation similar relative changes were observed in free and total (free + esterified) oxylipins in plasma and serum. Regarding EPA derived oxylipins, trends for a linear increase with dose can be deduced. However, interpretation of the quantitative oxylipin patterns between studies is hampered by strong inter-individual variances in oxylipin levels between and also within the studies. In the future, the reason for these varying oxylipin plasma concentrations needs to be clarified in order to understand oxylipin and n3-PUFA biology.*

\* Ostermann AI and Schebb NH. 2017. *Submitted for publication.*

Author contributions: AO, NHS: Designed study and wrote the manuscript.

## 2.1 Introduction

In many epidemiological and intervention studies, high endogenous levels of omega-3 polyunsaturated fatty acids (n3-PUFA), including eicosapentaenoic acid (C20:5 n3, EPA) and docosahexaenoic acid (C22:6 n3 DHA) have been correlated with beneficial effects on human health, e.g. in cardiovascular [1] or inflammatory diseases [2]. However, results are conflicting and in some studies these positive effects have not been observed, e.g. in intervention studies on the effectivity of n3-PUFAs on the relapse in Crohn's Disease [3], or on major cardiovascular events (fatal and nonfatal cardiovascular events and cardiac interventions) in a population with previous myocardial infarction, receiving medication [4]. Moreover, a recent meta-analysis did not find a risk lowering effect of n3-PUFAs for all-cause mortality, cardiac death, sudden death, myocardial infarction and stroke [5].

On a molecular level, a part of n3-PUFA related effects has been attributed to a shift in the pattern of lipid mediators formed in the arachidonic acid (ARA, C20:4 n6) cascade by competing with ARA for conversion in the three enzymatic pathways of this signaling cascade (Fig. 2.1 [2, 6]). Conversion of ARA by cyclooxygenases (COX) leads to prostaglandin (PG) H<sub>2</sub> which is further metabolized by downstream enzymes to series 2 prostanoids, such as PGE<sub>2</sub>, a potent mediator in the regulation of pain, fever and inflammation [2, 7, 8]. By contrast, conversion of EPA is slower, thereby reducing the levels of formed mediators [9] and leads to less potent series 3 PG [2, 8]. Similarly, leukotriene (LT) B<sub>4</sub>, formed by lipoxygenase (LOX) action on ARA, acts pro-inflammatory by neutrophil attraction [7], while its EPA derived counterpart (LTB<sub>5</sub>) shows much lower potency [2, 8]. Beyond that, EPA and DHA can also give rise to highly potent lipid mediators. For instance, in the third branch of the ARA cascade, enzymes of the cytochrome P450 (CYP) 2C and 2J family act as epoxygenases on PUFA. The main products of EPA and DHA, 17(18)-epoxy eicosatetraenoic acid (EpETE) and 19(20)-epoxy docosapentaenoic acid (EpDPE) are potent anti-arrhythmic acting mediators [10] and 19(20)-EpDPE has been shown to

inhibit angiogenesis, while Ep-FA deriving from ARA promote angiogenesis [11]. Also, multiple hydroxylation of EPA and DHA leads to potent inflammation resolving oxylipins, termed specialized pro-resolving mediators (SPM), like resolvins or maresins [12].

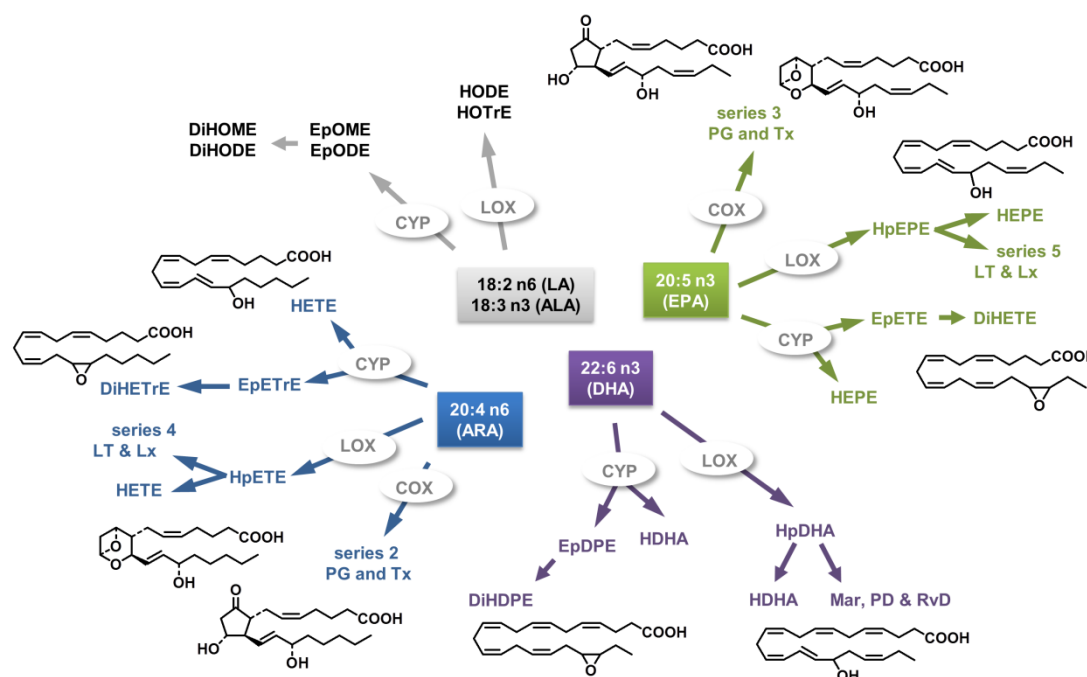


**Fig. 2.1:** Simplified overview over selected CYP, LOX and COX pathways of LA, ALA, ARA, EPA and DHA in the ARA cascade. HpETE – hydroperoxy eicosatetraenoic acid; Lx – lipoxin; Mar – maresin, PD – protectin; RvD – D series resolvins; HpEPE – hydroperoxy eicosapentaenoic acid.

Overall, the influence of EPA and DHA on the profile of lipid mediators formed in the ARA cascade is diverse and biological effects of n-3-PUFA seem to result more from a shift in the whole pattern of oxylipins rather than from changes of selected metabolites. For an interpretation of EPA and DHA derived effects and the characterization of the impact of individual metabolites, it is therefore important to monitor a comprehensive set of oxylipins from all branches of the ARA cascade and supplementation induced shifts therein [13, 14]. Oxylipin patterns in healthy subjects on different diets can be correlated with those during onset and progression of diseases allowing to evaluate the (patho-)physiological role of (n-3-PUFA derived) mediators. However, most studies in this field analyze and/or report only selected (groups) of oxylipins of interest,

e.g. SPM and Ep-FA [15], SPM and precursor thereof [16, 17], Ep-FA [18] or mainly ARA derived mediators [19].

Nonetheless, several studies characterized n3-PUFA (EPA+DHA) supplementation induced changes in a comprehensive set of oxylipins derived from different n6- and n3-PUFA (ARA, EPA and DHA amongst others) and across the different branches of the ARA cascade (COX, LOX, CYP and autoxidation) [13, 20-29] and in one study [30] the effects of individual EPA and n3 docosapentaenoic acid (n3-DPA) supplementation were compared. However, the outcome of these studies has not been systematically compared. The aim of the present work is therefore to summarize the results of n3-PUFA intervention, to evaluate if they lead to similar quantitative results and pinpoint differences which have to be addressed in future studies. In order to allow the quantitative comparison of the effects of n3-PUFA treatment on all three branches of the ARA cascade, only studies analyzing a comprehensive set of >30 oxylipins from different precursor FA and reporting mediators from different groups of oxylipins (e.g. hydroxy-, dihydroxy-, and epoxy-fatty acids) are included and a focus was set on supplementation induced changes in healthy subjects.

## **2.2 Dose, intervention period and study population**

EPA, DHA and other n3-PUFAs can be biosynthesized in humans from the essential n3-PUFA alpha linolenic acid (C18:3 n3, ALA) in multiple steps, involving conversion by delta-5 and delta-6 desaturases and elongases [31]. However, conversion rates of ALA to EPA are low in populations on a western diet rich in n6-PUFA [32], resulting in low shares of EPA and DHA in blood (red blood cells (RBC) and plasma) [33]. The way to supply humans with EPA and DHA is consumption of long-chain n3-PUFA rich seafood, like oily fish [1, 2], or by intake of dietary supplements [34]. Dietary recommendations for the uptake of EPA+DHA range from  $\geq 250$  mg/d to  $\geq 500$  mg/d (e.g. Academy of Nutrition and Dietetics, AHA, EFSA, WHO) [35] and according to the German Society for



Nutrition, prevention of primary coronary heart disease with a daily intake of up to 250 mg EPA and DHA seems probable [36]. However, in order to achieve the triglyceride lowering effects, daily doses need to be higher (2-4 g/d) and a higher intake is recommended for patients with coronary heart disease (~1g/d) [35]. Moreover, special recommendations for pregnant or lactating women concerning the intake of DHA exist [35].

In supplementation studies investigating the effect of n3-PUFA in healthy subjects [13, 20, 21, 23-28], daily intakes of EPA ranged from 0.36-1.9 g/d and DHA doses ranged from 0.24-1.5 g/d (Table 2.1). With a sum of EPA+DHA from 0.6-3.4 g/d, this is higher than the minimum dietary recommendations for the intake of n3-PUFA in healthy subjects. It should be noted that a linear relationship between dose and endogenous n3-PUFA levels in different blood compartments exists in this dose range (linearity at least up to 4 meals of oily fish per week, equaling 1.87 g EPA+DHA (1:1.2, w:w) per day [37]). At a dose of 3 g EPA+DHA (3:2, w:w) per day, incorporation of EPA into plasma phospholipids is still linear, while DHA incorporation seemed to reach saturation [38].

The effect of n3-PUFA supplementation on the oxylipin pattern in non-healthy subjects was investigated in patients with mild to moderate asthma [22], hyperlipidemia [25] and IgA nephropathy [29] and combined EPA and DHA doses ranged from 2.7-6.0 g/d (Table 2.1).

In most studies, EPA and DHA were administered as capsules, dominantly containing refined fish oil (Table 2.1). However, binding forms were slightly different which might have an impact on bioavailability of the PUFAs [39]. For instance, Schuchardt et al. used re-esterified triglycerides in their studies [25, 26], while n3-PUFA ethyl esters were used by Fischer and Konkel et al., Keenan et al. and Schebb et al. amongst others [13, 20-22, 24, 29]. Indeed, in some studies a higher bioavailability of re-esterified triglycerides in comparison to ethyl esters [39] was found which might influence the effect of n3-PUFA supplementation on the oxylipin pattern. However, not only the lipid binding

form is crucial for bioavailability of the fatty acids, but also galenic or matrix [39]. For example, pre-emulsified n3-PUFA ethyl esters show a significantly higher absorption and thus bioavailability [40]. Given the importance of the formation of an emulsion, the bioavailability of n3-PUFA from a supplementation product is thus influenced if it is ingested together with a meal containing a substantial amount of fat (releasing bile acids, and colipase).

The dietary intervention lasted 3-12 weeks in most studies investigating the effects of n3-PUFA on the oxylipin pattern, and one study monitored the effects up to 6 months and 12 months, respectively (Table 2.1). Heterogeneous study populations were used, comprising male and female subjects, aged roughly 21-70 years with a body mass index (BMI) of 19-35 kg/m<sup>2</sup> (Table 2.1). In Schuchardt et al., 2014 (A) only a single dose of omega-3 fatty acids was administered [26] and study participants from the study of Watkins et al. were older compared to other studies (75±6 years [27]).

Table 2.1: Overview over the study designs.

	Health status	Subjects			Intervention			Duration [weeks]	Comment	Ref
		Gender	Age [y]	BMI [kg/m <sup>2</sup> ]	N	EPA	Dose [g/d]			
<b>Supplementation with EPA+DHA</b>										
Fischer&Konkel et al., 2014	Healthy	M + F	18-60	M: 24.9±1.0 <sup>a</sup> F: 25.5±1.3 <sup>a</sup>	10+10	0.46 [Wk 1-4] 0.98 [Wk 5-8]	0.38 [Wk 1-4] 0.76 [Wk 5-8]		n3-PUFA as ethyl ester in capsules	Wk 9-16 w/washout; + sampling in week 1, 4, 8, 9 and 16 [20]
Keenan et al., 2012	Healthy	M + F	21-59	21-32	9+21	1.86	1.46		prescription n3-PUFA ethyl ester, capsules	[21]
Nording et al., 2013	Healthy	M + F	18-65	19-28	4+8	1.9	1.5		Fish oil in capsules	[23]
Schebb et al., 2014	Healthy	M + F	46-70	21-35	5+5	1.1	0.74		Fish oil as ethyl ester, capsules	[24]
Schuchardt et al., 2014 (A)	Healthy	M	26-36	22-29	6	1.008	0.672		Fish oil as rTAG, capsules	Single dose [26]
Schuchardt et al., 2014 (B)	Healthy	M	38±8 <sup>b</sup>	24.2±4.15 <sup>b</sup>	10	1.56	1.14		Fish oil as rTAG, capsules	[25]
Shearer et al., 2010	Healthy	M + F	33 (24, 51) <sup>c</sup>	25.5 (21, 29) <sup>c</sup>	4+6	4 <sup>c</sup> ; about 1.9 g/d EPA and 1.5 g/day DHA [21]			prescription n3-PUFA ethyl ester, capsules	[13]
Zhang et al., 2015	Healthy	M + F	24±2	-*	6+6	0.36-0.4	0.24-0.28		Fish oil in capsules	+ sampling on day 3, 7, 14 [28]
Watkins et al., 2016	Healthy	F	75±6	27.1±6.0	20	0.72	0.48		Fish oil in capsules	+ placebo group (olive oil) [27]
<b>Supplementation with other n3-PUFA</b>										
Lundström et al., 2013	Asthma	M + F	20-54	19-39	14+11	4	2		Capsules, ethyl ester	Cross over study with placebo (50:50 soybean: corn oil); 3 weeks washout [22]
Schuchardt et al., 2014 (B)	Hyperlipidemia	M	40±8	28.5±3.28	10	1.56	1.14		Fish oil as rTAG, capsules	[25]
Zivkovic et al., 2012	Nephropathy	-*	≤40 <sup>§</sup>	-*	7	1.9	1.5		Concentrated fish oil, n3-PUFA as ethyl ester in capsules [50]	+ placebo group (corn oil); + sampling at 6, 9, 12, 15, 18 months [29]
<b>Supplementation with other n3-PUFA</b>										
Markworth et al., 2016	Healthy	F	25.5±3.3	22.3±1.6	10	Day 1 : 2g; Day 2-7 : 1g			Day 1: 2 g purified FFA with 18 g olive oil in breakfast; Day 2-7: 2 g 1:1 FFA:olive oil with orange juice	Cross-over study with EPA, n3-DPA and placebo (olive oil), 2 weeks washout [30]

If not indicated otherwise, oxylipin concentrations were analysed at baseline and at the end of the supplementation period. \* no information provided; § information was taken from the inclusion criteria from the study; # oxylipins measured after 12 (n=4), 15 (n=2) or 24 (n=1) months of supplementation; d value refers to total dose of the prescription n3-PUFA ethyl ester product; a mean ± standard error of the mean; b mean ± standard deviation; c median (interquartile range)

### 2.3 Methods for the quantitative comparison of results

For the quantitative comparison of changes in the pattern of oxylipins and their precursors (linoleic acid (C18:2 n6, LA), ALA, ARA, EPA and DHA), fold changes between concentrations post- and pre-n3-PUFA-supplementation (post/pre) were calculated in the different studies, based on the means of the analytes pre- and post-supplementation provided in the respective study (Table 2.2). This relative comparison of study results was chosen to compensate for differences in absolute concentrations between the studies, originating, e.g., from different standards used for calibration [41]. Variances in the analytes' concentrations were not considered in this calculation. If sampling was conducted at more than one time point, basal levels of oxylipins and FA were compared to the longest supplementation period. If an analyte was described in the analytical method, or if an analyte was graphically presented in the manuscript, but no concentration was shown, authors were asked to kindly provide the exact concentration of the respective analytes. In case raw data (or raw means) were provided, calculations of the post/pre ratio for all analytes from the respective study were based on the raw data. For analytes below the limit of quantification (LOQ) the LOQ was used for calculation. Means from the raw data for the post/pre ratios were calculated if the analyte was detectable in  $\geq 50\%$  of the samples in one group. For the quantitative comparison of n3-PUFA induced effects on the oxylipin profile, exemplary oxylipins of the precursor PUFAs LA, ARA, ALA, EPA and DHA from all three enzymatic branches of the ARA cascade were chosen. The analytes were selected based on two criteria: i.) they were reported in most of studies and ii.) analogous biochemical formation route in the AA cascade: 15-LOX products, terminally epoxygenated PUFA and their hydrolyzation products. For oxylipins originating from the COX pathway, ARA derived products PGE<sub>2</sub> and thromboxane (Tx) B<sub>2</sub> were selected as well as their EPA derived counterparts (PGE<sub>3</sub> and TxB<sub>3</sub>).

## **2.4 Modulation of the n6- and n3-oxylipin pattern following n3-PUFA supplementation**

In order to understand oxylipin biology in the course of a disease or in response to a treatment, it would be most appropriate to analyze oxylipin concentrations in the tissue of interest. However, in humans this is rarely feasible. Therefore, plasma and serum are often used as a proximate for tissues to quantitatively evaluate changes in oxylipins, e.g. in response to a dietary intervention. Relative changes in exemplary plasma and serum oxylipins (post/pre fold change) from all three branches of the ARA cascade induced by supplementation with n3-PUFAs in different studies are presented in Table 2.2.

Based on the findings that low doses of EPA and DHA led to a maximum in the incorporation of EPA into plasma phosphatidylcholine after about 14 days of supplementation [37] and that EPA metabolites were rapidly increased after a single dose n3-PUFA [26], we assumed a maximum modulation of the oxylipin pattern after about 14 days. Thus, the oxylipin pattern obtained following 3-12 weeks of supplementation (Table 2.2) would be maximally modulated, allowing the direct comparison of changes between the studies.

The major portion of circulating oxylipins, esp. epoxy-FA and hydroxy-FA, is found esterified in lipids [24, 42]. While the role of esterified oxylipins in (patho-) physiology is not as well understood as the role of free oxylipins, esterified oxylipins have also been shown to be biologically active [43]. Thus, the question of analyzing free or esterified oxylipins is of importance for the interpretation of the results in a biological context. Liberation of oxylipins from their esterified form is often achieved using base hydrolysis, leading to a sum parameter of free and esterified oxylipins ("total oxylipins") [41]. In a direct comparison, relative changes induced by dietary n3-PUFA supplementation revealed similar trends in free and total oxylipins [24]. This finding is further supported by a comparison of changes induced in free and total oxylipins across different studies (Table 2.2). Although some trends were slightly different between free and total oxylipins (see below) the overall data indicates that after 3-12 weeks

of supplementation, shifts occurring in the oxylipin pattern are similarly represented by both, free and total oxylipins.

**Table 2.2:** Fold changes of precursor fatty acid and selected oxylipins. <sup>a</sup> no information provided; <sup>b</sup> analyte was below the limit of quantification in at least one of the groups (pre- or post-supplementation); <sup>c</sup> analyzed, but not shown; <sup>d</sup> analysis not possible due to analyte degradation during alkaline hydrolysis; \* post/pre ratios for FA calculated based on [mol%]; for all other studies, FA ratios were calculated based on [% of total FA]; # shown is comparison of supplementation vs. placebo group.

n3-PUFA	oxylipins	FA	ALA	13-HODE	12(13)- EHOME	12(13)- DIHOME	ARA	PGE <sub>2</sub>	TXB <sub>2</sub>	15-HETE	14(15)- EPETE	14(15)- DIHETE	DHA	17-HDHA	19(20)- EPDPE	19(20)- DHDPE
<b>free</b>																
Schebb et al., 2014	Plasma	RBC	0.94	0.97	0.53	0.9	1.3	<sup>a</sup>	<sup>a</sup>	1.5	1.8	2.5	1.2	<sup>a</sup>	1.2	1.4
Zhang et al., 2015	Plasma	<sup>a</sup>	<sup>a</sup>	<sup>a</sup>	<sup>a</sup>	<sup>a</sup>	<sup>a</sup>	<sup>b</sup>	<sup>b</sup>	<sup>b</sup>	<sup>b</sup>	7	<sup>a</sup>	1.2	<sup>b</sup>	<sup>a</sup>
Schuchardt et al., 2014 (B)	Serum	RBC	0.56	0.92	0.69	0.89	4.5	<sup>a</sup>	<sup>a</sup>	4.3	2.5	3.4	1.6	<sup>a</sup>	1.6	1.9
Watkins et al., 2016	Serum	Plasma	0.97	<sup>c</sup>	<sup>c</sup>	<sup>c</sup>	2.4	<sup>c</sup>	<sup>a</sup>	1.7	4.5	1.5	1.5	1.2	<sup>d</sup>	1.3
Zvkovic et al. 2012	Plasma	<sup>a</sup>	<sup>a</sup>	0.88	0.91	0.66	<sup>a</sup>	3.7	<sup>a</sup>	4.3	1.2	5.6	<sup>a</sup>	1.2	1.8	1.7
Lundström et al., 2013#	Serum	Serum PL	0.88	0.69	0.65	0.71	5.7	<sup>b</sup>	<sup>a</sup>	5.6	<sup>b</sup>	3.9	1.7	<sup>b</sup>	<sup>b</sup>	<sup>b</sup>
Schuchardt et al., 2014 (B)	Serum	RBC	0.68	0.94	0.54	0.76	3.5	<sup>a</sup>	<sup>a</sup>	2.2	1.4	3	1.7	<sup>a</sup>	0.84	2
<b>total</b>																
Fischer&Konkel et al. 2014	Plasma	RBC	0.81	<sup>a</sup>	<sup>a</sup>	<sup>a</sup>	3.4	<sup>d</sup>	<sup>d</sup>	3.2	5	3	1.4	2	2.2	1.9
Keenan et al., 2012*	Plasma	RBC	0.93	0.82	0.8	0.77	4.9	<sup>d</sup>	<sup>d</sup>	6.1	7.1	2	1.4	2.4	2.4	2.4
Schebb et al., 2014	Plasma	RBC	0.94	0.9	0.51	0.63	1.3	<sup>d</sup>	<sup>d</sup>	2.7	2.2	1.7	1.2	<sup>a</sup>	1.1	0.77
Shearer et al., 2010	Plasma	Plasma	0.99	0.86	0.88	1.2	8.5	<sup>d</sup>	<sup>d</sup>	5.5	4.8	4.1	2.7	2.1	2	2.1
<b>n6-PUFA</b>																
<b>free</b>																
Schebb et al., 2014	Plasma	RBC	0.91	<sup>a</sup>	0.98	1.2	0.93	<sup>a</sup>	<sup>a</sup>	0.95	0.92	0.89	1.4	2	2.2	1.9
Zhang et al., 2015	Plasma	<sup>a</sup>	<sup>a</sup>	<sup>a</sup>	<sup>a</sup>	<sup>a</sup>	<sup>a</sup>	<sup>b</sup>	0.7	0.74	<sup>b</sup>	1.4	1.4	2.4	2.4	2.4
Schuchardt et al., 2014 (B)	Serum	RBC	0.72	1.1	0.53	0.91	0.81	<sup>a</sup>	<sup>a</sup>	1.4	0.58	0.84	1.4	2.4	2.4	2.4
Watkins et al., 2016	Serum	Plasma	1	<sup>c</sup>	<sup>c</sup>	<sup>c</sup>	0.94	<sup>c</sup>	<sup>c</sup>	4.4	1.1	0.79	1.4	2.4	2.4	2.4
Zvkovic et al. 2012	Plasma	<sup>a</sup>	<sup>a</sup>	0.75	0.75	1	<sup>a</sup>	1	0.68	0.71	0.65	0.79	1.4	2.4	2.4	2.4
Lundström et al., 2013#	Serum	Serum PL	0.81	0.74	0.76	0.66	0.86	2.7	1.3	1	1.2	0.7	1.4	2.4	2.4	2.4
Schuchardt et al., 2014 (B)	Serum	RBC	0.74	0.67	0.36	0.83	0.93	<sup>a</sup>	<sup>a</sup>	0.93	0.38	0.82	1.4	2.4	2.4	2.4
<b>total</b>																
Fischer&Konkel et al. 2014	Plasma	RBC	0.94	<sup>a</sup>	<sup>a</sup>	<sup>a</sup>	0.95	<sup>d</sup>	<sup>d</sup>	0.85	0.92	0.95	2.7	2.1	2	2.1
Keenan et al., 2012*	Plasma	RBC	0.92	0.86	0.9	1.1	0.89	<sup>d</sup>	<sup>d</sup>	0.8	0.81	0.95	2.7	2.1	2	2.1
Schebb et al., 2014	Plasma	RBC	0.91	<sup>a</sup>	0.67	0.83	0.93	<sup>d</sup>	<sup>d</sup>	0.55	0.61	0.59	2.7	2.1	2	2.1
Shearer et al., 2010	Plasma	Plasma	0.98	0.87	0.93	0.92	0.88	<sup>d</sup>	<sup>d</sup>	0.8	0.92	0.89	2.7	2.1	2	2.1

In response to n3-PUFA supplementation, concentrations of free and total EPA and DHA metabolites in plasma and serum of healthy subjects increased. Generally, relative increases in EPA metabolites were more pronounced than changes in DHA metabolites, a trend that was found in all studies, and elevation in EPA and DHA oxylipins roughly corresponded to changes in the respective precursor FAs. Free DHA metabolites increased up to twofold, while changes in total DHA derived docosanoids were slightly higher in most studies (1.9-2.4-fold increase). However, in the study by Schebb et al., total 19(20)-EpDPE was only slightly increased (post/pre ratio of 1.1) and its hydrolysis product was decreased (post/pre ratio of 0.77). EPA oxylipins increased up to sevenfold and no trend was observable discriminating free (post/pre ratio of 1.5-7.0) and total oxylipins (post/pre ratio of 1.7-7.1). Differences in administered doses between the studies might be a variable leading to this variance (0.36 vs 1.9 g EPA/d see below).

It should be noted that high relative increase does not necessarily correspond to higher absolute concentration changes. For instance, in the study by Schuchardt et al. [25], relative changes in free 15-hydroxy eicosapentaenoic acid (HEPE) were more pronounced than changes in 17,18- dihydroxy eicosatetraenoic acid (DiHETE) (post/pre ration of 4.3 vs. 3.4), while the absolute increase in 17,18-DiHETE was much higher due to the higher concentrations of this analyte (post-pre<sub>15-HETE</sub> = 360 pM; post-pre<sub>17(18)-DiHETE</sub> = 1060 pM). Similarly, the relative increase in 19(20)-EpDPE was lower (post/pre = 1.6) compared to 15-HETE, while the absolute increase was higher (post-pre<sub>19(20)-EpDPE</sub> = 600 pM). Likewise, in the study by Keenan et al. [21], the post/pre ratio of total 17(18)-EpETE was 7.1 versus 2.0 for the hydrolyzation product 19,20-DiHETE, while the respective absolute differences (post-pre) were 4.4 and 7.0 nM. The relative modulation of 17-hydroxy docosahexaenoic acid (HDHA) was similar to 17(18)-DiHETE (2.4), while the concentration of the 17-HDHA was increased by 55 nM post supplementation [21]. In the other studies, similar trends can be found [13, 20, 24, 27, 28]. For the interpretation of biological effects it is thus crucial to not only consider relative changes, but also

absolute changes since one can assume that the concentration of the bioactive substance in the tissue mediates its effects.

Regarding (intra study) responses to n3-PUFA supplementation in the individual pathways of the ARA cascade, results between the studies are heterogenous. For instance, some studies indicated highest changes in the CYP pathway [20, 23]. However, a comparison of terminally epoxy-EPA and epoxy-DHA (CYP) with 15-LOX products (15-HEPE and 17-HDHA) in healthy subjects across different studies led to different results. For instance, changes in free 17(18)-EpETE compared to 15-HEPE were higher in the studies by Schebb et al. [24] and Watkins [27], while changes in 15-HEPE were more pronounced in the studies by Schuchardt et al. [25]. Similarly, results from total oxylipins show different outcomes: Fischer and Konkel [20] as well as Keenan [21] found higher modulation of 17(18)-EpETE and Schebb et al. [24] as well as Shearer et al. [13] found a higher modulation of 15-HEPE. A comparison of changes in 17-HDHA to 19(20)-EpDPE in healthy subjects was only possible for few studies and total oxylipins; however, results suggest a comparable modulation of both pathways [13, 20, 21]. In another study, a distinct decrease in Ep-FA derived from ARA, LA and ALA as well as DiH-FA from ARA (but not LA and ALA) was found, while changes in LOX products were inconsistent (Table 2.2 and [25]). Again, these trends were not found in all studies (Table 2.2).

Changes in the COX pathway could not be evaluated due to insufficient data availability (Table 2.2). Only Zhang et al. reported a decrease in  $\text{TxB}_2$  (post/pre ratio of 0.70 [28]), while other studies did not provide an information on  $\text{PGE}_2$  and  $\text{TxB}_2$ . Since most prostaglandins and thromboxanes are instable during alkaline hydrolysis [41], these analytes were not reported in the studies analyzing total oxylipin concentrations. However, due to their physiological function in platelet activation ( $\text{TxA}_2$ ) and regulation of inflammation ( $\text{PGE}_2$ ) [7, 8], low concentrations of these mediators would be expected in healthy subjects.



While ARA was slightly decreased in all studies, irrespective of the blood fraction analyzed (red blood cells, plasma, serum phospholipids (PL)), changes in free plasma ARA derived oxylipins in healthy subjects were inconsistent. For instance, while 14(15)- epoxy eicosatrienoic acid (EpETrE) was slightly increased in the studies by Watkins et al. (1.1 fold [27]), this analyte was slightly decreased in the study by Schebb et al. (fold change of 0.92 [24]) and highly decreased in the study by Schuchardt et al. (fold change of 0.58 [25]). 15-HETE and 14(15)-dihydroxy eicosatrienoic acid (DiHETrE) showed similar trends. By contrast, in the studies analyzing total oxylipins, ARA metabolites uniformly decreased (post/pre ratio of 0.95-0.55). Indeed, when evaluating changes in free ARA metabolites for each individual, it was shown that they were decreased in some, while they increased in others [23]. Thus, modulation of ARA derived oxylipins detectable in plasma seems to be highly variable between subjects. Changes in EPA and DHA oxylipins in response to n3-PUFA supplementation were also highly variable, but did show an increasing trend in most subjects [23]. This inconsistent trend in ARA oxylipins might be explained by the dietary and endogenous n6-PUFA status of the study subjects, strongly influencing the individual response of n6-PUFA derived oxylipins to n3-PUFA supplementation. By contrast, variance in the study population's dietary uptake of EPA and DHA is low, due to low background intake of EPA and DHA in comparison to the supplementation level, as discussed by Keenan et al. [21]. In response to n3-PUFA supplementation, oxylipins from the LA and ALA metabolomes were mostly decreased, as were their precursor FA.

Although serum and plasma are used in an analogous manner as a proximate to describe changes in tissue oxylipin concentrations, care must be taken when directly comparing absolute oxylipin concentrations from plasma and serum due to increased production of docosanoides and eicosanoids during coagulation. Regarding relative changes in oxylipins, the results from different studies (in healthy and diseased subjects) indicate that both, plasma and serum might be comparable in identifying trends in eicosanoids and other oxylipins induced by dietary supplementation. However, neither plasma, nor

serum oxylipins reflect the actual situation in an inflamed tissue. Serum can be regarded as “*ex vivo*” blood coagulation assay resulting in a massive activation of platelet COX-1 and 12-LOX. In order to induce an immunological response and thus to mimic inflammation, e.g., a septic shock, *ex vivo* assays with stimulation of whole blood with lipopolysaccharides (LPS) to induce monocyte activation [44] or with the calcium ionophore A23187 to induce platelet activation [45] are additionally used. Beyond increased TxB<sub>2</sub> formation, the production of other oxylipins from the COX and LOX pathways, esp. 12-LOX, have been shown to be increased in A23187 activated whole blood [46]. Fischer et al. [20] treated whole blood of subjects supplemented with n3-PUFA with the calcium ionophore A23187. Following supplementation with n3-PUFAs, the levels of LTB<sub>4</sub>, PGE<sub>2</sub> and TxB<sub>2</sub> were barely altered and concentrations of EPA derived counterparts LTB<sub>5</sub> and PGE<sub>3</sub> were low compared to ARA derived eicosanoids. Correlating LTB<sub>5</sub>/LTB<sub>4</sub> and PGE<sub>3</sub>/PGE<sub>2</sub> with the ratio of precursor FA revealed slopes <1, indicating a preference of ARA versus EPA for the formation of LTB and PGE. No change was found in TxB<sub>3</sub> following dietary intervention, probably due to insufficient supplementation doses to induce changes in TxB<sub>3</sub> formation [20]. Interestingly, while in non-activated plasma, LOX pathways did show a higher efficiency in converting EPA and DHA compared to ARA (esterified oxylipins, slope of the product ratios vs parent FA ratios correlations at least 1.9, except 7-HDHA [20]), ARA was more efficiently converted in Ca-ionophore activated whole blood (free oxylipins, slopes of the product ratios vs parent FA ratios correlations 0.01-1.3 [20]).

## **2.5 Dose and time dependent responses in the oxylipin pattern to dietary n3-PUFA supplementation**

Previous studies suggest a dose and time dependent response for the incorporation of EPA and DHA, e.g. into plasma lipid classes or blood cells in low doses which equaled up to four meals oily fish per week [37]. Interestingly, a maximum level of incorporation was reached in the different tissues and blood

compartments which showed a clear dose dependency [37]. However, the extent of incorporation was depended on the tissue and blood compartment. For instance, while the relative amount of EPA+DHA in plasma phosphatidylcholine was linear up to a dose corresponding to four meals oils fish per week (1.87 g/d), a saturation of EPA+DHA in red blood cells was found in the highest concentration [37]. Similarly, Flock et al. found a saturation of %EPA+DHA of total fatty acids in red blood cells in the highest dose supplemented (1800 mg(EPA+DHA)/day, ~5 months [47]). With regard to plasma phospholipids, a linear incorporation of EPA was found up to 3 g (EPA+DHA)/d (3:2, *w:w*) for 12 weeks, while DHA incorporation seemed to reach saturation at the same dose [38].

By contrast, almost no information is available on dose and time dependent changes in the oxylipin pattern in response to dietary n3-PUFA supplementation. In a study by Schuchardt et al. with a single dose n3-PUFA (1.008 g EPA and 0.672 g DHA), most free EPA metabolites in plasma were significantly elevated six hours post ingestion, indicating that EPA oxylipin level can be readily modified in a short period of time [26]. DHA and oxylipin level were not altered which is consistent with the overall lower relative modulation of DHA in response to n3-PUFA supplementation. In the study by Fischer and Konkell et al. the study participants received a daily dose of 460 mg EPA + 380 mg DHA for four weeks and twice as much in the following four weeks [20]. The ratio of the sum of CYP derived EPA and DHA epoxy and dihydroxy-metabolites and the sum of ARA analogs increased approximately twofold in the first week of intervention. In the following weeks only a slight increase occurred. With the doubled dose in week 4, the ratio was rapidly increased until week 8 by about 1.6-fold [20]. These results indicate a distinct time- and dose dependency in the modulation of metabolites in the third branch of the ARA cascade. Given the biological activity of the epoxy-n3-PUFA [10, 11], this warrants further investigation.

Doses supplied to healthy volunteers in studies investigating the effect of n3-PUFA supplementation on the oxylipin pattern were in the range of up to 3.4 g EPA+DHA and the intervention period in most studies was 3 to 12 weeks (Table 2.1). Based on the assumption that time dependent changes in EPA metabolites occur in a similar manner as changes in their precursor FA (see above), we compared the magnitude of change in different EPA derived oxylipins with the supplemented dose in order to evaluate dose response relations

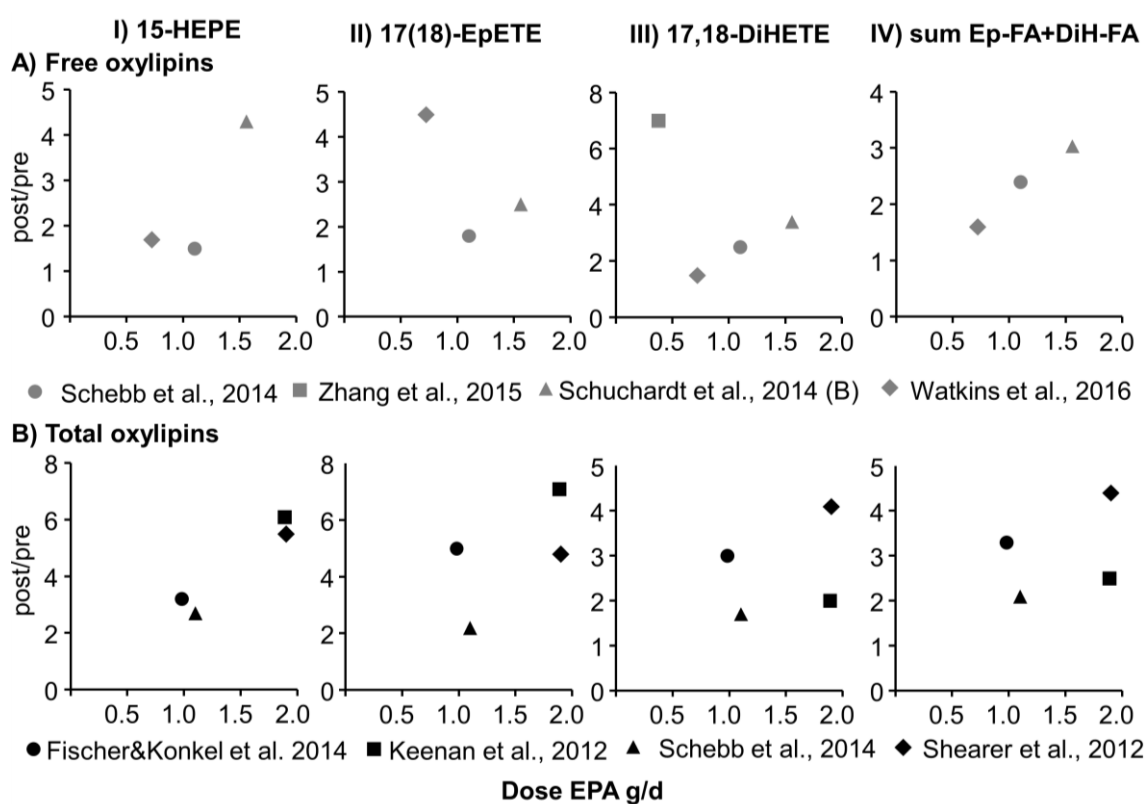


**Fig. 2.2:** Correlation of the post/pre concentration ratio (Table 2.1) for selected free **(A)** and total **(B)** EPA derived eicosanoids with the supplemented dose (Table 2.2) across the different studies.

Across the different studies, relative changes in total 15-HEPE seem to correlate linearly with the supplied dose (Fig. 2.2B I). However, total 17(18)-EpETE, 17(18)-DiHETE and the sum of both do not show a consistent trend across the studies (Fig. 2.2B II-IV). For free 15-HEPE and 17(18)-EpETE, a linear increase could be deduced combining the data of the studies by Schuchardt et al. and Schebb et al. However, observed changes in the study by

Watkins et al. did not correspond to the results (Fig. 2.2A I-II). Interestingly, relative changes in 17,18-DiHETE and in the sum of 17(18)-EpETE+17,18-DiHETE seem to increase linearly with the dose between the three studies. However, for 17,18-DiHETE, a lower dose of EPA in the study by Zhang et al led to a higher change (Fig. 2.2A III).

One should note that the correlations shown in Figure 2 can only be a rough estimate, because of different human subjects and different study designs. Taking the conflicting results on the clinical efficacy of n3-PUFA in different diseases into account, further studies on dose dependent modulations of the oxylipin profile are urgently needed. These studies should not only correlate changes in the overall oxylipin pattern with the n3-PUFA dose but also monitor the genetic variability, e.g. single-nucleotide polymorphism as well as expression levels of the enzymes from the pathways of the ARA cascade. This will not only allow deducing dose-response dependencies but also lead to a better understanding about the molecular mode of action of n3-PUFA and may explain why n3-PUFA are effective in some subjects while others do not respond to n3-PUFAs.

## **2.6 Inter-individual variations in responses to n3-PUFA supplementation**

Although the change of EPA and DHA derived oxylipins showed the same increasing trend, high variances were observed, esp. in changes of EPA and its metabolites between the studies. This is in accordance with findings within the different studies, showing high variances in the individual responses of the study participants to dietary intervention with n3-PUFA although compliance was high in the studies [21, 23, 25, 27].

Schuchardt et al. found that increases in serum EPA metabolites correlated well with increases of EPA in erythrocytes [25] and EPA metabolites in plasma correlated well with EPA plasma phospholipid level after a single dose of n3-

PUFA [26]. Consistently, Nording et al. described a correlation of changes in EPA/DHA in specific lipid classes (e.g. triglycerides, cholesterol ester) with their oxidative metabolites in plasma [23]. Moreover, it has been found that the study participants' individual responses in EPA+DHA in red blood cells (omega-3 index) [21] correlated well to the respective basal status, in a way that a lower basal omega-3 index was associated with higher supplementation induced increases. This was also found in a study by Flock et al., investigating the dose response of the omega-3 index to increasing doses of n3-PUFA supplementation. The authors found a positive correlation of changes with the initial omega-3 index. Furthermore, a lower bodyweight and a higher n3-PUFA dose were associated with a higher increase in the omega-3 index [47]. Keenan et al. correlated individual baseline PUFA and oxylipin concentrations with the respective dose-dependent change. The x-intercept of the resulting inverse correlation was introduced as the "change threshold". This concentration defines the threshold for supplementation induced changes by n3-PUFA. Study participants entering the study with this PUFA/oxylipin concentration will most likely show only little changes after supplementation. The larger the difference of a subject's basal PUFA/oxylipin status from the "change threshold" the higher the change that will be observed with supplementation [21].

These results indicate that changes in PUFA as well as oxylipin concentrations are dependent parameters and correlate with the basal level of PUFA/oxylipins. Thus, variances in basal n3-PUFA level might account for part of the observed differences in individual responses to n3-PUFA supplementation.

Fischer and Konkol et al. found a positive correlation between the (dose [mg/kg bodyweight/d]\*basal omega-3 index) and the omega-3 index in week 8 [20]. By contrast, in an explorative study by Nording et al., no significant correlations between changes in EPA, DHA, ARA or their oxylipins and age, body weight or BMI was found [23]. Similarly, Schebb et al. did not find statistically different concentrations in oxylipins before and after supplementation between men and women for most analytes [24].

Schuchardt et al. observed that variances between the study participants were much higher for oxylipins compared to fatty acids: While trends in fatty acids induced by n3-PUFA supplementation were similar between the individuals, trends in oxylipins differed [25]. These results indicate inter-individual differences in the metabolism of fatty acids. Indeed, Stephenson et al. reported differences in the response to n3-PUFA supplementation which were correlated to variants in the ALOX5 genotype [48]. In another study, it was shown that dietary intervention influenced the expression of different PUFA metabolizing enzymes, e.g. ALOX5, or CYP2J2, in study participants that did not show a response (in form of lowered triglyceride level) to n3-PUFA supplementation [49].

Most oxylipins in plasma are found in the lipoprotein fraction [42]. However, only little information exists on the profile of oxylipins in lipoproteins and their modulation, e.g. by n3-PUFA supplementation. In statin-treated, hypertriglyceridemic patients, the different lipoprotein fractions showed a distinct pattern of oxylipins, which shifted from dominantly ARA metabolites to EPA and DHA derived ones following supplementation with EPA and DHA. Thus, it seems likely that modulations in individual lipoprotein levels and distribution – e.g. dietary PUFA induced modulation of the LDL/HDL ratio – contribute to the varying plasma oxylipin levels observed in different subjects.

Overall, it seems crucial to address the high inter-individual variances in future studies, especially in the light of using oxylipins as biomarker for diseases.

## **2.7 Modulation of oxylipins by n3-supplementation in (the onset of) diseases**

Few studies investigated the effects of n3-PUFA supplementation on the oxylipin pattern in non-healthy subjects, including mild to moderate asthma [22], hyperlipidemia [25] and IgA nephropathy [29]. The changes in the oxylipin pattern in these subjects depicted in Table 2.2 were comparable to healthy

individuals. Indeed, Schuchardt et al. directly compared normo- vs. hyperlipidemic subjects and concluded that no differences between the oxylipin profiles in both study groups were observable [25]. Based on patients with n3-PUFA supplementation, Zivkovic et al. identified oxylipins which were changed the most between responders and non-responders in terms of n3-PUFA induced improved kidney function [29]. Here, the highest differences between both groups were not found for EPA and DHA epoxy- and dihydroxy-metabolites, but in hydroxy-LA and hydroxy-ARA. Based on this finding one could conclude that – at least plasma levels of – EPA and DHA oxylipins are not linked to the improvement of kidney function by n3-PUFA.

## **2.8 Conclusion**

In this short review we compared the effects of supplementation with the n3-PUFAs EPA and DHA on the oxylipin pattern across different studies. However, due to restrictions in data availability only few oxylipins could be quantitatively compared. In particular, it was not possible to evaluate changes in the COX branch of the ARA cascade and in bioactive SPMs.

Overall, EPA and DHA derived oxylipins were increased compared to baseline, while changes in ARA were less consistent with a trend to decreasing levels. However, interpretation of these results is hampered by high inter-individual variances in oxylipin concentration in response to n3-PUFA supplementation while changes in fatty acids were consistent. Nonetheless, the currently available data indicate that the response in the oxylipin profile to n3-PUFA supplementation correlates with the basal fatty acid status. However, only scarce information is available on dose- as well as time-responses.

Thus, in future studies it will be important to understand the underlying reasons for the high variability of inter-individual responses in oxylipins to n3-PUFA supplementation. Moreover, the investigation of time- and dose dependencies in n3-PUFA induced changes in the oxylipin pattern are still lacking. This



information will help to understand n3-PUFA biology, especially with regard to recent studies finding no beneficial effect of n3-PUFAs on human health, and to identify and establish oxylipin(ratios) as biomarker for disease status and the effectiveness of (pharmacological) treatment. Moreover, studies investigating the effect of the background diet (high n6, mediterranean) and supplementation with individual PUFAs [30] will be helpful to understand the regulation of the endogenous oxylipin profile.

## 2.9 References

1. Mozaffarian D, Wu JH. Omega-3 fatty acids and cardiovascular disease: effects on risk factors, molecular pathways, and clinical events. *J Am Coll Cardiol*. 2011;58(20):2047-2067.
2. Calder PC. Marine omega-3 fatty acids and inflammatory processes: Effects, mechanisms and clinical relevance. *Biochim Biophys Acta*. 2015;1851(4):469-484.
3. Feagan BG, Sandborn WJ, Mittmann U, Bar-Meir S, D'Haens G, Bradette M, Cohen A, Dallaire C, Ponich TP, McDonald JW, Hebuterne X, Pare P, Klvana P, Niv Y, Ardizzone S, Alexeeva O, Rostom A, Kiudelis G, Spleiss J, Gilgen D, Vandervoort MK, Wong CJ, Zou GY, Donner A, Rutgeerts P. Omega-3 free fatty acids for the maintenance of remission in Crohn disease: the EPIC Randomized Controlled Trials. *JAMA*. 2008;299(14):1690-1697.
4. Kromhout D, Giltay EJ, Geleijnse JM, Alpha Omega Trial G. n-3 fatty acids and cardiovascular events after myocardial infarction. *N Engl J Med*. 2010;363(21):2015-2026.
5. Rizos EC, Ntzani EE, Bika E, Kostapanos MS, Elisaf MS. Association between omega-3 fatty acid supplementation and risk of major cardiovascular disease events: a systematic review and meta-analysis. *JAMA*. 2012;308(10):1024-1033.
6. Wang W, Zhu J, Lyu F, Panigrahy D, Ferrara KW, Hammock B, Zhang G. omega-3 polyunsaturated fatty acids-derived lipid metabolites on angiogenesis, inflammation and cancer. *Prostaglandins Oth Lipid M*. 2014;113-115:13-20.
7. Funk CD. Prostaglandins and leukotrienes: advances in eicosanoid biology. *Science*. 2001;294(5548):1871-1875.
8. Gabbs M, Leng S, Devassy JG, Monirujjaman M, Aukema HM. Advances in Our Understanding of Oxylipins Derived from Dietary PUFAs. *Adv Nutr*. 2015;6(5):513-540.
9. Smith WL, Urade Y, Jakobsson PJ. Enzymes of the cyclooxygenase pathways of prostanoid biosynthesis. *Chem Rev*. 2011;111(10):5821-5865.
10. Arnold C, Markovic M, Blossey K, Wallukat G, Fischer R, Dechend R, Konkel A, von Schacky C, Luft FC, Muller DN, Rothe M, Schunck WH. Arachidonic acid-metabolizing cytochrome P450 enzymes are targets of {omega}-3 fatty acids. *J Biol Chem*. 2010;285(43):32720-32733.
11. Zhang G, Panigrahy D, Mahakian LM, Yang J, Liu JY, Stephen Lee KS, Wettersten HI, Ulu A, Hu X, Tam S, Hwang SH, Ingham ES, Kieran MW, Weiss RH, Ferrara KW, Hammock BD. Epoxy metabolites of docosahexaenoic acid (DHA) inhibit angiogenesis, tumor growth, and metastasis. *Proc Natl Acad Sci U S A*. 2013;110(16):6530-6535.
12. Serhan CN. Pro-resolving lipid mediators are leads for resolution physiology. *Nature*. 2014;510(7503):92-101.
13. Shearer GC, Harris WS, Pedersen TL, Newman JW. Detection of omega-3 oxylipins in human plasma and response to treatment with omega-3 acid ethyl esters. *J Lipid Res*. 2010;51(8):2074-2081.
14. Yang J, Schmelzer K, Georgi K, Hammock BD. Quantitative Profiling Method for Oxylipin Metabolome by Liquid Chromatography Electrospray Ionization Tandem Mass Spectrometry. *Anal Chem*. 2009;81(19):8085-8093.
15. Skarke C, Alamuddin N, Lawson JA, Li X, Ferguson JF, Reilly MP, FitzGerald GA. Bioactive products formed in humans from fish oils. *J Lipid Res*. 2015;56(9):1808-1820.
16. Barden A, Mas E, Croft KD, Phillips M, Mori TA. Short-term n-3 fatty acid supplementation but not aspirin increases plasma proresolving mediators of inflammation. *J Lipid Res*. 2014;55(11):2401-2407.

17. Mas E, Croft KD, Zahra P, Barden A, Mori TA. Resolvins D1, D2, and other mediators of self-limited resolution of inflammation in human blood following n-3 fatty acid supplementation. *Clin Chem*. 2012;58(10):1476-1484.
18. Akintoye E, Wu JH, Hou T, Song X, Yang J, Hammock B, Mozaffarian D. Effect of fish oil on monoepoxides derived from fatty acids during cardiac surgery. *J Lipid Res*. 2016;57(3):492-498.
19. Zulyniak MA, Perreault M, Gerling C, Spriet LL, Mutch DM. Fish oil supplementation alters circulating eicosanoid concentrations in young healthy men. *Metabolism*. 2013;62(8):1107-1113.
20. Fischer R, Konkel A, Mehling H, Blossey K, Gapelyuk A, Wessel N, von Schacky C, Dechend R, Muller DN, Rothe M, Luft FC, Weylandt K, Schunck WH. Dietary omega-3 fatty acids modulate the eicosanoid profile in man primarily via the CYP-epoxygenase pathway. *J Lipid Res*. 2014;55(6):1150-1164.
21. Keenan AH, Pedersen TL, Fillaus K, Larson MK, Shearer GC, Newman JW. Basal omega-3 fatty acid status affects fatty acid and oxylipin responses to high-dose n3-HUFA in healthy volunteers. *J Lipid Res*. 2012;53(8):1662-1669.
22. Lundstrom SL, Yang J, Brannan JD, Haeggstrom JZ, Hammock BD, Nair P, O'Byrne P, Dahlen SE, Wheelock CE. Lipid mediator serum profiles in asthmatics significantly shift following dietary supplementation with omega-3 fatty acids. *Molr Nutr Food Res*. 2013;57(8):1378-1389.
23. Nording ML, Yang J, Georgi K, Hegedus Karbowski C, German JB, Weiss RH, Hogg RJ, Trygg J, Hammock BD, Zivkovic AM. Individual variation in lipidomic profiles of healthy subjects in response to omega-3 Fatty acids. *PLoS One*. 2013;8(10):e76575.
24. Schebb NH, Ostermann AI, Yang J, Hammock BD, Hahn A, Schuchardt JP. Comparison of the effects of long-chain omega-3 fatty acid supplementation on plasma levels of free and esterified oxylipins. *Prostaglandins Oth Lipid M*. 2014;113-115:21-29.
25. Schuchardt JP, Schmidt S, Kressel G, Willenberg I, Hammock BD, Hahn A, Schebb NH. Modulation of blood oxylipin levels by long-chain omega-3 fatty acid supplementation in hyper- and normolipidemic men. *Prostaglandins Leukot Essent Fatty Acids*. 2014;90(2-3):27-37.
26. Schuchardt JP, Schneider I, Willenberg I, Yang J, Hammock BD, Hahn A, Schebb NH. Increase of EPA-derived hydroxy, epoxy and dihydroxy fatty acid levels in human plasma after a single dose of long-chain omega-3 PUFA. *Prostaglandins Oth Lipid M*. 2014;109-111:23-31.
27. Watkins BA, Kim J, Kenny A, Pedersen TL, Pappan KL, Newman JW. Circulating levels of endocannabinoids and oxylipins altered by dietary lipids in older women are likely associated with previously identified gene targets. *Biochim Biophys Acta*. 2016;1861(11):1693-1704.
28. Zhang X, Yang N, Ai D, Zhu Y. Systematic Metabolomic Analysis of Eicosanoids after Omega-3 Polyunsaturated Fatty Acid Supplementation by a Highly Specific Liquid Chromatography-Tandem Mass Spectrometry-Based Method. *J Proteome Res*. 2015;14(4):1843-1853.
29. Zivkovic AM, Yang J, Georgi K, Hegedus C, Nording ML, O'Sullivan A, German JB, Hogg RJ, Weiss RH, Bay C, Hammock BD. Serum oxylipin profiles in IgA nephropathy patients reflect kidney functional alterations. *Metabolomics*. 2012;8(6):1102-1113.

30. Markworth JF, Kaur G, Miller EG, Larsen AE, Sinclair AJ, Maddipati KR, Cameron-Smith D. Divergent shifts in lipid mediator profile following supplementation with n-3 docosapentaenoic acid and eicosapentaenoic acid. *Faseb Journal*. 2016;30(11):3714-3725.
31. Guillou H, Zadavec D, Martin PG, Jacobsson A. The key roles of elongases and desaturases in mammalian fatty acid metabolism: Insights from transgenic mice. *Prog Lipid Res*. 2010;49(2):186-199.
32. Burdge GC, Calder PC. Conversion of alpha-linolenic acid to longer-chain polyunsaturated fatty acids in human adults. *Reprod Nutr Dev*. 2005;45(5):581-597.
33. Stark KD, Van Elswyk ME, Higgins MR, Weatherford CA, Salem N, Jr. Global survey of the omega-3 fatty acids, docosahexaenoic acid and eicosapentaenoic acid in the blood stream of healthy adults. *Prog Lipid Res*. 2016;63:132-152.
34. Kutzner L, Ostermann AI, Konrad T, Riegel D, Hellhake S, Schuchardt JP, Schebb NH. Lipid Class Specific Quantitative Analysis of n-3 Polyunsaturated Fatty Acids in Food Supplements. *J Agric Food Chem*. 2017;65(1):139-147.
35. Flock MR, Harris WS, Kris-Etherton PM. Long-chain omega-3 fatty acids: time to establish a dietary reference intake. *Nutr Rev*. 2013;71(10):692-707.
36. Wolfram G, Bechthold A, Boeing H, Ellinger S, Hauner H, Kroke A, Leschik-Bonnet E, Linseisen J, Lorkowski S, Schulze M, Stehle P, Dinter J, German Nutrition S. Evidence-Based Guideline of the German Nutrition Society: Fat Intake and Prevention of Selected Nutrition-Related Diseases. *Ann Nutr Metab*. 2015;67(3):141-204.
37. Browning LM, Walker CG, Mander AP, West AL, Madden J, Gambell JM, Young S, Wang L, Jebb SA, Calder PC. Incorporation of eicosapentaenoic and docosahexaenoic acids into lipid pools when given as supplements providing doses equivalent to typical intakes of oily fish. *Am J Clin Nutr*. 2012;96(4):748-758.
38. Blonk MC, Bilo HJ, Nauta JJ, Popp-Snijders C, Mulder C, Donker AJ. Dose-response effects of fish-oil supplementation in healthy volunteers. *Am J Clin Nutr*. 1990;52(1):120-127.
39. Schuchardt JP, Hahn A. Bioavailability of long-chain omega-3 fatty acids. *Prostaglandins Leukot Essent Fatty Acids*. 2013;89(1):1-8.
40. Hussey EK, Portelli S, Fossler MJ, Gao F, Harris WS, Blum RA, Lates CD, Gould E, Abu-Baker O, Johnson S, Reddy KK. Relative Bioavailability of an Emulsion Formulation for Omega-3-Acid Ethyl Esters Compared to the Commercially Available Formulation: A Randomized, Parallel-Group, Single-Dose Study Followed by Repeat Dosing in Healthy Volunteers. *Clin Pharmacol Drug Dev*. 2012;1(1):14-23.
41. Willenberg I, Ostermann AI, Schebb NH. Targeted metabolomics of the arachidonic acid cascade: current state and challenges of LC-MS analysis of oxylipins. *Anal Bioanal Chem*. 2015;407(10):2675-2683.
42. Shearer GC, Newman JW. Lipoprotein lipase releases esterified oxylipins from very low-density lipoproteins. *Prostaglandins Leukot and Essent Fatty Acids*. 2008;79(6):215-222.
43. Hammond VJ, O'Donnell VB. Esterified eicosanoids: generation, characterization and function. *Biochim Biophys Acta*. 2012;1818(10):2403-2412.
44. Fu JY, Masferrer JL, Seibert K, Raz A, Needleman P. The induction and suppression of prostaglandin H2 synthase (cyclooxygenase) in human monocytes. *J Biol Chem*. 1990;265(28):16737-16740.
45. Young JM, Panah S, Satchawatcharaphong C, Cheung PS. Human whole blood assays for inhibition of prostaglandin G/H synthases-1 and -2 using A23187 and lipopolysaccharide stimulation of thromboxane B2 production. *Inflamm Res*. 1996;45(5):246-253.

46. Gomolka B, Siegert E, Blosser K, Schunck WH, Rothe M, Weylandt KH. Analysis of omega-3 and omega-6 fatty acid-derived lipid metabolite formation in human and mouse blood samples. *Prostaglandins Oth Lipid M.* 2011;94(3-4):81-87.
47. Flock MR, Skulas-Ray AC, Harris WS, Etherton TD, Fleming JA, Kris-Etherton PM. Determinants of erythrocyte omega-3 fatty acid content in response to fish oil supplementation: a dose-response randomized controlled trial. *J Am Heart Assoc.* 2013;2(6):e000513.
48. Stephensen CB, Armstrong P, Newman JW, Pedersen TL, Legault J, Schuster GU, Kelley D, Vikman S, Hartiala J, Nassir R, Seldin MF, Allayee H. ALOX5 gene variants affect eicosanoid production and response to fish oil supplementation. *J Lipid Res.* 2011;52(5):991-1003.
49. Rudkowska I, Paradis AM, Thifault E, Julien P, Barbier O, Couture P, Lemieux S, Vohl MC. Differences in metabolomic and transcriptomic profiles between responders and non-responders to an n-3 polyunsaturated fatty acids (PUFAs) supplementation. *Genes Nutr.* 2013;8(4):411-423.
50. Hogg RJ, Lee J, Nardelli N, Julian BA, Cattran D, Waldo B, Wyatt R, Jennette JC, Sibley R, Hyland K, Fitzgibbons L, Hirschman G, Donadio JV, Jr., Holub BJ, Southwest Pediatric Nephrology Study G. Clinical trial to evaluate omega-3 fatty acids and alternate day prednisone in patients with IgA nephropathy: report from the Southwest Pediatric Nephrology Study Group. *Clin J Am Soc Nephrol.* 2006;1(3):467-474.



# Chapter 3

## Determining the Fatty Acid Composition in Plasma and Tissues as Fatty Acid Methyl Esters Using Gas Chromatography – A Comparison of Different Derivatization and Extraction Procedures

*Analysis of the FA composition in biological samples is commonly carried out using gas liquid chromatography (GC) after transesterification to volatile FA methyl esters (FAME). We compared the efficacy of six frequently used protocols for derivatization of different lipid classes as well as for plasma and tissue samples. Transesterification with trimethylsulfonium hydroxide (TMSH) led to insufficient derivatization efficacies for polyunsaturated FAs (PUFA, <50%). Derivatization in presence of potassium hydroxide (KOH) failed at derivatizing free FAs (FFAs). Boron trifluoride (BF<sub>3</sub>) 7% in hexane/MeOH (1:1) was insufficient for the transesterification of cholesterol ester (CE) as well as triacylglycerols (TGs). In contrast, methanolic hydrogen chloride (HCl) as well as a combination of BF<sub>3</sub> with methanolic sodium hydroxide (NaOH+BF<sub>3</sub>) were suitable for the derivatization of FFAs, polar lipids, TGs and CEs (derivatization rate >80% for all tested lipids). Regarding plasma samples, all methods led to an overall similar relative FA pattern. However, significant differences were observed, e.g., for the relative amount of EPA+DHA in plasma. Absolute FA plasma concentrations differed considerably among the methods, with low yields for KOH and BF<sub>3</sub>. We also demonstrate that lipid extraction with tert-butyl methyl ether/methanol (MTBE/MeOH) is as efficient as the classical method according to Bligh and Dyer, making it possible to replace (environmentally) toxic chloroform. We conclude that HCl-catalyzed derivatization in combination with MeOH/MTBE extraction is the most appropriate among the methods tested for the analysis of FA concentrations and FA pattern in small biological samples.*

Reprinted from *Prostaglandins, Leukotrienes and Essential Fatty Acids*, vol. 91(6), Ostermann AI, Müller M, Willenberg I and Schebb NH, Determining the fatty acid composition in plasma and tissues as fatty acid methyl esters using gas chromatography – a comparison of different derivatization and extraction procedures, pp. 235-241, Copyright (2014), with permission from Elsevier.

Author contributions: AIO: Designed research, performed experiments and wrote the manuscript; MM: worked with the GC-FID method and performed extraction experiments as part of her master thesis under the supervision of AIO; IW: Designed research; NHS: Designed research and wrote the manuscript.

### 3.1 Introduction

For half a century, fatty acids have been routinely quantified using GC with flame ionization detection (GC-FID) following transesterification to FAMES [1]. This well-established technique is an integral tool in the characterization of authenticity and nutritional value of food. As food analysis is a highly regulated area, several standard methods for the analysis of FAs have been suggested by food authorities in the United States and European Union [2, 3].

With the finding that the dietary intake of long-chain PUFAs (LC-PUFAs) has direct impact on human health, numerous studies aimed to investigate the effects of a modulation of the PUFA pattern in blood and tissues in response to the diet [4-7]. At last, the broad recognition of the physiological importance of LC-n3-PUFA and their oxylipins caused a renaissance in GC-FID FAME analysis in bioanalysis laboratories. In fact, most modern liquid chromatography-mass spectrometry (LC-MS) based targeted oxylipin metabolomics studies are backed up by classic GC-FID FAME analysis of the precursor FA [8-12].

Compared to the area of food analysis dealing with rather large volumes, sample preparation and derivatization methods for the analysis of small amounts of tissue and low plasma volumes is less standardized. Most commonly acid derivatization with  $\text{BF}_3$  [5, 7, 10-14] or  $\text{HCl}$  [4, 15-17] are employed and have been used to characterize FA pattern in plasma and tissues [8, 15]. Moreover, TMSH [18-20] has been used in these kinds of studies and alkaline derivatization with sodium or potassium methanolate [6] or hydroxide [19] have been proven to be suitable for the analysis of different lipid classes. Moreover, combinations of different reagents, such as  $\text{BF}_3$  and methanolic sodium hydroxide, have been developed [21-23].

Lipid extraction is generally carried out according to Bligh and Dyer [24] or for samples with high fat content according to Folch [25, 26] albeit several years ago Matyash et al. described an extraction strategy allowing a replacement of



halogenated solvents [27]. Most studies start with an extraction of lipids from plasma or (homogenized) tissue, while few apply the derivatization agent without any prior sample preparation [15, 28].

Because GC-FID FAME analysis is such a well-established technique, only little information on method details and validation data are given in recent articles. As a consequence, it is difficult to deduce the most suited sample preparation method for quantitative FAME analysis in small biological samples based on current literature data. In effort to establish GC-FID FAME analysis in our laboratory, we compared the performance of six common derivatization methods. Most techniques led to comparable relative FA patterns. However, absolute concentrations of the different FA and sums of all FA determined in a plasma or tissue sample varied between the different methods. In this article, we therefore systematically elucidated reasons for these differences by analysis of derivatization efficacy for all relevant classes of lipids and different FA. Furthermore, we compared two different extraction protocols (Bligh and Dyer as well as MTBE/MeOH) and tested alkaline hydrolysis as additional sample preparation step to improve tissue homogenization and extraction.

## **3.2 Experimental**

### **3.2.1 Chemicals and biological material**

Chloroform (uvasolv grade), ethanol (uvasolv grade), ammonium acetate (p.a.), sodium chloride (p.a.) and KOH (p.a.) were obtained from Merck (Darmstadt, Germany). *n*-Hexane (hexane in the following) (HPLC grade), NaOH (p.a.) and MTBE (HPLC grade) were purchased from Carl Roth (Karlsruhe, Germany). TMSH was obtained from CS Chromatographie Service (Langerwehe, Germany). MeOH (HPLC grade) was purchased from J.T. Baker (Deventer, Holland). Methyl tricosanoate used as internal standard (FAME C23:0, >98%) and cholesteryl heptadecanoate (CE C17:0, >98%) were obtained from Santa

Cruz Biotechnology (Santa Cruz, CA, USA). Dihenarachidoyl-sn-glycero-3-phosphocholine (PC C21:0, >99%) was purchased from Avanti Polar Lipids (Alabaster, AL, USA). Arachidonic acid (C20:4n6), eicosapentaenoic acid (C20:5n3) and docosahexaenoic acid (C22:6n3) were obtained from Cayman Chemicals (Ann Arbor, MI, USA). Acetic acid (Acros Organics) was obtained from Fisher Scientific (Nidderau, Germany). Sodium bisulfate (p.a.) was obtained from Riedel de Haën (Seelze, Germany). All other chemicals were purchased from Sigma Aldrich (Schnelldorf, Germany). Rat liver tissues were collected from male Fischer 344 rats (250-300 g bodyweight, Charles River, Sulzfeld, Germany). Pooled human plasma was obtained from healthy male volunteers.

### **3.2.2 GC-FID analysis**

Gas liquid chromatography was carried out on a 30 m x 0.25 mm FAMEWAX capillary column with a 0.25 µm thick polar polyethylene coating (Restek, Bad Homburg, Germany) equipped with a 5 m x 0.25 mm Guard Column (Restek). Separation was performed with the following temperature gradient on a 6890 series GC instrument (Agilent, Weilbronn, Germany): 140 °C to 210 °C with 10 °C/min, 210 °C to 230 °C with 2 °C/min and 230 °C for 7 min (total run time 24 min). Helium was used as carrier gas at a constant flow of 1.5 mL/min. One microliter of the sample was injected into an injector kept at 275 °C and the split was set to 1:50. The flame ionization detector was operated at 300 °C with 45 mL/min hydrogen flow, 450 mL/min air flow and a make-up flow of 45 mL/min helium. Under these conditions, all biologically relevant FA were baseline separated as shown by a 37 FAME standard from Supelco (CRM47885, Sigma Aldrich) supplemented with 22:5n3 and 22:4n6 (Sigma Aldrich) as well as a 20 FAME fish oil mix (35066, Restek). ChemStation B01.03 (Agilent) was used for instrument control and data handling. Quantification of FAMES was carried out based on their peak areas compared to the internal standard (FAME C23:0) peak area by using response factors introduced by Ackman and Sipos [29, 30].

Linear range and the accuracy of the method were validated by the analysis of FAME standards (see above).

### 3.2.3 Sample preparation

#### Alkaline hydrolysis/sample saponification

10  $\mu\text{L}$  internal standard solution (IS; FAME C23:0, in chloroform/ethanol 1:9) and 10  $\mu\text{L}$  of antioxidant solution (0.2 mg/mL ethylenediaminetetraacetic acid, butylated hydroxytoluene and triphenylphosphine in methanol:water 50:50), were added to 35-45 mg liver tissue. Thereafter, 100  $\mu\text{L}$  MeOH and 60  $\mu\text{L}$  10 M aqueous sodium hydroxide were added and the samples were homogenized in a ball mill (20 Hz, 5 min, 22 °C, MM 400, Retsch, Haan, Germany). The crude suspension was then hydrolyzed for 30 min at 60 °C. Directly after hydrolysis, samples were neutralized (pH 6-7) on ice with 70  $\mu\text{L}$  of 50% acetic acid and extracted as described below.

#### Lipid extraction

Following addition of 10  $\mu\text{L}$  IS solution, pooled human plasma (50  $\mu\text{L}$ ) and rat liver tissue (35-45 mg) were extracted by the method of Bligh and Dyer [24] and Matyash [27] with slight modifications. For Bligh and Dyer [24] extraction, plasma was extracted with 750  $\mu\text{L}$  of chloroform:MeOH (1:2), and the liver tissue was homogenized with 750  $\mu\text{L}$  of chloroform:MeOH (1:2) and 50  $\mu\text{L}$  of water in a ball mill (see above). Thereafter, 250  $\mu\text{L}$  of chloroform as well as 250  $\mu\text{L}$  of water were added; the samples were mixed for 1.5 min and centrifuged for 10 min at 4500  $xg$  at room temperature. Following collection of the lower organic phase, the aqueous phase was re-extracted with 250  $\mu\text{L}$  of chloroform. The organic phases were combined and the sample was evaporated in a vacuum centrifuge (1 mbar, 35 °C; Christ, Osterode, Germany).

For the extraction according to Matyash [27] plasma was mixed with 300  $\mu\text{L}$  of MeOH and the liver tissue was homogenized with 300  $\mu\text{L}$  of MeOH and 50  $\mu\text{L}$  of

water in a ball mill (see above). Thereafter, 600  $\mu\text{L}$  of MTBE was added; the samples were vigorously shaken for 1.5 min and mixed with 300  $\mu\text{L}$  of 0.15 mmol/L ammonium acetate. After centrifugation for 5 min at 3500  $xg$  at 4  $^{\circ}\text{C}$  the upper organic layer was collected and the surface of the residual aqueous phase was washed with another 300  $\mu\text{L}$  MTBE. The organic phases were combined and evaporated in a vacuum centrifuge (see above).

### Derivatization

The dried lipid extracts were transesterified to FAME by six different methods as previously described with slight modifications [15, 19, 20, 22, 28]. For *TMSH derivatization*, the dried lipid extract was dissolved in 100  $\mu\text{L}$  of hexane and 50  $\mu\text{L}$  of methanolic TMSH (0.2 mol/L). The samples were shaken at 400 U/min for 30 min at room temperature [20]. For *BF<sub>3</sub> derivatization* the dried lipid extract was dissolved in 500  $\mu\text{L}$  BF<sub>3</sub> solution (12-14% in MeOH) and 500  $\mu\text{L}$  of hexane. The solution was heated for 1 h in a tightly closed vial in a metal block kept at 90-95 $^{\circ}\text{C}$ . After cooling, 750  $\mu\text{L}$  of water were added. The sample was shaken vigorously for 4 min, centrifuged at 3500  $xg$  for 5 min and the hexane layer was collected [28]. For the *HCl derivatization* the dried lipid extract was dissolved in 600  $\mu\text{L}$  of acetylchloride in MeOH (1:9) and 400  $\mu\text{L}$  hexane and the sample was heated to 90-95  $^{\circ}\text{C}$  for 1 h in a tightly closed vial. After cooling, 750  $\mu\text{L}$  of aqueous potassium carbonate (0.44 mol/L) were added. The sample was shaken vigorously for 4 min, centrifuged at 3500  $xg$  for 5 min and the hexane layer was collected [15]. For *KOH derivatization* the lipid extract was dissolved in 200  $\mu\text{L}$  of hexane and 100  $\mu\text{L}$  of methanolic KOH (2 mol/L). After incubation at room temperature for 5 min, 40 mg of sodium bisulfate were added and the supernatant was collected [19]. For the *combined NaOH+BF<sub>3</sub> protocol*, the dried lipid extract was dissolved in 100  $\mu\text{L}$  methanolic sodium hydroxide (0.5 mol/L) and heated for 15 min at 90-95  $^{\circ}\text{C}$  in a tightly closed vial. Thereafter, 500  $\mu\text{L}$  BF<sub>3</sub> solution (12-14% in MeOH) was added and the sample was heated for another 30 min at 90-95  $^{\circ}\text{C}$ . 750  $\mu\text{L}$  of saturated aqueous sodium chloride and 500  $\mu\text{L}$  of hexane were added after cooling of the sample. The sample was

shaken vigorously for 4 min, centrifuged at 3500  $xg$  for 5 min and the organic phase was collected [22].

Following all derivatization protocols, the organic phases were evaporated in a vacuum centrifuge (1 mbar, 35 °C; see above), reconstituted in 50  $\mu\text{L}$  of MTBE:MeOH (9:1) and analyzed by GC-FID. Only for direct TMSH derivatization the dried lipid extract was reconstituted in 50  $\mu\text{L}$  of methanolic TMSH (0.2 mol/L) and 50  $\mu\text{L}$  of MTBE and directly subjected to GC analysis [19].

The derivatization efficacies were analyzed by treating 5  $\mu\text{L}$  of a standard solution containing 2 mmol/L of FFAs, a phosphatidylcholine (PC), a CE and TGs, with 10  $\mu\text{L}$  IS as lipid extract.

### **3.3 Results**

#### **3.3.1 Derivatization efficacy for different lipid classes**

The efficacy of the six different protocols for the transesterification of FFA, a PC, TGs and a CE are shown in Fig. 3.1.

KOH led to good derivatization efficacies for PC and TG (>90%), while FFA as well as CE were not derivatized (<3%). Except for polyunsaturated FFA (derivatization  $\leq 11\%$ ), all tested lipid classes were acceptably methylated using TMSH ( $\geq 80\%$ ). Direct injection of the TMSH derivatization mixture into the hot injector (TMSH inj) led to higher but still low derivatization of polyunsaturated FFA ( $\leq 50\%$ ). Moreover, this procedure caused inefficient transesterification efficacies for TG C19:0 (rec=41%). Derivatization in presence of  $\text{BF}_3$  led to good efficacies (>95%) for FFA and the PC; however, the CE and TG were not efficiently transesterified ( $\leq 30\%$ ). Derivatization rates with methanolic HCl were good for all tested lipid classes (>80%). The protocol combining derivatization in

presence of methanolic NaOH+BF<sub>3</sub> also led to a good derivatization efficacy (≥85%) for all tested lipid classes.

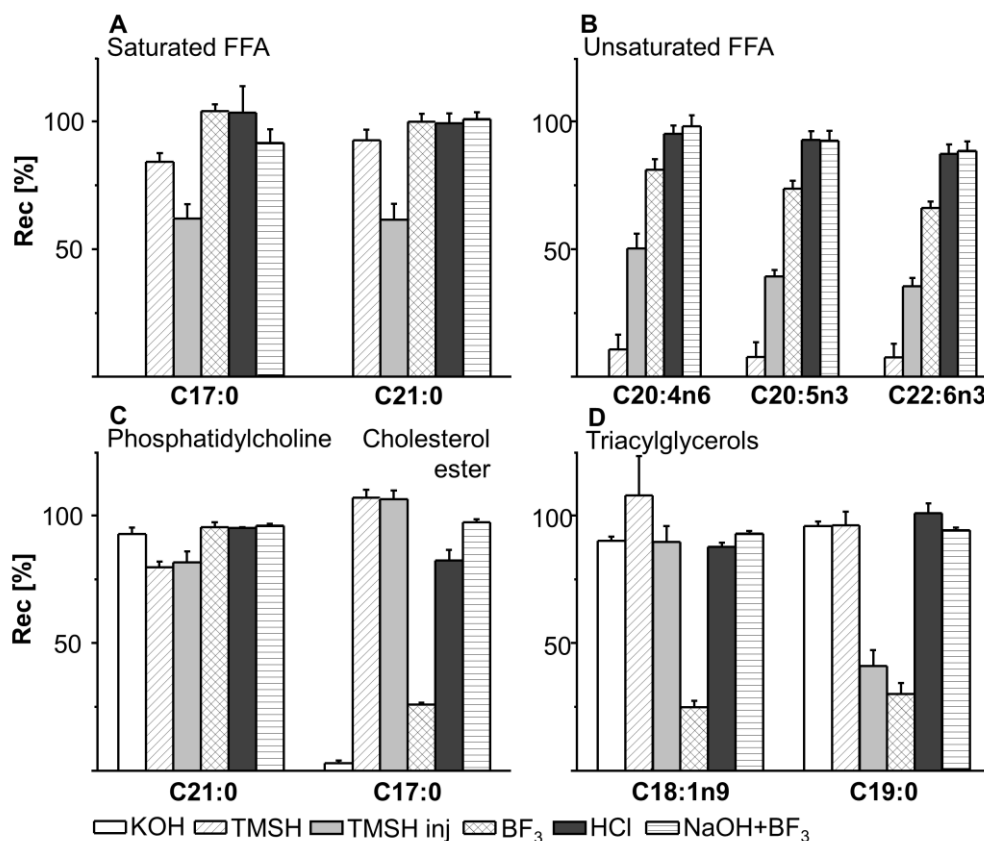


**Fig. 3.1:** Derivatization efficacy of FAME generation by the different methods: **A:** saturated FFAs C17:0 and C21:0, **B:** polyunsaturated FFAs C20:4n6, C20:5n3 and C22:6n3, **C:** PC C21:0 and CE C17:0 and **D:** TGs C18:1n9 and C19:0. For each lipid the recovery rate of a derivatized standard (200  $\mu$ M) is shown as mean  $\pm$  SD (n=5).

### 3.3.2 Derivatization of lipid extracts from plasma

The sums of quantified saturated FAs (SFA), monounsaturated FAs (MUFA), n3- and n6- PUFAs as well as the sum of all quantified FAs in human plasma extracted with MTBE/MeOH utilizing the six different derivatization protocols are summarized in Table 3.1. The plasma concentrations of the biologically relevant PUFA ALA, ARA, EPA and DHA are highlighted in Fig. 3.2A.

The concentrations of ALA, ARA, EPA and DHA were overall in the same range with all six protocols. However, the concentrations of these PUFA obtained with

KOH and  $\text{BF}_3$  derivatizations were significantly lower compared to HCl ( $p < 0.001$ , Fig. 3.2A). The sums of the concentrations of all detected SFA, MUFA and total n6- and n3-PUFA showed a similar trend (Table 3.1). As a consequence, the sum of the concentrations of all fatty acids was dramatically lower for the KOH and  $\text{BF}_3$  protocol (Table 3.1). For all other derivatization methods, the sums of SFA, MUFA, PUFA and total FA concentrations were comparable.

**Table 3.1:** Determined plasma PUFA levels utilizing different derivatization methods. Shown is the sum of the concentration and the relative amount of SFA, MUFA, n6-PUFA and n3-PUFA quantified in the same pooled human plasma (50  $\mu\text{L}$ ). All results are shown as mean  $\pm$  SD ( $n=5$ ).

Plasma [ $\mu\text{g/mL}$ ]	KOH	TMSH	TMSH direct injection	$\text{BF}_3$	HCl	$\text{NaOH}+\text{BF}_3$
SFA	810 $\pm$ 21	1200 $\pm$ 72	1200 $\pm$ 36	750 $\pm$ 15	1200 $\pm$ 16	1100 $\pm$ 39
MUFA	480 $\pm$ 13	910 $\pm$ 64	760 $\pm$ 57	390 $\pm$ 8.4	860 $\pm$ 14	870 $\pm$ 55
n6-PUFA	500 $\pm$ 12	1100 $\pm$ 100	820 $\pm$ 120	490 $\pm$ 8.1	1000 $\pm$ 24	1100 $\pm$ 120
n3-PUFA	190 $\pm$ 3.3	230 $\pm$ 38	240 $\pm$ 18	180 $\pm$ 5.5	300 $\pm$ 14	300 $\pm$ 15
total FA	2000 $\pm$ 49	3400 $\pm$ 270	3000 $\pm$ 230	1800 $\pm$ 37	3300 $\pm$ 69	3400 $\pm$ 230
<b>Relative distribution [%]</b>						
SFA	41 $\pm$ 1.0	35 $\pm$ 2.1	40 $\pm$ 1.2	42 $\pm$ 0.83	35 $\pm$ 0.49	33 $\pm$ 1.2
MUFA	24 $\pm$ 0.66	26 $\pm$ 1.9	25 $\pm$ 1.9	21 $\pm$ 0.47	26 $\pm$ 0.42	26 $\pm$ 1.6
n6-PUFA	25 $\pm$ 0.60	32 $\pm$ 2.9	27 $\pm$ 3.9	27 $\pm$ 0.45	30 $\pm$ 0.74	32 $\pm$ 3.5
n3-PUFA	9.5 $\pm$ 0.17	6.8 $\pm$ 1.1	8.1 $\pm$ 0.59	9.9 $\pm$ 0.31	9.0 $\pm$ 0.42	8.9 $\pm$ 0.46

The obtained variation of repeated measurements, calculated as standard deviation (SD) of five independent replicates differed considerably between the protocols. The lowest SD and thus the best precision for the sum of all FAs was found for HCl and  $\text{BF}_3$  with relative SDs of  $\leq 2\%$  compared to up to 8% for TMSH.

The six different protocols led to distinct differences in the relative pattern of SFA, MUFA and PUFA (Table 3.1). For n6-PUFA, for example, the relative amount of the different FA classes ranged from 25% (KOH) to 32% (TMSH and

NaOH+BF<sub>3</sub>) and for SFA between 33% (NaOH+BF<sub>3</sub>) and 42% (BF<sub>3</sub>). Regarding the relative content of EPA+DHA of all FA in plasma (a modification of the n3-index [31], Fig. 3.2B), the lowest value was calculated based on the data obtained by TMSH derivatization (5.3%), and the highest value resulted from the BF<sub>3</sub> method (8.3%). Derivatization with HCl, KOH and NaOH+BF<sub>3</sub> led to a consistent index of 7.4±0.2%. No statistical differences were observed between the three protocols (Fig. 3.2B). However, with 5.3% and 6.5%, both TMSH protocols led for the same samples to significantly lower, and BF<sub>3</sub> with 8.3% to significantly higher %EPA+DHA level compared to HCl.

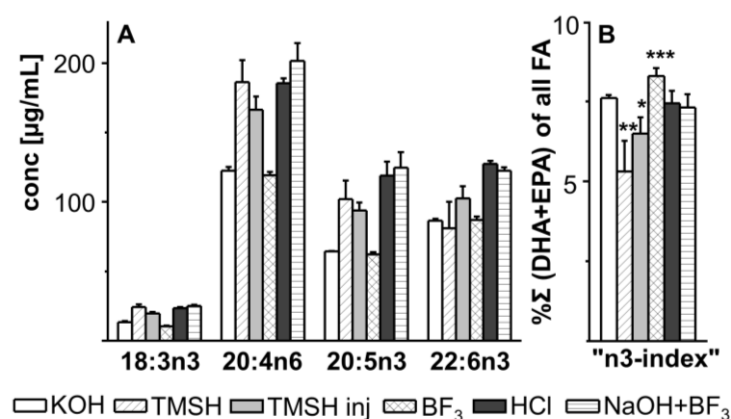


**Fig. 3.2:** Plasma PUFA levels determined with different derivatization methods. **A:** concentration of ALA (C18:3n3), ARA (C20:4n6), EPA (C20:5n3) and DHA (C22:6n3), **B:** Relative DHA+EPA content of all detected FA. For all samples the same pooled human plasma was extracted with MTBE/MeOH and analyzed. Significant differences were determined in comparison to the HCl method by independent sample t-test. \* p<0.05, \*\* p<0.005, \*\*\* p<0.001. All results are shown as mean ± SD (n=5).



### 3.3.3 Efficacies of the Bligh and Dyer versus the MTBE/MeOH extraction

The lipid extraction efficacy for plasma and liver tissue was compared for Bligh and Dyer and the MTBE/MeOH protocol (Tables 3.2 and 3.3). Derivatization of the resulting lipid extracts was carried out with the HCl and the combined NaOH+BF<sub>3</sub> method.

As summarized in Tables 3.2 and 3.3 both, the determined FA concentrations as well as the relative FA patterns and SDs were comparable for both protocols and derivatization techniques.

**Table 3.2:** Comparison of the lipid extraction efficacy of the protocol according to Bligh and Dyer and MTBE/MeOH using NaOH+BF<sub>3</sub> or HCl derivatization. Shown are the sums of the concentrations of SFA, MUFA, n6-PUFA and n3-PUFA quantified in the same pooled human plasma (50 µL). The relative DHA+EPA content of all detected FA is presented in the bottom panel of the table. All results are shown as mean ± SD (n=5).

Derivatization Plasma [µg/mL]	Bligh & Dyer	MTBE	Bligh & Dyer	MTBE
	NaOH + BF <sub>3</sub>		HCl	
SFA	1200 ± 80	1100 ± 39	1100 ± 33	1200 ± 16
MUFA	900 ± 65	870 ± 55	820 ± 27	860 ± 14
n6-PUFA	1100 ± 94	1100 ± 120	960 ± 37	1000 ± 24
n3-PUFA	290 ± 33	300 ± 15	280 ± 10	300 ± 14
total FA	3500 ± 270	3400 ± 230	3100 ± 110	3300 ± 69
%(EPA+DHA) of all FA	6.9 ± 0.81	7.3 ± 0.40	7.3 ± 0.28	7.4 ± 0.38

### 3.3.4 Saponification of tissue samples prior extraction

In addition to homogenization and extraction of liver, the tissue was heated under harsh alkaline conditions. This led to an almost complete dissolving of the tissue improving the handling of the following extraction. Lipid extraction was conducted by the methods of Bligh and Dyer and MTBE/MeOH, and HCl as well as NaOH+BF<sub>3</sub> were used for derivatization (Table 3.3).

Compared to the direct extraction, the sample saponification caused neither a difference in the absolute concentrations of the FAs, nor in the relative pattern of SFA, MUFA and PUFA. However, for both extraction protocols, there was a slight trend towards a higher extraction efficacy for the hydrolyzed samples

**Table 3.3:** Comparison of the extraction efficacy of the protocol according to Bligh and Dyer and MTBE/MeOH with either NaOH+BF<sub>3</sub> or HCl derivatization with or without alkaline hydrolysis prior extraction of liver samples. Shown are the sums of the concentrations of SFA, MUFA, n6-PUFA and n3-PUFA quantified in rat liver (35-45 mg) of the same animal. The relative DHA+EPA content of all detected FA is presented in the bottom panel of the table. All results are shown as mean  $\pm$  SD (n=5).

<b>Direct extraction of the sample</b>				
Derivatization Liver [ $\mu$ g/mg]	Bligh & Dyer	MTBE	Bligh & Dyer	MTBE
	NaOH + BF <sub>3</sub>		HCl	
SFA	16 $\pm$ 1.9	18 $\pm$ 2.1	15 $\pm$ 0.99	16 $\pm$ 1.6
MUFA	5 $\pm$ 0.96	6 $\pm$ 0.77	4.8 $\pm$ 0.46	5.2 $\pm$ 0.74
n6-PUFA	12 $\pm$ 0.42	12 $\pm$ 1.5	12 $\pm$ 0.48	12 $\pm$ 1.3
n3-PUFA	1.9 $\pm$ 0.36	2.1 $\pm$ 0.27	2 $\pm$ 0.25	5.9 $\pm$ 0.24
total FA	34 $\pm$ 3.6	38 $\pm$ 4.6	34 $\pm$ 2.2	35 $\pm$ 3.9
%EPA+DHA of all FA	4.3 $\pm$ 0.91	4.3 $\pm$ 0.56	4.5 $\pm$ 0.61	4.7 $\pm$ 0.42

<b>Alkaline hydrolysis prior extraction</b>				
Derivatization Liver [ $\mu$ g/mg]	Bligh & Dyer	MTBE	Bligh & Dyer	MTBE
	NaOH + BF <sub>3</sub>		HCl	
SFA	16 $\pm$ 0.87	16 $\pm$ 1.3	17 $\pm$ 1.2	17 $\pm$ 0.88
MUFA	5.6 $\pm$ 0.86	5.8 $\pm$ 1.4	5.5 $\pm$ 0.49	5.9 $\pm$ 0.37
n6-PUFA	13 $\pm$ 1.9	14 $\pm$ 2.9	13 $\pm$ 0.65	14 $\pm$ 0.58
n3-PUFA	2.3 $\pm$ 0.36	2.3 $\pm$ 0.5	2.3 $\pm$ 0.17	2.4 $\pm$ 0.17
total FA	37 $\pm$ 4	38 $\pm$ 6	38 $\pm$ 2.5	39 $\pm$ 2
%EPA+DHA of all FA	4.8 $\pm$ 0.81	4.7 $\pm$ 0.98	4.5 $\pm$ 0.27	4.7 $\pm$ 0.29

### 3.4 Discussion

FA quantification as FAMES by means of GC-FID is a well-established technique. Numerous studies describe the sample preparation procedure particularly derivatization to FAME [2, 3, 14, 15, 18, 20, 22, 24, 25, 27, 28]. However, for small biological samples a variety of different methods are used, making it difficult to deduce the most suitable. Therefore, we compared the most established derivatization methods to elucidate which is the most appropriate technique to analyze the PUFA pattern in plasma and tissue samples.

When analyzing standards of FFA, PC, CE and TG, our results show that only the derivatization protocols utilizing HCl and NaOH+BF<sub>3</sub> yielded FAME with satisfying efficacy (>80%). The other four protocols using BF<sub>3</sub>, KOH and TMSH failed to derivatize at least one of the lipids (Fig. 3.1), which are all present in plasma [32]. As described previously, KOH treatment does not esterify FFA to FAME [33]. Low efficacies were also observed for the derivatization of unsaturated FFA using TMSH (≤50%) with direct injection (pyrolysis of the salt formed from the FA and TMSH in the injector [34]) or derivatization at room temperature followed by evaporation. Similar observations have been made for TMSH derivatization before, e.g. Firl et al. reported lower recovery rates for PUFA in comparison to MUFA and SFA [19]. Interestingly, CE derivatization has been described to be problematic using TMSH because of long reaction times required [34]. However, our results indicate efficient transesterification. The BF<sub>3</sub> protocol is often used in literature for the derivatization of lipid extracts from biological samples [5, 7, 10-13, 31] or direct conversion of crude samples [28]. In our analysis, derivatization with 7% BF<sub>3</sub> in hexane/MeOH inefficiently transesterified CE and TG, two of the major lipid fractions in plasma [32]. However, it should be noted that the transesterification efficacy depends on the solvent composition [35]. Thus, a lower hexane/MeOH ratio could lead to a better conversion of CE and TG. When comparing different BF<sub>3</sub> protocols, it also should be noted that several described “BF<sub>3</sub> protocols” are two steps

procedures of an alkaline treatment followed by  $\text{BF}_3$  methylation [36], similar to the highly efficient protocol using  $\text{NaOH}+\text{BF}_3$  described here. Nevertheless, several authors report potential artifact formation by derivatization of PUFA with  $\text{BF}_3$ , hence giving reasons to prefer other derivatization procedures [37].

Despite the varying derivatization of the standards (Fig. 3.1), it is interesting that all derivatization protocols led to an overall similar relative pattern of SFA, MUFA and PUFA in plasma (Fig. 3.2B, Table 3.1). Particularly the determined relative amount of EPA and DHA in plasma, (a modification of the n3-index [31]) was fairly consistent between the methods (Fig. 3.2B). Hence, our results indicate that all protocols are suitable to detect changes in the relative FA pattern, as carried out in numerous studies [4-13, 19, 21, 23, 31]. However, due to the low derivatization efficacy for PUFA, TMSH led to an underestimation of the absolute and relative levels of n3-PUFA and thus to a significantly lower %EPA+DHA (Fig. 3.2B). Similarly, too low levels for SFA and MUFA in plasma are obtained for  $\text{BF}_3$  in hexane/MeOH (1:1), most likely caused by the low derivatization efficacy of CE and TG. In combination with the high transesterification rate of phospholipids by this  $\text{BF}_3$  protocol, the lipid fraction that contains most of all n3-PUFA in plasma [32], a significantly higher sum of %EPA and %DHA results (Fig. 3.2B).

These results demonstrate that great care should be taken when comparing relative FA pattern reported in different studies. Therefore, a comparison only seems possible between analyses using the HCl, KOH, and  $\text{NaOH}+\text{BF}_3$  derivatization protocols.

Regarding the absolute concentration of FA determined in plasma, much more pronounced differences were obtained between the protocols (Fig. 3.2A, Table 3.1). Following KOH and  $\text{BF}_3$  derivatization, the sum of all FA concentrations were with 2000 and 1800  $\mu\text{g}/\text{mL}$  almost 50% lower than for the TMSH, HCl and  $\text{NaOH}+\text{BF}_3$  protocols which led to concentrations of 3000-3400  $\mu\text{g}/\text{mL}$  (Table 3.1). This poor yield seems to be even problematic for the analysis of the relative FA pattern, e.g. by sacrificing detection sensitivity of low abundant FA.

Our results compelled us to conclude that among the procedures tested only HCl and NaOH+BF<sub>3</sub> are suitable protocols for the analysis of an overall FA pattern in plasma without discriminating individual classes of lipids. However, KOH derivatization leads to a consistent FA pattern in plasma, probably because of the low FFA content [32]. Thus, each derivatization method tested here might be suitable for specific samples. For example, BF<sub>3</sub> and KOH protocols might be applicable for the analysis of the relative FA pattern in samples rich in polar lipids, e.g. the composition of erythrocyte membranes.

Aside from the derivatization procedure, extraction of the lipids is the crucial sample preparation step for the analysis of biological samples. Utilizing a slightly modified extraction protocol as described by Matyash [27] about six years ago, a comparable extraction efficacy for plasma and tissues was found for the MTBE/MeOH extraction compared to the method of Bligh and Dyer [24] (Table 3.2 and Table 3.3). Based on the application of two derivatization protocols and the analysis of plasma and liver tissue, our results clearly demonstrate that both, the absolute concentration of FA as well as the relative FA pattern, are comparable between the two extraction protocols. Interestingly, the MTBE/MeOH extraction led to slightly higher concentrations of degradation-prone PUFA (Table 3.2 and Table 3.3). Thus, the extraction conditions seem to be milder in comparison to the traditional method. It should be noted that the results cannot be applied for the analysis of high fat tissues (>2% fat in the homogenate) where extraction to Folch yields better results than extraction according to Bligh and Dyer [26]. However, the good comparability of MTBE/MeOH with Bligh and Dyer encourages to further investigate if, for the analysis of high fat tissues, also Folch extraction could be replaced by this halogenated solvent-free procedure.

Regardless the method, extraction of tissues is a challenging task requiring labor-intensive and error-prone homogenization techniques. To improve extraction efficacy, we added a saponification step prior to sample preparation. The tissue almost dissolves in the applied sodium hydroxide solution within 30

min at 60 °C and the neutralized samples can be extracted as plasma or other liquid samples. As summarized in Table 3.3, the extraction efficacy for liver tissue was comparable for samples prepared with or without hydrolysis prior to extraction. Actually, the extraction is slightly, however not significantly, improved with saponification of the sample. Thus, it is concluded that saponification of tissue samples does not negatively influence fatty acid analysis. Therefore, this sample preparation strategy is a promising tool particularly for the FAME analysis of tough tissues, such as gut or other organs rich in connection tissue.

Overall, we suggest MTBE/MeOH extraction followed by HCl derivatization as sample preparation technique for FAME analysis in small amounts of biological samples, such as plasma and tissues. For the analysis of tissues, base hydrolysis prior extraction can be included in the sample preparation making homogenization easier and more reliable without negatively affecting the results. It should be noted that the combined protocol with NaOH+BF<sub>3</sub> is equally suitable, however, requires more working steps and has the risk of artifact formation [37]. The traditional extraction according to Bligh and Dyer also yields excellent results. Nonetheless, our data indicate no scientific need in continuing to use (environmentally) toxic chloroform for extraction.

Most importantly, our studies demonstrate that both the absolute concentrations, but also in part the relative FA pattern, significantly differ between derivatization methods. Therefore, we urge all authors of future articles using FAME analysis to provide details about their methods. Otherwise, a comparison of different studies might not be possible and potentially valuable information about PUFA biology might be lost.

### 3.5 References

1. Seppänen-Laakso T, Laakso I, Hiltunen R. Analysis of fatty acids by gas chromatography, and its relevance to research on health and nutrition. *Anal Chim Acta*. 2002;465(1-2):39-62.
2. Adam O, Beringer C, Kless T, Lemmen C, Adam A, Wiseman M, Adam P, Klimmek R, Forth W. Anti-inflammatory effects of a low arachidonic acid diet and fish oil in patients with rheumatoid arthritis. *Rheumatol Int*. 2003;23(1):27-36.
3. Adam O, Tesche A, Wolfram G. Impact of linoleic acid intake on arachidonic acid formation and eicosanoid biosynthesis in humans. *Prostag Leukotr Ess*. 2008;79(3-5):177-181.
4. Kratz M, Cullen P, Kannenberg F, Kassner A, Fobker M, Abuja PM, Assmann G, Wahrburg U. Effects of dietary fatty acids on the composition and oxidizability of low-density lipoprotein. *Eur J Clin Nutr*. 2002;56(1):72-81.
5. Lands WEM, Libelt B, Morris A, Kramer NC, Prewitt TE, Bowen P, Schmeisser D, Davidson MH, Burns JH. Maintenance of Lower Proportions of (N-6) Eicosanoid Precursors in Phospholipids of Human Plasma in Response to Added Dietary (N-3) Fatty-Acids. *Biochim Biophys Acta*. 1992;1180(2):147-162.
6. Sanders TAB, Younger KM. The Effect of Dietary-Supplements of Omega-3 Poly-Unsaturated Fatty-Acids on the Fatty-Acid Composition of Platelets and Plasma Choline Phosphoglycerides. *Brit J Nutr*. 1981;45(3):613-616.
7. Vognild E, Elvevoll EO, Brox J, Olsen RL, Barstad H, Aursand M, Osterud B. Effects of dietary marine oils and olive oil on fatty acid composition, platelet membrane fluidity, platelet responses, and serum lipids in healthy humans. *Lipids*. 1998;33(4):427-436.
8. Hudert CA, Weylandt KH, Lu Y, Wang J, Hong S, Dignass A, Serhan CN, Kang JX. Transgenic mice rich in endogenous omega-3 fatty acids are protected from colitis. *Proc Natl Acad Sci U S A*. 2006;103(30):11276-11281.
9. Keenan AH, Pedersen TL, Fillaus K, Larson MK, Shearer GC, Newman JW. Basal omega-3 fatty acid status affects fatty acid and oxylipin responses to high-dose n3-HUFA in healthy volunteers. *J Lipid Res*. 2012;53(8):1662-1669.
10. Schuchardt JP, Schmidt S, Kressel G, Dong H, Willenberg I, Hammock BD, Hahn A, Schebb NH. Comparison of free serum oxylipin concentrations in hyper- vs. normolipidemic men. *Prostag Leukotr Ess*. 2013;89(1):19-29.
11. Schuchardt JP, Schmidt S, Kressel G, Willenberg I, Hammock BD, Hahn A, Schebb NH. Modulation of blood oxylipin levels by long-chain omega-3 fatty acid supplementation in hyper- and normolipidemic men. *Prostag Leukotr Ess*. 2014;90(2-3):27-37.
12. Shearer GC, Harris WS, Pedersen TL, Newman JW. Detection of omega-3 oxylipins in human plasma and response to treatment with omega-3 acid ethyl esters. *J Lipid Res*. 2010;51(8):2074-2081.
13. Ma J, Folsom AR, Shahar E, Eckfeldt JH. Plasma fatty acid composition as an indicator of habitual dietary fat intake in middle-aged adults. The Atherosclerosis Risk in Communities (ARIC) Study Investigators. *Am J Clin Nutr*. 1995;62(3):564-571.
14. Morrison WR, Smith LM. Preparation of Fatty Acid Methyl Esters + Dimethylacetals from Lipids with Boron Fluoride-Methanol. *J Lipid Res*. 1964;5(4):600-608.
15. Lepage G, Roy CC. Direct Transesterification of All Classes of Lipids in a One-Step Reaction. *J Lipid Res*. 1986;27(1):114-120.

16. Stoffel W, Chu F, Ahrens EH. Analysis of Long-Chain Fatty Acids by Gas-Liquid Chromatography - Micromethod for Preparation of Methyl Esters. *Anal Chem.* 1959;31(2):307-308.
17. King IB, Lemaitre RN, Kestin M. Effect of a low-fat diet on fatty acid composition in red cells, plasma phospholipids, and cholesterol esters: investigation of a biomarker of total fat intake. *Am J Clin Nutr.* 2006;83(2):227-236.
18. Butte W. Rapid Method for the Determination of Fatty-Acid Profiles from Fats and Oils Using Trimethylsulfonium Hydroxide for Trans-Esterification. *J Chromatogr.* 1983;261(1):142-145.
19. Firl N, Kienberger H, Hauser T, Rychlik M. Determination of the fatty acid profile of neutral lipids, free fatty acids and phospholipids in human plasma. *Clin Chem Lab Med.* 2013;51(4):799-810.
20. Müller KD, Husmann H, Nalik HP, Schomburg G. Transesterification of Fatty-Acids from Microorganisms and Human Blood-Serum by Trimethylsulfonium Hydroxide (Tmsh) for Gc Analysis. *Chromatographia.* 1990;30(5-6):245-248.
21. Astorg P, Bertrais S, Laporte F, Arnault N, Estaquio C, Galan P, Favier A, Hercberg S. Plasma n-6 and n-3 polyunsaturated fatty acids as biomarkers of their dietary intakes: a cross-sectional study within a cohort of middle-aged French men and women. *Eur J Clin Nutr.* 2008;62(10):1155-1161.
22. Metcalfe LD, Schmitz AA, Pelka JR. Rapid Preparation of Fatty Acid Esters from Lipids for Gas Chromatographic Analysis. *Anal Chem.* 1966;38(3):514-515.
23. Weaver KL, Ivester P, Seeds M, Case LD, Arm JP, Chilton FH. Effect of Dietary Fatty Acids on Inflammatory Gene Expression in Healthy Humans. *J Biol Chem.* 2009;284(23):15400-15407.
24. Bligh EG, Dyer WJ. A Rapid Method of Total Lipid Extraction and Purification. *Can J Biochem Physiol.* 1959;37(8):911-917.
25. Folch J, Lees M, Stanley GHS. A Simple Method for the Isolation and Purification of Total Lipides from Animal Tissues. *J Biol Chem.* 1957;226(1):497-509.
26. Iverson SJ, Lang SL, Cooper MH. Comparison of the Bligh and Dyer and Folch methods for total lipid determination in a broad range of marine tissue. *Lipids.* 2001;36(11):1283-1287.
27. Matyash V, Liebisch G, Kurzchalia TV, Shevchenko A, Schwudke D. Lipid extraction by methyl-tert-butyl ether for high-throughput lipidomics. *J Lipid Res.* 2008;49(5):1137-1146.
28. Kang JX, Wang J. A simplified method for analysis of polyunsaturated fatty acids. *BMC Biochem.* 2005;6:5.
29. Ackman RG, Sipos JC. Application of Specific Response Factors in Gas Chromatographic Analysis of Methyl Esters of Fatty Acids with Flame Ionization Detectors. *J Am Oil Chem Soc.* 1964;41(5):377-378.
30. Craske JD, Bannon CD. Letter to the Editor. *J Am Oil Chem Soc.* 1988;65(7):1190-1191.
31. Harris WS, Von Schacky C. The Omega-3 Index: a new risk factor for death from coronary heart disease? *Prev Med.* 2004;39(1):212-220.
32. Hodson L, Skeaff CM, Fielding BA. Fatty acid composition of adipose tissue and blood in humans and its use as a biomarker of dietary intake. *Prog Lipid Res.* 2008;47(5):348-380.
33. Schreiner M. Principles for the Analysis of Omega-3 Fatty Acids. In: Teale MC, editor. *Omega 3 Fatty Acid Research.* New York: Nova Science Publishers; 2006. p. 1-25.



34. El-Hamdy AH, Christie WW. Preparation of Methyl-Esters of Fatty-Acids with Trimethylsulfonium Hydroxide - an Appraisal. *J Chromatogr.* 1993;630(1-2):438-441.
35. Carrapiso AI, Garcia C. Development in lipid analysis: Some new extraction techniques and in situ transesterification. *Lipids.* 2000;35(11):1167-1177.
36. Ackman RG. Remarks on official methods employing boron trifluoride in the preparation of methyl esters of the fatty acids of fish oils. *J Am Oil Chem Soc.* 1998;75(4):541-545.
37. Christie WW. In: Christie WW, editor. *Advances in Lipid Methodology - Two.* Dundee: The Oily Press; 1993. p. 69-111.



# Chapter 4

## Comparison of Sample Preparation Methods for the Quantitative Analysis of Eicosanoids and other Oxylipins in Plasma by Means of LC-MS/MS

*Oxylipins are potent lipid mediators. For the evaluation of their biological roles, several LC-MS based methods have been developed. While these methods are similar, the described sample preparation procedures for the extraction of oxylipins differ considerably. In order to deduce the most appropriate method for the analysis of non-esterified oxylipins in human plasma, we evaluated the performance of seven established sample preparation procedures. Six commonly used solid phase extraction (SPE) and one liquid-liquid extraction (LLE) protocol were compared based on the recovery of 13 added internal standards, extraction efficacy of oxylipins from plasma and reduction of ion-suppressing matrix. Dramatic differences in the performance in all three parameters were found. LLE with ethyl acetate was overall not a sufficient sample preparation strategy. The protocols using Oasis- and StrataX-material insufficiently removed interfering matrix compounds. Removal of matrix was nearly perfect on anion-exchanging BondElut cartridges and recovery of internal standards was good. However, extraction of unpolar epoxy fatty acids seemed to be better on a C18-material with removal of matrix by water and n-hexane prior elution with methyl formate.*

Adapted from *Analytical and Bioanalytical Chemistry*, Comparison of sample preparation methods for the quantitative analysis of eicosanoids and other oxylipins in plasma by means of LC-MS/MS, vol. 407(5), 2015, pp. 1403-1414, Ostermann AI, Willenberg I and Schebb NH. With permission of Springer.

Author contributions: AIO: Designed research, performed experiments and wrote the manuscript; IW: Contributed to research design and manuscript writing; NHS: Designed research and wrote the manuscript.

## 4.1 Introduction

Oxidative metabolites of polyunsaturated fatty acids (PUFA) are an important class of lipid mediators. The conversion of arachidonic acid (C20:4n6, ARA) by cyclooxygenases (COXs) and lipoxygenases (LOXs) leads to highly potent eicosanoids controlling a multitude of biological functions [1]. A large number of eicosanoids and oxidation products of other PUFA, particularly docosahexaenoic acid (C22:6n3, DHA) and eicosapentaenoic acid (C20:5n3, EPA), generally referred to as oxylipins, have been described in recent years [2, 3]. Their routes of formation are diverse, catalyzed by LOX, COX, Cytochrome P450 and soluble epoxide hydrolase among further enzymes and non-enzymatic (aut)oxidation [1, 3]. For many of the formed oxylipins, the biological role has not been fully understood, however, several are implicated to regulate physiological processes such as blood pressure, inflammation and pain, but also cellular functions, e.g. proliferation [1]. Quantitative analysis in biological samples is the key to a mechanistic understanding of the biological roles of oxylipins. Monitoring changes in a comprehensive pattern of oxylipins in different (patho)physiological conditions and in response to pharmacological treatment is one of the most promising strategies in the investigation of oxylipins. This led in the past, e.g. to the understanding of the remarkably different actions of n3- and n6-epoxides in angiogenesis and cancer growth [4, 5] as well as their antiarrhythmic effects [6] or the discovery of inflammation resolving hydroxy- [7] and multiple hydroxylated n3-PUFA, such as resolvins [2]. Several liquid chromatography (LC) mass spectrometry (MS) methods have been described allowing parallel quantification of a large number (~100) of oxylipins in biological matrices [8-11]. These approaches make targeted metabolomics analysis of the arachidonic acid cascade feasible because a comprehensive set of products is covered.

On the level of instrumental analysis, almost all current methods address the challenges of quantitative oxylipin analysis such as (i) very low concentrations (ii) huge concentration range of the different oxylipins in one sample (up to 104

fold) [12] and (iii) large number of structurally similar analytes with several (regio)isomers with a similar approach: Separation is carried out by modern reversed phase chromatography with sub-2- $\mu\text{m}$  particles. Electrospray ionization (ESI) is used in negative ion mode and the analytes are detected in selected reaction monitoring (SRM) mode on a highly sensitive triple quadrupole (QqQ) MS [8-11, 13]. In fact, even the same transitions are used for quantification, e.g., beta fragmentation of hydroxy-FA by collision-induced dissociation (CID) [11, 13]. Overall, the differences in the well-optimized methods are minor and mainly depend on analyte-coverage and sensitivity, most likely limited by standard availability and instrumental performance, respectively.

Regarding sample preparation the methods vary considerably. Mixing of the sample with organic solvents and direct injection is only possible for specific questions because of the low oxylipin concentrations in biological samples [14]. Thus, sample preparation techniques are required allowing efficient extraction from the matrix and pre-concentration prior instrumental analysis. For this purpose, both liquid-liquid extraction (LLE) with ethyl acetate (EA) [15] and different solid-phase extraction (SPE) protocols [6, 8, 10, 11, 13, 16, 17] have been described. For SPE, classical RP material [11, 16] as well as modern polymeric stationary phases with embedded polar groups such as Oasis HLB (Waters, Eschborn, Germany) [8, 10, 17] or StrataX (Phenomenex, Torrance, CA, USA) [9] are employed. Moreover, materials with anion exchange properties are used [6, 13] to extract the slightly acidic oxylipins from biological samples. Taking the different solvents used in the washing and eluting steps of the SPE into account, the described protocols are even more diverse.

Isotope-labeled internal standards (IS) are only available for few oxylipins because of the large diversity of analytes. As a consequence a single heavy atom labeled IS is used for a whole group of oxylipins, e.g.  $^2\text{H}_4\text{-PGE}_2$  for all prostaglandins (PGs) and 5-hydroxy eicosatetraenoic acid (HETE) for all hydroxy-FA [10]. Even though structurally similar IS are used, their retention

times differ. As a consequence, the IS cannot correct for all interferences caused by influence of matrix compounds on the ionization process. Ion suppression is in fact the Achilles heel for quantification using ESI-MS, since the signal is strongly affected by coeluting matrix compounds [18]. Thus, efficient removal of the matrix by sample preparation is the key for a successful quantification of oxylipins in complex biological samples.

However, neither the extraction efficacy of oxylipins from biological samples by the different sample preparation strategies nor their ability to remove ion-suppressing matrix compounds has been investigated so far. In the present study, we therefore compared the performance of seven commonly used sample preparation techniques for the analysis of free (i.e. non-esterified) oxylipins in human plasma. The methods were thoroughly evaluated according to three criteria: (i) IS recovery (ii) ion suppression and (iii) extraction efficacy. The most efficient sample preparation protocols are identified and could be used as a basis for further optimization procedures.

## 4.2 Experimental

### 4.2.1 Chemicals and biological materials

LC-MS grade acetonitrile (ACN), acetic acid (HAc) and methanol (MeOH) were from Fisher Scientific (Nidderau, Germany). Oxylipin standards and internal standards (Table 4.1) were purchased from Cayman Chemicals (local distributor: Biomol, Hamburg, Germany). Further standards such as epoxy octadecadienoic acids (EpODEs) and dihydroxy octadecadienoic acids (DiHODEs) were a kind gift from the laboratory of Bruce Hammock, UC Davis, CA, USA. 1-(1-(Ethyl-sulfonyl)piperidin-4-yl)-3-(4-(trifluoromethoxy)phenyl)urea synthesized as described [19] was used as internal standard 2 (IS 2). Sodium acetate was obtained from Merck (Darmstadt, Germany). *n*-Hexane (HPLC Grade) was purchased from Carl Roth (Karlsruhe, Germany) and formic acid

(Acros Organics) was obtained from Fisher Scientific (Nidderau, Germany). All other chemicals were from Sigma Aldrich (Schnelldorf, Germany). Pooled human plasma was generated by mixing ethylenediaminetetraacetic acid (EDTA) plasma obtained from healthy male volunteers. The pooled plasma was centrifuged (10 min, 4 °C, 10 000 xg) and stored at -80 °C in 1-2-mL aliquots.

#### 4.2.2 Oxylipin extraction

For each analysis, a freshly thawed 500 µL aliquot of the same human plasma pool was used. In the first step, 10 µL of IS solution in MeOH (100 nM of  $^2\text{H}_4$ -6-keto-PGF<sub>1 $\alpha$</sub> ,  $^2\text{H}_4$ -PGE<sub>2</sub>,  $^2\text{H}_4$ -PGD<sub>2</sub>,  $^2\text{H}_4$ -TxB<sub>2</sub>,  $^2\text{H}_4$ -LTB<sub>4</sub>,  $^2\text{H}_4$ -9-hydroxy octadecadienoic acid (HODE),  $^2\text{H}_8$ -5-HETE,  $^2\text{H}_8$ -12-HETE,  $^2\text{H}_6$ -20-HETE,  $^2\text{H}_{11}$ -14,15-dihydroxy eicosatrienoic acid (DiHETrE),  $^2\text{H}_{11}$ -14(15)-epoxy eicosatetraenoic acid (EpETrE),  $^2\text{H}_4$ -9(10)-epoxy octadecenoic acid (EpOME) and  $^2\text{H}_4$ -9(10)-dihydroxy octadecenoic acid (DiHOME) and 10 µL of antioxidant solution (0.2 mg/mL EDTA, butylated hydroxytoluene and triphenylphosphine in MeOH/water (50/50, v/v)) were added to the plasma. Extraction was carried out according to 6 different established SPE protocols (a detailed description of all procedures can be found in the appendix (App. Table 9.1.1)) and one LLE protocol:

For *LLE* [15], 500 µL of 1 M sodium acetate (pH 6.0) was added to 500 µL plasma. The sample was extracted twice with 750 µL EA. In each step, the sample was vortexed for 3 min and centrifuged for 5 min at 4 °C at 20 000 xg.

For *Oasis-EA* SPE [10] the plasma sample was mixed with 500 µL MeOH/water (5/95, v/v) acidified with 0.1% HAc. After centrifugation (10 min, 4 °C, 20 000 xg) the supernatant was loaded to a preconditioned Oasis HLB SPE-column (3 mL, 60 mg, 30 µm particles; Waters, Eschborn, Germany). The column was washed with 6 mL MeOH/water (5/95, v/v) acidified with 0.1% HAc and the cartridge was dried by low vacuum (~200 mbar) for 20 min. Oxylipins were eluted by gravity with 0.5 mL MeOH and 1.5 mL EA.

For the *Oasis-MeOH* SPE [17] the plasma sample was mixed with 500  $\mu\text{L}$  MeOH/water (40/60, v/v) acidified with 0.1% formic acid. The sample was centrifuged (10 min, 4  $^{\circ}\text{C}$ , 20 000 xg) and loaded to a preconditioned Oasis HLB SPE-column (3 mL, 60 mg, 30  $\mu\text{m}$  particles; Waters). The cartridges were washed with 3 mL of MeOH/water (20/80, v/v), acidified with 0.1% formic acid, dried with low vacuum ( $\sim$ 200 mbar, 20 min) and eluted by gravity with 2 mL of MeOH.

For the extraction on the anion exchange column BondElut Certify II [6, 13] the plasma was mixed with 500  $\mu\text{L}$  of 1 M sodium acetate buffer (pH 6.0) /MeOH (95/5, v/v). The sample was centrifuged (10 min, 4  $^{\circ}\text{C}$ , 20 000 xg) and the supernatant was loaded onto a preconditioned BondElut Certify II column (3 mL, 200 mg, 40  $\mu\text{m}$  particles; Agilent). The cartridges were washed with 3 mL of MeOH/water (50/50, v/v) and dried by low vacuum ( $\sim$ 200 mbar) for 20 min. Analytes were eluted with 2 mL of 75/25 (v/v) *n*-hexane/EA with 1% HAc (*AnionEx-Strong*) [6], or with 2 mL 25/75 (v/v) *n*-hexane/EA with 1% HAc (*AnionEx-Weak*) [13].

For *StrataX* SPE [9], 500  $\mu\text{L}$  plasma was mixed with 500  $\mu\text{L}$  MeOH/water (20/80, v/v) centrifuged (10 min, 4  $^{\circ}\text{C}$ , 20 000 xg) and loaded onto the preconditioned cartridge (3 mL, 100 mg, 33  $\mu\text{m}$ ; Phenomenex, Aschaffenburg, Germany). The columns were washed with 3.5 mL of 10% MeOH, dried ( $\sim$ 200 mbar, 20 min) and eluted by gravity with 1.0 mL of MeOH.

For the *SepPak* tC18 SPE [11,16] 500  $\mu\text{L}$  plasma were mixed with 1500  $\mu\text{L}$  MeOH/water (20/80, v/v), centrifuged (10 min, 4  $^{\circ}\text{C}$ , 20 000 xg) and acidified with 80  $\mu\text{L}$  pure HAc to a pH of 3.0 directly before loading onto the preconditioned SPE column (6 mL, 500 mg, 37-55  $\mu\text{m}$  particle, Waters). Samples were washed with 10 mL of water and 6 mL of *n*-hexane, dried and eluted by gravity with 8 mL of methyl formate.

All organic phases from the protocols were collected in sample tubes containing 6  $\mu\text{L}$  of 30% glycerol in MeOH. The extracts were centrifuged (10 min, 4  $^{\circ}\text{C}$ ,



20 000 xg) and evaporated in a vacuum centrifuge (1 mbar, 30 °C, 90-120 min; Christ, Osterode, Germany) until only the 2 µL glycerol plug was left. The dried residues were immediately frozen at -80 °C. Within 48 h the residues were reconstituted in 50 µL of MeOH containing 40 nM of IS2, centrifuged (10 min, 4 °C, 20 000 xg) and analyzed by LC-MS.

In a further set of samples, the IS was added after the LLE/SPE to the extracts to distinguish between a loss of IS during the extraction and a suppressed ESI signal. Samples for ion suppression analysis were prepared without addition of IS.

In order to investigate the effect of the cartridge size, the SepPak was carried out with a 3 mL (200 mg) cartridge and the AnionEx-Weak was additionally carried out on 6 mL cartridges (500 mg). The volumes for cleaning, equilibration, washing and elution were adjusted to the cartridge size. In brief, 3 mL SepPak cartridges were washed with 5 mL of water and 3 mL of *n*-hexane and eluted with 4 mL of methyl formate. Samples loaded on the 6 mL AnionEx columns were washed with one column volume of MeOH/water (50/50, v/v) and eluted with 5 mL of 25/75 (v/v) *n*-hexane/EA with 1% HAc.

#### **4.2.3 LC-MS analysis**

Quantification of oxylipins was carried out by LC-MS according to the method of Yang et al. [10, 20] adapted to the instrument in our laboratory as described in detail in the appendix (App. Meth. 9.1.1, Table 9.1.2).

In brief, separation was carried out utilizing an Agilent 1290 LC on an Agilent Zorbax Eclipse Plus C-18 reversed phase column (2.1 x 150 mm, particle size 1.8 µm) with a gradient of 0.1% aqueous HAc as solvent A and ACN/MeOH/HAc (800/150/1, v/v/v) as solvent B. Samples (5 µL) were injected by an xt-PAL autosampler (CTC Analytics, Zwingen, Switzerland). The outlet of the analytical column was connected to a Valco six-port two-position valve implemented in the MS allowing a reduced contamination of the MS source by

directing the void volume to waste. Mass spectrometric detection was carried out on an AB Sciex 6500 QTRAP instrument (AB Sciex, Darmstadt, Germany) in scheduled SRM mode following negative ion electrospray ionization. Instrument controlling was performed with Analyst 1.6.2. and data analysis was carried out with Multiquant 2.1.1. (AB Sciex).

Recovery of IS ( $^2\text{H}_4$ -6-keto-PGF $_{1\alpha}$ ,  $^2\text{H}_4$ -PGE $_2$ ,  $^2\text{H}_4$ -PGD $_2$ ,  $^2\text{H}_4$ -TxB $_2$ ,  $^2\text{H}_4$ -LTB $_4$ ,  $^2\text{H}_4$ -9-HODE,  $^2\text{H}_8$ -5-HETE,  $^2\text{H}_8$ -12-HETE,  $^2\text{H}_6$ -20-HETE,  $^2\text{H}_{11-14,15}$ -DiHETrE,  $^2\text{H}_{11-14(15)}$ -EpETrE,  $^2\text{H}_4$ -9(10)-EpOME and  $^2\text{H}_4$ -9,10-DiHOME) was calculated by an external calibration (2-40 nM) based on the peak areas. Quantification of oxylipins in plasma was performed by an external calibration using 13 deuterated internal standards (App. Table 9.1.2). For calibration, the analyte to IS area ratios were linearly fitted reciprocally weighted by concentration. Additionally, the IS 2 peak area (added in the last step of sample preparation) was monitored as measure for precision of injection and detection signal over the analysis batch and was found to be within (100±10%). For ion suppression analysis a 30 nM solution of the IS ( $^2\text{H}_4$ -PGE $_2$ ,  $^2\text{H}_4$ -PGD $_2$ ,  $^2\text{H}_4$ -TxB $_2$ ,  $^2\text{H}_4$ -LTB $_4$ ,  $^2\text{H}_4$ -9-HODE,  $^2\text{H}_8$ -5-HETE,  $^2\text{H}_8$ -12-HETE,  $^2\text{H}_6$ -20-HETE,  $^2\text{H}_{11-14,15}$ -DiHETrE,  $^2\text{H}_{11-14(15)}$ -EpETrE,  $^2\text{H}_4$ -9(10)-EpOME and  $^2\text{H}_4$ -9,10-DiHOME) in MeOH was post-columnly added to the eluate of the LC column (flow 0.8 mL/h) and the transitions of the compounds (App. Table 9.1.3) were monitored with a dwell time of 20 ms.

## 4.3 Results

### 4.3.1 Recoveries of internal standards

The % recoveries of the 13 deuterated IS spiked to 500  $\mu\text{L}$  human plasma using the SPE protocols are shown in Fig. 4.1 and recoveries with the LLE protocol are presented in the appendix Fig. 9.1.1. The results are also shown in more detail in the appendix (App. Fig. 9.1.2 and Table 9.1.4). With the LLE protocol,

recoveries of all 13 deuterated IS were below 40% (App. Fig. 9.1.1, Table 9.1.4), which is clearly below the performance of all SPE protocols (Fig. 4.1). Furthermore, the intersample (in batch) precision was low with a relative standard deviation (RSD) of the IS concentration of >34% for  $^2\text{H}_4$ -6-keto-PGF $_{1\alpha}$ ,  $^2\text{H}_4$ -TxB $_2$ ,  $^2\text{H}_4$ -PGE $_2$ ,  $^2\text{H}_4$ -PGD $_2$ ,  $^2\text{H}_4$ -LTB $_4$  and  $^2\text{H}_4$ -9,10-DiHOME and 15-26% for the other IS (App. Fig. 9.1.1, Table 9.1.4).

Using the Oasis-MeOH SPE protocol, recoveries of internal standards were below 62% (Fig. 4.1), except  $^2\text{H}_{11-14(15)}$ -EpETrE (68±2.1%). Compared to the other SPE protocols the recovery rates were generally low being the lowest among all protocols, e.g., for  $^2\text{H}_4$ -LTB $_4$ ,  $^2\text{H}_4$ -9,10-DiHOME,  $^2\text{H}_8$ -12-HETE and  $^2\text{H}_{11-14(15)}$ -EpETrE (Fig. 4.1).

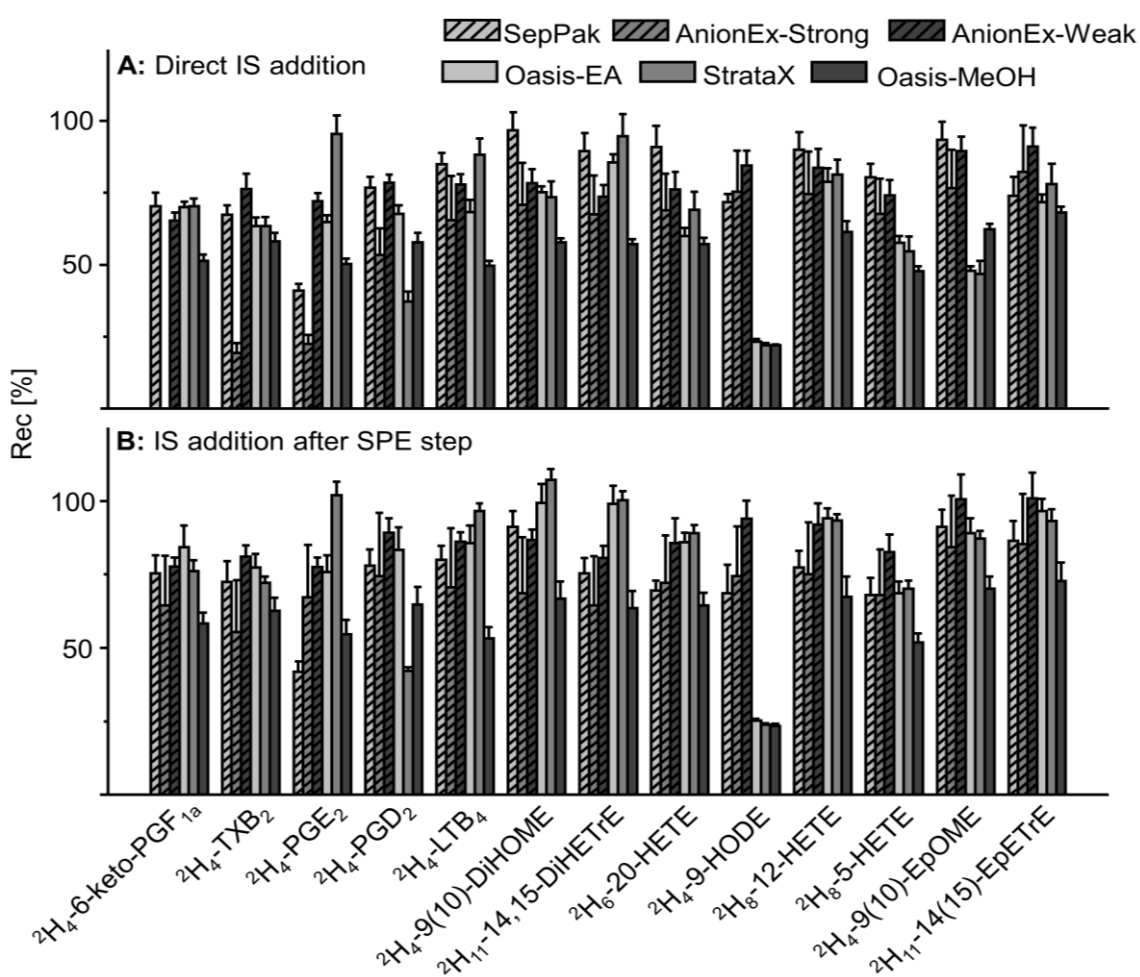


**Fig. 4.1:** Recoveries of internal standards (IS) for the tested SPE protocols. IS was added to the samples either at the beginning of the analysis (panel A) or after the SPE-step (panel B). Shown is the mean recovery rate ± SD (n=5).

Overall good recovery rates ( $\geq 65\%$ ) were obtained with the AnionEx-Weak protocol (Fig. 4.1). Following addition of the IS after the SPE step the determined IS concentrations were slightly higher. This indicates that small amounts of the analytes were lost during the SPE, probably due to incomplete elution from the sorbent bed. Using a less polar elution solvent (AnionEx-Strong), the polar IS  $^2\text{H}_4$ -6-keto-PGF $_{1\alpha}$ ,  $^2\text{H}_4$ -TxB $_2$ ,  $^2\text{H}_4$ -PGE $_2$  and  $^2\text{H}_4$ -PGD $_2$  were almost completely lost during SPE (recovery rates 0-54%) while recoveries were above 65% for all other IS. These losses are probably a result of insufficient elution during the SPE because recovery rates  $\geq 55\%$  were found when adding the IS directly after the SPE step (Fig. 4.1). The AnionEx-Strong protocol was designed for the analysis of medium to non-polar hydroxy-, dihydroxy- and epoxy-FA [6], thus low recovery rates of the polar prostanoids might be less important. However, it is interesting that even the recovery rates for the non-polar analytes were slightly better with a more polar elution solvent (AnionEx-Weak), though being acceptable ( $>65\%$ ) for the AnionEx-Strong. Moreover, the precision of the AnionEx-Strong protocol was low (RSD  $>17\%$  for medium to non-polar analytes) while RSD of the determined IS concentration in all other SPE protocols were  $<10\%$  (App. Table 9.1.4).

Good overall recoveries ( $\geq 68\%$ ) were observed for all IS with the SepPak protocol, except for  $^2\text{H}_4$ -PGE $_2$  (recovery  $41 \pm 2.4\%$ ). Losses during extraction can be ruled out, since there was no difference in the recovery rate of  $^2\text{H}_4$ -PGE $_2$  between the addition of IS at the beginning of the sample preparation and addition of the IS directly after the SPE step (Fig. 4.1, App. Fig. 9.1.2). This is consistent with the results from the ion suppression analysis for the  $^2\text{H}_4$ -PGE $_2$  and  $^2\text{H}_4$ -PGD $_2$  signal (Fig. 4.2A). Strong ion suppression of about 75% of the signal was observed exactly at the retention time of  $^2\text{H}_4$ -PGE $_2$  ( $t_R=4.56$  min) leading to the low recovery rate of  $^2\text{H}_4$ -PGE $_2$  with this protocol.

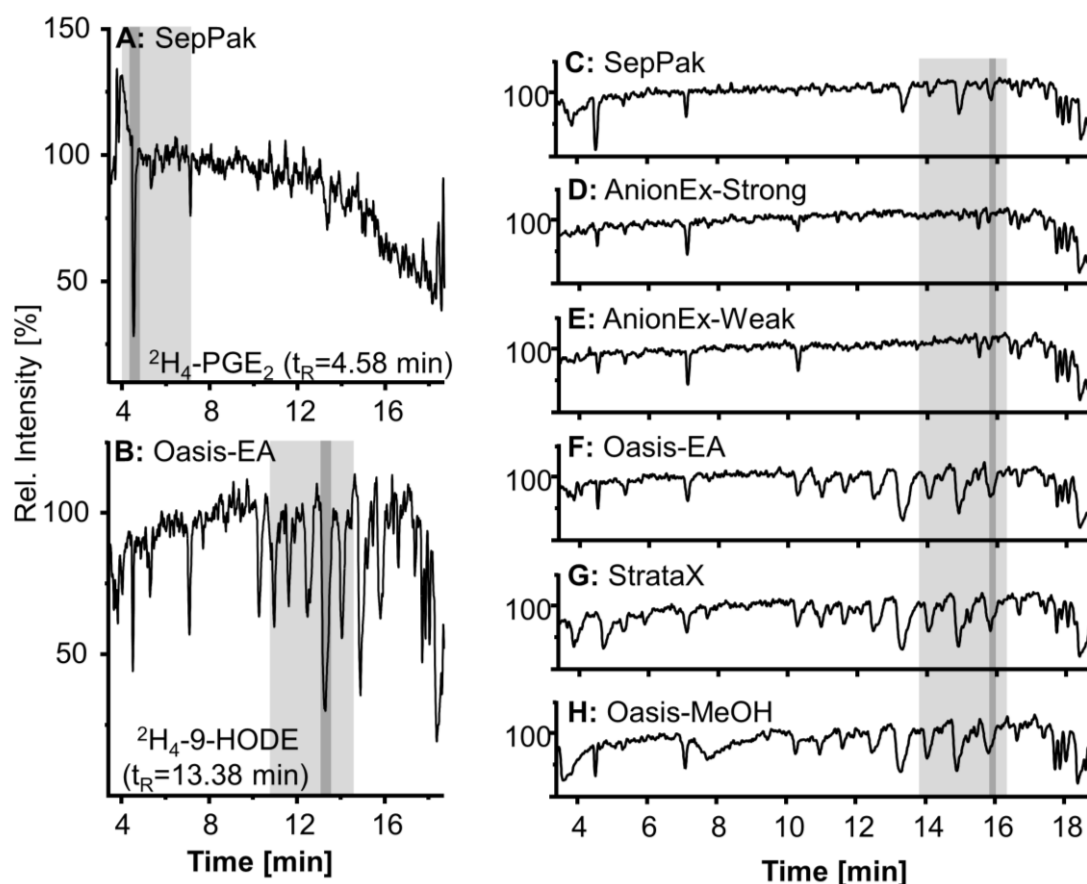


**Fig. 4.2:** Ion suppression analysis for (A)  $^2\text{H}_4\text{-PGE}_2$  with SepPak-SPE, (B)  $^2\text{H}_4\text{-9-HODE}$  with the Oasis-EA-SPE and (C-E) for  $^2\text{H}_4\text{-9(10)-EpOME}$  with all SPE protocols. The retention time window of each IS is highlighted in dark grey, the elution window of all analytes using this IS is depicted in light grey.

The Oasis-EA protocol yielded recovery rates  $\geq 64\%$  for all IS, except for  $^2\text{H}_4\text{-9-HODE}$ ,  $^2\text{H}_8\text{-5-HETE}$  and  $^2\text{H}_4\text{-9(10)-EpOME}$ . Nevertheless, when comparing recoveries with direct addition of IS and addition of IS after the SPE step it becomes clear that significant amounts of almost all IS were lost during the SPE step (e.g.,  $^2\text{H}_6\text{-20-HETE}$ ,  $^2\text{H}_4\text{-9(10)-EpOME}$  and  $^2\text{H}_{11-14(15)-EpETrE}$ ). For  $^2\text{H}_4\text{-9-HODE}$ , no differences in the recoveries were observed (Fig. 4.1, App. Fig. 9.1.2) when adding the IS before the SPE step or after the SPE step. As shown in Fig. 4.2B a significant ion suppression takes place in the  $^2\text{H}_4\text{-9-HODE}$  signal at its retention time providing a mechanistic explanation for the poor recovery rate. Similarly, the recovery rate of  $^2\text{H}_8\text{-5-HETE}$  with post-SPE addition of IS was with  $69\pm 4.1\%$  significantly lower than for the other medium to non-polar IS (e.g., 89-97% for both epoxides). Ion suppression also occurred for  $^2\text{H}_8\text{-5-HETE}$

(App. Fig. 9.1.3E), though not as pronounced as for  $^2\text{H}_4$ -9-HODE. Slight ion suppression was also observable for  $^2\text{H}_4$ -9(10)-EpOME (Fig. 4.2F) although the recovery rate with post-SPE addition of IS was 89%.

With the StrataX protocol, low recovery rates ( $\leq 55\%$ ) were observed for  $^2\text{H}_4$ -PGD<sub>2</sub>,  $^2\text{H}_4$ -9-HODE,  $^2\text{H}_8$ -5-HETE and  $^2\text{H}_4$ -9(10)-EpOME (Fig. 4.1). Ion suppression accounted significantly for the loss of  $^2\text{H}_4$ -9-HODE (App. Fig. 9.1.3D) and  $^2\text{H}_4$ -9(10)-EpOME (Fig. 4.2G), although  $^2\text{H}_4$ -9(10)-EpOME was also lost during the SPE step (Fig. 4.1). The loss of  $^2\text{H}_4$ -PGD<sub>2</sub> and  $^2\text{H}_8$ -5-HETE can in part also be explained by slight ion suppression (App. Fig. 9.1.3A, Fig. 9.1.3E). The low recovery rate of  $^2\text{H}_8$ -5-HETE could partly be explained by incomplete extraction (Fig. 4.1). Low extraction losses could also be observed for  $^2\text{H}_4$ -9,10-DiHOME and  $^2\text{H}_8$ -20-HETE (Fig. 4.1).

Overall, the ESI-signal in the ion suppression analysis was flattest with the AnionEx protocols followed by the SepPak protocol. Intense negative signals, particularly at late retention times occurred with the Oasis-EA, Oasis-MeOH and StrataX protocols (Fig. 4.2F-H, App. Fig. 9.1.3). A large number of oxylipins elutes at these retention times (App. Table 9.1.2). Thus, ion suppression strongly influenced the signal of these oxylipins.

### 4.3.2 Extraction of oxylipins from plasma

Aside from removing ion suppressing matrix compounds, SPE should lead to an efficient extraction of oxylipins from plasma. Since all IS were more or less affected by the matrix, the absolute peak areas were used as measure for the extraction efficacy of oxylipins. Table 4.1 shows the absolute areas of a representative set of oxylipins following extraction of 500  $\mu\text{L}$  plasma with the different protocols. The areas of all other determined analytes can be found in the appendix (App. Table 9.1.5). Consistent with the poor recovery of IS, the Oasis-MeOH protocol yielded low peak areas compared to the other protocols (e.g., prostanoids, diols, 20-HETE, 5-HETE). With the StrataX protocol low peak

areas were obtained, being in the lower range for several epoxy-FA and hydroxy-FA and lowest, e.g. for 9(10)-EpOME, 19(20)-epoxy docosapentaenoic acid (EpDPE), 9-HODE and 12-HETE. Furthermore, some epoxy-FA could not be detected at all, i.e., 11(12)-epoxy eicosatetraenoic acid (EpETE), 8(9)-EpETE and 13(14)-EpDPE (Table 4.1, App. Table 9.1.5). However, for several dihydroxy-FA, the StrataX protocol yielded absolute areas in the higher range being highest, e.g., for 14,15-DiHETrE or 17,18-dihydroxy eicosatetraenoic acid (DiHETE) (Table 4.1, Table 9.1.5).

Both AnionEx protocols led to absolute areas of epoxy-FA in the lower range compared to the other SPEs and several epoxy-FA could not be detected in the AnionEx extracts, e.g., 8(9)-EpETE and 13(14)-EpDPE (Table 4.1, App. Table 9.1.5). For various hydroxy-FA both protocols yielded areas in the higher range, e.g., 9-HODE and 12-HETE, while for dihydroxy-FA overall low peak areas were found, e.g. 14,15-DiHETrE (Table 4.1). The Oasis-EA protocol yielded intermediate results for the analytes. In a few cases, it led to the highest or lowest peak areas, e.g., 5,6-DiHETrE and 15(16)-epoxy octadecadienoic acid (EpODE) (App. Table 9.1.5).

The SepPak protocol yielded for many analytes the highest peak areas (Table 4.1, App. Table 9.1.5). Only for a few polar analytes, e.g., TxB<sub>2</sub> as well as PGE<sub>2</sub>, and for 15-oxo eicosatetraenoic acid (oxo-ETE) larger peaks were found with the other SPE protocols. Particularly non-polar epoxy-FA were found to be higher with this protocol (Table 4.1, App. Table 9.1.5): Compared to the AnionEx-Weak protocol up to 9-fold higher peak areas were found (16(17)-EpDPE, App. Table 9.1.5) and epoxides could be detected in human plasma which were below LOQ using AnionEx and StrataX protocols, e.g., 13(14)-EpDPE (Table 4.1).

**Table 4.1:** Peak areas of selected oxylipins obtained after the extraction of 500  $\mu$ L plasma. Shown is the mean  $\pm$  SD (n=5). The areas of all oxylipins detected are presented in the appendix, Table 9.1.5.

[1000 counts]	TxB <sub>2</sub>	PGE <sub>2</sub>	PGD <sub>2</sub>	9,10-DiHOME	14,15-DiHETrE	20-HETE	9-HODE
<b>SepPak</b>	31 $\pm$ 1.7	21 $\pm$ 2.2	30 $\pm$ 1.7	2200 $\pm$ 140	220 $\pm$ 16	29 $\pm$ 5	6500 $\pm$ 280
<b>AnionEx-Strong</b>	<LOQ*	15 $\pm$ 2.0*	22 $\pm$ 5.0*	1500 $\pm$ 300	180 $\pm$ 35	22 $\pm$ 4	6000 $\pm$ 1100
<b>AnionEx-Weak</b>	39 $\pm$ 0.72	36 $\pm$ 1.9	27 $\pm$ 2.1	1700 $\pm$ 53	190 $\pm$ 4.2	27 $\pm$ 2	6100 $\pm$ 180
<b>Oasis-EA</b>	44 $\pm$ 14	41 $\pm$ 4.4	18 $\pm$ 1.6	1500 $\pm$ 35	220 $\pm$ 7.4	24 $\pm$ 2	2400 $\pm$ 100
<b>StrataX</b>	29 $\pm$ 1.2	62 $\pm$ 6.7	4.9 $\pm$ 0.95	1400 $\pm$ 83	250 $\pm$ 19	24 $\pm$ 2	2200 $\pm$ 97
<b>Oasis-MeOH</b>	26 $\pm$ 2	26 $\pm$ 1.9	16 $\pm$ 2.2	1300 $\pm$ 36	150 $\pm$ 6.3	23 $\pm$ 3	2500 $\pm$ 110

	12-HETE	5-HETE	14(15)-EpETrE	9(10)-EpOME	13(14)-EpDPE	10(11)-EpDPE	8(9)-EpETrE
<b>SepPak</b>	580 $\pm$ 21	340 $\pm$ 21	48 $\pm$ 9.3	1200 $\pm$ 150	32 $\pm$ 6.1	63 $\pm$ 11	11.6 $\pm$ 2.2
<b>AnionEx-Strong</b>	860 $\pm$ 180	300 $\pm$ 60	8.8 $\pm$ 2	260 $\pm$ 53	<LOQ	11 $\pm$ 2	2.9 $\pm$ 0.56
<b>AnionEx-Weak</b>	740 $\pm$ 38	280 $\pm$ 8.3	10 $\pm$ 0.88	310 $\pm$ 18	<LOQ	14 $\pm$ 1	3.4 $\pm$ 0.51
<b>Oasis-EA</b>	370 $\pm$ 28	330 $\pm$ 13	23 $\pm$ 5.8	520 $\pm$ 160	6.8 $\pm$ 3.2	22 $\pm$ 8	9.1 $\pm$ 3.8
<b>StrataX</b>	320 $\pm$ 18	260 $\pm$ 11	11 $\pm$ 0.56	180 $\pm$ 16	<LOQ	13 $\pm$ 1	3.2 $\pm$ 0.44
<b>Oasis-MeOH</b>	330 $\pm$ 19	200 $\pm$ 26	15 $\pm$ 1.5	450 $\pm$ 29	7 $\pm$ 0.8	20 $\pm$ 1	4.4 $\pm$ 0.65

\*protocol not suited for the analysis of these oxylipins, IS rec <60%

### 4.3.3 Cartridge size

A possible reason for the differences in extraction efficacy is the varying cartridge size of the different SPE protocols (60-500 mg stationary phase) [1, 2, 8, 9, 11, 18, 21]. In order to assess the influence of the amount of stationary phase, the SepPak and AnionEx-Weak protocols were compared using 3 mL (200 mg) and 6 mL (500 mg) cartridges. The absolute areas of selected analytes are shown in Table 4.2 and all analytes are displayed in the appendix, Table 9.1.6. Using the SepPak protocol with the smaller column the peak areas were for most analytes in the same range as with the original protocol ( $\pm$ 20%), e.g., TxB<sub>2</sub>, 14,15-DiHETrE or 20-HETE. However, several analytes, especially epoxides, showed significantly higher absolute areas with the larger cartridge (120-290% of the area with the smaller cartridge), e.g. 9(10)-EpOME or 14(15)-EpETE (App. Table 9.1.5 and Table 9.1.6).

A similar trend was observed for the AnionEx-Weak SPE. With the larger column, peak areas of most analytes were within a range of  $\pm$ 20% of the



original protocol, while several analytes, mostly dihydroxy-FA, were in a range of 120-160% of the original protocol with extraction on the larger column, e.g., 13,14-dihydroxy docosapentaenoic acid (DiHDPE) or 13-hydroxy octadecatrienoic acid (HOTrE) (App. Table 9.1.5 and Table 9.1.6).

Nevertheless, when comparing the SepPak and the AnionEx-Weak SPE (both 500 mg, 6 mL cartridge) the absolute areas of most epoxides were still up to six- to seven-fold higher with the SepPak SPE, e.g., 16(17)-EpDPE and 9(10)-EpODE, while peak areas of dihydroxy-FA and hydroxy-FA was in the same range ( $\pm 20\%$ , App. Table 9.1.5 and Table 9.1.6 ).

**Table 4.2:** Effect of SPE-cartridge size on the extraction efficacy. Peak areas obtained after extraction of 500  $\mu$ L plasma on 6 mL cartridges (500 mg) were compared to 3 mL cartridges (200 mg). Shown is the mean  $\pm$  SD (n=5). The areas of all oxylipins detected are presented in the appendix Table 9.1.6).

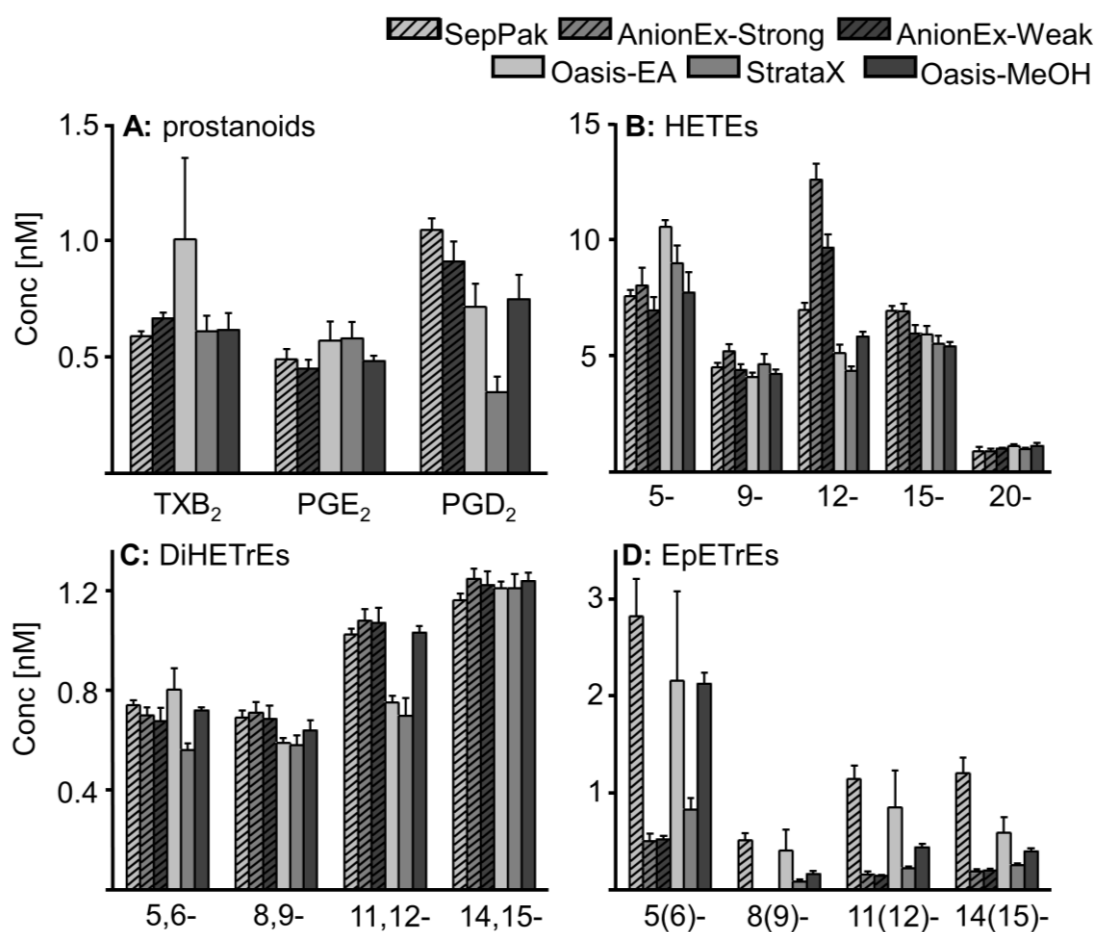
[1000 counts]	TxB <sub>2</sub>	PGE <sub>2</sub>	PGD <sub>2</sub>	9,10-DiHOME	14,15-DiHETrE	20-HETE	9-HODE
<b>SepPak 6 mL</b>	31 $\pm$ 1.7	21 $\pm$ 2.2	30 $\pm$ 1.7	2200 $\pm$ 140	220 $\pm$ 16	29 $\pm$ 5.2	6500 $\pm$ 280
<b>SepPak 3 mL</b>	36 $\pm$ 3.2	10 $\pm$ 0.9	23 $\pm$ 5.7	2100 $\pm$ 150	270 $\pm$ 30	29 $\pm$ 5.7	7400 $\pm$ 320
<b>AnionEx-Weak 3 mL</b>	39 $\pm$ 0.7	36 $\pm$ 1.9	27 $\pm$ 2.1	1700 $\pm$ 53	190 $\pm$ 4.2	27 $\pm$ 2.1	6100 $\pm$ 180
<b>AnionEx-Weak 6 mL</b>	40 $\pm$ 6.9	24 $\pm$ 4.3	24 $\pm$ 4.7	2000 $\pm$ 330	240 $\pm$ 48	28 $\pm$ 8.7	8200 $\pm$ 830

	12-HETE	5-HETE	14(15)-EpETrE	9(10)-EpOME	13(14)-EpDPE	10(11)-EpDPE	8(9)-EpETrE
<b>SepPak 6 mL</b>	580 $\pm$ 21	340 $\pm$ 21	48 $\pm$ 9.3	1200 $\pm$ 150	32 $\pm$ 6.1	63 $\pm$ 11	11.6 $\pm$ 2.2
<b>SepPak 3 mL</b>	660 $\pm$ 47	340 $\pm$ 41	17 $\pm$ 1.7	680 $\pm$ 46	20 $\pm$ 2.5	50 $\pm$ 5.1	7.2 $\pm$ 0.71
<b>AnionEx-Weak 3 mL</b>	740 $\pm$ 38	280 $\pm$ 8.3	10 $\pm$ 0.88	310 $\pm$ 18	<LOQ	14 $\pm$ 1.1	3.4 $\pm$ 0.51
<b>AnionEx-Weak 6 mL</b>	680 $\pm$ 92	300 $\pm$ 32	12 $\pm$ 2.3	280 $\pm$ 39	<LOQ	16 $\pm$ 3.3	3.9 $\pm$ 0.85

#### 4.3.4 Calculated concentrations

Finally, plasma concentrations of oxylipins were calculated using the analyte/IS ratio (App. Table 9.1.2) and external calibrations. Fig. 4.3 shows the concentrations of a representative set of eicosanoids determined with the different protocols. The concentration of all analytes can be found in the appendix, Table 9.1.7.



**Fig. 4.3:** Calculated oxylipin plasma concentrations with the different SPE protocols: **(A)** prostanoids **(B)** hydroxy-ARA, **(C)** dihydroxy-ARA and **(D)** epoxy-ARA. Internal standards used for the quantification of the analytes are shown in the appendix, Table 9.1.2. All results are shown as mean  $\pm$  SD ( $n=5$ ). It should be noted that panel A does not include the AnionEx-Strong protocol because it is not suited for the analysis of polar oxylipins.

For the ARA-derived polar prostanoids TxB<sub>2</sub>, PGE<sub>2</sub> and PGD<sub>2</sub>, which were all quantified with an isotopically labeled surrogate as IS, concentrations were in the same range with the different protocols. However, for TxB<sub>2</sub> the Oasis-EA led to a higher concentration and for PGD<sub>2</sub> the StrataX protocol yielded a significantly lower concentration. These results were consistent with the peak areas of the analytes which were highest for TxB<sub>2</sub> with the Oasis-EA and lowest for PGD<sub>2</sub> with the StrataX protocol (Table 4.1). Though group-specific IS were used (App. Table 9.1.2), all protocols also led to overall similar concentrations for HETEs and DiHETrEs. However, the plasma concentration of 12-HETE was significantly higher for both AnionEx protocols, consistent with the high peak areas for this analyte (Table 4.1). For 11,12-DiHETrE the Oasis-EA and the

StrataX protocol yielded lower concentrations compared to the other SPE protocols.

High differences were observed in the concentrations of epoxy-FA. Consistent with the peaks areas, the SepPak protocol clearly led to the highest concentrations followed by the Oasis-EA and the Oasis-MeOH protocol. Interestingly, the precision of the Oasis-EA protocol was low for some epoxides, e.g., 11(12)-EpETrE, 8(9)-EpETrE, 5(6)-EpETrE (RSD=43-53%). For the AnionEx SPE, 8(9)-EpETrE could not be quantified and 11(12)-EpETrE as well as 14(15)-EpETrE for example were detected in a concentration  $\leq 0.20$  nM while the SepPak protocol yielded concentrations  $\geq 1.1$  nM.

#### **4.4 Discussion**

The aim of the present study was to identify the most appropriate protocol for the analysis of free (non-esterified) oxylipins in EDTA plasma. Aside from analysis of total oxylipins after liberation of esterified oxylipins by saponification, quantification of free oxylipins in plasma is the most commonly carried out analysis in studies on the biology of oxylipins (for discussion, see [21, 22]).

Taking the high costs for standards, cartridges and instrument time into account, we did not perform the common tiered step-by-step-optimization procedure to develop a sample preparation strategy. Instead, we compared the efficacy of well-established sample preparation protocols. All these protocols are “fit for purpose” as they have been successfully used to study oxylipin biology: The Oasis-EA method is from the Hammock lab (Davis, CA, USA) [10] and has also been successfully employed by other groups [8]. Modifications of this protocol, e.g., with different eluents, are also commonly used and elution with methanol (Oasis-MeOH) according to Balvers et al. [17] was included in the comparison. The AnionEx SPE protocols originate from the contract research organization (CRO)/laboratory Lipidomix, Berlin, Germany and have been successfully employed by the groups of Schunck and Weylandt (Berlin,

Germany) [6, 13] among others. The StrataX and the SepPak SPE protocols are from the major laboratories in the field of oxylipin research, i.e., Dennis (San Diego, CA, USA) [9] and Serhan (Boston, MA, USA) [11]. Also, the LLE protocol is commonly used, e.g., by the lab of Fleming (Frankfurt, Germany) [15]. All methods were carried out as described by these groups. However, sample preparation was in some cases adapted for plasma and the overall procedure (waiting times, used glassware, plastic tubes, etc.) was kept the same in order to assure comparability (App. Table 9.1.1). The sample volume was set to 500  $\mu\text{L}$ , since lower volumes are, because of the low concentration of most oxylipins, doomed to failure in plasma despite highly sensitive LC-MS instruments [14].

Regarding the IS recovery rates (Fig. 4.1, App. Fig. 9.1.1, Fig. 9.1.2, Table 9.1.4), LLE and the Oasis-MeOH SPE are clearly outperformed by the other protocols. With the low IS recovery and the low precision, LLE is in our hands not an appropriate sample preparation for the analysis of oxylipins in plasma and thus excluded from further discussion. With acceptable recovery rates (>60%) for few oxylipins Oasis-MeOH SPE seems to be appropriate for specific questions. However, compared to the other protocols, there is no reason to choose this protocol in targeted oxylipin metabolomics particularly because eluting with MeOH and EA (Oasis-EA) yielded much better results and acceptable IS recoveries (>60%) except for  $^2\text{H}_4$ -9-HODE,  $^2\text{H}_8$ -5-HETE and  $^2\text{H}_4$ -9(10)-EpOME. The StrataX SPE showed a similar performance, leading to low recoveries (<60%) for four IS ( $^2\text{H}_4$ -PGD<sub>2</sub>,  $^2\text{H}_4$ -9-HODE,  $^2\text{H}_8$ -5-HETE and  $^2\text{H}_4$ -9(10)-EpOME). Ion suppression analysis of the extracts unveiled that both StrataX and Oasis SPE insufficiently remove interfering matrix compounds (Fig. 4.2, App. Fig. 9.1.3). These compounds led to massive ion suppression and caused for example the poor recovery of  $^2\text{H}_4$ -9-HODE (Fig. 4.2B, App. Fig. 9.1.3D) or  $^2\text{H}_4$ -9(10)-EpOME (Fig. 4.2F-H). In comparison, the SepPak and AnionEx SPE led to a better removal of matrix and the ion suppression signals were smoother and more flat (Fig. 4.2, App. Fig. 9.1.3). For the SepPak SPE only a single, strong signal occurred in the ion suppression analysis at  $t_{\text{R}}=4.56$

min. As a consequence, the recovery of the coeluting  $^2\text{H}_4\text{-PGE}_2$  is poor while the recovery rate of all other IS is good (68-97%). Nevertheless, the ion suppression analysis showed several signals of potentially interfering matrix compounds in the SepPak extract. However, these seem not to be prone to disturb the analysis since for example the small peak at 15.95 min does not cause a relevant suppression of the coeluting  $^2\text{H}_4\text{-9(10)-EpOME}$ . The ion suppression analysis of the AnionEx extracts was even superior and showed only few small peaks. Consistently, the IS recovery for the AnionEx-Weak is nearly perfect (all analytes  $\geq 65\%$ ). The AnionEx-strong SPE led also to good – however not better – recoveries for IS eluting later than  $^2\text{H}_4\text{-LTB}_4$ , while the polar oxylipins were lost.

The solvent used to elute the broad diversity of oxylipins from the SPE material has to be polar enough to elute the polar analytes (AnionEx-Strong vs. AnionEx-Weak), but must also possess a sufficiently strong elution power (see Oasis-EA vs. Oasis-MeOH) to elute all analytes quantitatively. While all protocols simply use polar eluents for equilibration, sample loading and washing followed by non-polar eluents for elution, the SepPak protocol utilizes the poor elution power of highly non-polar eluents for oxylipins: Here, the polar washing step (with water) is followed by a washing step with pure *n*-hexane (eluting potentially interfering lipids [23]), before the oxylipins are eluted with the medium polar methyl formate. This results in an efficient reduction of ion suppressing matrix, particularly compounds of low polarity are removed. Thus, at run times  $>10$  min, the ion suppression signal of the SepPak protocol is dramatically better than that of Oasis and StrataX protocols (Fig. 4.2, App. Fig. 9.1.3). Regarding IS recovery and ion suppression only the AnionEx-Weak protocol, making use of the acidic properties of all oxylipins (oxidative fatty acid derivatives) can compete with the SepPak protocol. Because of the poor recovery of  $^2\text{H}_4\text{-PGE}_2$  in the SepPak SPE (Fig. 4.1, Fig. 4.2), the AnionEx-weak SPE is overall the best protocol in terms of IS recovery.

It is somewhat striking that our results demonstrate that good IS recovery seems to not necessarily translate to a high extraction efficacy of oxylipins from the plasma matrix (Table 4.1, App. Table 9.1.5). While several oxylipins were extracted in the same range by SepPak, StrataX, AnionEx-Weak and Oasis-EA, e.g., TxB<sub>2</sub>, 9,10-DiHOME, 20-HETE, high differences were found for the extraction efficacy of analytes of low polarity, e.g., 9(10)-EpOME and 10(11)-EpDPE.

The AnionEx-Weak protocol led, even for the latest eluting epoxides, to a better extraction efficacy than the AnionEx-Strong protocol (Table 4.1), and thus is for all oxylipins investigated, clearly the more appropriate protocol compared to the AnionEx-Strong procedure. However, the peak areas of epoxides with the AnionEx-Weak were up to seven-fold lower compared to the SepPak SPE. Because of the flat ion suppression (Fig. 4.2E, App. Fig. 9.1.3), this effect might be caused by poor extraction efficacy rather than by ion suppression. Interestingly, the ratio between column dimension and sample volume (analyte and matrix amount) was found to be only of minor importance for the extraction efficacy. Even with a large 6 mL (500 mg) cartridge, the peak areas of epoxy-FA resulting from the AnionEx-Weak protocol were lower than those of the SepPak SPE (Table 4.2, App. Table 9.1.6).

The central aim of the LC-MS analysis of oxylipins is to provide quantitative information about their concentration in biological matrices. Compared to other LC-MS-based analyses, e.g., residues of pesticides where a heavy isotope surrogate is used as internal standard for each analyte, only few isotopically labeled oxylipins are available as IS. Thus, a single IS is used for the quantification of a group of oxylipins. Typically, <sup>2</sup>H<sub>4</sub>-PGE<sub>2</sub> is used for PGs, one or few deuterated hydroxy-FA are used as IS for the whole group of hydroxy-FA, one or few deuterated dihydroxy-FA for the class of dihydroxy-FA and so on. Though being structurally similar, the retention time of the analyte differs from that of the IS. Thus, the IS cannot compensate for ion suppressing effects from the matrix, which directly influence the calculated concentrations. As a

result, the different SPE protocols lead to significantly different plasma concentrations of the oxylipins (Fig. 4.3, App. Table 9.1.7). One example is the ion suppression observed for  $^2\text{H}_4\text{-PGE}_2$  with the SepPak protocol and the use of  $^2\text{H}_4\text{-PGE}_2$  for the quantification of other PGs and trihydroxy-ocadecenoic acids (TriHOMEs) as carried out in our method (App. Table 9.1.2). As shown in Fig. 4.3, the determined  $\text{PGE}_2$  levels are consistent with the other SPE methods because the use of the isotopologue as IS is correcting for the ion suppression. However, the use of  $^2\text{H}_4\text{-PGE}_2$  (rec=41±2.4%) for other PGs leads to an overestimation of the analytes and another IS, e.g.,  $^2\text{H}_4\text{-PGD}_2$  should be used for quantification of  $\text{PGE}_3$ , TriHOMEs,  $\text{PGF}_{2\alpha}$ ,  $\text{PGE}_1$  and  $\text{LXA}_4$ . With these adjustment, about 50% lower concentrations for these analytes result (App. Table 9.1.8) which are consistent with the concentrations obtained with the other protocols (App. Table 9.1.7).

Overall, the obtained concentrations of several prostanoids, hydroxy-FA and dihydroxy-FA were in same range, the determined concentrations of epoxy-FA were highly different (Fig. 4.3). Therefore, care must be taken when comparing results from studies using different SPE methods. In order to investigate the role of oxylipins in biology, their levels always have to be compared within the same study using exactly the same analytical method.

So what is the most appropriate protocol for the analysis of free oxylipins in plasma?

The Oasis-EA protocol efficiently extracts oxylipins from plasma (Table 4.1, App. Table 9.1.5). However, IS recovery and analytes are strongly affected by severe ion suppression caused by matrix compounds not removed by the sample preparation procedure (Fig. 4.1, Fig. 4.2, App. Fig. 9.1.2, Fig. 9.1.3, Table 9.1.4). Particularly, the concentration of analytes with a retention time >10 min could significantly be underestimated because the few IS used cannot compensate for the strong ion suppression in the analyte signals. Similarly, ion suppression was strong with StrataX and Oasis-MeOH protocols. Despite a near perfect removal of ion suppressing matrix and good recovery rates of

internal standards, the use of the AnionEx-Weak protocol seems to be problematic since the concentration of epoxy-FA is underpredicted or these potent lipid mediators [3, 6, 20] are not detected at all. The SepPak protocol showed good extraction efficacy and reduction of matrix compounds.

## **4.5 Conclusion**

Overall, our data clearly demonstrates that the AnionEx-Weak protocol is most efficient in removing interfering matrix components and leads to the overall best recovery rates of internal standards. However, the SepPak protocol led to higher peaks areas and concentrations of epoxy-FA indicating higher extraction efficiency of this analyte group from the plasma samples, while removal of interfering matrix was inferior compared to the AnionEx-Weak procedure.

It should be noted that the ion suppression effects presented here might affect other LC-MS methods in another way. Different gradients and RP columns will lead to slightly different elution profiles and different coelutions of oxylipins and matrix. Further, due to a high inter-individual and inter-species variability of biological samples, some of the observed ion suppression effects might be different in other samples. Moreover, our conclusions for extraction efficacy and precision are only valid for analysis of free oxylipins in human plasma. Other sample matrices, e.g. saponified samples or tissue extracts, might lead to different results and conclusions.



## 4.6 References

1. Buczynski MW, Dumlao DS, Dennis EA. Thematic Review Series: Proteomics. An integrated omics analysis of eicosanoid biology. *J Lipid Res.* 2009;50(6):1015-1038.
2. Serhan CN. Novel lipid mediators and resolution mechanisms in acute inflammation: to resolve or not? *Am J Pathol.* 2010;177(4):1576-1591.
3. Fischer R, Konkkel A, Mehling H, Blossey K, Gapelyuk A, Wessel N, von Schacky C, Dechend R, Muller DN, Rothe M, Luft FC, Weylandt K, Schunck WH. Dietary omega-3 fatty acids modulate the eicosanoid profile in man primarily via the CYP-epoxygenase pathway. *J Lipid Res.* 2014;55(6):1150-1164.
4. Panigrahy D, Edin ML, Lee CR, Huang S, Bielenberg DR, Butterfield CE, Barnes CM, Mammoto A, Mammoto T, Luria A, Benny O, Chaponis DM, Dudley AC, Greene ER, Vergilio JA, Pietramaggiori G, Scherer-Pietramaggiori SS, Short SM, Seth M, Lih FB, Tomer KB, Yang J, Schwendener RA, Hammock BD, Falck JR, Manthati VL, Ingber DE, Kaipainen A, D'Amore PA, Kieran MW, Zeldin DC. Epoxyeicosanoids stimulate multiorgan metastasis and tumor dormancy escape in mice. *J Clin Invest.* 2012;122(1):178-191.
5. Zhang G, Panigrahy D, Mahakian LM, Yang J, Liu J-Y, Stephen Lee KS, Wettersten HI, Ulu A, Hu X, Tam S, Hwang SH, Ingham ES, Kieran MW, Weiss RH, Ferrara KW, Hammock BD. Epoxy metabolites of docosahexaenoic acid (DHA) inhibit angiogenesis, tumor growth, and metastasis. *Proc Natl Acad Sci U S A.* 2013;110(16):6530-6535.
6. Arnold C, Markovic M, Blossey K, Wallukat G, Fischer R, Dechend R, Konkkel A, von Schacky C, Luft FC, Muller DN, Rothe M, Schunck WH. Arachidonic acid-metabolizing cytochrome P450 enzymes are targets of {omega}-3 fatty acids. *J Biol Chem.* 2010;285(43):32720-32733.
7. Chiu CY, Gomolka B, Dierkes C, Huang NR, Schroeder M, Purschke M, Manstein D, Dangi B, Weylandt KH. Omega-6 docosapentaenoic acid-derived resolvins and 17-hydroxydocosahexaenoic acid modulate macrophage function and alleviate experimental colitis. *Inflamm Res.* 2012;61(9):967-976.
8. Strassburg K, Huijbrechts AM, Kortekaas KA, Lindeman JH, Pedersen TL, Dane A, Berger R, Brenkman A, Hankemeier T, van Duynhoven J, Kalkhoven E, Newman JW, Vreeken RJ. Quantitative profiling of oxylipins through comprehensive LC-MS/MS analysis: application in cardiac surgery. *Anal Bioanal Chem.* 2012;404(5):1413-1426.
9. Dumlao DS, Buczynski MW, Norris PC, Harkewicz R, Dennis EA. High-throughput lipidomic analysis of fatty acid derived eicosanoids and N-acyl ethanolamines. *Biochim Biophys Acta.* 2011;1811(11):724-736.
10. Yang J, Schmelzer K, Georgi K, Hammock BD. Quantitative profiling method for oxylipin metabolome by liquid chromatography electrospray ionization tandem mass spectrometry. *Anal Chem.* 2009;81(19):8085-8093.
11. Masoodi M, Mir AA, Petasis NA, Serhan CN, Nicolaou A. Simultaneous lipidomic analysis of three families of bioactive lipid mediators leukotrienes, resolvins, protectins and related hydroxy-fatty acids by liquid chromatography/electrospray ionisation tandem mass spectrometry. *Rapid Commun Mass Spectrom.* 2008;22(2):75-83.

12. Schuchardt JP, Schmidt S, Kressel G, Dong H, Willenberg I, Hammock BD, Hahn A, Schebb NH. Comparison of free serum oxylipin concentrations in hyper- vs. normolipidemic men. *Prostag Leukotr Ess*. 2013;89(1):19-29.
13. Gomolka B, Siegert E, Blossey K, Schunck WH, Rothe M, Weylandt KH. Analysis of omega-3 and omega-6 fatty acid-derived lipid metabolite formation in human and mouse blood samples. *Prostag Oth Lipid M*. 2011;94(3-4):81-87.
14. Tsikas D, Zoerner AA. Analysis of eicosanoids by LC-MS/MS and GC-MS/MS: a historical retrospect and a discussion. *J Chromatogr B*. 2014;964:79-88.
15. Fromel T, Jungblut B, Hu J, Trouvain C, Barbosa-Sicard E, Popp R, Liebner S, Dimmeler S, Hammock BD, Fleming I. Soluble epoxide hydrolase regulates hematopoietic progenitor cell function via generation of fatty acid diols. *Proc Natl Acad Sci U S A*. 2012;109(25):9995-10000.
16. Giera M, Ioan-Facsinay A, Toes R, Gao F, Dalli J, Deelder AM, Serhan CN, Mayboroda OA. Lipid and lipid mediator profiling of human synovial fluid in rheumatoid arthritis patients by means of LC-MS/MS. *Biochim Biophys Acta*. 2012;1821(11):1415-1424.
17. Balvers MGJ, Verhoeckx KCM, Bijlsma S, Rubingh CM, Meijerink J, Wortelboer HM, Witkamp RF. Fish oil and inflammatory status alter the n-3 to n-6 balance of the endocannabinoid and oxylipin metabolomes in mouse plasma and tissues. *Metabolomics*. 2012;8(6):1130-1147.
18. Taylor PJ. Matrix effects: The Achilles heel of quantitative high-performance liquid chromatography-electrospray-tandem mass spectrometry. *Clinical Biochemistry*. 2005;38(4):328-334.
19. Schebb NH, Inceoglu B, Rose T, Wagner K, Hammock BD. Development of an ultra fast online-solid phase extraction (SPE) liquid chromatography electrospray tandem mass spectrometry (LC-ESI-MS/MS) based approach for the determination of drugs in pharmacokinetic studies. *Anal Methods*. 2011;3(2):420-428.
20. Inceoglu B, Wagner KM, Yang J, Bettaieb A, Schebb NH, Hwang SH, Morisseau C, Haj FG, Hammock BD. Acute augmentation of epoxygenated fatty acid levels rapidly reduces pain-related behavior in a rat model of type I diabetes. *Proc Natl Acad Sci U S A*. 2012;109(28):11390-11395.
21. Schebb NH, Ostermann AI, Yang J, Hammock BD, Hahn A, Schuchardt JP. Comparison of the effects of long-chain omega-3 fatty acid supplementation on plasma levels of free and esterified oxylipins. *Prostag Oth Lipid M*. 2014.
22. Shearer GC, Newman JW. Impact of circulating esterified eicosanoids and other oxylipins on endothelial function. *Current Atherosclerosis Reports*. 2009;11(6):403-410.
23. Yang R, Chiang N, Oh SF, Serhan CN. Metabolomics-lipidomics of eicosanoids and docosanoids generated by phagocytes. *Curr Protoc Immunol*. 2011;Chapter 14:Unit 14 26.

# Chapter 5

## Development of an Online-SPE-LC-MS/MS Method for 26 Hydroxylated Polyunsaturated Fatty Acids as Rapid Targeted Metabolomics Approach for the LOX, CYP and Autoxidation Pathways of the Arachidonic Acid Cascade

*Hydroxylated fatty acids (OH-FAs) are formed in all branches of the arachidonic acid (C20:4n6, ARA) cascade from polyunsaturated fatty acids (PUFA). OH-FAs act as potent lipid mediators and serve as activity marker for pathways of the ARA cascade, particularly the lipoxygenase branch. Current targeted metabolomics methods of the ARA cascade cover several OH-FAs among other oxylipins, yet they require long runtimes and laborious sample preparation. In the present study we developed a new rapid LC-MS method with automated sample preparation for the simultaneous quantification of 26 OH-FAs within 6.5 min. Crude biological samples are directly injected following addition of four isotopically labeled internal standards and centrifugation. The analytes are extracted from the matrix by means of online solid phase extraction on an Oasis HLB column at 3.5 mL min<sup>-1</sup> flow rate. LC separation was carried out on a RP-18 column with fused core 1.3 µm particles. The method showed a high sensitivity with a limit of detection of 0.5-10 fmol on column and a broad linear range. Intra- and inter-batch precision and accuracy for the analytes were characterized for cell culture medium as well as human plasma and were found to be generally within 100 ± 15%. The method was applied to the investigation of OH-FA formation in five cell lines following incubation with ARA, eicosapentaenoic acid (C20:5n3, EPA) and docosahexaenoic acid (C22:6n3, DHA). The colon cancer cell lines HCA-7 and SW-480, as well as the fibroblast line Balb/c 3T3 showed significant formation of OH-FAs in the cell culture medium, with dominant formation of 15-HETE, 18-HEPE, 20-HDHA and 8-HDHA from the precursor PUFAs.*

*Chromatographia*, Development of an Online-SPE-LC-MS/MS Method for 26 Hydroxylated Polyunsaturated Fatty Acids as Rapid Targeted Metabolomics Approach for the LOX, CYP, and Autoxidation Pathways of the Arachidonic Acid Cascade, vol. 78(5), 2015, pp. 415–428, Ostermann AI, Willenberg I, Weylandt KH and Schebb NH. With permission of Springer.

Author contributions: AIO, IW, NHS: Designed research, performed experiments and wrote the manuscript; KHW: Contributed to research design and manuscript writing.

## 5.1 Introduction

Oxidative metabolites of PUFA are an important class of lipid mediators. Particularly, the conversion of ARA by cyclooxygenases (COXs) and lipoxygenases (LOXs) to highly potent eicosanoids governing a multitude of biological functions has been intensively studied. Recent years have seen the discovery of a large number of eicosanoids and oxidation products of other PUFA, generally referred to as oxylipins. The routes of formation are diverse comprising in addition to the LOX and COX pathways conversion by cytochrome P450 enzymes and non-enzymatic (aut)oxidation [1]. The initially formed products can in turn be further converted by a multitude of other specific enzymes, such as prostaglandin synthases or soluble epoxide hydrolase leading to a large number of ARA-derived oxylipins [2].

OH-FAs are a main group of products, and are formed in all branches of the ARA cascade. In the conversion of ARA by COX-2, 15-hydroxy eicosatetraenoic acid (HETE) results as site product [3]. 5-LOX conversion of ARA leads to 5-hydroperoxy eicosatetraenoic acid (HpETE), 12-LOX conversion to 12-HpETE and 15-LOX conversion to 15-HpETE which can be further converted e.g., to leukotrienes or are reduced to 5-HETE, 12-HETE and 15-HETE [1]. Other important mediators formed from ARA, either by LOX action or by acetylated COX-2 after treatment with acetyl salicylic acid are the anti-inflammatory multihydroxylated lipoxins [4, 5]. Also, other PUFAs are substrates for these reactions, e.g., conversion of linoleic acid (C18:2n6, LA) and alpha-linolenic acid (C18:3n3, ALA) to 13-hydroxy octadecadienoic acid (HODE) and 13-hydroxy octadecatrienoic acid (HOTrE), respectively [6], or conversion of docosapentaenoic acid (C22:5n6, DPA) to 17-hydroxy-DPA or 10,17-dihydroxy-DPA which have been characterized as anti-inflammatory lipid mediators [7, 8].

In an analogous manner, OH-FAs result from reduction of hydroperoxides formed via autoxidation of PUFAs [9, 10]. Aside from analgesic and anti-inflammatory epoxy-FA formation by CYP2 isoforms [11, 12], the CYP branch of the ARA cascade can give rise to a diverse spectrum of OH-FAs. CYP4

enzymes catalyze predominantly hydroxylation at  $\omega$  or  $\omega-1$  position, yielding 20-HETE and 19-HETE, or the corresponding metabolites of other PUFA. 20-HETE has direct biological activity, acting as vasoconstrictor among other functions [13]. Moreover, CYP enzymes catalyze further hydroxylation of PUFA to several metabolites, such as 11-HETE, 12-HETE and 13-HETE [14].

The n3 PUFAs, particularly EPA and DHA are also efficiently metabolized by the pathways described above [2], thus adding a large number of OH-FAs with potential biological activity to the OH-FA lipidome. The formation of important OH-FAs derived from ARA, EPA and DHA is summarized in Fig. 5.1. Several of the EPA- and DHA-derived OH-FAs, such as 18-hydroxy eicosapentaenoic acid (HEPE), 17-hydroxy docosahexaenoic acid (HDHA) and 14-HDHA, are precursors of potent multiple hydroxylated lipid mediators such as resolvins, protectins and maresins [4, 15]. Of these, particularly for the 15-LOX-derived 17-HDHA, there are data indicating direct anti-inflammatory properties [8], comparable to the multihydroxylated resolvins [16-19].

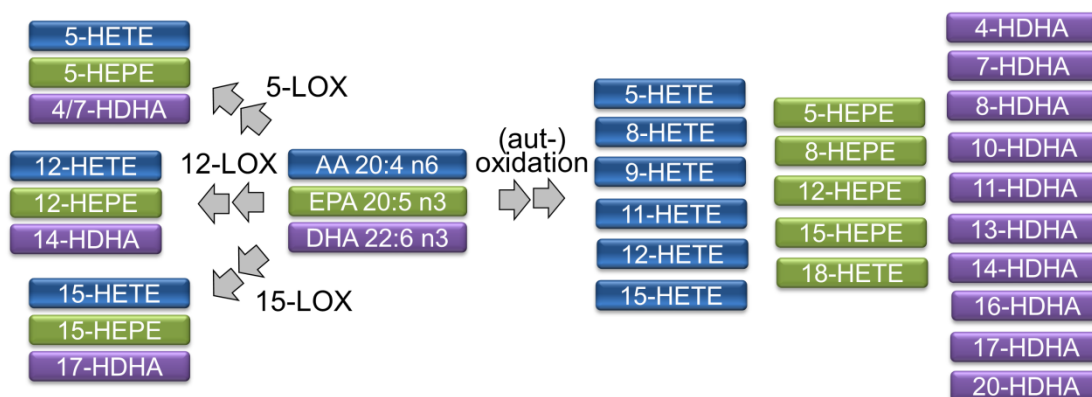


**Fig. 5.1:** Simplified overview about the formation routes of OH-FAs from ARA (red), EPA (green) and DHA (blue) analyzed in this study. Shown are the 5, 12, and 15 lipoxygenase pathways leading to OH-FAs via an intermediate formation of a hydroperoxide. Moreover, a large number of OH-FAs can be formed by (aut)oxidation shown on the right. Note: The CYP4 mediated  $\omega$  and  $\omega-1$  hydroxylations leading e.g. to 20-HETE are not included in the figure.

Quantification of OH-FAs can, therefore, be used to assess and understand the activity of multiple lipid metabolite formation pathways, e.g. to analyze LOX enzyme pathways, instead of analyzing the instable initially formed

hydroperoxides. In this context, reliable quantification methods for the determination of OH-FAs are indispensable. Several methods for the quantification of OH-FAs in biological matrices have been developed. In the past, gas chromatography mass spectrometry (GC-MS) following extraction and derivatization was used [20]. Though, this technique is still a powerful analytical tool [21], nowadays liquid chromatography mass spectrometry (LC-MS) is predominantly used for the quantitative analysis of a large number of oxylipins, such as OH-FAs. Some of these methods cover a large number of OH-FAs, e.g., 37 [22], 21 [23], 17 [24, 25] or 15 [26] among other oxylipins making a targeted metabolomics analysis of OH-FA formation feasible. However, with 15-26 min runtimes, these methods are rather long for modern ultra-high performance LC [22, 23, 26]. This impedes sample throughput and thus mechanistic studies on the formation and biological role of OH-FAs. In order to allow quantification of a comprehensive set of OH-FAs in a large number of samples, the aim of the present study was, therefore, the development of a rapid LC-MS method with automated sample preparation. The performance of the method was thoroughly characterized and the method was validated for direct analysis of plasma and cell culture samples. The applicability is demonstrated by the comparison of the OH-FA pattern in four different human and one murine cell line, formed upon incubation with PUFA ethyl esters. The results of this study provide new interesting insights in the OH-FA generation in cell lines, which warrants further investigation

## **5.2 Experimental**

### **5.2.1 Chemicals and Biological Materials**

Dulbecco's modified Eagle's medium (DMEM), fetal calf serum (FCS) and all other cell culture reagents were purchased from Biochrom (Berlin, Germany). LC-MS grade acetonitrile (ACN), acetic acid (HAc) and methanol (MeOH) were from Fisher Scientific (Nidderau, Germany). Oxylipin standards and internal

standards (Table 5.1) were purchased from Cayman Chemicals (local distributor: Biomol, Hamburg, Germany). All other chemicals were purchased from Sigma Aldrich (Schnelldorf, Germany). HCA-7 cells were from the European Collection of Cell Cultures (ECACC, Salisbury, United Kingdom) and all other cell lines were from the German Collection of Microorganisms and Cell Cultures (DSMZ, Braunschweig, Germany). Pooled human EDTA plasma was obtained from healthy male volunteers.

### 5.2.2 LC-MS analysis

Quantification of OH-FAs was carried out by LC-MS with automated sample preparation by online-SPE in backflush mode (Fig. 5.2) as described [27]. Two binary Agilent 1290 pumps and an Agilent 1290 column oven (Agilent, Waldbronn, Germany) equipped with a high-pressure six-port two-position valve (valve 1, Fig. 5.2) were used. Samples were kept at 4 °C in an xt-PAL autosampler (CTC Analytics, Zwingen, Switzerland) with an injection loop of 20  $\mu\text{L}$  and a 100  $\mu\text{L}$  syringe; wash solution 1 was 0.1% HAc in water and wash solution 2 was ACN. The complete setup is shown in Fig. 5.2. At the beginning of each analysis, 5  $\mu\text{L}$  of the sample was transferred through a 0.3  $\mu\text{m}$  SS frit (1.3  $\mu\text{L}$ ) inlet filter (Agilent part number 5067-4638) and valve 1 to the 1 x 20 mm Oasis-HLB SPE column (particle size 25  $\mu\text{m}$ , Waters, Eschborn, Germany) with a flow of 3.5  $\text{mL min}^{-1}$  0.1% aqueous HAc (solvent A) delivered by pump 1 (Fig. 5.2). After 30 s, the six-port valve 1 (Fig. 5.2) was switched and the analytes were eluted in reversed direction (backflush) with the LC flow (0.5  $\text{mL min}^{-1}$ ) of pump 2. The valve was switched back after 1.5 min. Separation of hydroxy-FAs was achieved on a 50 x 2.1 mm Kinetex RP-C18 column filled with 1.3  $\mu\text{m}$  fused core particles with 100 Å pores (Phenomenex, Torrance, CA USA) equipped with a Crude Catcher inlet filter (Phenomenex). The outlet of the analytical column and the waste line of the SPE-column were connected to a Valco six-port two-position valve (valve 2, Fig. 5.2) implemented in the MS. Valve 2 was switched after 1.5 min allowing the separate collection of the aqueous waste and reducing contamination of the MS source.

For pump 1, solvent A was 0.1% HAc and solvent B was 95/5 ACN/water acidified with 0.1% HAc (v/v). Gradients and flow rates are depicted in Fig. 5.2. Separation was carried out by the isocratic flow of pump 2 which comprised of 55% solvent B (800/150/1 ACN/MeOH/HAc v/v) and 45% solvent A (water/solvent B 95/5, v/v, acidified with 0.1% HAc). After the separation is completed at 5.0 min, the column is cleaned for 0.6 min with 100% solvent B (~2 void volumes) and equilibrated at 55% B for 0.3 min as well as during the next injection cycle and the SPE extraction (~4 void volumes).

Mass spectrometric detection was carried out on an AB Sciex 6500 QTRAP instrument (AB Sciex, Darmstadt, Germany) in selected reaction monitoring (SRM) mode following negative electrospray ionization. The instrument was operated with the following parameters: ion spray voltage -4.5 kV, entrance potential -10 V, curtain gas 35 psi, gas 1 and gas 2 both 60 psi, temperature 500 °C. The collision-activated dissociation (CAD) gas was set to high (12 psi) and declustering potential (DP), collision energy (CE) and collision cell exit potential (CXP) were optimized for each transition as shown in Table 5.1. Nitrogen was used as nebulizer, desolvation and collision gas. The instrument was operated in scheduled SRM mode with a detection window of  $\pm 12.5$  s around the expected retention time and a maximum cycle time of 0.5 s. Quantification was performed by an external calibration using 4 deuterated internal standards (IS, Table 5.1). For calibration, the analyte to IS area ratios were linearly fitted reciprocally weighted by concentration. Instrument controlling was performed with Analyst 1.6.1 and data analysis was carried out with Multiquant 2.2 (AB Sciex).

**Table 5.1:** Parameters of the online-LC-ESI(-)-MS/MS method for the determination of the concentration of hydroxy-fatty acids in biological samples. Shown are all analytes covered by the current method, the mass transition used for quantification in scheduled SRM mode, the electronical MS parameters declustering potential (DP), collision energy (CE), collision cell exit potential (CXP), the internal standard (IS), the retention time and its standard deviation (SD), peak width (full width at half maximum height (FWHM)), limit of detection (LOD,  $s/n > 3$ ) and limit of quantification (LLOQ,  $s/n > 9$ , accuracy  $\pm 15\%$ ). It should be noted, that the actual dynamic range for the quantification in the sample matrix depends on the dilution (2-4 fold for plasma and media) during sample preparation.



Table 5.1:

Analyte	Mass transition		MS Parameters			IS	Retention time <sup>1</sup>		Peak width <sup>2</sup>	LOD	Calibration			R <sup>2</sup>
	m/z (MS1)	m/z (MS3)	DP (V)	CE (V)	CXP (V)		(min)	SD (S)			LOD (nM)	lower conc (nM) <sup>3</sup>	upper conc (nM) <sup>4</sup>	
LA	295.2	195.2	-80	-26	-9	d4-9-HODE	2.38	0.8	2.6	0.4	1	2000	0.999	
	295.2	171.1	-80	-26	-7	d4-9-HODE	2.41	0.9	2.8	0.1	0.4	2000	0.999	
ALA	293.2	195.1	-70	-24	-8	d4-9-HODE	1.9	1.8	3.9	0.1	0.25	500	0.999	
	293.2	171.2	-65	-22	-8	d4-9-HODE	1.83	1.5	3.6	0.1	0.25	500	0.999	
MA	319.2	289.1	-80	-24	-6	d6-20-HETE	2.06	1	2.9	1	2	500	0.996	
	319.2	219.2	-60	-20	-8	d8-12-HETE	2.59	1	3	0.5	1	500	0.999	
	319.2	167.2	-60	-23	-7	d8-12-HETE	2.8	1	2.9	0.1	0.25	500	0.999	
	319.2	155.2	-60	-22	-6	d8-12-HETE	2.95	0.9	3	1	5	500	0.999	
	319.2	179.2	-60	-20	-8	d8-12-HETE	2.96	0.9	3.1	0.25	0.5	500	0.999	
	319.2	167.2	-60	-23	-7	d8-5-HETE	3.1	1.3	3.2	1	2	500	0.999	
	319.2	115.2	-60	-21	-7	d8-5-HETE	3.24	1.4	3.5	0.1	0.25	500	0.999	
EPA	317.2	259.2	-55	-17	-7	d4-9-HODE	1.9	0.8	2.9	0.25	0.5	500	0.999	
	317.2	219.2	-60	-20	-10	d4-9-HODE	2.06	0.8	2.9	0.5	1	500	0.999	
	317.2	155.2	-60	-20	-8	d4-9-HODE	2.14	1	2.9	0.25	0.5	500	0.999	
	317.2	179.2	-65	-20	-8	d4-9-HODE	2.18	1.5	3.7	0.25	0.5	500	0.999	
	317.2	115.1	-60	-20	-6	d4-9-HODE	2.31	1.6	3.9	0.25	0.5	500	0.998	
DHA	343.2	241.2	-55	-19	-7	d8-12-HETE	2.5	1.5	3.7	0.5	1	20	0.997	
	343.2	233.2	-55	-19	-7	d8-12-HETE	2.7	1.5	3.8	0.25	0.5	20	0.998	
	343.2	193.1	-55	-19	-7	d8-12-HETE	2.81	1.6	3.6	0.5	1	20	0.998	
	343.2	201.2	-60	-20	-6	d8-12-HETE	2.71	1.6	3.8	2	3	500	0.998	
	343.2	153.2	-45	-21	-7	d8-12-HETE	2.91	1.6	3.9	0.25	0.5	20	0.998	
	343.2	205.2	-50	-19	-7	d8-12-HETE	2.88	0.9	2.8	0.5	1	500	0.999	
	343.2	121.1	-45	-20	-7	d8-5-HETE	3.06	0.6	3.1	0.5	1	20	0.996	
	343.2	141.2	-55	-19	-7	d8-5-HETE	3.08	2.1	3.3	1	2	500	0.999	
	343.2	189.2	-50	-19	-7	d8-5-HETE	3.18	1.3	3.3	1	2	20	0.997	
	343.2	101.1	-55	-19	-7	d8-5-HETE	3.62	0.6	3.6	0.25	1	500	0.999	

A breakthrough of OH-FAs was analyzed by connecting the outlet of the SPE column (Fig. 5.2) to the MS (split 1:10) and injecting 5-20  $\mu\text{L}$  of a 40 nM standard in ACN while keeping the flow at  $3.5 \text{ mL min}^{-1}$  100% 0.1% acetic acid for 1 min. The transfer time to elute the analytes from the SPE column was assessed by removing the analytical column from the setup (Fig. 5.2) and directly monitoring the eluate of the SPE column by the flow delivered from pump 2.

Carry over was determined by injecting the highest standard (500 nM of OH-FAs except for 2000 nM of HODEs) and a subsequent injection of MeOH. Carry over was calculated based on the peak area observed in the MeOH injection.

### 5.2.3 Sample preparation

The only sample preparation step carried out was mixing the sample with IS solution yielding a final IS concentration of 20 nM followed by centrifugation at 20 000  $\times g$  at 4 °C for 5 min. Cell culture medium samples and plasma samples were either mixed with IS solution in ACN 1:1 (*v/v*; 50  $\mu\text{L}$ +50  $\mu\text{L}$ ; 200  $\mu\text{L}$ +200  $\mu\text{L}$ ) or 1:4 (*v/v*; 25  $\mu\text{L}$ +75  $\mu\text{L}$ ). For determination of accuracy and precision, DMEM (supplemented with 10% FCS, glutamine, penicillin and streptomycin (see below)) and human plasma spiked with a low, medium and high (10, 30, 100 nM) concentration of the analytes were analyzed as quality control samples. The recovery of the OH-FAs was calculated based on the determined concentrations in the quality control samples after subtraction of the determined concentration in non-spiked matrix samples. Three independently prepared samples were analyzed within one batch, and the three samples were analyzed in three different batches on three different days.

### 5.2.4 Cell culture

HCA-7, HCT-116, SW480 and HT-29 cells were cultured in DMEM with 10% FCS, 2 mM glutamine, penicillin (100 IU  $\text{mL}^{-1}$ ) and streptomycin (100  $\mu\text{g mL}^{-1}$ )

in a humidified 37 °C incubator with 5% carbon dioxide. Stock cultures were split at a confluence of 70-80% by using trypsin/EDTA and seeded in 6-well plate dishes at a density of 500 000 cells/well (HCA-7) and 750 000 cells/well (HCT-116, SW480 and HT-29), respectively (8.96 cm<sup>2</sup> growth area per well). Balb/c 3T3 cells were cultured accordingly using Dulbecco's modified Eagle's medium/Hams F12 1:1 (DMEM Hams F12) with 5% FCS, 2 mM glutamine, penicillin (100 IU mL<sup>-1</sup>) and streptomycin (100 µg mL<sup>-1</sup>) and were seeded in 6-well plate dishes at a density of 250 000 cells/well. 24 h after seeding, the medium was removed and replaced by 2 mL medium freshly supplemented with a stock solution of ARA, EPA or DHA ethyl ester (EE) (50 mM in ethanol) yielding a concentration of 50 µM. The same incubations were carried out with and without cells. Medium was sampled before and after 24 hours of incubation and all experiments were carried out in quadruplicates.

## **5.3 Results and Discussion**

### **5.3.1 Online-SPE-LC-MS**

A central aim of our study was the development of a LC-MS method for the rapid quantification of the major OH-FAs from all the biologically relevant PUFAs: LA, ALA, ARA, EPA and DHA. In order to allow high throughput, the analysis time was kept short and the manual sample preparation was minimized. As demonstrated for the analysis of epoxy-FAs and dihydroxy-FAs [28], sample preparation in oxylipin analysis can be reduced by means of online-SPE. Similar to this study, online-SPE was carried out with a basic backflush set-up (Fig. 5.2) using an SPE column filled with large particles at high flow rates [28-30]. The setup was extended by a second six-port valve allowing the separate collection of aqueous from organic waste thus preventing contamination of the MS-source by directing the void volume of the analytical column to waste (Fig. 5.2) [27].

The OH-FAs were fully extracted by the online-SPE using Oasis HLB material (Waters) which is commonly used for the offline SPE of oxylipins [25, 26]. No breakthrough was detected following injections of standards in ACN up to an injection volume of 20  $\mu\text{L}$ . Thus, it can be assumed that the analytes are robustly and efficiently extracted following injection of 5  $\mu\text{L}$  biological samples containing less organic solvent. After switching of the six-port valve 1 (Fig. 5.2), the analytes were rapidly eluted from the SPE column by the flow of pump 2 and transfer of all OH-FAs was completed after 1.2 min. The six-port valve could, therefore, be switched back at 1.5 min before the elution and detection of the OH-FAs.

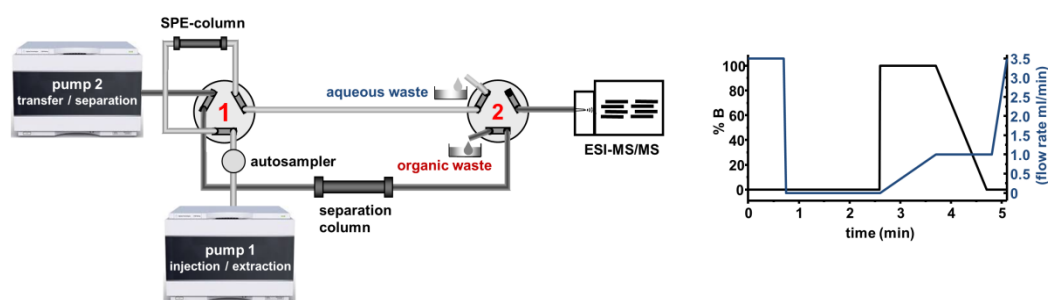


**Fig. 5.2:** Online-SPE-LC-MS setup (**left**). Following addition of IS solution and centrifugation the crude samples are directly injected. The samples are transferred onto the SPE column by the flow of pump 1. The flow rate and gradient of pump 1 are depicted on the **right**. After 0.5 min the six-port valve 1 is switched and the analytes are transferred from the SPE to the separation column and separated by the isocratic flow of pump 2. The second valve further prevents contamination of the MS source and allows collecting the aqueous waste separately from the organic waste.

The used separation column combines the high chromatographic resolution of an efficient mass transfer and high surface area of small particles with equal distribution of diffusion paths of fused core particles [31]. Indeed the separation efficiency of the OH-FAs was high, leading to narrow peaks with a full width at half maximal height (FWHM) of about 3 s corresponding to a high number of theoretical plates, e.g.,  $19 \times 10^5$  for 8-HETE (Fig. 5.3C; Table 5.1). The structurally similar analytes eluted in a short retention time window of 1.8 min between 1.8 and 3.6 min total analysis time (Fig. 5.3). The best separation was obtained using isocratic conditions for transfer and separation.

Despite the application of online-SPE, narrow peaks (small FWHM) were obtained for HODEs, HOTrEs, HETEs and HEPEs. Also, the stronger retained HDHAs showed only low or moderate tailing. Only for 4-HDHA, eluting more than 0.5 minutes later than all other OH-FAs, significant tailing was observed, which was with a FWHM of 3.6 sec still acceptable (Fig. 5.3).

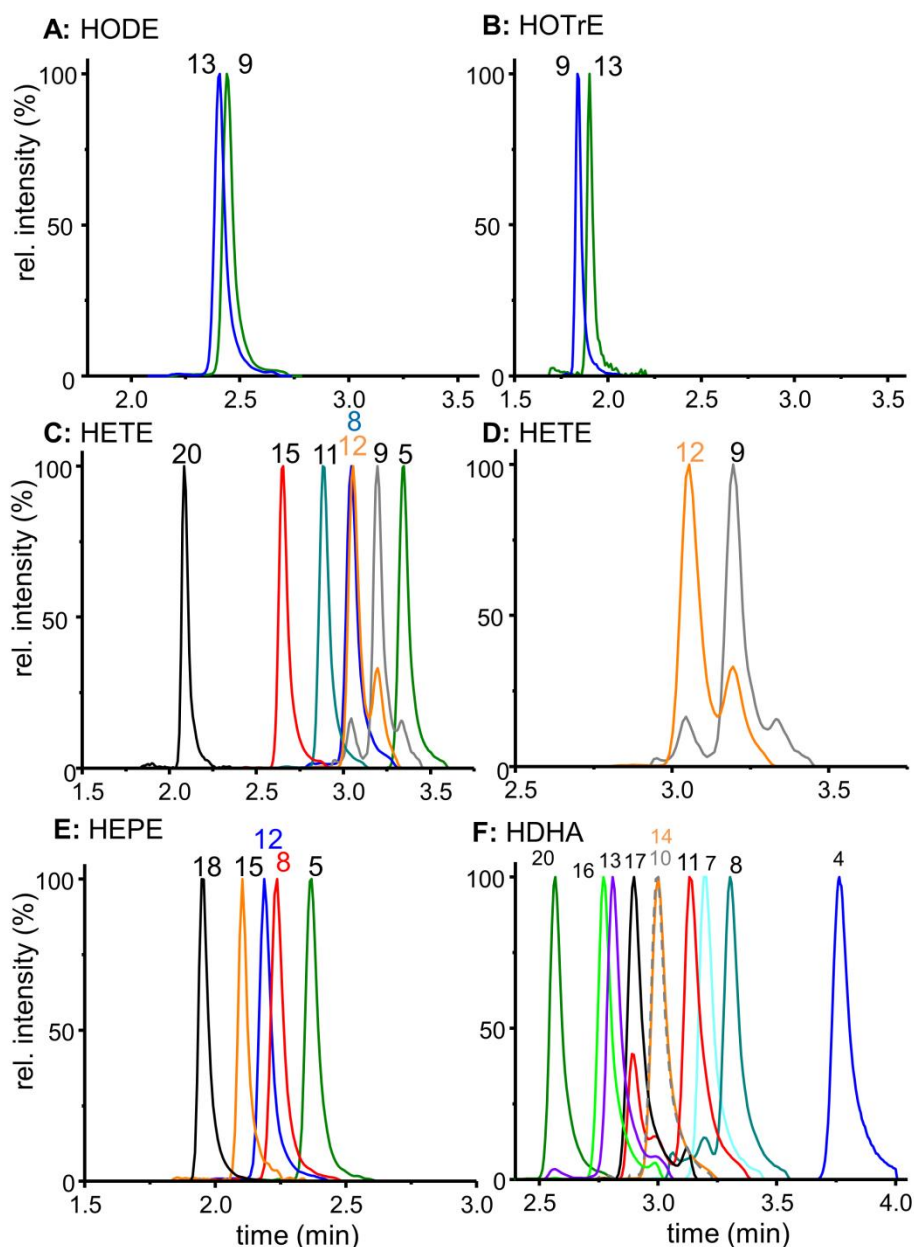


**Fig. 5.3:** Separation efficiency of the developed method. Shown are the SRM signals used for quantification following injection of a multianalyte standard (20 nM). **A:** LA derived HODEs, **B:** ALA derived HOTrEs, **C:** ARA derived HETEs, **E:** EPA derived HEPEs and **F:** DHA (22:6) derived HDHAs. The critical separation pair 12-/9-HETE is shown superimposed in panel **D**.

As a result of the separation efficiency, the OH-FA regioisomers were well resolved. For example, 5 of the 7 analyzed HETEs and 4 out of 5 analyzed HEPEs were (almost) baseline separated (Fig. 5.3). Nevertheless, several regioisomers eluted together. Almost perfect co-elution occurred for 8-HETE and 12-HETE as well as 10-HDHA and 14-HDHA, whereas regioisomers of HODEs and HOTrEs as well as 12-HETE and 9 HETE, 12-HEPE and 8-HEPE and different HDHAs were not fully separated (Fig. 5.3). Moreover, the OH-FAs of the different PUFA coeluted.

Regarding these limitations, it should be noted that even methods using longer separation columns (with more theoretical plates), slower gradients and thus longer runtimes do not allow to fully resolve the structurally so similar OH-FAs chromatographically. For example, in the method of Yang et al. [24, 25] and Strassburg et al. [26], using a 150 x 2.1 mm column with 1.8  $\mu\text{m}$  or 2.7  $\mu\text{m}$  particles and gradients of 21-25 min, co-elutions occurred. Likewise, the retention times of the method used by Gomolka et al. on a 150 x 2.1 mm column with 3.5  $\mu\text{m}$  particles were similar, indicating the co-elution of several OH-FAs [23]. Also, after derivatization to *N*-(4-aminomethylphenyl) pyridinium amides – improving ESI(+) detection sensitivity – co-elutions occurred, e.g., of 11-HETE and 12-HETE [32]. Overall it has to be concluded that reversed phase chromatography alone is not sufficient for a specific detection of OH-FAs. Since regioisomers have the same (exact) mass (Table 5.1), detection in selected reaction monitoring, based on the different fragmentation of the regioisomers is indispensable to specifically quantify the OH-FAs independently from one another by means of LC-MS.

Similar to previous LC-MS methods [22, 25, 26, 33, 34], detection was carried out following negative ESI ionization based on the fragment resulting from  $\beta$ -cleavage of the carbon-carbon-bond adjacent to the hydroxyl group. Taking localization of the negative charge at the carboxyl group into account, the dominant fragment ions with chain lengths according to the position of the hydroxyl group ( $n$ ) or  $n-1$  were used for quantification (Table 5.3). Only for 11-

HDHA, 17-HDHA and 20-HDHA different transition ions were used as described [23].

Following injection of standard mixtures, multiple peaks were observed in the signals of several transitions (Fig. 5.3). For example, the transition  $m/z$  319→167 (9-HETE) yielded a signal for 9-HETE, 12-HETE and 15-HETE and  $m/z$  319→179 (12-HETE) for 12-HETE and 9-HETE (Fig. 5.3). Moreover, in the transition of  $m/z$  343→121 (11-HDHA) a strong signal is observed for 17-HDHA (Fig. 5.3, App. Fig. 9.2.1). Thus, SRM detection of OH-FAs is – as well known for other oxylipins [25] – far away of being fully specific and analysis of OH-FAs requires an efficient chromatography.

In the presented method, only one critical separation pair [25], with interfering SRM transitions and incomplete chromatographic separation, was identified: 12-HETE and 9-HETE (Fig. 5.3). MS/MS analysis of both compounds failed to deduce a fragment which was exclusively formed by one of the two analytes allowing a more specific detection. All dominant fragments formed from the  $[M-H]^-$  ion of 9-HETE resulted also from 12-HETE fragmentation (see fragmentation pattern in [35]). Nevertheless, the separation was sufficient for reproducible integration yielding good accuracy and precision of both HETEs (see below).

The limit of detection (LOD) for the different OH-FAs, defined as signal/noise ratio ( $s/n$ ) = 3, was determined as 0.1-2 nM (Table 5.1) corresponding to 0.5-10 fmol on column. With this performance, the method is more sensitive or comparable to state of the art targeted metabolomics LC-MS methods of oxylipins with LODs of 0.2-4.2 nM [26], 0.01-0.21 ng (~30-600 fmol) [23], 10-30 pg (~30-90 fmol) [36], 0.1-1 pg (~0.3-3 fmol) [22], 10-20 pg (~30-60 fmol) [33] and 0.2-10 pg (~0.6-30 fmol) on column [32] or reported lower limits of quantification (LLOQs) of 0.1-5 nM [25].

Using four deuterated OH-FAs as IS at a concentration of 20 nM, an excellent linear correlation of the signal was obtained ( $R^2 > 0.997$ ). The LLOQ, defined as  $s/n = 9$  and  $\pm 15\%$  accuracy of the calibration curve, ranged for the OH-FAs

between 0.25-5 nM. This sensitivity allows the quantification of a large number of OH-FA in cell culture samples (see below). However, the low concentration of several OH-FA in plasma and serum samples [6, 37] might require a pre-concentration on the SPE column and thus higher injection volumes than tested in this study. For all analytes, the upper limit of quantification was not reached by the highest standard injected indicating a dynamic range of more than three orders of magnitude. Despite the use of SPE, carry over was found to be negligible, being highest for the strongest retained 4-HDHA with  $0.11 \pm 0.01\%$  ( $n=3$ ) and lowest for the polar 9-HOTrE with  $0.05 \pm 0.001\%$  ( $n=3$ ).

The performance of the method for the quantitative analysis of OH-FAs in biological samples was characterized oriented on the Guideline on bioanalytical method validation of the European Medicine Agency 2011 (EMA/CHMP/EWP/192217/2009). For this purpose, matrix samples were spiked at low (10 nM), medium (30 nM) and high analyte levels (100 nM) and analyzed within one batch and in different batches. Two types of biological matrices were used: (i) cell culture medium (DMEM) with 10% FCS representing the matrix of the samples from cell culture analyzed below and (ii) human plasma as matrix containing more protein, lipids and other potentially interfering matrix compounds.

**Table 5.2:** Recovery of IS in cell culture medium and plasma. Recovery was determined based on the peak area of the IS relative to the IS peak area in a matrix-free standard of the same concentration (20 nM). Shown are mean and SD of quadruplicate injections of 24 independently prepared samples per matrix.

	sample:IS	d6-20-HETE	d4-9-HODE	d8-12-HETE	d8-5-HETE
cell medium	1:1	80 ± 9	80 ± 5	76 ± 10	76 ± 10
	1:4	96 ± 12	98 ± 8	94 ± 12	93 ± 12
plasma	1:1	80 ± 9	80 ± 5	76 ± 10	76 ± 10
	1:4	100 ± 10	83 ± 5	92 ± 10	92 ± 11

The only sample preparation step was mixing the sample with IS 1:1 or 1:4 followed by centrifugation. As shown in Table 5.2, the recovery rates of the internal standards obtained in both matrices were higher than 75% indicating efficient extraction from the matrix and low ion suppression. It is interesting that



these levels exceed by far the IS recovery rates for OH-FAs described for classical offline SPE using the same Oasis HLB material [26].

For the analysis of cell culture samples, the accuracy for all spike-levels was good (within  $100\pm 15\%$ , Table 5.3). Similarly, high intra-batch and inter-batch precisions of better than 15% were found. As expected, the variation increased getting close to the LLOQ. Thus, the OH-FAs with a better, i.e., lower LLOQ were determined in the low spiked levels at higher precision (Table 5.3). No apparent differences were observed for mixing IS 1:1 or 1:4 (v/v), indicating dilution integrity and thus efficient removal of potentially interfering matrix from cell culture medium by the online-SPE step.

For the analysis of plasma mixed 1:1 (v/v) with IS solution, the matrix influenced the signals of the OH-FAs. For the early eluting HEPEs, 13-HODE and 13-HOTrE using  $^2\text{H}_4$ -9-HODE as IS slightly too high recovery rates (120-130%) were observed. This could be caused by a higher ion suppression at the IS retention time of 2.4 min compared to the slightly different retention time window of the analytes (Table 5.1). At a higher dilution with IS (1:4, v/v), acceptable recovery rates ( $100\pm 15\%$ ) were observed and thus matrix effects could be diluted out. This supports the assumption that the higher than supposed levels at 1:1 dilution are caused by ion suppression/ion enhancement effects of the matrix. All other OH-FAs were determined with good accuracy in spiked quality control plasma at both dilutions, except for few outliers (8-HETE, 12-HETE and 9-HETE with still tolerable recovery rates of about 72-80%). Overall intra- and inter-batch precision was high and better than 15% (Table 5.3). However, for 1:1 dilution of plasma, few analytes such as 20-HETE or 17-HDHA were determined at low concentrations with low precision. This high variation might be problematic for the analysis of biological samples by masking physiological effects.

**Table 5.3:** Accuracy and precision of the method. Cell culture medium including 10% FCS and human plasma were spiked at low, medium and high concentration (10, 30, 100 nM) of the OH-FAs. The samples were either prepared by mixing 1:1 (v/v) or 1:4 (v/v) with IS solution as indicated in the rows. Recovery (accuracy) and SD (variation) were determined for 3 independent samples analyzed within one batch (intra batch accuracy & precision) and within 3 batches on 3 different days (inter batch accuracy & precision).

		LA		ALA		ARA								
		13-HODE	9-HODE	13-HOTrE	9-HOTrE	20-HETE	15-HETE	11-HETE	8-HETE	12-HETE	9-HETE	5-HETE		
plasma	1:1	intra 10	78±7	97±7	135±4	101±1	108±16	105±8	102±3	78±5	76±2	80±12	96±3	
		intra 30	94±16	100±7	134±6	106±3	107±7	107±0	107±3	79±3	78±2	92±4	105±6	
		intra 100	97±1	96±2	123±1	100±4	99±6	98±1	100±1	73±1	72±3	82±6	100±3	
	inter	10	91±26	98±14	143±7	107±4	112±45	93±9	110±11	77±4	84±7	81±19	96±6	
		30	91±21	97±3	134±5	104±6	108±4	106±13	111±1	82±3	82±7	90±7	106±7	
		100	93±14	98±2	125±4	101±4	100±9	102±8	102±5	75±7	76±6	88±1	101±5	
	1:4	intra	10	109±2	96±1	118±17	102±2	94±2	102±2	104±6	73±23	81±2	89±6	96±4
			30	102±7	93±10	110±14	104±3	92±12	97±8	106±2	76±13	80±6	97±23	100±2
			100	94±1	95±1	108±2	105±1	99±4	99±3	101±3	83±1	79±2	80±7	92±3
		inter	10	111±3	95±3	108±18	112±16	97±19	108±10	100±3	72±3	79±8	79±10	92±5
			30	103±4	93±5	114±2	108±9	111±22	100±13	109±3	77±7	80±3	90±9	99±2
			100	96±2	97±2	111±1	109±3	99±7	105±8	106±4	79±5	78±3	80±4	99±6
cell medium	1:1	intra 10	99±3	100±4	103±5	100±2	99±9	106±5	110±7	107±5	101±7	101±7	103±2	
		intra 30	95±3	97±3	96±5	97±2	97±0	101±4	97±4	97±4	95±5	97±5	99±2	
		intra 100	88±3	88±2	87±3	87±2	87±3	96±1	93±2	96±5	91±2	89±5	91±3	
	inter	10	101±7	101±3	104±5	94±5	104±12	109±11	111±3	107±9	104±3	96±3	102±2	
		30	95±3	97±3	97±2	97±2	100±5	102±1	104±6	103±5	104±7	97±7	100±1	
		100	88±2	89±3	89±2	89±3	88±3	96±8	91±5	95±6	93±8	94±3	91±2	
	1:4	intra	10	97±5	96±4	93±6	92±5	109±13	105±6	104±4	100±7	105±5	99±4	105±1
			30	93±3	95±3	91±4	90±2	102±6	100±3	99±4	103±4	96±7	92±9	97±5
			100	89±5	92±4	86±4	87±3	89±2	95±3	95±5	95±4	95±4	90±5	91±2
		inter	10	98±2	99±2	99±2	94±7	93±11	108±5	105±0	102±10	101±0	93±6	107±3
			30	94±3	95±3	90±1	90±3	101±7	102±4	101±1	103±4	98±5	101±6	102±1
			100	87±4	89±10	87±2	86±2	88±5	98±6	95±4	96±5	97±2	94±4	94±0

Table 5.3: Continued.

		EPA					DHA					
		18- HEPE	15- HEPE	8- HEPE	12- HEPE	5- HETE	17- HDHA	14- HDHA	7- HDHA	4- HDHA		
plasma	1:1	intra 10	131±3	125±2	131±6	123±5	124±3	81±10	90±10	88±3	90±3	
		intra 30	134±2	125±4	125±3	121±5	123±3	90±4	98±3	89±3	92±6	
		intra 100	122±3	121±3	117±2	113±3	115±2	83±1	91±3	81±3	87±3	
	inter	10	132±5	122±9	127±6	123±6	118±4	119±41	99±2	83±3	89±5	
		30	129±5	123±5	122±6	119±7	120±5	98±8	92±7	87±4	93±4	
		100	120±3	120±5	116±2	115±3	114±1	85±2	88±9	82±4	87±3	
	1:4	intra	10	115±2	108±10	113±4	114±7	104±7	107±6	100±8	93±8	90±2
			30	110±5	115±3	110±3	112±3	106±2	92±14	96±2	93±6	90±2
			100	110±1	108±2	105±2	105±1	102±2	93±0	96±4	88±2	85±2
		inter	10	112±8	112±12	107±2	108±3	101±8	96±9	91±11	84±3	85±4
			30	110±2	112±6	107±2	109±5	104±3	103±1	96±13	91±8	89±7
			100	108±5	106±5	104±5	104±5	102±7	101±13	100±3	89±4	84±7
cell medium	1:1	intra 10	102±2	102±3	99±3	92±1	99±3	95±14	108±16	92±7	96±3	
		intra 30	96±3	93±6	95±3	93±3	94±4	92±10	94±2	88±6	93±3	
		intra 100	86±3	86±3	87±2	86±2	87±1	96±7	93±2	83±1	88±2	
	inter	10	102±3	102±3	98±3	93±2	97±1	92±7	106±16	83±3	93±2	
		30	92±4	92±5	91±2	89±5	92±5	93±7	88±4	87±4	90±3	
		100	85±2	85±1	86±1	85±2	85±1	86±5	89±7	82±4	87±5	
	1:4	intra	10	99±6	97±8	94±10	91±2	97±6	104±21	104±11	98±12	101±2
			30	90±4	92±3	90±3	89±2	91±1	96±9	101±5	97±6	96±2
			100	88±5	88±3	87±5	88±5	87±3	91±7	97±4	92±3	91±4
		inter	10	101±4	103±4	97±8	89±6	97±8	110±15	106±7	104±7	93±14
			30	91±2	92±3	90±4	88±3	87±6	94±9	101±6	100±5	95±3
			100	85±3	87±4	86±6	87±3	85±5	97±6	95±6	92±4	90±4

Based on these method characteristics, it is concluded that the developed rapid analysis method allows the sensitive determination OH-FAs in crude medium and plasma samples with good accuracy and precision. With the simultaneous detection of 26 analytes the developed method allows determining a comprehensive pattern of enzymatically and non-enzymatically formed OH-FAs. This makes a targeted metabolomics analysis of the pathways of the ARA cascade easily feasible. Only the method described by Dennis and Coworkers

[22] covers with 37 more OH-FAs, whereas other targeted metabolomics methods of the ARA cascade provide only quantitative information on fewer OH-FAs, e.g., 21 [23], 17 [24, 25] 15 [26] and 14 [33]. With a total analysis time of 6.5 min, the developed method is at the same time faster and can compete with all other approaches in terms of sensitivity, accuracy and precision (see above). Only the method of Miller is with 6 min equally fast, but covers only 3 OH-FAs [34]. Most importantly, the developed method allows the direct injection of samples after IS addition and centrifugation due to automated sample preparation by online-SPE. All other LC-MS-based targeted metabolomics approaches for the analysis of OH-FAs utilize classical (offline) SPE impeding sample throughput. Since sample preparation and analysis time is fast, our approach allows the analysis of about 200 samples per day by a single operator. This makes – for the first time – a detailed analysis of the formation of OH-FAs as lipid mediators and pathway markers in the ARA cascade in large sample sets, e.g., from cell cultures, feasible.

### **5.3.2 Analysis of OH-FA pattern in cell culture**

Cell culture of cell lines from different human tissues has become the standard tool for the mechanistic investigation of cellular pathways and regulatory networks. Surprisingly few information is available on the oxylipin pattern formed by these models [35, 38-40]. This may be explained by the long runtimes and laborious sample preparation of today's LC-MS-based targeted metabolomics methods.

In order to demonstrate that our rapid approach is well-suited for mechanistic studies of lipid mediator formation in cell culture, we investigated 4 human colon carcinoma cell lines and a murine fibroblast cell line after incubation with the ethyl ester of either ARA, EPA or DHA (50  $\mu$ M). Before incubation, no or very low OH-FA levels (<10 nM) were detected in the cell supernatant media. Similarly, in non-supplemented medium no relevant formation of OH-FAs (<10 nM) was found. By contrast, following 24 h incubation of cell culture

medium with 50  $\mu\text{M}$  PUFA-EE a strong formation of OH-FAs was observed in HCA-7, SW-480 and Balb/c 3T3 cells (Fig. 5.4), whereas HT-29 and HCT-116 cells showed no product formation compared to cell free controls (App. Fig. 9.2.2).

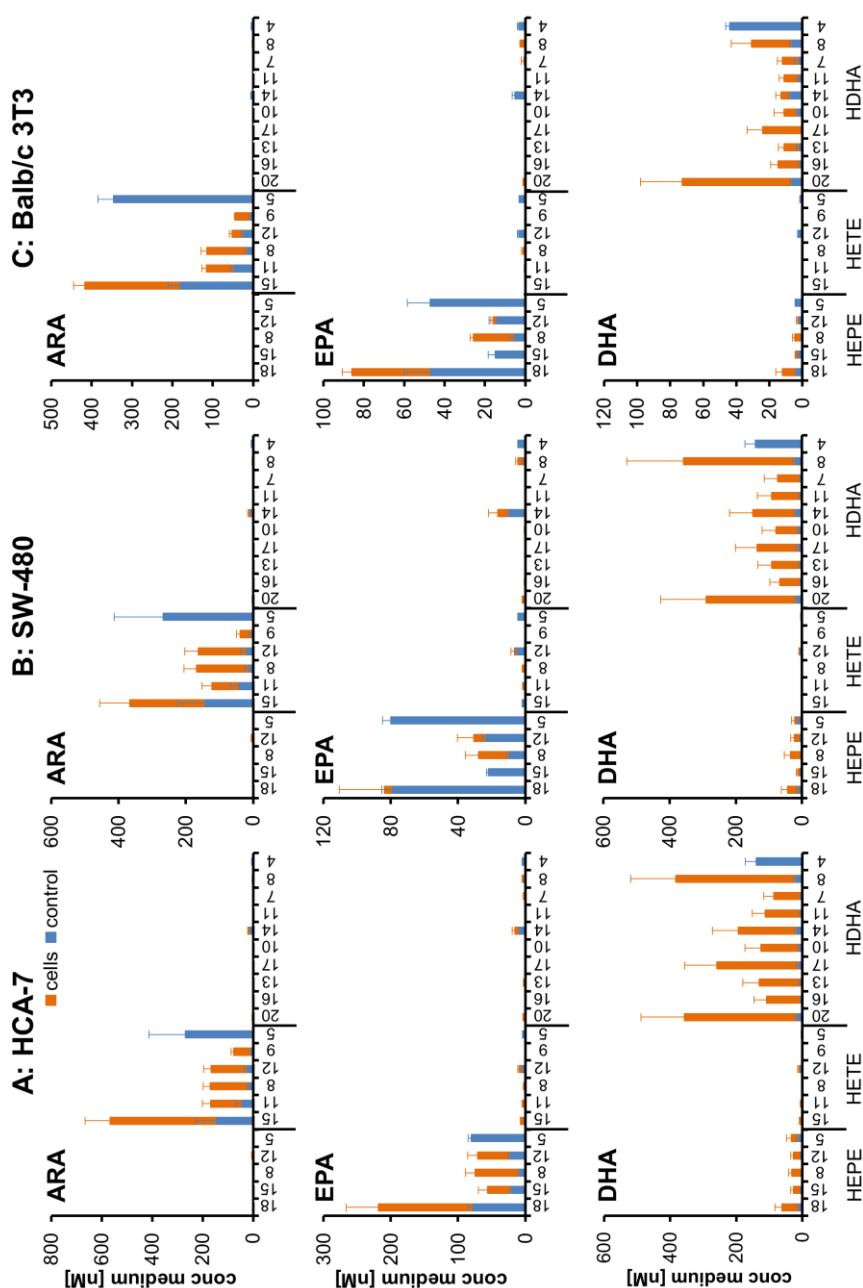


**Fig. 5.4:** Formation of OH-FAs in cell culture medium. HCA-7 (A), SW480 (B) and BALB/c 3T3 (C) were incubated with PUFA ethyl esters (50  $\mu\text{M}$ ) for 24 hours. Shown is the concentration of an incubation with (dark grey) and without cells (light grey) reflecting formation by hydrolysis and autoxidation. Incubations for every cell line were carried out with ARA, EPA and DHA. The concentrations in the media before incubation and in incubations without addition of PUFA were below 10 nM (not shown). All results are given as mean $\pm$ SD (n=4).

Incubation of HCA-7 cells with ARA-EE led to a dominant formation of 15-HETE ( $567\pm 100$  nM) followed by about 200 nM of 11-HETE, 8-HETE and 12-HETE (Fig. 5.4A, left column). In presence of EPA-EE 18-HEPE was detected at highest concentration ( $218\pm 48$  nM) followed by 15-HEPE, 8-HEPE, and 12-HEPE with about 60 nM. DHA-EE was converted by the HCA-7 cells to a diverse pattern of HDHAs with highest concentration for 20-HDHA ( $357\pm 131$  nM) and 8-HDHA ( $383\pm 137$  nM), followed by 17-HDHA ( $259\pm 98$  nM) and 14-HDHA ( $194\pm 78$  nM), whereas for 16-HDHA, 13-HDHA, 10 HDHA, 11-HDHA and 7-HDHA a concentration of about 100 nM was found. SW480 cells produced overall the same pattern and concentration of HETEs and HDHAs following incubation with ARA-EE and DHA-EE respectively (Fig. 5.4B). 15-HETE as well as 20-HDHA and 8-HDHA were formed dominantly. Interestingly, the conversion of EPA by SW480 cells was much lower compared to HCA-7 cells (Fig. 5.4B, middle). A similar low conversion of EPA was observed for the fibroblasts Balb/c 3T3 which only exceeded the control incubations without cells for 18-HEPE and 8-HEPE (Fig. 5.4C middle). For Balb/c 3T3, the conversion rate of DHA was also about five fold lower than for the two colon cell lines (Fig 5.4C, bottom). However, the overall pattern of metabolites formed was consistent: All HDHAs were generated except for 4-HDHA with a dominant formation of 20-HDHA, 8-HDHA and 17-HDHA. Generation of HETE from ARA EE was also slightly lower; however, with  $417\pm 28$  nM 15-HETE was formed in the same range as with the other cell lines. The overall similar pattern of OH-FAs generated by these three cell lines implies a rather unspecific formation, or common pathways in the two colon cell lines and the fibroblast cell line. Nevertheless, when assaying the colon carcinoma cell lines HT-29 and HCT-116 under the same conditions, no or only slightly elevated concentrations of OH-FAs compared to the control could be detected. This indicates that formation of OH-FA is highly cell line-dependent. For all incubations, high standard deviations ( $>35\%$ ) in the determined OH-FA concentrations were observed, e.g. 8-HDHA and 20-HDHA (Fig. 5.4). Because the precision in spiked medium (see above) was generally  $\leq 15\%$  (Table. 5.3) it is concluded

that these high variations are based on differences in the incubations rather than low performance of the analytical method.

Regarding the control incubations of culture media without cells, high concentrations of OH-FAs were detected; particularly of 15-HETE, 5-HETE, 18-HEPE, 5-HEPE and 4-HDHA. Thus, relevant hydrolysis of the PUFA-EE to PUFA and hydroxylation occurs directly in the medium (Fig. 5.4). This might primarily be triggered by components of the fetal calf serum added to the cell culture media, and could be due to auto-oxidation processes in this context. However, levels in the presence of the HCA-7 cells discussed above exceeded the concentration in the controls by at least a factor of 2-3. Thus, dominant routes of formation for the OH-FAs observed with this cell line and for HDHAs as well as 11-, 8- and 12-HETE by SW480 and Balb/c 3T3 seem to be absorption of PUFA-EEs in the cell, enzymatic hydrolysis and conversion to OH-FAs with subsequent release to the cell culture medium.

It is interesting that the concentrations of 5-LOX products, i.e., 5-HETE, 5-HEPE and 4-HDHA were slightly lower (3-20%) in the presence of the cells compared to control incubations without cells. It is reasonable to assume that these OH-FAs are also formed in the media during incubation with cells. The initially formed 5-HETE, 5-HEPE and 4-HDHA are probably then absorbed and converted by the HCA-7, SW-480 and Balb/c 3T3 cells instead of being released to the medium. Different fates of the OH-FAs in the cells can be considered, ranging from esterification and incorporation into lipids [37], conjugation to glucuronic acid (phase II metabolism) [41, 42] or processing to further lipid mediators, e.g., multihydroxylated PUFA [5]. For 5-HETE further oxidation to 5-oxo-ETE by 5-hydroxyeicosanoid dehydrogenase (5-HEDH) [43] as well as hydroxylation by 15-LOX to 5,15-DiHETE [44] are well-characterized pathways. The n3-PUFAs EPA and DHA may undergo similar conversions, e.g., to oxo metabolites [45] or multiple hydroxylated derivatives which are in part potent inflammation resolving mediators [5]. As incorporation in lipids and conjugation are usually rather unspecific for the different OH-FAs, the clearance

of the 5-LOX products from the cell culture media might indicate a further processing of 5-HETE, 5-HEPE and 4-HDHA to new oxylipins in the cell lines tested.

12-HETE, 12-HEPE and 14-HDHA are formed by HCA-7, SW-480 and Balb/c 3T3 cells (Fig. 5.4). However, the formation of these OH-FAs does not dominate over the formation of other OH-FAs indicating only low 12-LOX activity in the cells. The dominant formation of 15-HETE and 17-HDHA could indicate that the cell lines express active 15-LOX. However, HCA-7 cells overexpress COX-2 [46, 47] and it is well known that COX-2 has a side activity to generate 15-HETE [3], which might explain part of the 15-HETE formation by HCA-7. Using the OH-FA levels released to the cell culture medium as LOX pathway marker, the FA-OH pattern does not suggest specifically high activity of LOX enzymes in any of the cell lines tested. This is consistent with reports about expression of LOX enzymes in the cell lines without any activation, showing no 15-LOX activity for HCT-116 [48] and low expression of 5-, 12- and 15-LOX by SW-480 cells [49]. However, significant expression of 15-LOX in HT-29 [49] as well as 5-LOX expression in HCT-116, HT-29 and HCA-7 has been described [50-52] and for HT-29 and HCT-116 even the formation of leukotriene B<sub>4</sub> – a downstream 5-LOX product – could be shown [52]. In Balb/c 3T3 significant formation of 9-HODE and 13-HODE was observed upon epidermal growth factor hormone stimulation which was attributed to LOX activity [40].

Since two of the active (HCA-7 and SW480) and both inactive (HT-29 and HCT 116) were human cell lines originating from colorectal adenocarcinomas [46, 49, 52], this shows that the capability to generate OH-FAs can vary strongly even in cell lines derived from the same tissue and species. Further research will have to address lipid metabolite profiles in direct samples from human colorectal cancer.

Dennis and coworkers carried out incubations with ARA, EPA and DHA and found an impressive pattern of oxylipins in stimulated RAW264.7 macrophages [38]. Consistent with our observations, they found a strong elevation of 20-



HDHA, 16-HDHA and 8-HDHA in Toll-like receptor 4 activated 264.7 cells. Interestingly, no increase in 18-HEPE following EPA treatment was observed. However, it is questionable if these studies are comparable (different cell lines, stimulation vs. no stimulation).

Overall it is striking that 18-HEPE and 20-HDHA are formed most dominantly in three different cell lines. While some authors indicate 18-HEPE as CYP metabolite [38], no detailed information about an enzymatic route of formation is available for this compound. Regarding the formation by radical chain reaction during autoxidation, these OH-FAs are most likely formed via an initial abstraction of a proton at the bisallylic carbon ( $\omega$ -5) of the fatty acid chain of both n3-PUFA, i.e the bisallylic proton located closest to the  $\omega$  end of the fatty acid chain. Interestingly, the dominantly formed OH-FA of the n6-PUFA ARA is 15-HETE, which is initially also formed by abstraction of the proton at the bisallylic carbon at position 13 which is closest to the  $\omega$ -end of the fatty acid chain. Because of the mesomeric stabilization of the intermediately formed radical, protons are preferentially abstracted at bisallylic carbons in radical chain reactions during autoxidation and 11-HpETE and 15-HpETE are the dominating primary products of autoxidation of ARA [9]. Accordingly, for EPA initial abstraction of protons at C7, C10, C13 or C16 occurs [10]. Thus, the formation of 18-HEPE and 20-HDHA is consistent with the expected preferred autoxidation products of the PUFA. Nevertheless, an enzymatic conversion cannot be ruled out because particularly 18-HEPE is formed dominantly compared to other expected metabolites in HCA-7 and Balb/c 3T3 cells. In order to address these questions, the OH-FA pattern of more cell lines should be evaluated and compared with the pattern observed in tissues. With the help of different responses in different cell lines and other molecular biological study approaches, e.g., using expression analysis and co-incubations with inhibitors, the formation pathways of these oxylipins could probably be elucidated in more detail. The rapid LC-MS method described here provides an excellent tool for these studies.

## 5.4 Conclusion

A new rapid LC-MS method for the targeted metabolomics analysis of OH-FA formation within the ARA cascade has been developed and validated for biological samples. With the parallel determination of 26 analytes, the method allows the determination of a comprehensive pattern of OH-FAs. Being equally or more sensitive, the method is with a runtime of 6.5 min, significantly faster than previous methods. Most importantly, the method allows the direct analysis of crude samples after IS addition and centrifugation, thus making the analysis of large sample sets at low cost per sample feasible.

Among the five cell lines tested, two did not release OH-FA after incubation with ARA, EPA and DHA (HT-29 and HCT-116), as compared to media-only control experiments. It is noteworthy, however, that incubation of cell culture medium containing FCS with PUFA-EE alone (without cells present) led to a formation of relevant concentrations of OH-FAs—therefore, media-only control experiments are necessary in order to correctly assess the cellular component of metabolite formation. A significant formation of OH-FA was found for three out of five cell lines, the colon cancer cell lines HCA-7 and SW480, as well as the fibroblast cell line Balb/c 3T3. The dominantly formed OH-FA metabolites were 15-HETE from ARA, 18-HEPE from EPA and 20-HDHA from DHA.

## 5.5 References

1. Buczynski MW, Dumlao DS, Dennis EA. Thematic Review Series: Proteomics. An integrated omics analysis of eicosanoid biology. *J Lipid Res.* 2009;50(6):1015-1038.
2. Fischer R, Konkell A, Mehling H, Blossey K, Gapelyuk A, Wessel N, von Schacky C, Dechend R, Muller DN, Rothe M, Luft FC, Weylandt K, Schunck WH. Dietary omega-3 fatty acids modulate the eicosanoid profile in man primarily via the CYP-epoxygenase pathway. *J Lipid Res.* 2014;55(6):1150-1164.
3. Mulugeta S, Suzuki T, Hernandez NT, Griesser M, Boeglin WE, Schneider C. Identification and absolute configuration of dihydroxy-arachidonic acids formed by oxygenation of 5S-HETE by native and aspirin-acetylated COX-2. *J Lipid Res.* 2010;51(3):575-585.
4. Serhan CN. Pro-resolving lipid mediators are leads for resolution physiology. *Nature.* 2014;510(7503):92-101.
5. Weylandt KH, Chiu CY, Gomolka B, Waechter SF, Wiedenmann B. Omega-3 fatty acids and their lipid mediators: towards an understanding of resolvin and protectin formation. *Prostag Oth Lipid M.* 2012;97(3-4):73-82.
6. Schuchardt JP, Schmidt S, Kressel G, Dong H, Willenberg I, Hammock BD, Hahn A, Schebb NH. Comparison of free serum oxylipin concentrations in hyper- vs. normolipidemic men. *Prostag Leukotr Ess.* 2013;89(1):19-29.
7. Dangi B, Obeng M, Nauroth JM, Teymourlouei M, Needham M, Raman K, Arterburn LM. Biogenic Synthesis, Purification, and Chemical Characterization of Anti-inflammatory Resolvins Derived from Docosapentaenoic Acid (DPAn-6). *J Biol Chem.* 2009;284(22):14744-14759.
8. Chiu CY, Gomolka B, Dierkes C, Huang NR, Schroeder M, Purschke M, Manstein D, Dangi B, Weylandt KH. Omega-6 docosapentaenoic acid-derived resolvins and 17-hydroxydocosahexaenoic acid modulate macrophage function and alleviate experimental colitis. *Inflamm Res.* 2012;61(9):967-976.
9. Porter NA, Lehman LS, Weber BA, Smith KJ. Unified Mechanism for Poly-Unsaturated Fatty-Acid Autoxidation - Competition of Peroxy Radical Hydrogen-Atom Abstraction, Beta-Scission, and Cyclization. *J Am Chem Soc.* 1981;103(21):6447-6455.
10. Yin H, Brooks JD, Gao L, Porter NA, Morrow JD. Identification of novel autoxidation products of the omega-3 fatty acid eicosapentaenoic acid in vitro and in vivo. *J Biol Chem.* 2007;282(41):29890-29901.
11. Konkell A, Schunck WH. Role of cytochrome P450 enzymes in the bioactivation of polyunsaturated fatty acids. *Biochim Biophys Acta.* 2011;1814(1):210-222.
12. Inceoglu B, Wagner K, Schebb NH, Morisseau C, Jinks SL, Ulu A, Hegedus C, Rose T, Brosnan R, Hammock BD. Analgesia mediated by soluble epoxide hydrolase inhibitors is dependent on cAMP. *Proc Natl Acad Sci U S A.* 2011;108(12):5093-5097.
13. Miyata N, Roman RJ. Role of 20-hydroxyeicosatetraenoic acid (20-HETE) in vascular system. *J Smooth Muscle Res.* 2005;41(4):175-193.
14. Bylund J, Kunz T, Valmsen K, Oliw EH. Cytochromes P450 with bisallylic hydroxylation activity on arachidonic and linoleic acids studied with human recombinant enzymes and with human and rat liver microsomes. *J Pharmacol Exp Ther.* 1998;284(1):51-60.

15. Buckley CD, Gilroy DW, Serhan CN. Proresolving Lipid Mediators and Mechanisms in the Resolution of Acute Inflammation. *Immunity*. 2014;40(3):315-327.
16. Bento AF, Claudino RF, Dutra RC, Marcon R, Calixto JB. Omega-3 Fatty Acid-Derived Mediators 17(R)-Hydroxy Docosahexaenoic Acid, Aspirin-Triggered Resolvin D1 and Resolvin D2 Prevent Experimental Colitis in Mice. *J Immunol*. 2011;187(4):1957-1969.
17. Gonzalez-Periz A, Planaguma A, Gronert K, Miquel R, Lopez-Parra M, Titos E, Horrillo R, Ferre N, Deulofeu R, Arroyo V, Rodes J, Claria J. Docosahexaenoic acid (DHA) blunts liver injury by conversion to protective lipid mediators: protectin D1 and 17S-hydroxy-DHA. *Faseb Journal*. 2006;20(14):2537-+.
18. Lima-Garcia JF, Dutra RC, da Silva KABS, Motta EM, Campos MM, Calixto JB. The precursor of resolvin D series and aspirin-triggered resolvin D1 display anti-hyperalgesic properties in adjuvant-induced arthritis in rats. *Br J Pharmacol*. 2011;164(2):278-293.
19. Neuhofer A, Zeyda M, Mascher D, Itariu BK, Murano I, Leitner L, Hochbrugger EE, Fraisl P, Cinti S, Serhan CN, Stulnig TM. Impaired Local Production of Proresolving Lipid Mediators in Obesity and 17-HDHA as a Potential Treatment for Obesity-Associated Inflammation. *Diabetes*. 2013;62(6):1945-1956.
20. Wilson R, Lyall K. Simultaneous determination by GC-MS of epoxy and hydroxy FA as their methoxy derivatives. *Lipids*. 2002;37(9):917-924.
21. Tsikas D, Zoerner AA. Analysis of eicosanoids by LC-MS/MS and GC-MS/MS: a historical retrospect and a discussion. *J Chromatogr B*. 2014;964:79-88.
22. Dumlao DS, Buczynski MW, Norris PC, Harkewicz R, Dennis EA. High-throughput lipidomic analysis of fatty acid derived eicosanoids and N-acyl ethanolamines. *Biochim Biophys Acta*. 2011;1811(11):724-736.
23. Gomolka B, Siegert E, Blossey K, Schunck WH, Rothe M, Weylandt KH. Analysis of omega-3 and omega-6 fatty acid-derived lipid metabolite formation in human and mouse blood samples. *Prostag Oth Lipid M*. 2011;94(3-4):81-87.
24. Inceoglu B, Wagner KM, Yang J, Bettaieb A, Schebb NH, Hwang SH, Morisseau C, Haj FG, Hammock BD. Acute augmentation of epoxygenated fatty acid levels rapidly reduces pain-related behavior in a rat model of type I diabetes. *Proc Natl Acad Sci U S A*. 2012;109(28):11390-11395.
25. Yang J, Schmelzer K, Georgi K, Hammock BD. Quantitative profiling method for oxylipin metabolome by liquid chromatography electrospray ionization tandem mass spectrometry. *Anal Chem*. 2009;81(19):8085-8093.
26. Strassburg K, Huijbrechts AM, Kortekaas KA, Lindeman JH, Pedersen TL, Dane A, Berger R, Brenkman A, Hankemeier T, van Duynhoven J, Kalkhoven E, Newman JW, Vreeken RJ. Quantitative profiling of oxylipins through comprehensive LC-MS/MS analysis: application in cardiac surgery. *Anal Bioanal Chem*. 2012;404(5):1413-1426.
27. Willenberg I, Elsner L, Steinberg P, Schebb NH. Development of an online-SPE-LC-MS method for the investigation of the intestinal absorption of 2-amino-1-methyl-6-phenylimidazo[4,5-b]pyridine (PHIP) and its bacterial metabolite PHIP-M1 in a Caco-2 Transwell system. *Food Chem*. 2015;166:537-543.
28. Schebb NH, Huby M, Morisseau C, Hwang SH, Hammock BD. Development of an online SPE-LC-MS-based assay using endogenous substrate for investigation of soluble epoxide hydrolase (sEH) inhibitors. *Anal Bioanal Chem*. 2011;400(5):1359-1366.

29. Schebb NH, Flores I, Kurobe T, Franze B, Ranganathan A, Hammock BD, Teh SJ. Bioconcentration, metabolism and excretion of triclocarban in larval Qurt medaka (*Oryzias latipes*). *Aquatic Toxicology*. 2011;105(3-4):448-454.
30. Schebb NH, Inceoglu B, Rose T, Wagner K, Hammock BD. Development of an ultra fast online-solid phase extraction (SPE) liquid chromatography electrospray tandem mass spectrometry (LC-ESI-MS/MS) based approach for the determination of drugs in pharmacokinetic studies. *Anal Methods*. 2011;3(2):420-428.
31. Hsieh Y, Duncan CJG, Brisson JM. Fused-core silica column high-performance liquid chromatography/tandem mass spectrometric determination of rimonabant in mouse plasma. *Anal Chem*. 2007;79(15):5668-5673.
32. Bollinger JG, Thompson W, Lai Y, Oslund RC, Hallstrand TS, Sadilek M, Turecek F, Gelb MH. Improved Sensitivity Mass Spectrometric Detection of Eicosanoids by Charge Reversal Derivatization. *Anal Chem*. 2010;82(16):6790-6796.
33. Masoodi M, Mir AA, Petasis NA, Serhan CN, Nicolaou A. Simultaneous lipidomic analysis of three families of bioactive lipid mediators leukotrienes, resolvins, protectins and related hydroxy-fatty acids by liquid chromatography/electrospray ionisation tandem mass spectrometry. *Rapid Commun Mass Spectrom*. 2008;22(2):75-83.
34. Miller TM, Donnelly MK, Crago EA, Roman DM, Sherwood PR, Horowitz MB, Poloyac SM. Rapid, simultaneous quantitation of mono and dioxygenated metabolites of arachidonic acid in human CSF and rat brain. *J Chromatogr B*. 2009;877(31):3991-4000.
35. Harkewicz R, Fahy E, Andreyev A, Dennis EA. Arachidonate-derived dihomoprostaglandin production observed in endotoxin-stimulated macrophage-like cells. *J Biol Chem*. 2007;282(5):2899-2910.
36. Masoodi M, Eiden M, Koulman A, Spaner D, Volmer DA. Comprehensive Lipidomics Analysis of Bioactive Lipids in Complex Regulatory Networks. *Anal Chem*. 2010;82(19):8176-8185.
37. Schebb NH, Ostermann AI, Yang J, Hammock BD, Hahn A, Schuchardt JP. Comparison of the effects of long-chain omega-3 fatty acid supplementation on plasma levels of free and esterified oxylipins. *Prostag Oth Lipid M*. 2014.
38. Norris PC, Dennis EA. Omega-3 fatty acids cause dramatic changes in TLR4 and purinergic eicosanoid signaling. *Proc Natl Acad Sci U S A*. 2012;109(22):8517-8522.
39. Norris PC, Reichart D, Dumlao DS, Glass CK, Dennis EA. Specificity of eicosanoid production depends on the TLR-4-stimulated macrophage phenotype. *J Leukoc Biol*. 2011;90(3):563-574.
40. Glasgow WC, Eling TE. Epidermal Growth-Factor Stimulates Linoleic-Acid Metabolism in Balb/C 3t3-Fibroblasts. *Mol Pharmacol*. 1990;38(4):503-510.
41. Little JM, Kurkela M, Sonka J, Jantti S, Ketola R, Bratton S, Finel M, Radominska-Pandya A. Glucuronidation of oxidized fatty acids and prostaglandins B1 and E2 by human hepatic and recombinant UDP-glucuronosyltransferases. *J Lipid Res*. 2004;45(9):1694-1703.
42. Turgeon D, Chouinard S, Belanger P, Picard S, Labbe JF, Borgeat P, Belanger A. Glucuronidation of arachidonic and linoleic acid metabolites by human UDP-glucuronosyltransferases. *J Lipid Res*. 2003;44(6):1182-1191.
43. Grant GE, Rokach J, Powell WS. 5-Oxo-ETE and the OXE receptor. *Prostaglandins Other Lipid Mediat*. 2009;89(3-4):98-104.

44. Green FA. Transformations of 5-Hete by Activated Keratinocyte 15-Lipoxygenase and the Activation Mechanism. *Lipids*. 1990;25(10):618-623.
45. Powell WS, Gravel S, Gravelle F. Formation of a 5-oxo metabolite of 5,8,11,14,17-eicosapentaenoic acid and its effects on human neutrophils and eosinophils. *J Lipid Res*. 1995;36(12):2590-2598.
46. Sharma RA, Gescher A, Plastaras JP, Leuratti C, Singh R, Gallacher-Horley B, Offord E, Marnett LJ, Steward WP, Plummer SM. Cyclooxygenase-2, malondialdehyde and pyrimidopurine adducts of deoxyguanosine in human colon cells. *Carcinogenesis*. 2001;22(9):1557-1560.
47. Sheng H, Shao J, Kirkland SC, Isakson P, Coffey RJ, Morrow J, Beauchamp RD, DuBois RN. Inhibition of human colon cancer cell growth by selective inhibition of cyclooxygenase-2. *J Clin Invest*. 1997;99(9):2254-2259.
48. Yoshinaga M, Buchanan FG, DuBois RN. 15-LOX-1 inhibits p21 (Cip/WAF1) expression by enhancing MEK-ERK1/2 signaling in colon carcinoma cells. *Prostaglandins Other Lipid M*. 2004;73(1-2):111-122.
49. Bednar W, Holzmann K, Marian B. Assessing 12(S)-lipoxygenase inhibitory activity using colorectal cancer cells overexpressing the enzyme. *Food and Chemical Toxicology*. 2007;45(3):508-514.
50. Melstrom LG, Bentrem DJ, Salabat MR, Kennedy TJ, Ding XZ, Strouch M, Rao SM, Witt RC, Ternent CA, Talamonti MS, Bell RH, Adrian TA. Overexpression of 5-Lipoxygenase in Colon Polyps and Cancer and the Effect of 5-LOX Inhibitors In vitro and in a Murine Model. *Clin Cancer Res*. 2008;14(20):6525-6530.
51. Tavolari S, Bonafe M, Marini M, Ferreri C, Bartolini G, Brighenti E, Manara S, Tomasi V, Laufer S, Guarnieri T. Licofelone, a dual COX/5-LOX inhibitor, induces apoptosis in HCA-7 colon cancer cells through the mitochondrial pathway independently from its ability to affect the arachidonic acid cascade. *Carcinogenesis*. 2008;29(2):371-380.
52. Lepage C, Liagre B, Cook-Moreau J, Pinon A, Beneytout JL. Cyclooxygenase-2 and 5-lipoxygenase pathways in diosgenin-induced apoptosis in HT-29 and HCT-116 colon cancer cells. *Int J Oncol*. 2010;36(5):1183-1191.

# Chapter 6

## **Modulation of the Endogenous Omega-3 Fatty Acid and Oxylipin Profile *in vivo* – A Comparison of the *fat-1* Transgenic Mouse with C57BL/6 Wildtype Mice on an Omega-3 Fatty Acid Enriched Diet\***

*Dietary intervention and genetic fat-1 mice are two models for the investigation of effects associated with omega-3 polyunsaturated fatty acids (n3-PUFA). In order to assess their power to modulate the fatty acid and oxylipin pattern, we thoroughly compared fat-1 and wild-type C57BL/6 mice on a sunflower oil diet with wild-type mice on the same diet enriched with 1% EPA and 1% DHA for 0, 7, 14, 30 and 45 days. Feeding led after 14-30 days to a high steady state of n3-PUFA in all tissues at the expense of n6-PUFAs. Levels of n3-PUFA achieved by feeding were higher compared to fat-1 mice, particularly for EPA (max. 1.7% in whole blood of fat-1 vs. 7.8% following feeding). Changes in PUFAs were reflected in most oxylipins in plasma, brain and colon: Compared to wild-type mice on a standard diet, arachidonic acid metabolites were overall decreased while EPA and DHA oxylipins increased with feeding more than in fat-1 mice. In plasma of n3-PUFA fed animals, EPA and DHA metabolites from the lipoxygenase and cytochrome P450 pathways dominated over ARA derived counterparts. Fat-1 mice show n3-PUFA level which can be reached by dietary interventions, supporting the applicability of this model in n3-PUFA research. However, for specific questions, e.g., the role of EPA derived mediators or concentration dependent effects of (individual) PUFA, feeding studies are necessary.*

\* Ostermann AI, Waindok P, Schmidt MJ, Chiu C-Y, Smyl C, Rohwer N, Weylandt KH and Schebb NH. 2017. *Submitted for publication.*

Author contributions: AIO: Designed research, performed experiments and wrote manuscript; PW: Performed experiments; MJS: Performed experiments as part of his internship under the supervision of AIO; CYC, CS: Performed animal experiments; NR, KHW NHS: Designed research and wrote the manuscript.

## 6.1 Introduction

It has long been suggested that dietary intake of long-chain n3 polyunsaturated fatty acids (n3-PUFA), especially of eicosapentaenoic acid (C20:5 n3, EPA) and docosahexaenoic acid (C22:6 n3, DHA), is associated with beneficial health effects [1, 2]. Strong evidence exists for an improvement of cardiometabolic health by lowering blood triglyceride levels and cardiovascular outcomes, such as sudden cardiac death [2]. Furthermore, anti-inflammatory [1, 2] and anti-angiogenic [3, 4] effects have been described and DHA plays an important role in neurodevelopment [5]. Part of the effects might be explained by direct physiological actions of n3-PUFA. They have been shown to act directly on membrane ion channels, or to reduce expression of inflammatory genes via nuclear factor-kappaB (NFκB), e.g. by interacting with peroxisome proliferator-activated receptor gamma (PPARγ) [1, 2]. Moreover, n3-PUFA serve as substrates in the arachidonic acid (C20:4 n6, ARA) cascade. In this signaling cascade, ARA is converted via three enzymatic pathways and autoxidation to oxidative metabolites, called oxylipins, several of which are biologically highly active: (I) Cyclooxygenase (COX) conversion of ARA yields series-2 prostanoids, like the potent prostaglandin (PG) E<sub>2</sub> which is involved in the regulation of pain, fever and inflammation or thromboxane (Tx) A<sub>2</sub> which is involved in platelet aggregation [6-8]. (II) Lipoxygenase (LOX) action on ARA leads to multiple biologically active classes of lipid mediators via hydroperoxy intermediates, such as leukotrienes (LT), e.g. LTB<sub>4</sub>, involved in the chemotaxis of neutrophils, lipoxins with anti-inflammatory properties or hydroxy-fatty acids (OH-FA) [6-8]. (III) Finally, cytochrome P450 (CYP) enzymes can convert ARA to OH- and epoxy-FA (Ep-FA). For instance, ω-hydrolase activity of CYP enzymes can yield the vasoconstrictory 20-hydroxyeicosatetraenoic acid (20-HETE) formed by members of the CYP4A or 4F family [6, 8, 9]. Conversion of ARA by CYP2C and 2J, e.g., leads to vasodilatory, anti-inflammatory, analgesic and angiogenic acting Ep-FA [6, 8-11] which are further metabolized to less potent dihydroxy-FA (DiH-FA) by the soluble epoxide hydrolase [6, 8, 12]. The effect of n3-PUFA on this important signaling cascade is multifaceted. On the



one hand, by competing with ARA for conversion, the formation of potent ARA derived mediators, such as pro-inflammatory PGE<sub>2</sub> and LTB<sub>4</sub> is reduced, while their EPA derived counterparts, PGE<sub>3</sub> and LTB<sub>5</sub> have been shown to be less potent [1, 8]. On the other hand, enzymatic conversion of EPA and DHA can yield highly potent lipid mediators: CYP catalyzed epoxidation leads, e.g., to anti-arrhythmic acting 17(18)-epoxy eicosatetraenoic acid (EpETE) from EPA and 19(20)-epoxy docosapentaenoic acid (EpDPE) from DHA [13]. Interestingly, while these Ep-FA share the anti-inflammatory action of the corresponding ARA oxylipins [3], 19(20)-EpDPE has been shown to inhibit angiogenesis in contrast to ARA derived Ep-FA [4]. Moreover, multiple hydroxylation leads to highly potent, specialized pro-resolving lipid mediators (SPM) such as resolvins and protectins [14, 15].

Regarding the clinical relevance of n3-PUFA in different diseases the results of epidemiological and intervention studies are conflicting [1, 2, 16]. Moreover, molecular modes of action for individual effects of n3-PUFA have not been fully unveiled, and dose dependencies remain largely unclear [1, 2]. In order to address these questions, appropriate experimental models allowing a defined modulation of the endogenous n3-PUFA and oxylipin profile are required.

In humans and other mammals EPA and DHA can be synthesized endogenously by combined elongation (ELOVL2 and 5 (human gene name indicated)), desaturation (delta 5 (FADS1) and delta 6 (FADS2) desaturase) and  $\beta$ -oxidation reactions from the essential n3-PUFA alpha linolenic acid (C18:3 n3, ALA) [17, 18]. However, conversion rates are low on a diet rich in linoleic acid (C18:2 n6, LA), as it is the case for a typical western diet (soy, corn and sunflower oil based) [17]. Additionally, mammals lack an n3 desaturase for the endogenous conversion of n6 to n3-PUFA [18]. Therefore, EPA and DHA have to be directly supplied, either by consumption of n3-PUFA rich food, like fish, algae or krill [19] or by ingestion of supplementation products [20]. In *in vivo* studies, animal diets are often enriched with EPA and DHA containing oils to modulate the endogenous n3-PUFA profile. This approach has been used in

different disease models for the investigation of n3-PUFA associated biology, e.g. in inflammatory diseases, such as colon inflammation [21, 22], arthritis [23, 24], hypertension [25], liver injury [26] or Parkinson's Disease [27].

Another approach to investigate physiological effects of elevated endogenous n3-PUFA concentrations is the use of the *fat-1* transgenic mouse model. The DNA of these mice has been edited to carry the *fat-1* gene of the nematode *Caenorhabditis elegans* encoding an n3 fatty acid desaturase catalyzing the conversion of n6 to n3 fatty acids [28]. This leads to a massively decreased endogenous n6/n3-ratio in *fat-1* mice fed with a standard n6-PUFA rich diet compared to wild type (WT) animals, e.g. from 46.6 (WT) to 2.9 (*fat-1*) in erythrocytes [28]. Therefore, *fat-1* mice have been used in many studies for the investigation of n3-PUFA associated effects, e.g. in inflammation, including colitis [29, 30], hepatitis [31], pancreatitis [32], different types of cancer, such as liver [33], colitis-associated colon cancer [34, 35] and melanoma [36] as well as Parkinson's Disease [37] or chemically induced diabetes [38].

In most studies using *fat-1* mice, selected FA and/or (variations of) the n6/n3-PUFA ratio in tissues are used as biomarker of the endogenous n3-PUFA status [29-39]. Only little attention has been paid to the modulation of n3- and n6-PUFA oxylipins in *fat-1* compared to wild type mice. In disease models a focus was set on selected oxylipins, such as PGE and/or PGD from ARA and/or EPA [29, 30, 34, 36, 38], SPMs [30], precursor thereof [33] and few others [30, 34, 38]. A comprehensive set of free oxylipins in *fat-1* mice has only been described in plasma [40] and total (free and esterified) OH-FA have been described in plasma and tissues [39]. Almost no data is available on the differences in fatty acids and oxylipins in between *fat-1* versus WT mice after dietary supplementation with n3-PUFA. The only available study compares the effects of nine weeks of feeding on selected oxylipins and fatty acids in kidney tissue [41]. Therefore, in the present study we thoroughly investigated the modulations of both, the total fatty acid and oxylipin profile in *fat-1* vs. WT mice on standard, sunflower oil based diet and the same diet enriched with n3-PUFA

(1% EPA and 1% DHA). Not only is a comprehensive set of tissues and blood (including plasma and blood cells) analyzed, we also show the time course of effects occurring on a diet enriched with n3-PUFA over a feeding period of 7-45 days. This study provides fundamental insights on the breadth of effects on the lipidome caused by the insertion of the fat-1 gene into the murine DNA in the context of a diet high in n6-PUFA compared to an n3-PUFA dietary intervention as well as the time dependency of nutrition induced changes.

## **6.2 Experimental**

### **6.2.1 Chemicals**

Acetic acid and methanol (Optima LC/MS Grade) as well as acetonitrile (HPLC-MS grade) were obtained from Fisher Scientific (Schwerte, Germany) and ammonium acetate (p.a.) was purchased from Merck (Darmstadt, Germany). Methyl *tert*-butyl ether and *n*-hexane (HPLC grade) were obtained from Carl Roth (Karlsruhe, Germany). Methyl tricosanoate (FAME C23:0) was obtained from Santa Cruz Biotechnology (Heidelberg, Germany). Oxylin and deuterated oxylin standards were purchased from Cayman Chemicals (local distributor: Biomol, Hamburg, Germany). Further oxylin standards (Epoxy octadecadienoic acids (EpODEs) and dihydroxy octadecadienoic acids (DiHODEs)) were a kind gift from the laboratory of Bruce Hammock (UC Davis, CA, USA). Ethyl acetate, methyl formate and all other chemicals were purchased from Sigma Aldrich (Taufkirchen, Germany).

### **6.2.2 Feeding experiment**

Pellets for the feeding experiment were based on a standard experimental diet from ssniff (product number: E15051; ssniff Spezialdiäten GmbH, Soest, Germany) with 10% fat. The fat used for the standard diet was refined sunflower oil (Henry Lamotte Oils, Bremen, Germany) enriched with 0.2% (w/w)

tocopherol mix (Covi-Ox T 70 EU, BASF, Ludwigshafen). The n3-PUFA rich diet was the same diet containing 1% EPA and 1% DHA as ethyl esters. The fatty acid concentrations of the chow and details on the actual fatty acid composition of the diets can be found in the supplementary information (App. Table 9.3.1).

Animals were cared for in accordance with the institution's guidelines for experimental animals. The animal protection committee of the local authorities approved all experiments. Transgenic *fat-1* mice were generated as described [28] and phenotyping (ratio of n6/n3-PUFA) from tails was carried out using gas chromatography. For the feeding experiment female C57BL/6 WT and *fat-1* mice of 9-10 weeks of age were used (n=6). Before the experiment, mice were kept on a diet with 3.3% fat (1.8% LA, 0.23% ALA in the diet, App. Table 9.3.2) with water and food supply ad libitum. WT mice were kept on the experimental diets for 7, 14, 30 and 45 days. *Fat-1* mice were kept on the standard sunflower diet for 30 days. One group of WT and *fat-1* animals was sacrificed on day 0. Animals were killed by cervical dislocation and organs (liver, kidney, spleen, brain and colon) as well as blood (by cardiac puncture) were collected. 10  $\mu$ L of whole blood were directly diluted with 50  $\mu$ L of deionized water. For plasma and blood cell generation, blood was directly centrifuged (800 xg, 10 min, 4 °C). Plasma was collected and blood cells were washed once with phosphate buffered saline (containing 1.5 mg/mL ethylenediaminetetraacetic acid (EDTA)) and reconstituted to the original blood volume in phosphate buffered saline. All samples were stored at -80 °C until further analysis

### 6.2.3 Fatty acid analysis

Fatty acid composition was analyzed in all collected blood fractions (60  $\mu$ L diluted whole blood, 50  $\mu$ L plasma and 100  $\mu$ L reconstituted blood cells) and tissues (30-35 mg) as described [42 (see Chapter 3)]. Briefly, blood and tissues were extracted with methanol/ methyl *tert*-butyl ether (1:2, v/v) and derivatized to fatty acid methyl esters (FAME) with methanolic hydrogen chloride (acetylchloride in methanol (1:10, v/v)). FAMES were analyzed by means of gas

chromatography with flame ionization detection (GC-FID) on a 6890 series instrument (Agilent Technologies, Waldbronn, Germany) equipped with a 30 m x 0.25 mm FAMEWAX column (0.25  $\mu$ m film) and a 5 m x 0.25 mm deactivated guard column of intermediate polarity (Restek GmbH, Bad Homburg, Germany), using FAME C23:0 as internal standard. Peak integration was performed with Chemstation B01.03 (Agilent). For the calculation of the relative pattern and absolute fatty acid concentrations response factors were used [42 (see Chapter 3), 43]. Results are presented as mean  $\pm$  standard error of the mean (SEM).

#### **6.2.4 Oxylipin analysis**

Extraction and analysis of oxylipins from plasma (200  $\mu$ L) and colon (50 $\pm$ 5 mg) was carried out as described [44 (see Chapter 4), 45]. Brain (50 $\pm$ 5 mg) was homogenized following addition of internal standards and antioxidant solution [44 (see Chapter 4), 45] in 750  $\mu$ L ethyl acetate and 500  $\mu$ L water (pH 6) by a ball mill using two 3 mm metal beads (25 Hz, 5 min, Retsch, Haan, Germany). Following homogenization and centrifugation (20 000  $\times g$ , 5 min, 4  $^{\circ}$ C), the organic phase was collected and the sample extracted with another 750  $\mu$ L ethyl acetate. The combined organic phases were evaporated using a vacuum centrifuge (Christ, Osterode am Harz, Germany) and the dried lipid extract was reconstituted in 300  $\mu$ L methanol. All samples were diluted to 6 mL with water and acidified with acetic acid (to pH 3) directly before extraction. The acidified samples were brought onto a C18 solid phase extraction cartridge (500 mg, Macherey-Nagel, Düren, Germany) and eluted using methyl formate [44 (see Chapter 4), 45]. Oxylipins were quantified by liquid chromatography-mass spectrometry (LC-MS) following negative electrospray ionization on a QTrap6500 mass spectrometer (Sciex, Darmstadt, Germany) operated in scheduled selected reaction monitoring mode [44 (see Chapter 4), 45]. Analyst 1.6.2 (Sciex) was used for data acquisition and Multiquant 2.1.1 (Sciex) was used for data analysis. Hemolytic plasma samples and samples with high TxB<sub>2</sub> and 12-HETE – indicating improper anticoagulation – were excluded from analysis. Results are presented as mean  $\pm$  SEM.

## 6.3 Results

### 6.3.1 Behaviour and bodyweight

During the experiment, no differences in animal behavior were observed. Bodyweight means of the groups ranged from 17.9 to 21.7 g. Compared to baseline, groups on a standard sunflower based, n6-PUFA rich diet (WT-STD) showed a slight decrease in bodyweight, whereas groups on a sunflower based diet enriched with n3-PUFA (WT-STD+n3) did not show a consistent trend. *Fat-1* mice at baseline were a little lighter than WT mice and their bodyweight did not change during the feeding period (App. Fig. 9.3.1). These results indicate no differences in feeding behavior between the groups.

### 6.3.2 Fatty acid profile

Fig. 6.1 and Table 6.1 show the relative pattern of selected FA as well as the FA profile grouped as saturated fatty acids (SFA), monounsaturated fatty acids (MUFA) and n6- and n3-polyunsaturated fatty acids (PUFA) during the course of the feeding time. The full FA profile of blood and tissues is found in the Appendix (App. Table 9.3.3A+B).

After 30 days on a sunflower oil based diet, low in n3-PUFA (WT-STD, App. Table 9.3.1), EPA was <0.05% in most investigated tissues and blood, except for whole blood (Fig. 6.1, Table 6.1). DHA levels ranged from 0.73% (colon) to 7.4% (kidney) and were higher in brain (17%, Fig. 6.1, Table 6.1). ARA levels increased over the feeding period slightly in most tissues reaching 20-23% in whole blood, plasma, blood cells, kidney and spleen (Fig. 6.1, Table 6.1). Lowest levels were found in colon (5.7%), the only tissue in which ARA decreased over the feeding time (Table 6.1, App. Table 9.3.3B). Interestingly, ALA levels in all tissues and blood decreased over the feeding period in all groups (App. Table 9.3.3B) due to the low ALA content of sunflower oil (0.29-0.34% of ALA in all diets, App. Table 9.3.1).

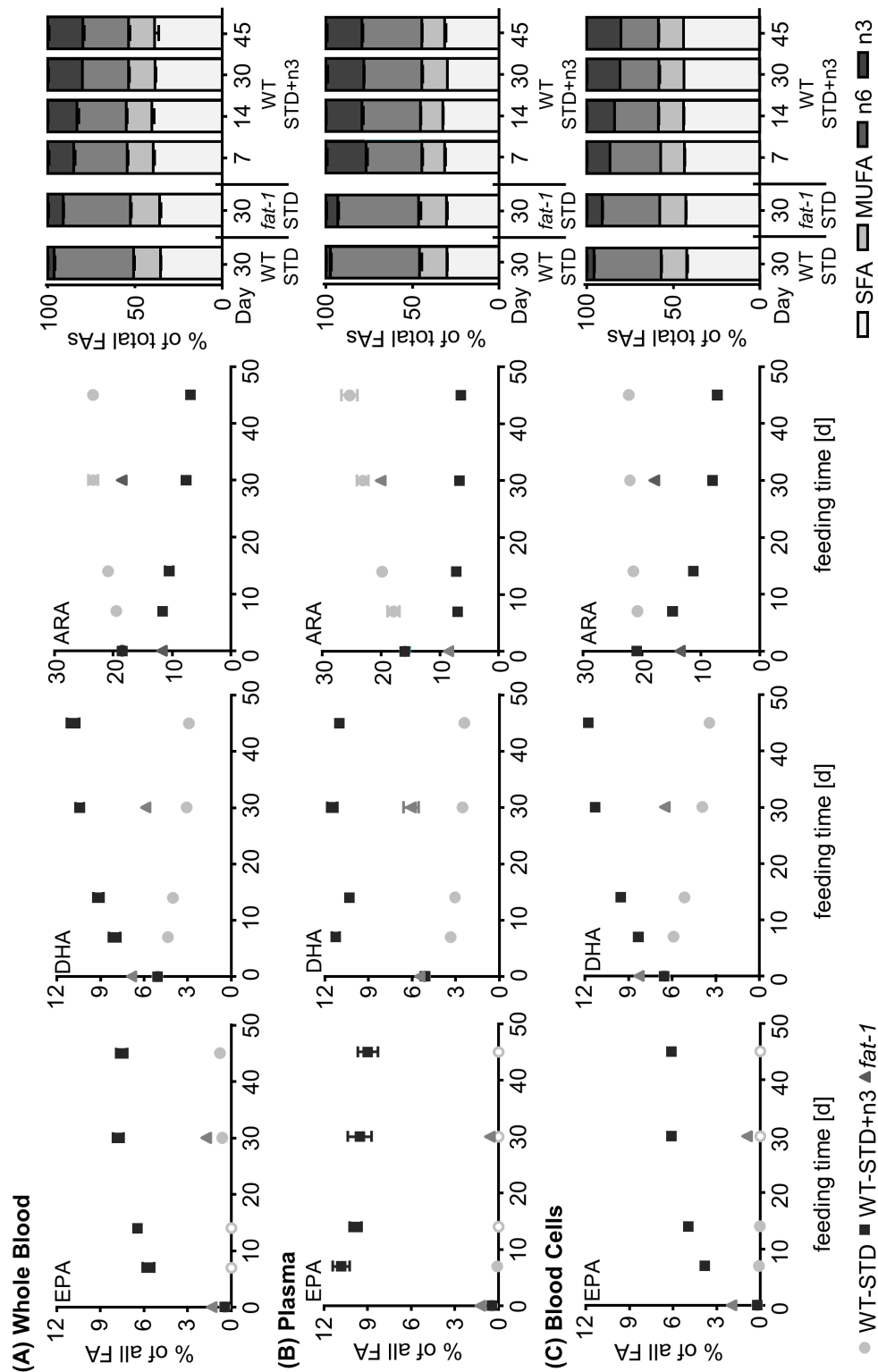


**Fig. 6.1:** Relative amounts of EPA, DHA and ARA as well as the relative distribution of n3- and n6-PUFA, MUFA and SFA in transgenic *fat-1* mice and wild type animals (WT-STD) after 30 days on a sunflower oil based diet, as well as in wild type mice on the same diet enriched with EPA and DHA (WT-STD+n3) during the course of the feeding period (45 days) in (A) whole blood, (B) plasma and (C) blood cells. Analytes that were below the limit of quantification are marked with a white filling in the diagram.

**Feeding of a diet enriched in n3-PUFA** (1% EPA and 1% DHA as ethyl ester, WT-STD+n3, App. Table 9.3.1) led to a massive increase in the relative and absolute concentrations of these FA in blood and all investigated tissues (Fig. 6.1, Table 6.1, App. Fig. 9.3.2). The fatty acid pattern changed most during the first seven days of supplementation and no further increase of n3-PUFAs was found in plasma (Fig. 6.1). Constant levels (steady state) were reached after 14-30 days of feeding in brain, spleen as well as kidney (Table 6.1) and after 30 days in blood cells as well as whole blood (Fig. 6.1). For liver and colon tissue, relative amounts of EPA and DHA varied more between the different time points, however, the data also suggests that a steady state was reached at least after 30 days of feeding (Table 6.1). When comparing the levels of EPA and DHA after 30 days of n3-PUFA supplementation to levels in tissues and blood of mice at the beginning of the feeding experiment, changes in EPA were more pronounced (App. Fig. 9.3.2): While the mean %difference  $[(c(FA)_{WT-STD+n3, D30} - c(FA)_{WT, D0})/c(FA)_{WT, D0} * 100]$  in DHA was about 100% (except in colon and brain, with an increase of at most 35%), EPA was increased by about 2000-5000% in whole blood, blood cells, plasma, liver, kidney and spleen. Again, changes in colon and brain were lower (400% and 1200%, respectively). Relative increases in the elongation product of EPA, n3 docosapentaenoic acid (C22:5n3, n3-DPA), ranged from 160% (colon) to 480% (liver, App. Fig. 9.3.2). In response to n3-PUFA supplementation, SFA and MUFA changed only slightly (Fig. 6.1, Table 6.1, App. Fig. 9.3.3), while n6-PUFA levels were uniformly decreased. For instance, ARA as a major n6-PUFA, showed a 40-85% decrease in all tissues and blood, except brain (App. Fig. 9.3.2). It should be noted that due to the high content in the experimental sunflower based diets, the other main n6-PUFA, LA, was slightly higher compared to baseline in most tissues of the feeding groups.

Over all groups (*fat-1*, WT-STD and WT-STD+n3) the sum of SFA and MUFA was comparable (Fig. 6.1, Table 6.1, App. Fig. 9.3.3), ranging between 50-60% in most investigated tissues and blood. In colon and brain the sums of SFA and MUFA were slightly higher (62-70%, Table 6.1).



**Table 6.1:** Relative amounts of EPA, DHA and ARA as well as the sum of n6-PUFA, n3-PUFA, MUFA and SFA in liver, kidney, spleen, colon and brain tissue in WT (WT-STD) and *fat-1* mice after 30 days on a standard sunflower oil based diet and in WT mice on the same diet enriched with EPA and DHA (WT-STD+n3) during the course of the feeding period (day7-45).

		EPA	DHA	ARA	n6-PUFA	n3-PUFA	MUFA	SFA
<b>Liver</b>								
WT-STD	Day 30	<LOQ	3.7±0.2	15.9±0.9	39.5±0.8	3.8±0.2	24±2	33±1
<i>fat-1</i>	Day 30	0.16±0.02	6.8±0.5	13.2±0.7	36.7±0.6	7.2±0.5	24±2	32±1
WT-STD+n3	Day 7	6.1±0.4	14.7±0.3	7.8±0.2	26.8±0.6	22.3±0.6	13.5±0.5	37.4±0.3
	Day 14	4.4±0.2	11.1±0.4	5.9±0.4	27±1	17.0±0.6	21±1	35.1±0.8
	Day 30	5.4±0.4	14.1±0.8	5.1±0.2	26.3±0.5	21±1	19±2	34.7±0.5
	Day 45	4.2±0.5	12.5±0.5	6.1±0.2	29±1	18.1±0.9	18.9±0.6	34.4±0.5
<b>Kidney</b>								
WT-STD	Day 30	0.015±0.002	7.4±0.6	22±2	38.8±0.7	7.7±0.6	16±2	38.0±0.6
<i>fat-1</i>	Day 30	1.01±0.07	12.1±0.3	20.3±0.6	35.5±0.5	13.9±0.4	12.1±0.5	38.5±0.3
WT-STD+n3	Day 7	4.6±0.1	14.9±0.7	12.9±0.8	27.8±0.3	20.6±0.8	13±1	39.1±0.3
	Day 14	5.2±0.2	16.3±0.7	10.9±0.6	25.7±0.2	22.6±0.8	13±1	38.7±0.2
	Day 30	6.3±0.3	18.0±0.5	10.3±0.4	24.6±0.2	25.5±0.6	11.0±0.7	39.0±0.2
	Day 45	6.2±0.2	16.5±0.7	9.5±0.5	25.2±0.3	23.9±0.9	13±1	38.1±0.4
<b>Spleen</b>								
WT-STD	Day 30	0.035±0.007	2.6±0.1	20.4±0.8	39±1	3.0±0.1	16±2	42.8±0.5
<i>fat-1</i>	Day 30	1.6±0.2	4.9±0.6	14±1	31.2±0.2	9±1	18±3	41±1
WT-STD+n3	Day 7	3.58±0.07	9.8±0.3	10.5±0.5	25.7±0.4	17.8±0.4	13.3±0.9	43.2±0.2
	Day 14	4.0±0.1	10.3±0.2	8.3±0.4	23.4±0.4	18.7±0.4	14.8±0.7	43.0±0.3
	Day 30	4.3±0.1	11.2±0.2	7.7±0.2	23.2±0.2	20.1±0.5	13.1±0.7	43.6±0.3
	Day 45	3.8±0.2	10.5±0.6	6.9±0.5	23.6±0.2	19±1	16±2	42.1±0.9
<b>Colon</b>								
WT-STD	Day 30	0.048±0.010	0.73±0.13	5.7±1.0	35.5±0.8	0.96±0.15	35±1	29.0±0.8
<i>fat-1</i>	Day 30	0.65±0.22	1.5±0.5	4.7±1.4	32±1	2.9±0.8	35±2	31±1
WT-STD+n3	Day 7	1.8±0.3	3.5±0.4	2.8±0.8	28.8±0.6	6.7±0.7	32±2	32.9±0.8
	Day 14	2.8±0.4	5.0±0.5	3.6±0.6	26.0±0.6	9.2±0.8	30±1	34.6±0.7
	Day 30	2.0±0.2	4.5±0.3	1.8±0.4	27.5±0.6	7.7±0.5	30.5±0.9	34.2±0.6
	Day 45	3.0±0.4	5.7±0.2	3.5±0.4	27.4±0.5	10.2±0.6	27.4±0.8	35.0±0.3
<b>Brain</b>								
WT-STD	Day 30	<LOQ	17.1±0.3	11.3±0.2	15.5±0.3	17.2±0.3	20.5±0.6	46.8±0.2
<i>fat-1</i>	Day 30	0.066±0.005	16.3±0.9	9.8±0.8	14.0±0.9	16.5±0.9	25±3	45±1
WT-STD+n3	Day 7	0.15±0.02	16.7±0.4	10.3±0.3	14.3±0.4	17.1±0.4	23±1	46.0±0.4
	Day 14	0.14±0.01	17.4±0.3	10.6±0.2	14.6±0.3	17.9±0.3	20.9±0.7	46.6±0.3
	Day 30	0.18±0.01	19.0±0.3	9.5±0.2	13.2±0.2	19.6±0.3	21.2±0.5	46.0±0.2
	Day 45	0.16±0.01	17.4±0.5	8.8±0.2	15.8±0.4	15.8±0.6	20±1	48.7±0.3

After **30 days of feeding** a standard sunflower oil based diet, level of EPA in blood in tissues of *fat-1* mice ranged from  $0.066\pm 0.005\%$  (brain) to  $1.7\pm 0.2\%$  (whole blood, Fig. 6.1, Table 6.1). EPA level in WT mice on the same diet (WT-STD) were  $<0.05\%$  in most tissues and blood (Fig. 6.1, Table 6.1). 30 days of n3-PUFA supplementation led to EPA levels which were about 200-600% higher (and up to 1500% and 3300% in plasma and liver, App. Fig. 9.3.4) as compared to *fat-1* mice and ranged from  $2.0\pm 0.2\%$  (colon) to  $9.5\pm 0.8\%$  (plasma, Fig. 6.1, Table 6.1). EPA level in brain was  $0.18\pm 0.01\%$  (Table 6.1). In *fat-1* mice n3-DPA level ranged from  $0.14\pm 0.03\%$  (plasma) to  $2.7\pm 0.3\%$  (spleen, App. Table 9.3.3B). Levels of n3-DPA in WT mice on the same diet were much lower with highest amounts found in blood cells ( $0.38\pm 0.10\%$ , App. Table 9.3.3B). After 30 days of feeding a chow enriched in n3-PUFA to WT mice, large differences in n3-DPA levels compared to *fat-1* mice were observed in plasma and liver (App. Fig. 9.3.4), yet, levels were roughly in the same range, yielding  $0.42\pm 0.01\%$  (brain) to  $1.90\pm 0.02\%$  (blood cells, App. Table 9.3.3B). Spleen showed a high level of n3-DPA with  $4.6\pm 0.1\%$ . DHA levels in *fat-1* mice were 2- to 42-fold (and 250-fold in brain) higher than EPA concentrations and were found in the range of  $1.5\pm 0.5\%$  (colon) to  $16.3\pm 0.9\%$  (brain, Fig. 6.1, Table 6.1). Except for brain, DHA level in tissues and blood of WT animals on the same diet were about twofold lower in comparison to *fat-1* mice, while DHA level after 30 days of n3-PUFA supplementation were in roughly twofold higher compared to DHA in *fat-1* mice (mean %difference of about 100%, App. Fig. 9.3.4), ranging between  $4.5\pm 0.3\%$  (colon) and  $19.0\pm 0.3\%$  (brain, Fig. 6.1, Table 6.1). In brain, DHA levels differed least between the groups (Table 6.1). ARA levels in *fat-1* mice were lowest in colon ( $4.7\pm 1.4\%$ ) and highest in whole blood, blood cells, plasma and kidney (18-20%, Fig. 6.1, Table 6.1). In WT mice on the same diet ARA level were slightly higher (Fig. 6.1, Table 6.1). After n3-PUFA supplementation, ARA levels were roughly 40-60% lower compared to *fat-1* mice (App. Fig. 9.3.4) and ranged from  $1.8\pm 0.4\%$  (colon) to  $10.3\pm 0.4\%$  (kidney, Fig. 6.1, Table 6.1).

The **n6/n3 ratio** in blood and tissues as well as the **sum of %EPA and %DHA** (%EPA+DHA) in blood cells, a modification of the omega-3 index [46], as marker for the endogenous n3-PUFA status after 30 days of EPA and DHA supplementation in comparison to *fat-1* and WT animals on the standard sunflower oil based diet are presented in Fig. 6.2. The ratios during the feeding course and data on the tissues are shown in the appendix, Table 9.3.4. Massive differences were found in the n6/n3 ratio in the same tissue between the different groups. The ratios in different tissues and in blood within the same feeding group, however, were comparable, with the exception of colon and brain (Fig. 6.2A+B). Of other tissues and blood, highest n6/n3 ratios were found in WT animals on the STD diet with 5.1-20, compared to 2.5-6.9 in *fat-1* mice, thus, exceeding levels in *fat-1* mice approximately 2- to 3.5-fold (Fig. 6.2A+B). With EPA and DHA supplementation, the n6/n3 ratio decreased below two throughout all tissues (except colon and brain). Compared to *fat-1* mice, feeding thus led to 2.6- to 4.5-fold lower n6/n3 ratios, and compared to WT mice on the STD diet to 5.4- to 13-fold lower n6/n3 ratios. Colon tissue showed remarkably high n6/n3 ratios (Fig. 6.2B), however, relative changes between feeding groups were comparable to other tissues. In brain, the n6/n3 ratio was below one in all groups. It was only slightly modulated by n3-supplementation (Fig. 6.2B). Compared to WT mice on the STD diet ( $3.93 \pm 0.08\%$ ), %EPA+DHA in blood cells of *fat-1* mice was about twofold higher ( $7.4 \pm 0.2\%$ ) and fourfold elevated in STD+n3 fed WT animals, reaching  $17.4 \pm 0.2\%$  (Fig. 6.2C).

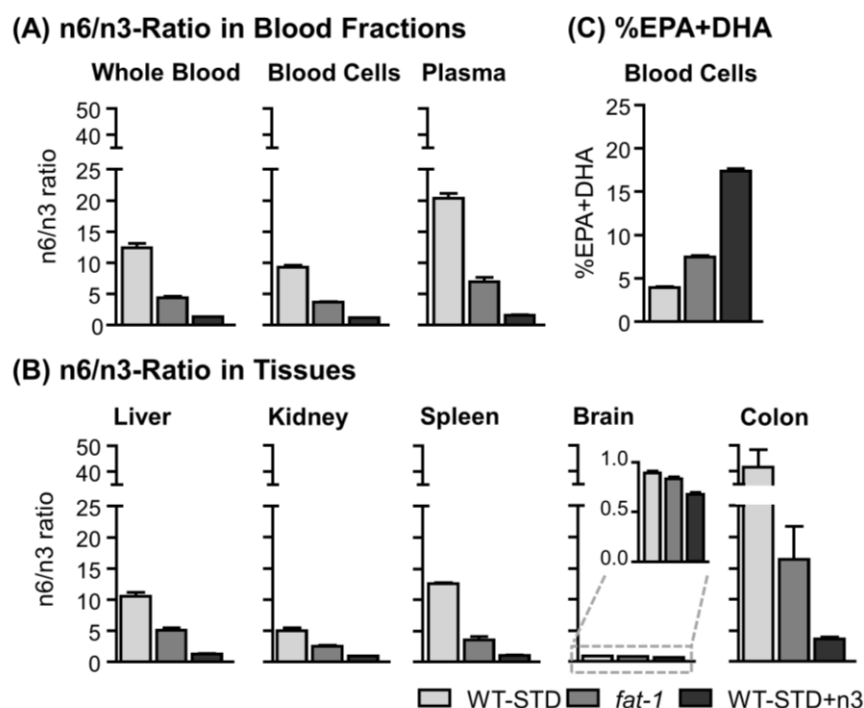


**Fig. 6.2:** n6/n3 ratio in blood (A) and in tissues (B), as well as %EPA+DHA in blood cells (C) in transgenic *fat-1* mice and wild type animals (WT-STD) on a standard sunflower oil based diet, as well as in wild type mice on the same diet enriched with EPA and DHA (WT-STD+n3) after 30 days of feeding. The n6/n3 ratio was calculated as  $\Sigma\%(C18:2\ n6, C18:3\ n6, C20:3\ n6, C20:4\ n6, C22:4n6) / \Sigma\%(C18:3\ n3, C20:5\ n3, C22:5\ n3, C22:6\ n3)$ .

### 6.3.3 Oxylipin pattern

Oxylipins were analyzed in selected tissues, i.e. plasma, colon and brain. Concentrations of all oxylipins covered by the LC-MS method in all feeding groups in plasma, colon and brain are presented in the appendix, Table 9.3.5. Since a steady state in the nutrition induced changes in fatty acids (see above) was reached after 30 days, the differences between the groups are highlighted for this time point in Fig. 6.3 for selected oxylipins from EPA, DHA and ARA in plasma, brain and colon.

**Feeding of a diet enriched with n3-PUFA** (1% EPA and 1% DHA as ethyl ester, WT-STD+n3) led to high changes in the oxylipin pattern of plasma, brain and colon already in the first seven days of supplementation. Thereafter, concentrations remained almost constant showing only minor trends towards a further increase (App. Table 9.3.5). However, the levels of several oxylipins,

such as OH-FA of EPA and DHA in plasma, varied strongly, showing no clear trend between day 7 and 45 of feeding (App. Table 9.3.5). After 30 days of feeding, EPA metabolites showed the highest change of all oxylipins derived from EPA, DHA and ARA with a mean %increase of over 500% for many compounds in plasma, brain and colon as compared to baseline (App. Fig. 9.3.6). Increases in DHA oxylipins were also massive e.g., mean %difference of >500% for HDHAs in plasma and EpDPEs in colon, however, for other analytes more moderate in comparison to EPA oxylipins (App. Fig. 9.3.6). Most ARA derived eicosanoids decreased in plasma and the investigated tissues (up to about 90% for 12-HETE in colon, App. Fig. 9.3.6). For few analytes, a slight increase was found, e.g. TxB<sub>2</sub> (41%) or 12-HETE (140%) in plasma (App. Fig. 9.3.6). As observed for the parent FA, ALA metabolites decreased massively. This trend was also found for ALA metabolites in WT and *fat-1* animals on the STD diet (App. Table 9.3.5).

After **30 days of feeding** a standard n6-PUFA rich sunflower oil based diet, concentrations of **EPA metabolites** in plasma of *fat-1* mice were overall in the low nM range with highest concentrations found for 17(18)-DiHETE (5.3±0.8 nM, Fig. 6.3, App. Table 9.3.5). In comparison to WT animals after 30 days on the same diet, concentrations in plasma of *fat-1* animals were highly elevated (up to 15-fold for 12- hydroxy eicosapentaenoic acid (12-HEPE)) and many analytes were found which were not detectable in STD fed WT animals, e.g. 17(18)-EpETE, 5-HEPE or 18-HEPE (Fig. 6.3). Compared to *fat-1* animals, WT mice on a diet enriched with n3-PUFA showed massively higher concentrations of EPA derived oxylipins (up to 7000% for 12-HEPE, Fig. 6.3, App. Fig. 9.3.7). After n3-PUFA feeding, highest concentrations were found for OH-FA (6.3-240 nM) followed by DiH-FA (1.5-14 nM) and Ep-FA (0.94-1.1 nM, Fig. 6.3, App. Table 9.3.5). Resolvins were below the limit of quantification (<LOQ) in plasma of the feeding groups and the only EPA derived prostanoid found in detectable concentrations was TxB<sub>3</sub> in animals on the STD+n3 diet (Fig. 6.3).

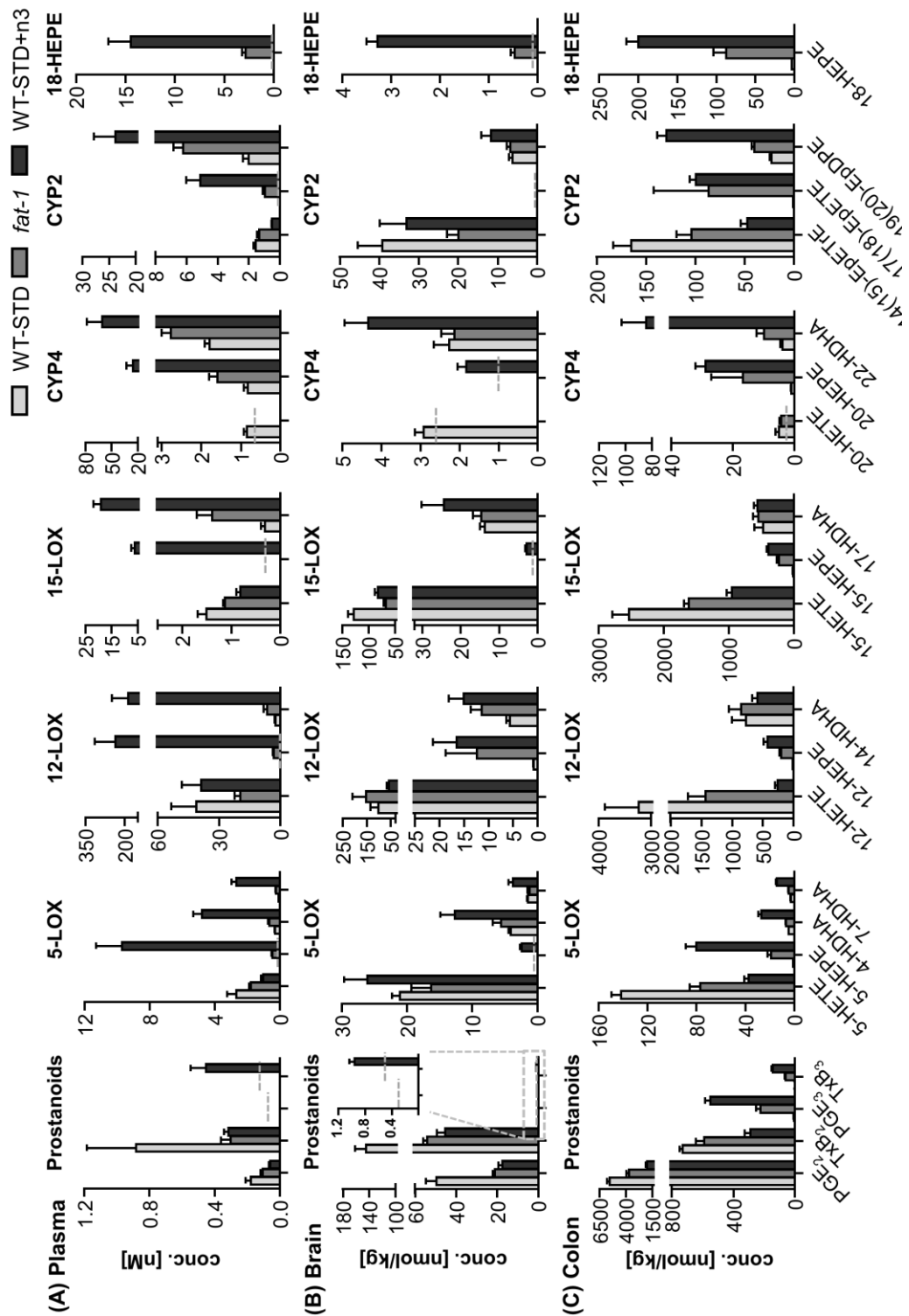


**Fig. 6.3:** Concentrations of oxylipins in plasma of transgenic *fat-1* mice and wild type animals (WT-STD) on a sunflower oil based diet, as well as in wild type mice on the same diet enriched with EPA and DHA (WT-STD+n3) after 30 days of feeding. Shown are concentrations of selected prostanoids, 5-LOX, 12-LOX, 15-LOX, CYP4 and CYP2 products of ARA, EPA and DHA as well as 18-HEPE in (A) plasma, (B) brain and (C) colon. The lower limit of quantification (LLOQ) for the analyte is indicated in case it was not exceeded in >50% of the samples per group.

Comparing the ratio of precursor PUFA and their oxidative products in all three groups, an almost linear correlation ( $R^2 > 0.8$ ) resulted for CYP and LOX metabolites (Fig. 6.4) which was also observed for DHA metabolites. The slope of  $>2$  indicates that moderate changes in the concentrations of EPA or DHA led to a more pronounced change in the concentrations of their oxylipins.

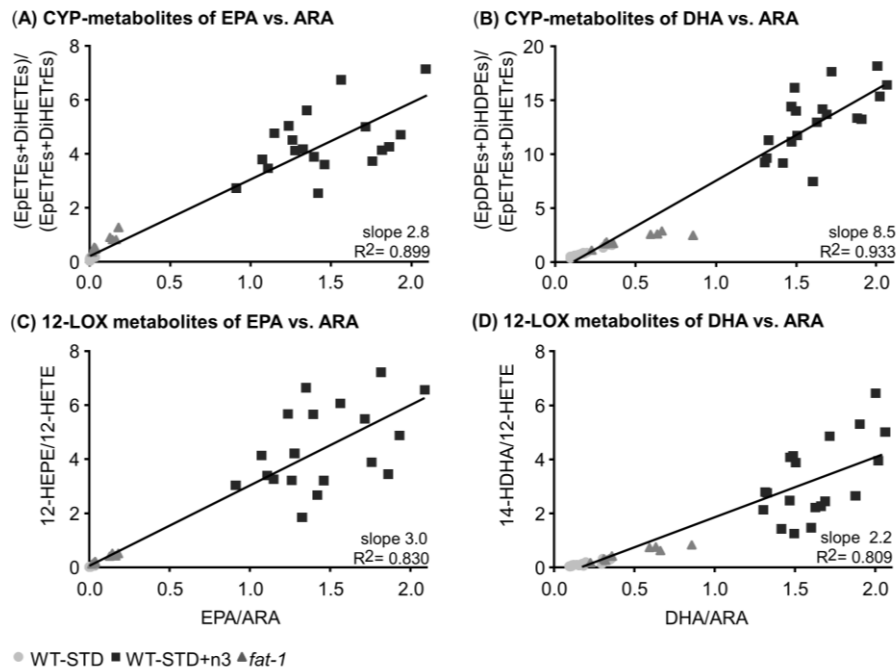


**Fig. 6.4:** Correlation between plasma n3-PUFA/n6-PUFA oxylipins and the ratio of their precursor fatty acids: The ratio of CYP metabolites (sum of epoxy-FA and dihydroxy-FA) from EPA (A) and DHA (B) and the respective ARA metabolites are plotted against the ratio of their precursor PUFA. In panel C-D the same correlation is shown for selected 12-LOX metabolites (12-HETE and 14-HDHA). The slope of the linear regression and the correlation coefficient were calculated based on all feeding groups of the experiment.

In brain, only few EPA derived oxylipins were found in *fat-1* animals and mice on the STD diet, whereas all OH-FA, some Ep-FA, 19(20)-DiHDPE, TxB<sub>3</sub> and PGD<sub>3</sub> were found in mice supplemented with n3-PUFA, though in low nmol/kg concentrations (up to  $17 \pm 5$  nmol/kg for 12-HEPE, Fig. 6.3, App. Table 9.3.5). In colon tissue, differences observed between *fat-1* mice and WT animals on the STD diet were massive, e.g. 74-fold higher concentrations for 17(18)-EpETE and 27-fold higher levels for 18-HEPE while differences between *fat-1* and n3 supplemented animals were more moderate (on average 2-4 fold higher in WT-STD+n3, Fig. 6.3). Overall, concentrations of EPA oxylipins in colon were much

higher compared to plasma and brain and ranged in *fat-1* and n3-PUFA supplemented animals from DiH-FA, dominantly found in low nmol/kg concentrations (0.65-8.6 nmol/kg; except 17,18-DiHETE), to Ep-FA (9-100 nmol/kg) and OH-FA (3.3-430 nmol/kg) to prostanoids in the high nmol/kg range (60-830 nmol/kg, Fig. 6.3, App. Table 9.3.5). Interestingly, resolvin (Rv) E2 was found in colon tissue of n3-supplemented mice ( $1.7\pm 0.2$  nmol/kg) while no other resolvin could be detected in the other assayed tissues (App. Table 9.3.5).

All **DHA metabolites** covered by the method (except RvD1) were found in plasma of all feeding groups. Concentrations in *fat-1* mice ranged up to  $9.3\pm 1.4$  nM for 19(20)-dihydroxy docosapentaenoic acid (DiHDPE) and were on average two- to threefold higher than in WT mice on the same diet (Fig. 6.3, App. Table 9.3.5). WT mice after n3-PUFA feeding showed about fourfold higher concentrations than *fat-1* mice for DiH-FA and Ep-FA (mean %difference of about 300%), while OH-FA, were elevated up to 2800% (14-hydroxy docosahexaenoic acid (14-HDHA), App. Fig. 9.3.7). Highest concentrations in DHA metabolites after n3-PUFA feeding were found for HDHAs (2.7-190 nM) followed by DiHDPEs and EpDPEs (1.6-31 nM, Fig. 6.3, App. Table 9.5.5). DHA metabolites in brain were in the low nmol/kg range in all groups (1-24 nmol/kg, Fig. 6.3, App. Table 9.3.5), with most DiHDPEs being <LOQ. While DHA levels in all groups were similar, differences in DHA docosanoids between *fat-1* and n3-PUFA fed mice were pronounced, being with a mean% difference of 220-230% highest for 7-HDHA and 19(20)-DiHDPE (Fig. 6.3, App. Fig. 9.3.7). As observed for EPA metabolites, amounts of DHA oxylipins in colon were higher compared to plasma and brain, reaching high nmol/kg concentrations for some HDHAs (up to  $850\pm 200$  nmol/kg for 14-HDHA in *fat-1* mice, App. Table 9.3.5). By contrast, most DiHDPEs, except 19,20-DiHDPE, were found in low nmol/kg concentrations (up to  $8.6\pm 0.4$  nmol/kg for 4,5-DiHDPE in WT-STD+n3 mice, App. Table 9.3.5). Levels in *fat-1* mice compared to WT mice on the STD diet were on average twofold higher and WT mice supplemented with n3-PUFA showed again two to threefold higher concentrations as compared to *fat-1* mice (Fig. 6.3). Concentration differences for some HDHAs were higher (mean



%difference of up to 780% for 22-HDHA, App. Fig. 9.3.7). Interestingly, 17-HDHA concentrations in colon were comparable between the three groups and 14-HDHA was lowest in n3 supplemented mice (Fig. 6.3).

Except for 12-HETE, concentrations of **ARA metabolites** in plasma were low (between  $0.060 \pm 0.008$  nM for  $\text{PGE}_2$  in WT-STD+n3 mice and  $6.3 \pm 0.9$  nM for 5(6)-epoxy eicosatrienoic acid (EpETrE) in WT-STD mice) in all three feeding groups on day 30 (Fig. 6.3, App. Table 9.3.5). It is notable that compared to EPA and DHA derived LOX and CYP products, ARA products were much lower in plasma of WT mice after n3-PUFA supplementation while the product pattern was dominated by ARA derived eicosanoids in WT mice on the standard sunflower oil based diet (Fig. 6.3). Concentrations of most ARA derived eicosanoids in n3-PUFA fed animals, except  $\text{TxB}_2$  and 12-HETE, were about 50-60% lower as compared to *fat-1* mice (App. Fig. 9.3.7) and differences between *fat-1* and WT-STD mice were in the same range (Fig. 6.3, App. Table 9.3.5). In brain of all feeding groups at day 30, diH-FA of ARA were found in low nmol/kg concentrations (0.51-1.3 nmol/kg), followed by ep-FA (10-81 nmol/kg) and OH-FA (2.9-150 nmol/kg). Prostanoids were found in concentrations up to  $750 \pm 40$  nmol/kg ( $\text{PGD}_2$ , WT-STD, Fig. 6.3, App. Table 9.3.5). Highest change between the groups was found for  $\text{TxB}_2$  (with a factor of 2.7) between WT-STD and *fat-1* mice (Fig. 6.3). It is interesting that concentrations of most ARA derived eicosanoids were slightly higher in WT-STD+n3 mice compared to *fat-1* mice (Fig. 6.3, App. Table 9.3.5). ARA eicosanoid levels in colon reached  $\mu\text{mol/kg}$  concentrations for some prostanoids, e.g.  $\text{PGE}_2$  and  $\text{PGD}_2$ , and HETEs, such as 11-HETE and 15-HETE (Fig. 6.3), while diH-ARA were found in low nmol/kg concentrations (0.8-11 nmol/kg, App. Table 9.3.5). Changes between the groups (WT-STD vs. *fat-1* vs. WT-STD+n3) were comparable, roughly twofold for most analytes (Fig. 6.3).

## 6.4 Discussion

A low dietary content of n3-PUFA has been implicated in a variety of pathophysiological processes and could impair human health. However, neither the breadth of biological effects of n3-PUFA nor the underlying molecular mechanisms are completely understood. Therefore, predictive (animal) models are needed which allow investigating the biology of n3-PUFA and their metabolites. In recent years, a transgenic mouse model with high endogenous levels of n3-PUFA has been established which is in addition to feeding studies, providing n3-PUFA with the diet, frequently used for this purpose and has shown beneficial effects of increased endogenous n3-PUFA levels in a wide variety of disease models [29-36, 38]. The aim of the present study was to thoroughly characterize and compare the power of the transgenic model and a feeding approach to modulate the endogenous fatty acid and oxylipin profile.

Feeding of n3-PUFAs EPA and DHA with the diet led to massively higher concentrations of respective fatty acids in blood and tissues compared to WT mice on a standard sunflower oil based diet as reported earlier in rodents [13, 21-24]. In men, similar observations were made following EPA+DHA supplementation, however, changes were more moderate caused by lower supplementation levels of n3-PUFA [47-52]. After 14-30 days of feeding a sunflower oil based diet enriched with 1% EPA and 1% DHA, levels of both FA reached a maximum steady state. This data suggests that studies aiming to investigate the effect of n3-PUFA need to implement a pre-feeding period of at least 14-30 days to elicit the full effects of n3-PUFA.

*Fat-1* mice showed lower concentrations of n3-PUFA as compared to supplemented WT mice which was most pronounced for EPA, being 2.7-34 fold lower in blood and tissues, while DHA concentrations were at most threefold lower at maximum steady state at 30 days and thereafter (Fig. 6.1, Table 6.1). This can be explained by the genetic background of these animals. In the *fat-1* mouse model the *fat-1* gene of the roundworm *C. elegans* was introduced into the DNA of C57BL/6 wildtype mice. As a consequence, homo- and

heterozygote animals can biosynthesize n3- from n6-PUFA [28]. In *C. elegans*, different n6-PUFA, such as LA, C20:3 n6 and ARA are converted by the n3 desaturase, encoded by the *fat-1* gene, resulting in ALA, C20:4 n3 and EPA, respectively [53]. The roundworm lacks further elongase activity. Therefore, the biosynthetic fatty acid pathway stops at EPA, being the most abundant PUFA in the worm [53]. By contrast, in mammals EPA is further elongated to n3-DPA which in turn is converted via C24:5 n3 to DHA (conversion by elongase and delta-6 desaturase with subsequent  $\beta$ -oxidation in peroxisomes) [17, 18]. These reactions occur at high rates, e.g. 63% (EPA to n3-DPA) and 37% (n3-DPA to DHA) in humans [54]. EPA biosynthesis in mammals from the essential ALA, however, is low – caused by the rate limiting desaturation of ALA to C18:4 n3 in combination with high dietary LA and low ALA consumption [17, 18]. This results in low endogenous EPA levels compared to DHA, being <0.05% in WT mice on a standard sunflower oil based diet in most tissues and blood (Fig. 6.1, Table 6.1) or two- to tenfold lower than DHA in blood of non-supplemented humans [47-52].

Due to n3 desaturase activity in *fat-1* mice, endogenous EPA formation is higher compared to WT mice. However, further metabolism by mammalian enzymes again resulted in high DHA concentrations compared to EPA e.g., 6.8% (DHA) vs. 0.16% (EPA) in liver, which is consistent with previous results [31]. Thus, n3 desaturase activity led to high DHA levels in *fat-1* while EPA levels were in the low range.

Levels of intermediary formed n3-DPA were in the same range as EPA levels in *fat-1* mice, supporting higher conversion rates of EPA to n3-DPA than of n3-DPA to DHA as observed in humans [54]. This finding is also supported by levels of n3-DPA in STD fed WT mice, which were higher compared to EPA levels in all investigated tissues and blood cells. However, it should be noted, that n3-DPA is not only formed as intermediate in the conversion of EPA to DHA, but also in the process of DHA retroconversion: Following a single dose of 3 mg [<sup>13</sup>C]22:6-triacylglycerol to male rats (300 g), retroconversion was found to

be 9% of the total plasma [ $^{13}\text{C}$ ]22:6 n3 (estimated by [ $^{13}\text{C}$ ]22:5 n3+[ $^{13}\text{C}$ ]20:5 n3 in plasma lipids) [55].

The n6/n3 ratio, a frequently used marker to describe the endogenous n3-PUFA status [21, 27, 30, 31, 34, 36, 56] was reduced in *fat-1* compared to WT animals on a standard diet. Although calculated slightly different, the observed n6/n3 ratios were comparable, however, a little higher than ratios observed by Kang et al. [28]. This reduction in the n6/n3 ratio observed in *fat-1* mice has been associated with protection in different disease models, including colon inflammation and hepatitis [29-36, 38]. Feeding of WT animals with a diet enriched with 1% EPA and 1% DHA led to notably lower n6/n3 ratios. It remains to be determined if this is also associated with a higher degree of protection. In a model of Parkinson's Disease this seems to be the case: *Fat-1* mice did not show a neuroprotective effect [37], while n3-PUFA supplementation did [27]. The lack of efficiency in the *fat-1* mouse model might be due to a lower modulation of the endogenous n3 and n6 PUFA profile compared to supplementation, as discussed by Bousquet et al. [37].

The %EPA+DHA in blood cells for the description of the endogenous n3-PUFA status is a modification of the omega-3 index which is discussed as a risk factor for cardiovascular diseases in humans [46, 57]. In *fat-1* mice, %EPA+DHA in blood cells was  $7.4\pm 0.2\%$ . Translating from mouse to men, these levels were in the range of an omega-3 index that has been shown to be correlated with a lower cardiovascular risk, e.g. for an acute coronary syndrome event or for mortality from coronary heart disease (omega-3 index  $>8\%$ , [46, 57]). %EPA+DHA in blood cells of *fat-1* mice was also comparable to the omega-3 index observed in healthy volunteers following supplementation (0.46-1.6 mg/d EPA and 0.38-1.1 g/d DHA for up to 12 weeks) which ranged from 8.4-11% (calculated from the means presented for EPA and DHA as %of total FA [47, 49, 50]). However, the ratio of DHA to EPA in *fat-1* mice was seven while in humans after supplementation this ratio was on average two [47, 49, 50]. Thus, individual level of EPA and DHA were differently modulated in *fat-1* mice

compared to n3-PUFA supplementation with almost equal amounts of EPA and DHA. Keeping in mind that EPA and DHA effects might be different (e.g. EpDPEs were more effective in reducing pain than EpETEs in a model of pain associated with inflammation [58]), care must be taken when directly transferring results obtained from the *fat-1* mouse model to humans. By contrast, using feeding approaches, experiments can be designed with defined treatment regimens and optimized n3-PUFA concentrations mimicking dietary ingestion of n3-PUFAs in humans.

In response to higher endogenous level of n3-PUFA induced by supplementation or insertion of the *fat-1* gene, the share of n6-PUFA, such as ARA and related FA, was decreased which is consistent with previous findings in n3-PUFA fed animals on a dietary background high in LA [13, 23, 24] and *fat-1* mice [29-31, 33-38]. Thus, EPA and DHA supplementation directly led to a notable displacement of ARA, which is a common explanation for their anti-inflammatory action [1-3]. This theory is based on the assumption that most ARA derived oxylipins act pro-inflammatory and that n3-PUFA compete for conversion by the same enzymes yielding, e.g., less potent, EPA derived PGE<sub>3</sub> or LTB<sub>5</sub> [1, 8]. Our study supports this replacement of ARA by n3-PUFA on the level of oxylipins, reflecting the changes observed for PUFA (Fig. 6.3): While oxylipin levels in WT animals on a standard diet – in line with the high ARA level – were dominated by ARA derived oxylipins, the pattern shifted to n3-PUFA derived ones in *fat-1* and n3-PUFA fed animals. This is consistent with previous results, showing similar trends for free oxylipins [40] and esterified OH-FA [39] in *fat-1* mice as well as for esterified CYP metabolites in plasma and tissues of rodents [13] and for free and/or esterified oxylipins in plasma of humans [47-52]. It should be noted that in general the modulation of the oxylipin pattern was more pronounced for n3-supplemented than for *fat-1* mice compared to WT mice on the standard diet. As a result, n3-PUFA feeding led overall to higher concentrations of n3-PUFA derived oxylipins and lower ARA derived eicosanoids (except in brain) compared to *fat-1* mice. This was most

pronounced in plasma for EPA metabolites, thereby reflecting the high difference in EPA between *fat-1* and n3-PUFA fed mice.

As shown in Fig. 6.3 for exemplary oxylipins, the product patterns of the LOX (5, 12 and 15) and CYP (hydroxylation and epoxygenation) pathways in plasma after n3-PUFA feeding were dominated by EPA and DHA oxylipins. This is somewhat remarkable, since ARA remained a dominating PUFA (6.7% ARA vs. 9.5% EPA vs. 11% DHA in plasma of WT-STD+n3 mice, Fig. 6.1) and indicates a preferred formation of n3-PUFA oxylipins over ARA derived ones. The ratio of substrates and products for CYP and LOX (Fig. 6.4), found in this study suggests that a preference of the enzymes could explain part of the effect. However, the moderate preference of, e.g., epoxygenating and hydroxylating CYP enzymes for DHA or EPA over ARA (ARA:EPA:DHA 1:4:1.5 for CYP2J2) [13, 59] alone seems not to sufficiently explain the massive difference observed in the overall pattern of oxylipins in plasma. Interestingly, in tissues, the dominance of LOX and CYP derived n3-PUFA oxylipins was less pronounced and concentrations were mostly in a similar range as ARA derived eicosanoids which indicates a tissue specific regulation. Nevertheless, our findings once more show that a moderate shift in the fatty acid pattern causes a pronounced increase in their oxidation products.

In contrast, only a slight shift in ARA derived eicosanoids to n3-PUFA oxylipins was observed for COX products in plasma and tissues. While absolute concentrations of COX derived ARA metabolites were similarly decreased as LOX and CYP products, EPA metabolite concentrations in *fat-1* and n3-PUFA fed mice were still very low compared to their ARA derived counterparts. This can be explained by the low conversion rate of n3-PUFA by COX [60] leading on the one hand to low EPA-product formation and on the other hand to inhibition of ARA conversion by COXs.

It is interesting that, compared to plasma and brain, the highest concentrations of oxylipins from all three branches of the ARA cascade were found in colon, although the share of n3-PUFA among all FA in colon was lowest in all

investigated tissues and blood. Particularly COX metabolites were found in high concentrations, indicating an important role in homeostasis. Distinct differences in the oxylipin pattern were found between *fat-1* and WT mice on the STD diet in colon. While relative changes in ARA and DHA metabolites were moderate, EPA metabolites from all enzymatic pathways were massively increased in *fat-1* compared to WT-STD mice. This high increase may in part explain the effectiveness of the *fat-1* model in colitis and colitis-associated colon cancer [29, 30, 34, 35]. Not only were pro-inflammatory ARA derived metabolites, such as COX products, decreased (see above) but also were most EPA derived mediators elevated. While specialized pro-resolving mediators (SPM) derived from EPA were not found in colon tissue of *fat-1* mice, 18-HEPE, as anti-inflammatory pathway indicator and precursor for E series resolvins [61] with unclear formation pathway, was highly increased. Since RvE1 has previously been found in the same concentration range as PGE3 in inflamed colon of *fat-1* mice [30], this might indicate elevated resolvin formation in case of an inflammation. Also, 17(18)-EpETE, precursor to the potent anti-inflammatory mediator 12-OH-17,18-EpETE [62], was elevated. Although 12-OH-17,18-EpETE was not found in colon tissue, it might as well be formed upon inflammatory stimuli.

In brain, only slight modulations in the overall fatty acid profile were found between the groups compared to the other tissues investigated. In comparison to WT mice on the STD diet, DHA concentrations were slightly lower in *fat-1* after 30 days on the same diet and slightly higher after 30 days of n3-PUFA supplementation. This low modulation of DHA in adult mice with a developed brain [63] is consistent with previous findings in adult rats. Bourre et al. showed that neither feeding an n3-PUFA deprived diet for seven months to adult rats [64] nor eight weeks of feeding a diet containing 1.5% fish oil altered the brain DHA level [65]. However, with higher concentrations of fish oil in the diet, the DHA content in brain increased [65]. It should be noted that in contrast to slight changes in DHA concentrations, DHA oxylipins were elevated about twofold between WT-STD/*fat-1* and *fat-1*/WT-STD+n3. On the one hand, a higher

substrate availability from plasma, a main source of brain DHA [66] might have led to the observed increase. On the other hand, oxylipins formed in other tissues might have been transported to the brain tissue. However, it should be noted that the animals were not perfused before collection of organs and residual blood might have been present in the tissue analyzed, although highest care was taken during sample preparation. Thus, the observed modulation in brain oxylipins may have resulted from residual blood in the tissue. Nonetheless, the pronounced effect on brain oxylipin levels by n3-PUFA warrants further investigation.

Overall, the fatty acid and oxylipin pattern in *fat-1* mice and n3 supplemented mice were modulated to higher concentrations of n3-PUFA and their metabolites in blood and tissues compared to WT mice on a standard sunflower diet, which is associated with a protection against different diseases. In general, the modulation in *fat-1* mice was lower compared to n3-PUFA supplementation. The applicability of the *fat-1* mouse model to investigate n3-PUFA associated effects, however, has been demonstrated in various disease models, e.g. colon inflammation or hepatitis [29-36, 38]. Since levels of EPA+DHA in blood cells of *fat-1* mice were comparable to humans after supplementation, this model mimics n3-PUFA concentrations readily achievable with dietary supplementation. However, levels of the individual FA, particularly EPA were different, which might result in different physiological effects. An advantage of the *fat-1* mouse model in comparison to feeding of n3-PUFA is the possibility of using one standard diet for the experimental groups. Therefore, confounding factors which might be introduced by the use of different experimental diets [56] or degradation of oxidation prone PUFA to potentially bioactive compounds [67] are reduced. However, for several questions, this model might not be suitable, particularly for the investigation of concentration dependent effects or the optimization of the dietary n6/n3 ratio needed for protection against diseases [68]. Here, feeding studies using defined concentrations of n3-PUFA in the diet in combination with an effective feeding regime are the most suitable approach. Another drawback of the *fat-1* mouse model is that a discrimination between



individual effects derived from DHA and EPA is not possible while the diet for feeding studies can be modulated accordingly.

Given the large amount of biologically relevant effects observed in studies using *fat-1* mice, these results indicate that efficacy of n3-PUFA, and their derived oxylipins, might thus be found already in the context of rather low endogenous levels of n3-PUFA which could be easily achieved – and even surpassed – by dietary interventions. However, for some questions, e.g. the in depth and concentration dependent effects of (individual) n3-PUFA in vivo, feeding studies remain the model of choice.

## 6.5 References

1. Calder PC. Marine omega-3 fatty acids and inflammatory processes: Effects, mechanisms and clinical relevance. *Biochim Biophys Acta*. 2015;1851(4):469-484.
2. Mozaffarian D, Wu JH. Omega-3 fatty acids and cardiovascular disease: effects on risk factors, molecular pathways, and clinical events. *J Am Coll Cardiol*. 2011;58(20):2047-2067.
3. Wang W, Zhu J, Lyu F, Panigrahy D, Ferrara KW, Hammock B, Zhang G. omega-3 polyunsaturated fatty acids-derived lipid metabolites on angiogenesis, inflammation and cancer. *Prostaglandins Oth Lipid M*. 2014;113-115:13-20.
4. Zhang G, Panigrahy D, Mahakian LM, Yang J, Liu JY, Stephen Lee KS, Wettersten HI, Ulu A, Hu X, Tam S, Hwang SH, Ingham ES, Kieran MW, Weiss RH, Ferrara KW, Hammock BD. Epoxy metabolites of docosahexaenoic acid (DHA) inhibit angiogenesis, tumor growth, and metastasis. *Proc Natl Acad Sci U S A*. 2013;110(16):6530-6535.
5. Innis SM. Dietary (n-3) fatty acids and brain development. *J Nutr*. 2007;137(4):855-859.
6. Buczynski MW, Dumlao DS, Dennis EA. Thematic Review Series: Proteomics. An integrated omics analysis of eicosanoid biology. *J Lipid Res*. 2009;50(6):1015-1038.
7. Funk CD. Prostaglandins and leukotrienes: advances in eicosanoid biology. *Science*. 2001;294(5548):1871-1875.
8. Gabbs M, Leng S, Devassy JG, Monirujjaman M, Aukema HM. Advances in Our Understanding of Oxylipins Derived from Dietary PUFAs. *Adv Nutr*. 2015;6(5):513-540.
9. Panigrahy D, Greene ER, Pozzi A, Wang DW, Zeldin DC. EET signaling in cancer. *Cancer Metastasis Rev*. 2011;30(3-4):525-540.
10. Inceoglu B, Wagner K, Schebb NH, Morisseau C, Jinks SL, Ulu A, Hegedus C, Rose T, Brosnan R, Hammock BD. Analgesia mediated by soluble epoxide hydrolase inhibitors is dependent on cAMP. *Proc Natl Acad Sci U S A*. 2011;108(12):5093-5097.
11. Inceoglu B, Wagner KM, Yang J, Bettaieb A, Schebb NH, Hwang SH, Morisseau C, Haj FG, Hammock BD. Acute augmentation of epoxygenated fatty acid levels rapidly reduces pain-related behavior in a rat model of type I diabetes. *Proc Natl Acad Sci U S A*. 2012;109(28):11390-11395.
12. Morisseau C, Hammock BD. Epoxide hydrolases: mechanisms, inhibitor designs, and biological roles. *Annu Rev Pharmacol Toxicol*. 2005;45:311-333.
13. Arnold C, Markovic M, Blossey K, Wallukat G, Fischer R, Dechend R, Konkel A, von Schacky C, Luft FC, Muller DN, Rothe M, Schunck WH. Arachidonic acid-metabolizing cytochrome P450 enzymes are targets of {omega}-3 fatty acids. *J Biol Chem*. 2010;285(43):32720-32733.
14. Serhan CN. Pro-resolving lipid mediators are leads for resolution physiology. *Nature*. 2014;510(7503):92-101.
15. Weylandt KH, Chiu CY, Gomolka B, Waechter SF, Wiedenmann B. Omega-3 fatty acids and their lipid mediators: Towards an understanding of resolvin and protectin formation Omega-3 fatty acids and their resolvin/protectin mediators. *Prostaglandins Oth Lipid M*. 2012;97(3-4):73-82.

16. Weylandt KH, Serini S, Chen YQ, Su HM, Lim K, Cittadini A, Calviello G. Omega-3 Polyunsaturated Fatty Acids: The Way Forward in Times of Mixed Evidence. *Biomed Res Int.* 2015;2015:143109.
17. Burdge GC, Calder PC. Conversion of alpha-linolenic acid to longer-chain polyunsaturated fatty acids in human adults. *Reprod Nutr Dev.* 2005;45(5):581-597.
18. Guillou H, Zadavec D, Martin PG, Jacobsson A. The key roles of elongases and desaturases in mammalian fatty acid metabolism: Insights from transgenic mice. *Prog Lipid Res.* 2010;49(2):186-199.
19. Bimbo AP. Sources of omega-3 fatty acids. In: Jacobsen C, Nielsen NS, Frisenfeldt Horn A, Moltke Sørensen A-D, editors. *Food enrichment with omega-3 fatty acids.* Cambridge: Woodhead Publishing Limited; 2013. p. 27-107.
20. Kutzner L, Ostermann AI, Konrad T, Riegel D, Hellhake S, Schuchardt JP, Schebb NH. Lipid Class Specific Quantitative Analysis of n-3 Polyunsaturated Fatty Acids in Food Supplements. *J Agric Food Chem.* 2017;65(1):139-147.
21. Camuesco D, Galvez J, Nieto A, Comalada M, Rodriguez-Cabezas ME, Concha A, Xaus J, Zarzuelo A. Dietary olive oil supplemented with fish oil, rich in EPA and DHA (n-3) polyunsaturated fatty acids, attenuates colonic inflammation in rats with DSS-induced colitis. *J Nutr.* 2005;135(4):687-694.
22. Nieto N, Torres MI, Rios A, Gil A. Dietary polyunsaturated fatty acids improve histological and biochemical alterations in rats with experimental ulcerative colitis. *J Nutr.* 2002;132(1):11-19.
23. Olson MV, Liu YC, Dangi B, Paul Zimmer J, Salem N, Jr., Nauroth JM. Docosahexaenoic acid reduces inflammation and joint destruction in mice with collagen-induced arthritis. *Inflamm Res.* 2013;62(12):1003-1013.
24. Volker DH, FitzGerald PE, Garg ML. The eicosapentaenoic to docosahexaenoic acid ratio of diets affects the pathogenesis of arthritis in Lew/SSN rats. *J Nutr.* 2000;130(3):559-565.
25. Ulu A, Harris TR, Morisseau C, Miyabe C, Inoue H, Schuster G, Dong H, Iosif AM, Liu JY, Weiss RH, Chiamvimonvat N, Imig JD, Hammock BD. Anti-inflammatory Effects of omega-3 Polyunsaturated Fatty Acids and Soluble Epoxide Hydrolase Inhibitors in Angiotensin-II-Dependent Hypertension. *J Cardiovasc Pharmacol.* 2013;62(3):285-297.
26. Harris TR, Kodani S, Yang J, Imai DM, Hammock BD. An omega-3-enriched diet alone does not attenuate CCl4-induced hepatic fibrosis. *J Nutr Biochem.* 2016;38:93-101.
27. Bousquet M, Saint-Pierre M, Julien C, Salem N, Jr., Cicchetti F, Calon F. Beneficial effects of dietary omega-3 polyunsaturated fatty acid on toxin-induced neuronal degeneration in an animal model of Parkinson's disease. *FASEB Journal.* 2008;22(4):1213-1225.
28. Kang JX, Wang J, Wu L, Kang ZB. Transgenic mice: fat-1 mice convert n-6 to n-3 fatty acids. *Nature.* 2004;427(6974):504.
29. Gravaghi C, La Perle KM, Ogrodowski P, Kang JX, Quimby F, Lipkin M, Lamprecht SA. Cox-2 expression, PGE(2) and cytokines production are inhibited by endogenously synthesized n-3 PUFAs in inflamed colon of fat-1 mice. *J Nutr Biochem.* 2011;22(4):360-365.
30. Hudert CA, Weylandt KH, Lu Y, Wang J, Hong S, Dignass A, Serhan CN, Kang JX. Transgenic mice rich in endogenous omega-3 fatty acids are protected from colitis. *Proc Natl Acad Sci U S A.* 2006;103(30):11276-11281.

31. Schmocker C, Weylandt KH, Kahlke L, Wang J, Lobeck H, Tiegs G, Berg T, Kang JX. Omega-3 fatty acids alleviate chemically induced acute hepatitis by suppression of cytokines. *Hepatology*. 2007;45(4):864-869.
32. Weylandt KH, Nadolny A, Kahlke L, Kohnke T, Schmocker C, Wang J, Lauwers GY, Glickman JN, Kang JX. Reduction of inflammation and chronic tissue damage by omega-3 fatty acids in fat-1 transgenic mice with pancreatitis. *Biochim Biophys Acta*. 2008;1782(11):634-641.
33. Weylandt KH, Krause LF, Gomolka B, Chiu CY, Bilal S, Nadolny A, Waechter SF, Fischer A, Rothe M, Kang JX. Suppressed liver tumorigenesis in fat-1 mice with elevated omega-3 fatty acids is associated with increased omega-3 derived lipid mediators and reduced TNF-alpha. *Carcinogenesis*. 2011;32(6):897-903.
34. Jia Q, Lupton JR, Smith R, Weeks BR, Callaway E, Davidson LA, Kim W, Fan YY, Yang PY, Newman RA, Kang JX, McMurray DN, Chapkin RS. Reduced colitis-associated colon cancer in fat-1 (n-3 fatty acid desaturase) transgenic mice. *Cancer Research*. 2008;68(10):3985-3991.
35. Nowak J, Weylandt KH, Habbel P, Wang J, Dignass A, Glickman JN, Kang JX. Colitis-associated colon tumorigenesis is suppressed in transgenic mice rich in endogenous n-3 fatty acids. *Carcinogenesis*. 2007;28(9):1991-1995.
36. Xia SH, Wang JD, He CW, Hong S, Serhan CN, Kang JX. Melanoma growth is reduced in fat-1 transgenic mice: Impact of omega-6/omega-3 essential fatty acids. *Proc Natl Acad Sci U S A*. 2006;103(33):12499-12504.
37. Bousquet M, Gue K, Emond V, Julien P, Kang JX, Cicchetti F, Calon F. Transgenic conversion of omega-6 into omega-3 fatty acids in a mouse model of Parkinson's disease. *J Lipid Res*. 2011;52(2):263-271.
38. Bellenger J, Bellenger S, Bataille A, Massey KA, Nicolaou A, Rialland M, Tessier C, Kang JX, Narce M. High Pancreatic n-3 Fatty Acids Prevent STZ-Induced Diabetes in Fat-1 Mice: Inflammatory Pathway Inhibition. *Diabetes*. 2011;60(4):1090-1099.
39. Chiu CY, Smyl C, Dogan I, Rothe M, Weylandt KH. Quantitative Profiling of Hydroxy Lipid Metabolites in Mouse Organs Reveals Distinct Lipidomic Profiles and Modifications Due to Elevated n-3 Fatty Acid Levels. *Biology (Basel)*. 2017;6(1).
40. Astarita G, McKenzie JH, Wang B, Strassburg K, Doneanu A, Johnson J, Baker A, Hankemeier T, Murphy J, Vreeken RJ, Langridge J, Kang JX. A protective lipidomic biosignature associated with a balanced omega-6/omega-3 ratio in fat-1 transgenic mice. *PLoS One*. 2014;9(4):e96221.
41. Kelton D, Lysecki C, Aukema H, Anderson B, Kang JX, Ma DWL. Endogenous synthesis of n-3 PUFA modifies fatty acid composition of kidney phospholipids and eicosanoid levels in the fat-1 mouse. *Prostaglandins Leukot Essent Fatty Acids*. 2013;89(4):169-177.
42. Ostermann AI, Muller M, Willenberg I, Schebb NH. Determining the fatty acid composition in plasma and tissues as fatty acid methyl esters using gas chromatography - a comparison of different derivatization and extraction procedures. *Prostaglandins Leukot Essent Fatty Acids*. 2014;91(6):235-241.
43. Craske JD, Bannon CD. Letter to the Editor. *J Am Oil Chem Soc*. 1988;65(7):1190-1191.

44. Ostermann AI, Willenberg I, Schebb NH. Comparison of sample preparation methods for the quantitative analysis of eicosanoids and other oxylipins in plasma by means of LC-MS/MS. *Anal Bioanal Chem.* 2015;407(5):1403-1414.
45. Willenberg I, Rund K, Rong S, Shushakova N, Gueler F, Schebb NH. Characterization of changes in plasma and tissue oxylipin levels in LPS and CLP induced murine sepsis. *Inflammation Research.* 2016;65(2):133-142.
46. Harris WS, Von Schacky C. The Omega-3 Index: a new risk factor for death from coronary heart disease? *Prev Med.* 2004;39(1):212-220.
47. Fischer R, Konkell A, Mehling H, Blosssey K, Gapelyuk A, Wessel N, von Schacky C, Dechend R, Muller DN, Rothe M, Luft FC, Weylandt K, Schunck WH. Dietary omega-3 fatty acids modulate the eicosanoid profile in man primarily via the CYP-epoxygenase pathway. *J Lipid Res.* 2014;55(6):1150-1164.
48. Keenan AH, Pedersen TL, Fillaus K, Larson MK, Shearer GC, Newman JW. Basal omega-3 fatty acid status affects fatty acid and oxylipin responses to high-dose n3-HUFA in healthy volunteers. *J Lipid Res.* 2012;53(8):1662-1669.
49. Schebb NH, Ostermann AI, Yang J, Hammock BD, Hahn A, Schuchardt JP. Comparison of the effects of long-chain omega-3 fatty acid supplementation on plasma levels of free and esterified oxylipins. *Prostaglandins Oth Lipid M.* 2014;113-115:21-29.
50. Schuchardt JP, Schmidt S, Kressel G, Willenberg I, Hammock BD, Hahn A, Schebb NH. Modulation of blood oxylipin levels by long-chain omega-3 fatty acid supplementation in hyper- and normolipidemic men. *Prostaglandins Leukot Essent Fatty Acids.* 2014;90(2-3):27-37.
51. Schuchardt JP, Schneider I, Willenberg I, Yang J, Hammock BD, Hahn A, Schebb NH. Increase of EPA-derived hydroxy, epoxy and dihydroxy fatty acid levels in human plasma after a single dose of long-chain omega-3 PUFA. *Prostaglandins Oth Lipid M.* 2014;109-111:23-31.
52. Shearer GC, Harris WS, Pedersen TL, Newman JW. Detection of omega-3 oxylipins in human plasma and response to treatment with omega-3 acid ethyl esters. *J Lipid Res.* 2010;51(8):2074-2081.
53. Watts JL, Browse J. Genetic dissection of polyunsaturated fatty acid synthesis in *Caenorhabditis elegans*. *Proc Natl Acad Sci U S A.* 2002;99(9):5854-5859.
54. Pawlosky RJ, Hibbeln JR, Novotny JA, Salem N, Jr. Physiological compartmental analysis of alpha-linolenic acid metabolism in adult humans. *J Lipid Res.* 2001;42(8):1257-1265.
55. Brossard N, Croset M, Pachiaudi C, Riou JP, Tayot JL, Lagarde M. Retroconversion and metabolism of [13C]22:6n-3 in humans and rats after intake of a single dose of [13C]22:6n-3-triacylglycerols. *Am J Clin Nutr.* 1996;64(4):577-586.
56. Kang JX. Fat-1 transgenic mice: A new model for omega-3 research. *Prostaglandins Leukot Essent Fatty Acids.* 2007;77(5-6):263-267.
57. von Schacky C. The Omega-3 Index as a risk factor for cardiovascular diseases. *Prostaglandins Oth Lipid M.* 2011;96(1-4):94-98.
58. Morisseau C, Inceoglu B, Schmelzer K, Tsai HJ, Jinks SL, Hegedus CM, Hammock BD. Naturally occurring monoepoxides of eicosapentaenoic acid and docosahexaenoic acid are bioactive antihyperalgesic lipids. *J Lipid Res.* 2010;51(12):3481-3490.

59. Westphal C, Konkell A, Schunck WH. Cytochrome p450 enzymes in the bioactivation of polyunsaturated Fatty acids and their role in cardiovascular disease. *Adv Exp Med Biol.* 2015;851:151-187.
60. Smith WL, Urade Y, Jakobsson PJ. Enzymes of the cyclooxygenase pathways of prostanoid biosynthesis. *Chem Rev.* 2011;111(10):5821-5865.
61. Serhan CN, Petasis NA. Resolvins and protectins in inflammation resolution. *Chem Rev.* 2011;111(10):5922-5943.
62. Kubota T, Arita M, Isobe Y, Iwamoto R, Goto T, Yoshioka T, Urabe D, Inoue M, Arai H. Eicosapentaenoic acid is converted via omega-3 epoxygenation to the anti-inflammatory metabolite 12-hydroxy-17,18-epoxyeicosatetraenoic acid. *Faseb Journal.* 2014;28(2):586-593.
63. Semple BD, Blomgren K, Gimlin K, Ferriero DM, Noble-Haeusslein LJ. Brain development in rodents and humans: Identifying benchmarks of maturation and vulnerability to injury across species. *Progress in Neurobiology.* 2013;106:1-16.
64. Bourre JM, Dumont OS, Piciotti MJ, Pascal GA, Durand GA. Dietary alpha-linolenic acid deficiency in adult rats for 7 months does not alter brain docosahexaenoic acid content, in contrast to liver, heart and testes. *Biochim Biophys Acta.* 1992;1124(2):119-122.
65. Bourre JM, Bonneil M, Dumont O, Piciotti M, Calaf R, Portugal H, Nalbone G, Lafont H. Effect of increasing amounts of dietary fish oil on brain and liver fatty composition. *Biochim Biophys Acta.* 1990;1043(2):149-152.
66. Spector AA. Plasma free fatty acid and lipoproteins as sources of polyunsaturated fatty acid for the brain. *J Mol Neurosci.* 2001;16(2-3):159-165.
67. Wang W, Yang H, Johnson D, Gensler C, Decker E, Zhang G. Chemistry and biology of omega-3 PUFA peroxidation-derived compounds. *Prostaglandins Other Lipid Mediat.* 2016.
68. Simopoulos AP. The importance of the ratio of omega-6/omega-3 essential fatty acids. *Biomed Pharmacother.* 2002;56(8):365-379.

# Chapter 7

## A Diet Rich in Omega-3 Fatty Acids Enhances Expression of Soluble Epoxide Hydrolase in Murine Brain\*

*Several studies suggest that intake of omega-3 polyunsaturated fatty acids (n3-PUFA) beneficially influence cognitive function. However, effects on the adult brain are not clear. Little is known about the impact of dietary intervention on the fatty acid profile in adult brain, the modulation in the expression of enzymes involved in fatty acid biosynthesis and metabolism as well as changes in resulting oxylipins. These questions were addressed in the present study in two independent n3-PUFA feeding experiments in mice. Supplementation of eicosapentaenoic acid (EPA) and docosahexaenoic acid (DHA, 1% each in in the diet) for 30 days to adult NMRI and C57BL/6 mice led to a distinct shift in the brain PUFA pattern. While n3-PUFAs EPA, n3-docosapentaenoic acid and DHA were elevated, many n6-PUFAs were significantly decreased (except, e.g. C20:3 n6 which was increased). This shift in PUFAs was accompanied by immense differences in concentrations of oxidative metabolites derived from enzymatic conversion of PUFAs, esp. arachidonic acid which products were uniformly decreased, and a modulation in the activity and expression pattern of delta-5 and delta-6 desaturases. In both mouse strains a remarkable increase in the soluble epoxide hydrolase (sEH) activity (decreased epoxy-fatty acids (FA) concentrations and epoxy-FA to dihydroxy-FA-ratios) as well as sEH expression was observed. Taking the high biological activity of epoxy-FA, e.g. on blood flow and nociceptive signaling into account, this finding might be of relevance for the effects of n3-PUFAs in neurodegenerative diseases. On any account, our study suggests a new distinct regulation of brain PUFA and oxylipin pattern by supplementation of n3-PUFAs to adult rodents*

\* Ostermann AI, Reutzel M, Hartung N, Franke N, Kutzner L, Schoenfeld K, Weylandt KH, Eckert GP and Schebb NH. 2017. *Submitted for publication.*

Author contributions: AIO: Designed research, performed experiments, and wrote manuscript; RM, NH, FN, LK, KS: Performed experiments; KHW: Contributed to research design; GPE, NHS: Designed research and wrote the manuscript.

## 7.1 Introduction

The dietary intake of long chain (LC) n3 polyunsaturated fatty acids (n3-PUFA), especially of eicosapentaenoic acid (C20:5 n3, EPA) and docosahexaenoic acid (C22:6 n3, DHA) is associated with beneficial effects on human health [1, 2]. Aside from blood triglyceride and blood pressure lowering as well as anti-inflammatory effects, improvement of cognition in adults by dietary n3-PUFA is intensively discussed [3, 4] and the importance of n3-PUFA, especially DHA, in neurodevelopment is well established [3, 5]. Moreover, several studies suggest that intake of LC n3-PUFA in adults may prevent neuronal degradation and thus contribute to the maintenance of normal brain function and cognition in elderly people [5, 6]. DHA is the main n3-PUFA in brain [5, 7] and most effects of n3-PUFA have been attributed to this FA, however evidence exists that other n3-PUFA, such as EPA or n3 docosapentaenoic acid (C22:5 n3, n3-DPA) also show distinct effects in the brain [7].

Aside from incorporation into the membranes, PUFA can be metabolized in the brain (Fig. 7.1). Though endogenous synthesis of n3-PUFA in the brain is low compared to the uptake from plasma unesterified fatty acid pool [8], brain tissue possesses all enzymes to convert one PUFA into another. Reactions involved in the biosynthesis of DHA from alpha-linolenic acid (C18:3 n3, ALA) include conversion by delta 5 and delta 6 desaturase (FADS1 and FADS2), elongases in the endoplasmic reticulum (ELOVL2 and 5) and  $\beta$ -oxidation in peroxisomes [9]. LC-n3-PUFA in brain tissue are dominantly found in phospholipids and can be converted in the arachidonic acid (ARA) cascade to eicosanoids and other oxylipins upon liberation by phospholipases. Several of the originating lipid mediators are implicated in brain (patho)physiology [7, 10]. Oxylipins are formed via three enzymatic pathways as well as autoxidation [11, 12]: Constitutively expressed cyclooxygenase (COX) 1 and COX2, the latter of which is induced e.g. during inflammation, give rise to prostaglandins (PG). Conversion by lipoxygenases (LOX) leads to hydroxperoxy FA, which can be further metabolized to, e.g., leukotrienes or hydroxy-FA. Cytochrome P450 enzymes



can act either as  $\omega$ -hydroxylases, yielding e.g. terminally hydroxylated PUFA, or as epoxygenases, yielding epoxy-FA [13]. The latter act anti-inflammatory, vasodilatory and analgesic [13, 14] and are inactivated by the soluble epoxide hydrolase to dihydroxy-FA [15]. In addition multiple hydroxylated n3-PUFA, so called specialized pro-resolving lipid mediators (SPM) such as resolvines, maresines and protectins are described as potent oxylipins (Fig. 7.1).

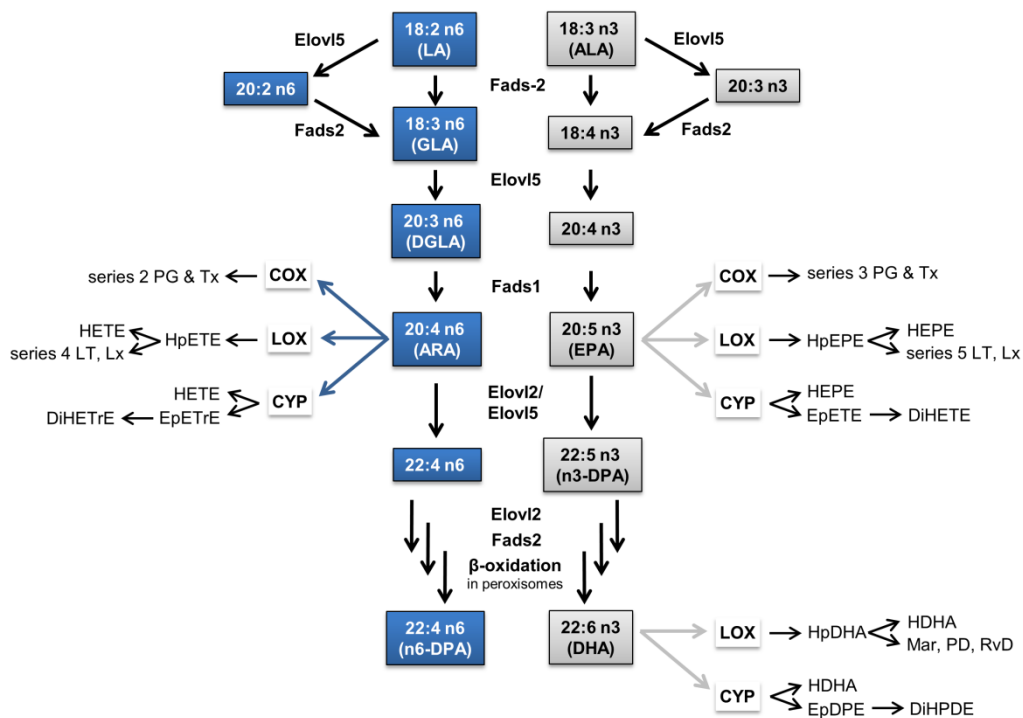


**Fig. 7.1:** Biosynthesis of long chain n3-polyunsaturated fatty acids from LA and ALA and selected oxygenation reactions of ARA, EPA and DHA within the ARA cascade. Elov1 – elongases; HpETE – hydroperoxy eicosatetraenoic acid; HETE – hydroxy eicosatetraenoic acid; Lx – lipoxin; LT – leukotriene; EpETrE – epoxy eicosatrienoic acid; DiHETrE – dihydroxy eicosatrienoic acid; HpEPE – hydroperoxy eicosapentaenoic acid; HEPE - hydroxy eicosapentaenoic acid; EpETE – epoxy eicosatetraenoic acid; DiHETE – dihydroxy eicosatetraenoic acid; HpDPA – hydroperoxy docosahexaenoic acid; HDHA – hydroxy docosahexaenoic acid; Mar – maresin, PD – protectin; RvD – D series resolvins.

Despite the tremendous interest of n3-PUFA supplementation on brain physiology and cognitive function, only little information is available on the modulation of PUFA metabolizing enzymatic pathways in the brain. Therefore, in the present study we investigated the modulation of key enzymes from the fatty acid biosynthesis (Fads1, Fads2) and metabolism (Ptgs-2 (COX2), EPHX2

(sEH)) after dietary intervention with n3-PUFA in murine brain based on activity markers quantified by means of targeted oxylipin and fatty acid metabolomics.

## **7.2 Experimental**

### **7.2.1 Chemicals**

Acetic acid and methanol (Optima LC/MS Grade) as well as acetonitrile (HPLC-MS grade) were from Fisher Scientific (Schwerte, Germany) and ammonium acetate (p.a.) was purchased from Merck (Darmstadt, Germany). Methyl tert-butyl ether, *n*-hexane (HPLC grade) and sodium acetate (p.a.) were obtained from Carl Roth (Karlsruhe, Germany). Oxylipin and deuterated oxylipin standards were obtained from Cayman Chemicals (local distributor: Biomol, Hamburg, Germany). Methyl pentacosanoate, ethyl acetate, methyl formate, and all other chemicals were purchased from Sigma Aldrich (Taufkirchen, Germany).

### **7.2.2 Feeding experiment**

Diets were obtained from ssniff GmbH, Soest, Germany. A standard diet (product number: E15051) with 10% fat from refined sunflower oil (Henry Lamotte Oils, Bremen, Germany) enriched with 0.2% tocopherol mix (Covi-Ox T 70 EU, BASF, Ludwigshafen) was used as control (STD). The same diet containing 1% EPA and 1% DHA as ethyl esters was used as n3-PUFA rich diet (STD+n3). For the feeding experiments, female C57BL/6 and NMRI mice (Charles River, Sulzfeld, Germany) of 9-10 weeks of age were used (n=6-8) and kept on the standard sunflower oil (STD) or the n3-PUFA enriched diet (STD+n3) for 30 days. The animals had access to food and water ad libitum.

### 7.2.3 Fatty acid and oxylipin analysis

Lipids were extracted from brain tissue ( $15\pm 2$  mg) using methanol/methyl tert-butyl ether (1:2, v/v) and (trans-)esterified to fatty acid methyl esters (FAME) with methanolic hydrogen chloride as described [16 (see Chapter 3)]. The method was extended to cover C20:3 n9, C22:5 n6 (n6-DPA) and 20:4 n3 allowing to calculate wt %n3 and wt %n6 in HUFA. FAMEs were analyzed by means of gas chromatography with flame ionization detection [16 (see Chapter 3)] and quantified using methyl pentacosanoate as internal standard. For oxylipin analysis, brain from C57BL/6 mice ( $50\pm 5$  mg) was homogenized following addition of internal standards and antioxidant solution [17 (see Chapter 4), 18] in 750  $\mu$ L ethyl acetate and 500  $\mu$ L water (pH 6). Brain tissue was homogenized in a ball mill using two 3 mm metal beads (25 Hz, 5 min, Retsch, Haan, Germany). Following centrifugation (20 000 xg, 5 min, 4 °C), the organic phase was collected and the sample was extracted with another 750  $\mu$ L ethyl acetate. The dried lipid extract was reconstituted in 300  $\mu$ L methanol, diluted with water to 6 mL and acidified with acetic acid (to pH 3). Extraction was carried out on C18 material (500 mg, Macherey-Nagel, Düren, Germany) as described [17 (see Chapter 4), 18] using methyl formate as eluent. Brain tissue from NMR1 mice was pulverized in liquid nitrogen in a mortar and  $50\pm 5$  mg were homogenized, after addition of internal standards and antioxidant solution [17 (see Chapter 4), 18], in acidified methanol (0.2% formic acid) using a ball mill (15 Hz, 8 min, see above). After centrifugation (20 000 xg, 5 min, 4 °C), the supernatant was diluted with 1 M sodium acetate (pH 6.0) to 3 mL and extracted on an unpolar (C8)/anion exchange mixed mode material (Bond Elut Certify II, 200 mg, Agilent) using ethyl acetate/*n*-hexane (75:25 v/v) with 1% acetic acid as eluent [17 (see Chapter 4)]. Oxylipins were quantified by liquid chromatography-mass spectrometry (LC-MS) following negative electrospray ionization on a QTrap6500 mass spectrometer (Sciex, Darmstadt, Germany) operated in scheduled selected reaction monitoring mode [17 (see Chapter 4), 18]. All results are presented as mean  $\pm$  standard error of the mean (SEM).

#### 7.2.4 Transcription analysis by quantitative real-time PCR (qRT-PCR)

For qRT-PCR analysis, cerebrum cortex tissue from NMRI mice was used. Due to limitations of cerebrum tissue, tissue from the cerebellum of C57BL/6 mice had to be used for qRT-PCR analysis. Brain tissues were stabilized with RNAlater (Qiagen, Hilden, Germany) according to the manufacturer's instructions and stored at -80 °C. Total RNA was isolated from brain tissue (~20 mg) using the RNeasy Mini Kit (Qiagen) according to the manufacturer's instructions. Quantification of RNA and assessment of purity was conducted using a NanoDrop™ 2000 c spectrophotometer (Thermo Fisher Scientific, Waltham, MA, USA). To remove residual genomic DNA, total RNA was treated with TURBO DNA-free™ Kit according to the manufacturer's instructions (Thermo Fisher Scientific). First strand cDNA was synthesized from total RNA (1 µg) using the iScript cDNA synthesis kit (BioRad, Munich, Germany) according to the manufacturer's instructions. qRT-PCR was performed on a Cfx 96 Touch™ real time PCR detection system (BioRad). All Primers were received from Biomol (Biomol, Hamburg, Germany) except EPHX2 (BioRad). Oligonucleotide primer sequence, product sizes and primer concentrations for qRT-PCR are displayed in Table 7.1. DNA for qRT-PCR was diluted 1:10 with RNase free water (Qiagen) before use and experiments were performed in triplicates. qRT-PCR cycling conditions for *Fads2* were 95 °C for 3 min followed by 50 cycles of 95 °C for 10 s, 58 °C for 45 s and 72 °C for 29 s. q-PCR conditions for *Ptgs2* were 95 °C for 3 min followed by 45 cycles 95 °C for 10 s, 56 °C for 30 s and 72 °C for 29 s. qRT-PCR cycling conditions for *Fads1* were 95 °C for 3 min followed by 50 cycles of 95 °C for 10 s, 58 °C for 45 s and 72 °C for 29 s. qRT-PCR conditions for *EPHX2* were 95 °C for 3 min followed by 40 cycles of 95 °C for 10 s, 56 °C for 30 s and 72 °C for 29 s. Gene expression was analysed using the  $2(-\Delta\Delta Cq)$  method using BioRad Cfx manager (BioRad) and Biogazelle qbase+ (Biogazelle, Zwijnaarde, Belgium) and normalized to the levels of  $\beta 2$  microglobulin (B2M) and phosphoglycerat kinase 1 (PGK1).

**Table 7.1:** Oligonucleotide primer sequences, product sizes and primer concentrations for qRT-PCR.

Gene	Primer Sequence	Product size (bp)	Primer conc. (nm)
EPHX2 <sup>1</sup>	N/A	N/A	sixfold dilution (6x)
Fads1	5'-aagcacatgccatacaacca-3' 5'-cagcggcatgtaagtgaaga-3'	177	200
Fads2	5'-aaagagcctgcatgtgttg-3' 5'-gatgccgtagaaagggatgt-3'	250	100
Ptgs2	5'-tgatcgaagactacgtgcaa-3' 5'-gtgagtcctatgtccaggag-3'	229	100

bp base pairs, conc. Concentration

<sup>1</sup>commercial primer, no information available (N/A)

### 7.3 Results and Discussion

The aim of this study was the investigation of the effect of n3-PUFA supplementation on the activity of PUFA metabolizing enzymes in murine brain. Utilizing targeted oxylipin metabolomics and fatty acid analysis accompanied by qRT-PCR, changes in the product patterns of the enzymes were correlated to their transcription levels in brain.

During the feeding experiments, no differences in feeding and animal behavior were observed. Feeding of a diet containing 1% EPA and 1% DHA as ethyl esters led to slight changes in the overall fatty acid pattern (Fig. 7.2 I). However, changes in the brain PUFA composition of the animals were distinct (Fig. 7.2 II). In C57BL/6 mice, concentrations of most ALA downstream products, covered by the method, were increased compared to baseline (from 6.1±0.5 to 6.9±0.4 µg/mg for DHA, from <0.002 to 0.084±0.005 µg/mg for EPA and from 0.037±0.003 to 0.18±0.01 µg/mg for n3-DPA, respectively, Fig. 7.2 IIA, App. Table 9.4.1), while concentrations of arachidonic acid (C20:4 n6, ARA) were decreased (from 4.6±0.4 to 3.9±0.3 µg/mg, Fig. 7.2 IIA, App. Table 9.4.1). Consequently, downstream products of ARA, C22:4 n6 and n6 docosapentaenoic acid (C22:5 n6, n6-DPA) formed from ARA by elongation

(C22:4 n6) with subsequent desaturation and  $\beta$ -oxidation in peroxisomes (n6-DPA)[19] were also found at significantly lower concentrations (Fig. 7.2 IIA). Interestingly, levels of C20:3 n6 (dihomo gamma-linolenic acid, DGLA), precursor of ARA in the fatty acid biosynthesis, were increased (Fig. 7.2 IIA), indicating elevated conversion of linoleic acid (C18:2 n6, LA) to longer chain PUFA, which is further supported by the D6D index (Fig. 7.2 IVA, see below). The desaturation product of LA, gamma-linolenic acid (C18:3 n6, GLA) was below the limit of detection in both feeding groups (Fig. 7.2 IIA, STD and STD+n3), suggesting that this FA is quickly further metabolized. This is consistent with previous results, reporting that the first step in the conversion of LA/ALA (the desaturation of LA/ALA by delta-6 desaturase (Fads2)) [19, 20] to longer chain PUFA is rate limiting. An independent feeding experiment (new batch of n3-PUFA chow, different animal facility, different mouse strain (NMRI)) led to same effects (Fig. 7.2 B), though absolute PUFA concentrations were slightly lower. Changes observed in the absolute fatty acid pattern were reflected in relative levels (App. Fig. 9.4.1, Table 9.4.2).

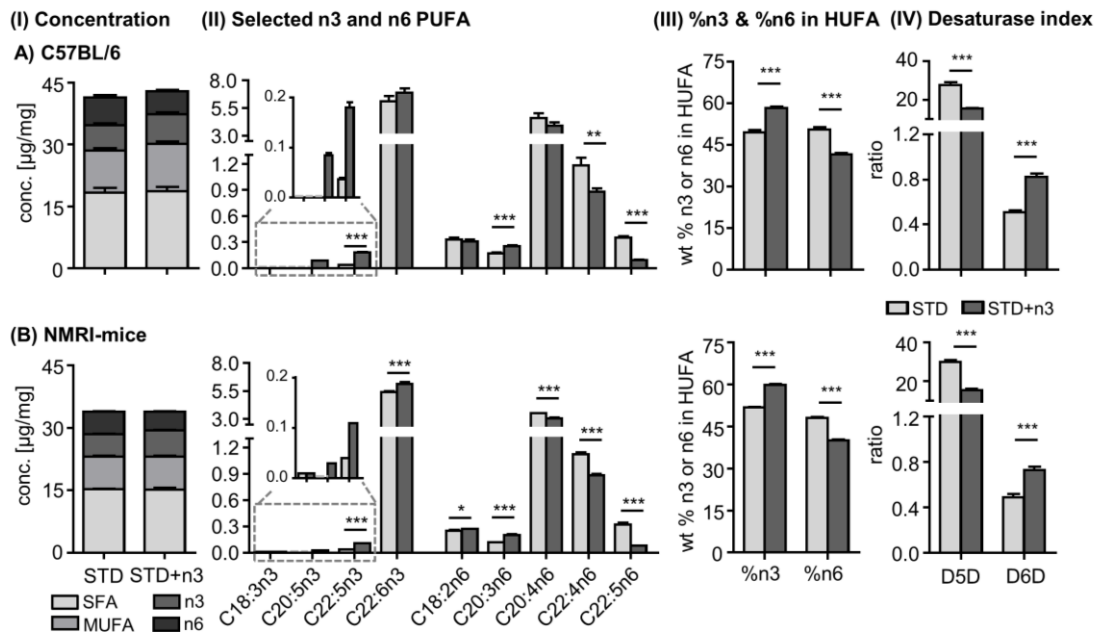


**Fig. 7.2:** Fatty acid concentrations in brain tissue of C57BL/6 (A) and NMRI-mice (B) fed with a standard sunflower oil based diet (STD) or the same diet enriched with n3-PUFA (STD+n3). Shown are (I) relative amounts of saturated (SFA), monounsaturated (MUFA), n3 and n6 polyunsaturated fatty acids (PUFA) as well as (II) selected n3- and n6-PUFA. n9-PUFA are not shown in (I) due to relative amounts below 0.2 % of total FA. The LOQ for an analyte is indicated as dashed line in case it was not exceeded in >50% of the samples per group. (III) wt%n3 and wt%n6 in HUFA (highly unsaturated fatty acids) were calculated as follows, modified from [21] (C20:3 n9 not quantified): %n3 in HUFA =  $100 \times (C20:5 \text{ n3} + C22:5 \text{ n3} + C22:6 \text{ n3}) / (C20:3 \text{ n6} + C20:4 \text{ n6} + C22:4 \text{ n6} + C22:5 \text{ n6} + C20:5 \text{ n3} + C22:5 \text{ n3} + C22:6 \text{ n3})$ ; %n6 in HUFA =  $100 \times (C20:3 \text{ n6} + C20:4 \text{ n6} + C22:4 \text{ n6} + C22:5 \text{ n6}) / (C20:3 \text{ n6} + C20:4 \text{ n6} + C22:4 \text{ n6} + C22:5 \text{ n6} + C20:5 \text{ n3} + C22:5 \text{ n3} + C22:6 \text{ n3})$ . (IV) Desaturase indices of the delta-5 desaturase (D5D) and delta-6desaturase (D6D) were calculated according to [29]:  $D5D = C20:4 \text{ n6} / C20:3 \text{ n6}$  and  $D6D = C20:3 \text{ n6} / C18:2$ . Statistical differences were determined with a two-tailed t-test for unpaired samples (\*  $p < 0.05$ , \*\*  $p < 0.01$ , \*\*\*  $p \leq 0.0001$ ). No t-test was performed for C 18:3 n3 and C20:5 n3. Results are shown as mean  $\pm$  SEM.

In both models, feeding of the n3-PUFA enriched diet massively changed the %n3 and %n6 in HUFA ratio (modified from [21]) in the cerebral tissue (Fig. 7.2 III). The changes in PUFAs in cerebrum are consistent with previous studies in rodents: Following three weeks of feeding an almost identical (~1% EPA and DHA) diet to rats (four weeks of age), Arnold et al. found an increase from 16% to 20% DHA and a decrease in ARA (13% to 11%) and n6-DPA (2.7% to 0.9%), while EPA levels (0.1%) were not altered [22]. However, Bourre et al. found almost no increase in DHA (12.1% vs 12.3%) and no change in EPA in 190-200 g rats after a feeding period of 8 weeks with 1.5% fish oil in the diet, while other downstream products of LA/ARA pathways were similarly modulated as

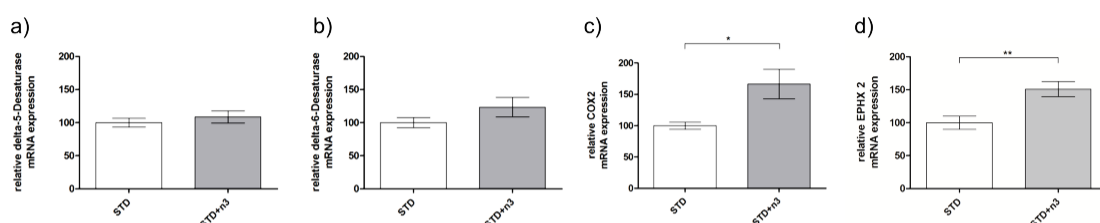
observed here (slight increase in DGLA and n3-DPA, decrease in ARA, n6-DPA and 22:4 n6) [23]. With a higher concentration of fish oil in the diet, the FA pattern, including DHA and EPA, was stronger modulated [23]. When looking at observed the effects, one could argue that the low ALA (and other n3-PUFA) content in the control diet (sunflower oil) led to a depletion of n3-PUFA in the brain of the control group causing the differences to the DHA/EPA feeding group. Indeed, Joffre et al. demonstrated that 4 months old C57BL/6 mice growing up on an n3-PUFA deficient diet had lower DHA and EPA brain levels than animals on a balanced n6/n3 diet [24]. However, Bourre et al. found that feeding a diet low in ALA over 7 months did not affect brain DHA content of adult rats [25]. Our experiment was carried out in grown up mice, aged 9-10 weeks, when the brain development is almost finished [26]. Thus, it is somewhat remarkable that the rather short DHA and EPA supplementation (30 days) could significantly change brain PUFA pattern. These findings are consistent with our recent study in old (24 month) mice, showing that fish oil supplementation by oral gavage for 21 days significantly increased DHA but not EPA levels in the brain [27]. Extrapolating from mice to men, this indicates that brain lipid composition may be directly and rapidly influenced by diet in adult age. This is consistent with the improved cognition in healthy subjects following n3-PUFA supplementation demonstrating a direct effect on brain physiology [5, 6].

The change in PUFA levels in brain compelled us to ask the question how PUFA metabolizing enzymes in brain are modulated by n3-PUFA supplementation. This is of particular importance in the context that the index of delta-5 desaturase (D5D) activity significantly increased in blood/plasma of human subjects supplemented with fish oil, whereas the index of delta-6 desaturase (D6D) activity decreased post-supplementation [28, 29]. Utilizing the product/substrate ratios of FA as marker for D5D and D6D activity (FAMES C20:4 n6/C20:3 n6 as marker of D5D activity and C20:3 n6/C18:2 n6 for D6D [29]), we evaluated the effect of n3-PUFA feeding on these key enzymes in PUFA synthesis. In both mouse strains the brain PUFA composition indicated a



massive change in the activity of the two desaturases. The D6D index was highly increased. This is consistent with the finding that feeding of EPA/DHA significantly induced gene transcription of *Fasd1* in cerebrum cortex tissue isolated from NMRI mice (Fig. 7.3 e), indicating that the increase in D6D activity was at least partly due to elevated enzyme levels. The D5D index however, was significantly decreased, while expression analysis of *Fads1* (D5D) showed an increase similar to *Fads2* (D6D, Fig. 7.3). In the cerebellum of C57BL/6 mice D5D and D6D activity indices were similarly modulated compared to NMRI mice, while expression of both desaturase genes was barely influenced in the cerebellum, with a slight tendency to an upregulation in *Fads2* (Fig. 7.3 a,b).

(I) C57BJ6/L mice



(II) NMRI mice

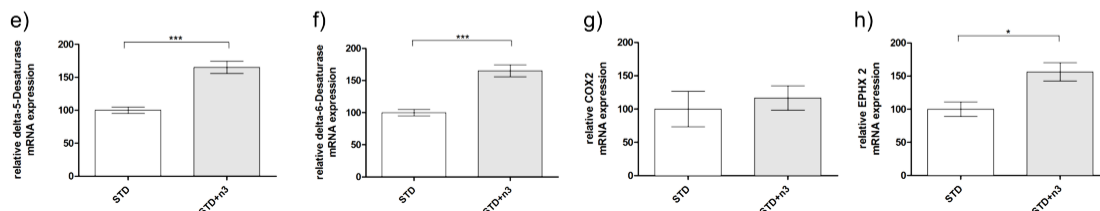


**Fig. 7.3:** Relative normalized mRNA (a, b, c, d, e, f, g, h) expression from C57BL/6 (a-d) and NMRI (e-h) mice of delta-5-desaturase (a, e), delta-6-desaturase (b, f), cyclooxygenase 2 (COX2; c, g) and epoxide hydrolase 2 (EPHX2; d, h) in brain homogenate determined using quantitative real-time PCR; mRNA expression of LA is 100 %; n = 7-8; mean  $\pm$  SEM; unpaired t-test with \*P < 0.05; \*\*P < 0.01; \*\*\*P < 0.001; mRNA expression is normalized to the expression levels of  $\beta$ 2 microglobulin (B2M) and phosphoglycerat kinase 1 (PGK1).

In *Fads2*-null mice fed a high n6/n3-PUFA diet, *Fads1* mRNA levels were significantly higher in liver tissue. However, diet and genotype had little effect on brain PUFAs in those mice [30]. Feeding rats an n3-PUFA deficient diet up-regulated D6D activity and mRNA levels in the liver but neither D5D nor D6D activity nor gene expression were changed in the brain [31]. Expression levels of *Fads2* decreased in growing finishing pigs when DHA was introduced into the diet [32]. Mice fed EPA-rich vegetable or fish oils showed lower *Fads1* mRNA

levels in liver tissue. *Fads2* mRNA levels were only enhanced by the EPA-rich camelina sativa seed oil lacking any DHA [33]. Moreover, it was shown in rats that dietary intervention, in form of n3-PUFA deprivation, led to an increased elongase (2 and 5) and desaturase ( $\Delta^5$ - and  $\Delta^6$ ) expression in liver, while no effect on brain was found [34]. These results suggest that higher levels of, e.g. DGLA leading to a higher D5D activity as observed in NMRI and C57BL/6 mice might also be a result of an increased expression or activity of *Fads2* in liver. The observed modulation in brain PUFA and the D5D/D6D indices might thus be a result of changed PUFA supply from the plasma rather than from changes in brain enzyme activities. However, NMRI mice clearly showed a modulation of mRNA level between animals on a standard sunflower oil based diet and mice supplemented with n3-PUFA. While D6D activity as well as *Fads1* and *Fads2* expression levels were elevated, D5D activity was decreased. However, there is evidence from gene expression data that *Fads2* correlates with *Fads1* brain expression in human and mice [35] and it has been shown that in *Fads1*-null mice PUFA levels determined in brain and liver reflected decreased D5D and normal D6D activity [36]. Keeping in mind that the plasma unesterified fatty acid pool is the main source for brain PUFA, the discrepancy between the D5D index (estimated by the ratio of C20:4 n6 to C20:3 n6) and elevated *Fads1* expression levels, could be a result of a depletion of ARA in plasma in response to n3-PUFA supplementation, as shown previously in plasma of rats on an almost identical diet (see above) [22].

Evidence exists that fatty acid uptake from plasma is not selective, i.e. EPA and DHA are transported similarly into the brain [37]. However, consistent with previous findings [22-24], EPA level in brain were very low in comparison to DHA level. It has been shown that EPA in brain is quickly metabolized, with  $\beta$ -oxidation playing an important role [37, 38]. Although conversion of EPA to DHA plays a minor role in the metabolism of EPA (radioactivity found in DHA was only 0.064% of a single injection of 10  $\mu$ Ci  $^{14}$ C-EPA into rat brain [38]), increased *Fads2* level might be a response to sub-chronical (30 days) exposure to high plasma level of EPA. However, this question warrants further

investigation. In this context, it will be important to investigate the effect of EPA alone on the expression of fatty acid metabolizing enzymes.

The effect of n3-PUFA feeding on selected enzymes of the AA cascade was investigated by quantitative targeted metabolomics utilizing the tissue concentration of selected oxylipins as pathways markers (Fig. 7.4). For COX activity, the concentrations of PGE<sub>2</sub>, PGD<sub>2</sub>, PGF<sub>2α</sub> and 6-keto-PGF<sub>1α</sub> (prostacyclin (PGI<sub>2</sub>) hydrolyzation product) as well as thromboxane (Tx) B<sub>2</sub> were evaluated. In both models n3-PUFA feeding massively decreased the brain levels of these prostanoids. This is consistent with a previous study, showing that n3-PUFA feeding (17 weeks) to 70 weeks old rats led to decreased level of PGE<sub>2</sub>, PGD<sub>2</sub> and PGF<sub>2α</sub> in brain cortex [39]. mRNA levels of Ptgs2 encoding for COX2 indicate that expression changes were not responsible for decreased levels in prostanoids: Feeding of EPA/DHA had no effect on gene expression of Ptgs2 encoding for COX2 in cerebrum cortex tissue isolated from NMRI mice (Fig. 7.2 g) and in the cerebellum of C57BL/6 mice Ptgs2 expression was significantly enhanced (Fig. 7.2 c) which might reflect a compensatory up-regulation of COX2 gene expression. Another explanation for the observed lower concentrations of ARA prostanoids might be a lower substrate availability, since ARA levels were slightly decreased in brain following n3-PUFA supplementation. Moreover, EPA can be converted in the COX pathway of the ARA cascade to series 3 PGs, at conversion rates much lower compared to ARA[40], thereby reducing level of potent, inflammation mediating ARA metabolites, like PGE<sub>2</sub>, which is a common explanation for the anti-inflammatory effects of n3-PUFA [1, 2]. Concentrations of most EPA derived oxylipins were low, probably because of low EPA concentrations in combination with low conversion rates (Fig. 7.4). However, the slight change in substrate availability might not compensate for the massive decrease observed in ARA eicosanoids. As discussed for PUFA, changes in peripherally formed prostanoids, which might pass the blood-brain barrier, as shown exemplary for PGE<sub>1</sub> in rats [41] and PGD<sub>2</sub> in mice [42], might account for part of the observed changes in prostanoid concentrations. However, uptake of PG from plasma was

low [41, 42]. Since the expression of 15-hydroxyprostaglandin dehydrogenase, an important enzyme in the inactivation of PGs, is low in adult brain tissue and PGs are deprotonated at physiological pH, indicating low diffusion rates [43], an active transport, e.g. via organic anion transporter 3 (Oat3) or multidrug resistance-associated protein 4 (Mrp4) [43] through the blood-brain barrier is likely. Thus, decreased concentrations of PG observed in this study could be a result from increased efflux.

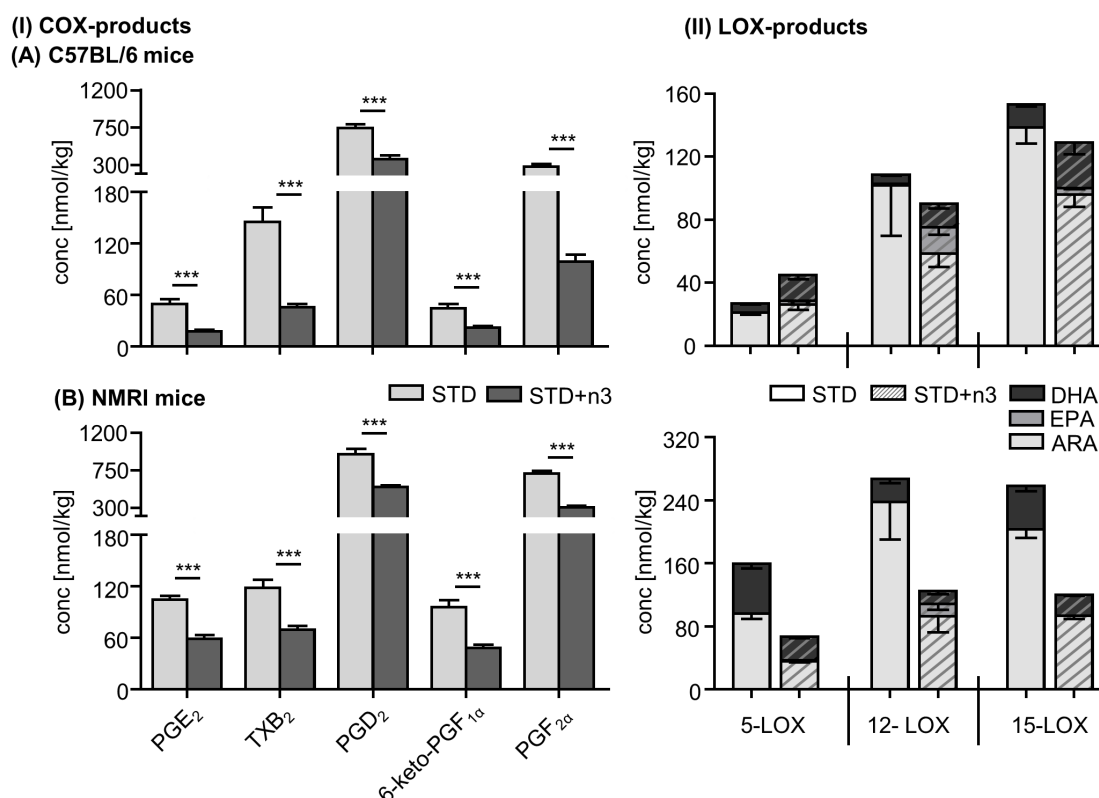


**Fig. 7.4:** Concentrations of AA derived COX products PGE<sub>2</sub>, TxB<sub>2</sub>, PGD<sub>2</sub>, 6-keto-PGF<sub>1α</sub> and PGF<sub>2α</sub> in (A) C57BL/6 mice and (B) NMRI mice fed with a standard sunflower oil based diet (STD) or the same diet enriched with n3-PUFA (STD+n3). From all EPA derived prostanoids covered by the LC-MS method, only PGD<sub>3</sub> and TxB<sub>3</sub> could be quantified in STD+n3 fed mice. Concentrations were  $3.1 \pm 0.3$  nmol/kg and  $0.96 \pm 0.08$  nmol/kg in C57BL/6 mice and  $2.7 \pm 0.2$  nmol/kg and  $0.8 \pm 0.1$  nmol/kg in NMRI mice for PGD<sub>3</sub> and TxB<sub>3</sub>, respectively. Statistical differences were determined using a two-tailed t-test for unpaired samples (\*  $p < 0.05$ , \*\*\*  $p \leq 0.001$ ). (II) Comparison of 5-LOX products (5-HETE, 5-HEPE, 4- and 7-HDHA), 12-LOX products (12-HETE, 12-HEPE, 14-HDHA) and 15-LOX products (8- and 15-HETE, 8- and 15-HEPE, 10- and 17-HDHA) of ARA, EPA and DHA in the STD and STD+n3 feeding groups of (A) C57BL/6 and (B) NMRI mice. EPA derived 5-LOX and 15-LOX products were <LOQ (5-HEPE: 0.5; 8-HEPE: 0.63 and 15-HEPE: 1.25 nmol/kg) in C57BL/6 mice of the STD feeding group. EPA derived 5-LOX and 12-LOX products were <LOQ (5-HEPE: 0.5 and 12-HEPE: 0.63 nmol/kg) in NMRI mice of the STD feeding group and 15-LOX products were <LOQ (8-HEPE: 0.63 and 15-HEPE: 1.25 nmol/kg) in NMRI mice of both feeding groups.

The LOX products of EPA and DHA increased in C57BL/6 mice following n3-PUFA supplementation (Fig. 7.2), while ARA derived LOX products decreased in both models as described in previous studies in plasma and serum of men [44-47]. Consistently, feeding of n3-PUFAs (17-weeks) to 70 weeks old rats led to increases in EPA and DHA derived LOX products, while ARA lox products were not altered [39]. However, the levels of the LOX products did not show a consistent trend regarding a modulation of LOX activity in the two mouse strains (Fig. 7.4).

Changes in the activity of the “third branch” of the ARA cascade were evaluated using the levels of epoxy-FA and dihydroxy-FA as marker (Table 7.2). Exceeding the commonly observed replacement of n6-PUFA derived epoxy-FA by n3-epoxy-FA in plasma or serum of men [45-47] or in plasma and tissues of rats (however not in cerebral cortex showing elevated epoxy-ARA) [22], the overall sum of epoxy-FA levels in brain as well as the epoxy-FA/dihydroxy-FA ratios (in NMRI mice) were markedly reduced (Table 7.2). This indicates a higher activity of the soluble epoxide hydrolase (sEH), i.e. EPHX2. Using the tissue concentration of epoxy-FA and the ratio of epoxy- to dihydroxy-FA from LA as a sensitive marker for sEH activity [48], decreased concentrations in epoxy-FA levels were observed in both models, being statistically highly significant in NMRI mice. Consistently, all ARA derived epoxy-FA in C57BL/6 and NMRI mice and corresponding epoxy/diol ratios in NMRI mice were decreased. In C57BL/6 mice, concentrations of DHA derived epoxy-FA (13(14)-, 16(17)-, 19(20)- epoxy docosapentaenoic acid (EpDPE)) and dihydroxy-FA (19,20- dihydroxy docosapentaenoic acid (DiHDPE)) were elevated in response to n3-PUFA supplementation. This can be explained by the higher enzyme specificity towards n3-PUFA, e.g. ARA:EPA:DHA 1:4.2:1.5 of CYP2J2, a PUFA-epoxygenase [13, 22], in combination with a slight shift in the brain PUFA pattern (decrease in ARA, increase in DHA). Nonetheless, the ratio of the main DHA metabolite 19(20)-EpDPE/19,20-DiHDPE also reflected the increased sEH activity. In NRMI mice, the levels of DHA epoxy-FA were even decreased following n3-PUFA supplementation indicating a massively higher sEH activity,

which is additionally supported by an increase in the hydrolyzation product of 19(20)-EpDPE, 19,20-DiHDPE. Though not all epoxy-FA and epoxy/dihydroxy-FA ratios showed a statistically significant reduction in response to n3-PUFA treatment, level of LA, ARA and DHA metabolites clearly indicated that n3-PUFA treatment increased sEH activity in the brain in both models.

**Table 7.2:** Concentrations of epoxy-fatty acids (Ep-FA), dihydroxy-FA (DiH-FA) as well as the ratio of the corresponding Ep-FA/DiH-FA in brain tissue of (A) C57BL/6 mice and (B) NMRI mice fed with STD-diet and n3-PUFA enriched STD diet. Additionally, selected sums of Ep-FA and DiH-FA along with their respective ratios are shown. Enzymatically formed products of LA (EpOME/DiHOME), ARA (EpETrE/DiHETrE), and DHA (EpDPE/DiHDPE) are presented. Due to chemical instability, 5(6)-EpETrE, and 4(5)-DiHDPE were not evaluated. Statistical differences were determined with a two-tailed t-test for unpaired samples. Results are shown as mean  $\pm$  SEM.

**A) C57BL/6**

FA precursor	isomer	STD			STD+n3			t-test		
		Ep-FA	DiH-FA	ratio	EP-FA	DiH-FA	ratio	Ep-FA	DiH-FA	ratios
LA	9,10	8.0 $\pm$ 1	1.9 $\pm$ 0.2	4.5 $\pm$ 0.9	6.3 $\pm$ 1.2	1.3 $\pm$ 0.1	4.8 $\pm$ 0.7	n.s.	<0.01	n.s.
	12,13	8.8 $\pm$ 2	3.5 $\pm$ 0.2	2.6 $\pm$ 0.5	7.1 $\pm$ 1.3	2.2 $\pm$ 0.2	3.1 $\pm$ 0.4	n.s.	<0.01	n.s.
	sum	17 $\pm$ 3	5.4 $\pm$ 0.4	3.2 $\pm$ 0.6	13 $\pm$ 2	3.5 $\pm$ 0.3	3.7 $\pm$ 0.5	n.s.	<0.01	n.s.
ARA	8,9	22 $\pm$ 4	<0.5 <sup>+</sup>	- <sup>+</sup>	16 $\pm$ 3	<0.5 <sup>+</sup>	- <sup>+</sup>	n.s.		
	11,12	64 $\pm$ 11	0.73 $\pm$ 0.07	86 $\pm$ 9	48 $\pm$ 11	0.56 $\pm$ 0.04	85 $\pm$ 19	n.s.	n.s.	n.s.
	14,15	39 $\pm$ 6	1.3 $\pm$ 0.1	29 $\pm$ 3	33 $\pm$ 7	1.03 $\pm$ 0.04	31 $\pm$ 6	n.s.	<0.01	n.s.
	sum	130 $\pm$ 20	2.1 $\pm$ 0.2	57 $\pm$ 7	97 $\pm$ 21	1.59 $\pm$ 0.07	59 $\pm$ 11	n.s.	<0.05	n.s.
DHA	7,8	- <sup>#</sup>	<1 <sup>+</sup>	- <sup>+</sup>	- <sup>#</sup>	<1 <sup>+</sup>	- <sup>+</sup>			
	10,11	5.3 $\pm$ 1.1	<0.25 <sup>+</sup>	- <sup>+</sup>	7.2 $\pm$ 1	<0.25 <sup>+</sup>	- <sup>+</sup>	n.s.		
	13,14	4.3 $\pm$ 0.8	<0.25 <sup>+</sup>	- <sup>+</sup>	6.4 $\pm$ 1	<0.25 <sup>+</sup>	- <sup>+</sup>	n.s.		
	16,17	4.1 $\pm$ 0.7	<0.5 <sup>+</sup>	- <sup>+</sup>	5.9 $\pm$ 1	<0.5 <sup>+</sup>	- <sup>+</sup>	n.s.		
	19,20	6.3 $\pm$ 0.9	1.6 $\pm$ 0.2	3.9 $\pm$ 0.4	12 $\pm$ 3	4.8 $\pm$ 0.6	2.6 $\pm$ 0.5	n.s.	<0.001	n.s.
	sum	20 $\pm$ 3	1.6 $\pm$ 0.2	12 $\pm$ 1	31 $\pm$ 6	4.9 $\pm$ 0.6	6.9 $\pm$ 1.3	n.s.	<0.001	<0.05
	sum of all	160 $\pm$ 20	9.1 $\pm$ 0.6	18 $\pm$ 2	140 $\pm$ 20	10 $\pm$ 1	15 $\pm$ 2	n.s.	n.s.	n.s.

Table 7.2: Continued

B) NMRI

FA precursor	isomer	STD			STD+n3			t-test		
		EP-FA	DiH-FA	ratio	EP-FA	DiH-FA	ratio	EP-FA	DiH-FA	ratios
LA	9,10	7.1±1.0	2.0±0.2	3.5±0.3	3.1±0.4	1.7±0.1	1.7±0.2	<0.01	n.s.	<0.01
	12,13	6.7±0.8	2.4±0.2	2.8±0.3	3.2±0.4	2.0±0.1	1.6±0.2	<0.01	n.s.	<0.01
	sum	14±2	4.5±0.3	3.1±0.3	6.3±0.8	3.7±0.3	1.7±0.2	<0.01	n.s.	<0.01
ARA	8,9	54±8	0.76±0.09	78±14	13±2	<0.5*	- <sup>+</sup>	<0.001		
	11,12	50±8	0.98±0.09	55±10	14±3	0.44±0.02	34±7	<0.001	<0.001	n.s.
	14,15	69±9	1.8±0.2	42±7	27±5	0.80±0.03	35±6	<0.001	<0.001	n.s.
	sum	170±20	3.4±0.4	57±10	55±10	1.23±0.04	45±8	<0.001	<0.0001	n.s.
DHA	7,8	- <sup>#</sup>	<1*	- <sup>+</sup>	- <sup>#</sup>	<1*	- <sup>+</sup>			
	10,11	18±3	0.35±0.06	58±10	6.3±1.1	0.26±0.01	24±4	<0.01	n.s.	<0.01
	13,14	10±1	0.38±0.07	30±5	3.6±0.7	<0.25*	- <sup>+</sup>	<0.01		
	16,17	8.7±1.2	0.75±0.11	14±3	3.8±0.7	<0.5*	- <sup>+</sup>	<0.01		
	19,20	38±4	2.5±0.3	17±3	16±2	4.8±0.3	3.4±0.3	<0.001	<0.001	<0.001
	sum	75±9	3.9±0.8	24±4	30±4	5.2±0.5	5.8±0.7	<0.001	n.s.	0.001
sum of all		260±40	12±1	67±11	91±14	10±1	13±1	<0.001	n.s.	<0.01

\* Analyte was <LOQ in >50% of the samples of one group. In this case the LOQ is shown.

# Analyte was not included in LC-MS-method.

<sup>+</sup> If the concentration of either Ep-FA or DiH-FA was <LOQ in more than 50% of the samples of one group, or if the analyte was not included in the LC-MS method, no ratio was calculated.

Consistently, a significant increase in EPHX2 mRNA levels in response to n3-PUFA feeding was found in the cerebrum of NRMI mice and cerebellum of C57BL/6 (Fig. 7.2 d,h). In the rodent brain, sEH is expressed in the white matter mainly neuronal and not vascular or glial [49, 50]. A modulation of sEH activity regulating the endogenous levels of epoxy-FA in the brain is of high biological relevance, because epoxy-FA derived from ARA (EpETrEs, EETs) are key mediators in the brain [49, 50]. Similar to their action in the periphery, epoxy-ARA regulate vascular tone and cerebral blood flow [50]. Moreover, they show distinct effects in the central nervous system (CNS), including astrocyte-mediated coupling and pain processing [14, 50, 51]. It is highly remarkable that the analgesic action is effective in both, inflammatory as well as non-inflammatory pain [51]. Administration of epoxy-FA or increasing epoxy-FA concentration, e.g., by application of potent inhibitors of sEH (sEHi), protects against neuronal cell death caused by ischemia [52] and higher sEH activity is correlated to a higher stroke risk [49, 53]. Elevation of epoxy-FA can also be

protective in subarachnoid hemorrhage [54]. In addition to their vasodilatory effects, part of this protection could be caused by the anti-inflammatory action of epoxy-FA leading to reduced pro-inflammatory cytokine production [55]. However, the anti-inflammatory efficacy in the CNS is not as established as in the periphery [50]. Though a large number of molecular targets of epoxy-FA could be uncovered, including the transient receptor potential vanilloid-4 (TRPV4) as well as peroxisome proliferator-activated receptor (PPAR) and a potential G-coupled receptor, their molecular mode of action remains largely unclear [15, 50]. It is important to notice, that not only epoxy-ARA is biologically active, but also other epoxy-FA, particularly epoxy-EPA and epoxy-DHA. When sEHi are used to increase epoxy-FA levels, particularly in neuronal tissue – because of the high DHA content – epoxy-DHA is similarly elevated compared to epoxy-ARA [51]. With respect to nociceptive signaling, DHA epoxides were equally potent in reducing local pain elicited by carrageenan injection in rats as epoxy-ARA, while the effect of DHA metabolites lasted longer [56]. Regarding their vascular effects, EPA and DHA epoxides activate large-conductance calcium-activated potassium channels in coronary vascular smooth muscle cells [57, 58]. In these experiments, one DHA-epoxide was over 1000-times more potent than the ARA derived ones [57]. Speculating that epoxy-FA from n3-PUFA are also more active in CNS function, the increase in sEH activity following n3-PUFA supplementation might be a homeostatic response to control action of epoxy-FA, e.g. increased vasodilation in brain. Taken the role of elevated/decreased sEH activity in the (patho)physiology in the CNS into account, the finding that n3-PUFA supplementation increases sEH activity warrants further investigation. In case n3-epoxy-FA are indeed more active than n6-epoxy-FA, this finding may also pave the route for a new pharmacological intervention by combined administration of sEH inhibitors with n3-PUFA, e.g. in prevention and treatment of a stroke or inflammatory and non-inflammatory pain.



## 7.4 References

1. Calder PC. Marine omega-3 fatty acids and inflammatory processes: Effects, mechanisms and clinical relevance. *Biochim Biophys Acta*. 2015;1851(4):469-484.
2. Mozaffarian D, Wu JH. Omega-3 fatty acids and cardiovascular disease: effects on risk factors, molecular pathways, and clinical events. *J Am Coll Cardiol*. 2011;58(20):2047-2067.
3. Jiao J, Li Q, Chu J, Zeng W, Yang M, Zhu S. Effect of n-3 PUFA supplementation on cognitive function throughout the life span from infancy to old age: a systematic review and meta-analysis of randomized controlled trials. *Am J Clin Nutr*. 2014;100(6):1422-1436.
4. Nelson EB, Van Elswyk ME. Limitations of the review and meta-analysis of the role of n-3 long-chain PUFA supplementation and cognitive function. *Am J Clin Nutr*. 2015;101(6):1305-1306.
5. Weiser MJ, Butt CM, Mohajeri MH. Docosahexaenoic Acid and Cognition throughout the Lifespan. *Nutrients*. 2016;8(2):99.
6. Kulzow N, Witte AV, Kerti L, Grittner U, Schuchardt JP, Hahn A, Floel A. Impact of Omega-3 Fatty Acid Supplementation on Memory Functions in Healthy Older Adults. *J Alzheimers Dis*. 2016;51(3):713-725.
7. Dyall SC. Long-chain omega-3 fatty acids and the brain: a review of the independent and shared effects of EPA, DPA and DHA. *Front Aging Neurosci*. 2015;7:52.
8. Demar JC, Jr., Ma K, Chang L, Bell JM, Rapoport SI. alpha-Linolenic acid does not contribute appreciably to docosahexaenoic acid within brain phospholipids of adult rats fed a diet enriched in docosahexaenoic acid. *J Neurochem*. 2005;94(4):1063-1076.
9. Nara T, Li Y, Nakamura M. Delta-6 desaturase gene expression is regulated by both SREBP-1 and PPAR alpha. *Faseb Journal*. 2004;18(8):C269-C269.
10. Bazinet RP, Laye S. Polyunsaturated fatty acids and their metabolites in brain function and disease. *Nat Rev Neurosci*. 2014;15(12):771-785.
11. Buczynski MW, Dumlao DS, Dennis EA. Thematic Review Series: Proteomics. An integrated omics analysis of eicosanoid biology. *J Lipid Res*. 2009;50(6):1015-1038.
12. Gabbs M, Leng S, Devassy JG, Monirujjaman M, Aukema HM. Advances in Our Understanding of Oxylipins Derived from Dietary PUFAs. *Adv Nutr*. 2015;6(5):513-540.
13. Westphal C, Konkel A, Schunck WH. Cytochrome p450 enzymes in the bioactivation of polyunsaturated Fatty acids and their role in cardiovascular disease. *Adv Exp Med Biol*. 2015;851:151-187.
14. Inceoglu B, Wagner K, Schebb NH, Morisseau C, Jinks SL, Ulu A, Hegedus C, Rose T, Brosnan R, Hammock BD. Analgesia mediated by soluble epoxide hydrolase inhibitors is dependent on cAMP. *Proc Natl Acad Sci U S A*. 2011;108(12):5093-5097.
15. Morisseau C, Hammock BD. Impact of Soluble Epoxide Hydrolase and Epoxyeicosanoids on Human Health. *Annual Review of Pharmacology and Toxicology*, Vol 53, 2013. 2013;53:37-58.
16. Ostermann AI, Muller M, Willenberg I, Schebb NH. Determining the fatty acid composition in plasma and tissues as fatty acid methyl esters using gas chromatography - a comparison of different derivatization and extraction procedures. *Prostaglandins Leukot Essent Fatty Acids*. 2014;91(6):235-241.

17. Ostermann AI, Willenberg I, Schebb NH. Comparison of sample preparation methods for the quantitative analysis of eicosanoids and other oxylipins in plasma by means of LC-MS/MS. *Anal Bioanal Chem.* 2015;407(5):1403-1414.
18. Willenberg I, Rund K, Rong S, Shushakova N, Gueler F, Schebb NH. Characterization of changes in plasma and tissue oxylipin levels in LPS and CLP induced murine sepsis. *Inflamm Res.* 2016;65(2):133-142.
19. Guillou H, Zadravec D, Martin PG, Jacobsson A. The key roles of elongases and desaturases in mammalian fatty acid metabolism: Insights from transgenic mice. *Prog Lipid Res.* 2010;49(2):186-199.
20. Burdge GC, Calder PC. Conversion of alpha-linolenic acid to longer-chain polyunsaturated fatty acids in human adults. *Reprod Nutr Dev.* 2005;45(5):581-597.
21. Lands B. A critique of paradoxes in current advice on dietary lipids. *Prog Lipid Res.* 2008;47(2):77-106.
22. Arnold C, Markovic M, Blossey K, Wallukat G, Fischer R, Dechend R, Konkel A, von Schacky C, Luft FC, Muller DN, Rothe M, Schunck WH. Arachidonic acid-metabolizing cytochrome P450 enzymes are targets of {omega}-3 fatty acids. *J Biol Chem.* 2010;285(43):32720-32733.
23. Bourre JM, Bonneil M, Dumont O, Piciotti M, Calaf R, Portugal H, Nalbone G, Lafont H. Effect of increasing amounts of dietary fish oil on brain and liver fatty composition. *Biochim Biophys Acta.* 1990;1043(2):149-152.
24. Joffre C, Gregoire S, De Smedt V, Acar N, Bretillon L, Nadjar A, Laye S. Modulation of brain PUFA content in different experimental models of mice. *Prostaglandins Leukot Essent Fatty Acids.* 2016;114:1-10.
25. Bourre JM, Piciotti M, Dumont O, Pascal G, Durand G. Dietary linoleic acid and polyunsaturated fatty acids in rat brain and other organs. Minimal requirements of linoleic acid. *Lipids.* 1990;25(8):465-472.
26. Semple BD, Blomgren K, Gimlin K, Ferriero DM, Noble-Haeusslein LJ. Brain development in rodents and humans: Identifying benchmarks of maturation and vulnerability to injury across species. *Prog Neurobiol.* 2013;106-107:1-16.
27. Afshordel S, Hagl S, Werner D, Rohner N, Kogel D, Bazan NG, Eckert GP. Omega-3 polyunsaturated fatty acids improve mitochondrial dysfunction in brain aging--impact of Bcl-2 and NPD-1 like metabolites. *Prostaglandins Leukot Essent Fatty Acids.* 2015;92:23-31.
28. Al-Hilal M, AlSaleh A, Maniou Z, Lewis FJ, Hall WL, Sanders TAB, O'Dell SD, Team MS. Genetic variation at the FADS1-FADS2 gene locus influences delta-5 desaturase activity and LC-PUFA proportions after fish oil supplement. *J Lipid Res.* 2013;54(2):542-551.
29. Cormier H, Rudkowska I, Lemieux S, Couture P, Julien P, Vohl MC. Effects of FADS and ELOVL polymorphisms on indexes of desaturase and elongase activities: results from a pre-post fish oil supplementation. *Genes Nutr.* 2014;9(6):437.
30. Su H, Zhou D, Pan YX, Wang X, Nakamura MT. Compensatory induction of Fads1 gene expression in heterozygous Fads2-null mice and by diet with a high n-6/n-3 PUFA ratio. *J Lipid Res.* 2016;57(11):1995-2004.
31. Hofacer R, Jandacek R, Rider T, Tso P, Magrisso IJ, Benoit SC, McNamara RK. Omega-3 fatty acid deficiency selectively up-regulates delta6-desaturase expression and activity

- indices in rat liver: prevention by normalization of omega-3 fatty acid status. *Nutr Res.* 2011;31(9):715-722.
32. De Tonnac A, Labussiere E, Vincent A, Mouro J. Effect of alpha-linolenic acid and DHA intake on lipogenesis and gene expression involved in fatty acid metabolism in growing-finishing pigs. *Br J Nutr.* 2016;116(1):7-18.
  33. Tejera N, Vauzour D, Betancor MB, Sayanova O, Usher S, Cochard M, Rigby N, Ruiz-Lopez N, Menoyo D, Tocher DR, Napier JA, Minihane AM. A Transgenic Camelina sativa Seed Oil Effectively Replaces Fish Oil as a Dietary Source of Eicosapentaenoic Acid in Mice. *J Nutr.* 2016;146(2):227-235.
  34. Igarashi M, Ma K, Chang L, Bell JM, Rapoport SI. Dietary n-3 PUFA deprivation for 15 weeks upregulates elongase and desaturase expression in rat liver but not brain. *J Lipid Res.* 2007;48(11):2463-2470.
  35. Rizzi TS, van der Sluis S, Derom C, Thiery E, van Kesteren RE, Jacobs N, Van Gestel S, Vlietinck R, Verhage M, Heutink P, Posthuma D. FADS2 Genetic Variance in Combination with Fatty Acid Intake Might Alter Composition of the Fatty Acids in Brain. *PLoS One.* 2013;8(6):e68000.
  36. Powell DR, Gay JP, Smith M, Wilganowski N, Harris A, Holland A, Reyes M, Kirkham L, Kirkpatrick LL, Zambrowicz B, Hansen G, Platt KA, van Sligtenhorst I, Ding ZM, Desai U. Fatty acid desaturase 1 knockout mice are lean with improved glycemic control and decreased development of atheromatous plaque. *Diabetes Metab Syndr Obes.* 2016;9:185-199.
  37. Chen CT, Bazinet RP. beta-oxidation and rapid metabolism, but not uptake regulate brain eicosapentaenoic acid levels. *Prostaglandins Leukot Essent Fatty Acids.* 2015;92:33-40.
  38. Chen CT, Liu Z, Bazinet RP. Rapid de-esterification and loss of eicosapentaenoic acid from rat brain phospholipids: an intracerebroventricular study. *J Neurochem.* 2011;116(3):363-373.
  39. Hashimoto M, Katakura M, Tanabe Y, Al Mamun A, Inoue T, Hossain S, Arita M, Shido O. n-3 fatty acids effectively improve the reference memory-related learning ability associated with increased brain docosahexaenoic acid-derived docosanoids in aged rats. *Biochim Biophys Acta.* 2015;1851(2):203-209.
  40. Smith WL, Urade Y, Jakobsson PJ. Enzymes of the cyclooxygenase pathways of prostanoid biosynthesis. *Chem Rev.* 2011;111(10):5821-5865.
  41. Taogoshi T, Nomura A, Murakami T, Nagai J, Takano M. Transport of prostaglandin E1 across the blood-brain barrier in rats. *J Pharm Pharmacol.* 2005;57(1):61-66.
  42. Suzuki F, Hayashi H, Hayaishi O. Transport of Prostaglandin-D2 into Brain. *Brain Research.* 1986;385(2):321-328.
  43. Tachikawa M, Hosoya K, Terasaki T. Pharmacological significance of prostaglandin E2 and D2 transport at the brain barriers. *Adv Pharmacol.* 2014;71:337-360.
  44. Fischer R, Konkel A, Mehling H, Blosser K, Gapelyuk A, Wessel N, von Schacky C, Dechend R, Muller DN, Rothe M, Luft FC, Weylandt K, Schunck WH. Dietary omega-3 fatty acids modulate the eicosanoid profile in man primarily via the CYP-epoxygenase pathway. *J Lipid Res.* 2014;55(6):1150-1164.
  45. Schebb NH, Ostermann AI, Yang J, Hammock BD, Hahn A, Schuchardt JP. Comparison of the effects of long-chain omega-3 fatty acid supplementation on plasma levels of free and esterified oxylipins. *Prostaglandins Oth Lipid M.* 2014;113-115:21-29.

46. Schuchardt JP, Schmidt S, Kressel G, Willenberg I, Hammock BD, Hahn A, Schebb NH. Modulation of blood oxylipin levels by long-chain omega-3 fatty acid supplementation in hyper- and normolipidemic men. *Prostaglandins Leukot Essent Fatty Acids*. 2014;90(2-3):27-37.
47. Schuchardt JP, Schneider I, Willenberg I, Yang J, Hammock BD, Hahn A, Schebb NH. Increase of EPA-derived hydroxy, epoxy and dihydroxy fatty acid levels in human plasma after a single dose of long-chain omega-3 PUFA. *Prostaglandins Oth Lipid M*. 2014;109-111:23-31.
48. Ostermann AI, Herbers J, Willenberg I, Chen R, Hwang SH, Greite R, Morisseau C, Gueler F, Hammock BD, Schebb NH. Oral treatment of rodents with soluble epoxide hydrolase inhibitor 1-(1-propanoylpiperidin-4-yl)-3-[4-(trifluoromethoxy)phenyl]urea (TPPU): Resulting drug levels and modulation of oxylipin pattern. *Prostaglandins Oth Lipid M*. 2015;121(Pt A):131-137.
49. Iliff JJ, Alkayed NJ. Soluble Epoxide Hydrolase Inhibition: Targeting Multiple Mechanisms of Ischemic Brain Injury with a Single Agent. *Future Neurol*. 2009;4(2):179-199.
50. Iliff JJ, Jia J, Nelson J, Goyagi T, Klaus J, Alkayed NJ. Epoxyeicosanoid signaling in CNS function and disease. *Prostaglandins Oth Lipid M*. 2010;91(3-4):68-84.
51. Inceoglu B, Wagner KM, Yang J, Bettaieb A, Schebb NH, Hwang SH, Morisseau C, Haj FG, Hammock BD. Acute augmentation of epoxygenated fatty acid levels rapidly reduces pain-related behavior in a rat model of type I diabetes. *Proc Natl Acad Sci U S A*. 2012;109(28):11390-11395.
52. Liu Y, Wan Y, Fang Y, Yao E, Xu S, Ning Q, Zhang G, Wang W, Huang X, Xie M. Epoxyeicosanoid Signaling Provides Multi-target Protective Effects on Neurovascular Unit in Rats After Focal Ischemia. *J Mol Neurosci*. 2016;58(2):254-265.
53. Fairbanks SL, Young JM, Nelson JW, Davis CM, Koerner IP, Alkayed NJ. Mechanism of the sex difference in neuronal ischemic cell death. *Neuroscience*. 2012;219:183-191.
54. Siler DA, Martini RP, Ward JP, Nelson JW, Borkar RN, Zuloaga KL, Liu JJ, Fairbanks SL, Raskin JS, Anderson VC, Dogan A, Wang RK, Alkayed NJ, Cetas JS. Protective role of p450 epoxyeicosanoids in subarachnoid hemorrhage. *Neurocrit Care*. 2015;22(2):306-319.
55. Koerner IP, Zhang W, Cheng J, Parker S, Hurn PD, Alkayed NJ. Soluble epoxide hydrolase: regulation by estrogen and role in the inflammatory response to cerebral ischemia. *Front Biosci*. 2008;13:2833-2841.
56. Morisseau C, Inceoglu B, Schmelzer K, Tsai HJ, Jinks SL, Hegedus CM, Hammock BD. Naturally occurring monoepoxides of eicosapentaenoic acid and docosahexaenoic acid are bioactive antihyperalgesic lipids. *J Lipid Res*. 2010;51(12):3481-3490.
57. Ye D, Zhang D, Oltman C, Dellsperger K, Lee HC, VanRollins M. Cytochrome p-450 epoxygenase metabolites of docosahexaenoate potently dilate coronary arterioles by activating large-conductance calcium-activated potassium channels. *J Pharmacol Exp Ther*. 2002;303(2):768-776.
58. Lauterbach B, Barbosa-Sicard E, Wang MH, Honeck H, Kargel E, Theuer J, Schwartzman ML, Haller H, Luft FC, Gollasch M, Schunck WH. Cytochrome P450-dependent eicosapentaenoic acid metabolites are novel BK channel activators. *Hypertension*. 2002;39(2 Pt 2):609-613.

# Chapter 8

## Future Perspectives

Overall, this thesis aimed to establish sample preparation techniques and analytical tools to investigate the modulation of the endogenous fatty acid and oxylipin pattern. The methods were used to thoroughly characterize the total fatty acid and free oxylipin profile in tissues and blood in two frequently used models for the investigation of n3-PUFA related effects. Though time dependent changes in blood and a large number of tissues were described in detail, several questions remain: A large portion of oxylipins is found esterified in lipids, e.g. polar lipids such as phosphatidylcholine or phosphatidylserine. These bound oxylipins, and thus changes in their levels, were not monitored in the thesis. Moreover, it would be highly relevant to investigate changes in the different fractions of blood, i.e. lipoproteins and membranes of different types of blood cells. For this purpose in the future, separation of cells, membranes, lipoproteins and lipid classes before analysis would be highly interesting allowing evaluation of n3-PUFA induced changes in more detail.

A key finding of this thesis is that the overall fatty acid profile of the adult murine brain is only slightly modulated by n3-PUFA, while distinct changes occurred in the profile of polyunsaturated fatty acids and oxylipins. The relevance of these findings is supported by two independent feeding experiments showing the same effect. Using concentrations of products and ratios of products and substrates as activity markers as well as transcription analysis, a significant increase in the expression of the soluble epoxide hydrolase, the enzyme hydrolyzing bioactive epoxy-FA to their less potent dihydroxy-FA, was found. Epoxy- ARA play an important role in the regulation of cerebral blood flow, vascular tone and inflammatory as well as non-inflammatory pain. Assuming a

similar or even a higher potency of epoxy-FA from EPA and DHA, as is the case in the periphery, the increase in the soluble epoxide hydrolase might be a compensatory mechanism to regulate epoxy-FA level.

Based on these results, it would be highly interesting to investigate whether an increase in endogenous epoxy-FA from EPA and DHA in cerebral tissue, either by administration of potent inhibitors of the soluble epoxide hydrolase or by direct administration of epoxy-FA, might induce effects discussed for n3-PUFAs, like improvement of cognitive function and reduction of memory loss. The results from these experiments would additionally provide insights in the molecular mechanisms.

Interestingly, increased expression of the soluble epoxide hydrolase has been associated with a higher risk for stroke, while dietary intake of n3-PUFA has been correlated with a reduced risk of stroke. Thus, it would be of high importance to evaluate a combined treatment with inhibitors of the soluble epoxide hydrolase and n3-PUFAs as a new pharmaceutical approach to prevent or treat stroke.

.

# Summary

Although the dietary intake of omega-3 polyunsaturated fatty acids (n3-PUFA) has been associated with beneficial effects in different diseases, their importance for human health has not been fully unveiled. Additionally, many questions regarding the power to modulate the endogenous profile of oxidative PUFA metabolites – oxylipins – remain (see Chapter 2). To answer these questions and for the investigation of n3-PUFA related effects, powerful analytical methods are needed in order to characterize modulations in the endogenous profile of fatty acids and oxylipins, e.g. upon dietary intervention. Thus, the first part of this thesis deals with the optimization of sample preparation procedures for the quantification of total fatty acids and free oxylipins in biological samples.

An important step in the analysis of the total fatty acid profile in biological samples is the (trans-)esterification of lipids in order to generate fatty acid methyl esters which can be analyzed by gas chromatography with flame ionization detection. Therefore, in chapter 3, different commonly used derivatization techniques were compared regarding their power to efficiently derivatize different lipid classes found in biological samples, such as plasma and tissues. Using lipid standards, it was found that transesterification to methyl esters using methanolic hydrogen chloride was most efficient, while other methods showed a discrimination of specific lipid classes. In plasma, this resulted in distinct differences in the determined fatty acid profile. Moreover, a halogenated-solvent free method based on methyl tert-butyl ether and methanol was found to be equivalent for the extraction of lipids from small liver and plasma samples to a standard, chloroform/methanol based extraction procedure.

Chapter 4 and 5 describe different approaches for the extraction of free oxylipins from plasma and cell culture medium. For the extraction of free oxylipins of all different classes, including prostaglandins, epoxy- and hydroxy-fatty acids amongst others, solid-phase extraction is commonly applied. Due to the low concentration of most free oxylipins in plasma, extraction of the analytes as well as removal of interfering matrix have to be efficient. Thus, in chapter 4, commonly used solid phase extraction procedures for free oxylipins were compared regarding their power to selectively extract free oxylipins from plasma. In the interpretation of the results a focus was set on extraction efficiency of internal standards from plasma samples and the removal of ion suppressing matrix. Using a mixed phase comprising of a strong anion exchanger and C8 material, good recoveries of internal standards and reduction of ion suppressing matrix was found. However, extraction of unpolar epoxy-FA seemed to be more efficient using a protocol based on C18 material.

In chapter 5 a fast, online-solid phase extraction liquid chromatography-mass spectrometry (online-SPE LC-MS) method for the quantification of hydroxylated fatty acids was developed. Following minimal manual sample preparation by mixing the sample with a methanolic internal standard solution, extraction and separation of the 26 hydroxy-FA were performed within a total analysis time of 6.5 min. The method showed good sensitivity compared to state of the art targeted metabolomics LC-MS methods for oxylipins, narrow peaks of about 3 sec at half maximum height and acceptable inter- as well as intra-batch precision for the extraction of analytes from plasma and cell culture medium. The method was used to characterize the pattern of hydroxy-FA formed in different cell lines upon incubation with ARA, eicosapentaenoic acid (EPA) and docosahexaenoic acid (DHA).

In the second part of the thesis the modulation of the endogenous fatty acid and oxylipin pattern in two common in vivo models for the investigation of n3-PUFA biology was thoroughly characterized by applying the methods developed in chapter 3 and 4: On the one hand feeding of mice with a diet enriched with n3-PUFAs EPA and DHA and on the other hand transgenic *fat-1* mice which are



able to endogenously convert n6- to n3-PUFA. Feeding of mice with an n3-PUFA enriched diet (1% EPA and 1% DHA ethyl ester in the diet) led to a time dependent increase of EPA and DHA in blood and tissues, reaching a maximum steady state after 14-30 days in all investigated tissues and blood. Compared to wild type mice fed 30 days a standard sunflower oil based diet, *fat-1* mice on the same diet and wild type mice on the n3-PUFA enriched diet showed remarkably higher amounts of EPA and DHA in blood and tissues at the expense of n6-PUFAs, especially ARA. However, the levels of n3-PUFAs following feeding were higher compared to *fat-1* mice, especially EPA (7.8% following feeding vs. 1.7% in whole blood of *fat-1* mice). Trends observed in the fatty acid profile were reflected in most oxylipins in plasma, colon and brain. Taking into account that the *fat-1* mouse model has been shown to be a powerful model for the investigation of n3-PUFA related effects, the results suggest that effects of n3-PUFA might already be found at endogenous n3-PUFA levels which are achievable by dietary intervention.

Following feeding of a diet enriched with n3-PUFA, the oxylipin pattern in brain was highly modulated, while changes in the overall fatty acid pattern were low. This interesting finding was further investigated in chapter 7. In two independent feeding experiments it was found that although the overall pattern of saturated FA, monounsaturated FA and PUFAs was barely modulated, distinct changes were induced in individual PUFAs following 30 days of feeding a diet enriched with n3-PUFAs (1% EPA and 1% DHA ethyl ester in the diet). Moreover, in both models a massive shift in the pattern of oxylipins from all three enzymatic branches of the ARA cascade was observed. Using ratios of products and substrates as enzyme activity marker and transcription analysis, a distinct modulation of the delta-5 and delta-6 desaturases and a significant increase in the soluble epoxide hydrolase (sEH) was unveiled. Taking the role of epoxy-FA in cerebral blood flow and vascular tone as well as elevated sEH activity for the risk of stroke into account, this finding warrants further investigation since it might be important for the understanding of the role of n3-PUFA in memory loss or stroke.



# Appendix

## 9.1 Chapter 4

**Table 9.1.1:** Overview of the sample preparation steps for the SPE protocols

	Column Preparation	Sample Preparation (500 µL plasma)	Sample Loading	Sample Wash	Elution
<b>Oasis-EA</b> (Oasis HLB, 3 mL, 60 mg, 30 µm)	1 x EA 1 x MeOH 2 x 5% MeOH, 0.1% HAc	1:1 dilution with 5% MeOH, 0.1% HAc Centrifugation		2 x 5% MeOH, 0.1% HAc	0.5 mL MeOH 1.5 mL EA
<b>SepPak</b> (SepPak tC18, 6 mL, 500mg, 37-55 µm)	3 x MeOH 3 x H <sub>2</sub> O	+ 1.5 mL 20% MeOH Centrifugation + 80 µL conc HAc (sample: pH 3)		10 mL H <sub>2</sub> O 6 mL Hex	8 mL Methyl Formate
<b>BondElut</b> (Bond Elut Certify II, 3 mL, 200 mg, 47-60 µm)	1 x MeOH 1 x 0.1 mol/L NaAc, 5% MeOH	1:1 dilution with 1 mol/L NaAc, 5% MeOH (pH 6.0) Centrifugation		1 x MeOH/H <sub>2</sub> O (50/50, v/v)	<b>AnionEx-weak</b> 2.0 mL n-Hex/EA (25/75, v/v) + 1% HAc ----- <b>AnionEx-strong</b> 2.0 mL n-Hex/EA (75/25, v/v) + 1% HAc
<b>StrataX</b> (StrataX, 3 mL, 100 mg, 33 µm)	3.5 mL MeOH 3.5 mL H <sub>2</sub> O	1:1 dilution with 20% MeOH Centrifugation		3.5 mL 10% MeOH	1.0 mL MeOH
<b>Oasis-MeOH</b> (Oasis HLB, 3 mL, 60 mg, 30 µm)	1 x EA 1 x MeOH 1 x 20% MeOH, 0.1% FA	1:1 dilution with 40% MeOH, 0.1% FA Centrifugation		1 x 20% MeOH, 0.1% FA	2.0 mL MeOH

### Meth. 9.1.1: LC-MS oxylipin analysis

#### LC-MS oxylipin analysis

Prior analysis, the samples were kept at 4°C in a HTS xt-PAL autosampler (CTC Analytics, Switzerland, local distributor: Axel Semrau, Sprockhövel, Germany) equipped with a 20 µL sample loop and 100 µL syringe.

A 5 µL aliquot of the sample solution is injected in the flow of an 1290 LC System (Agilent, Weilbronn, Germany), on an Agilent Zorbax Eclipse Plus C-18 reversed phase column (dimensions 2.1 x 150 mm, particle size 1.8 µm) with a Phenomenex C-18 SecurityGuard Ultra C18 cartridge as precolumn (cat. nr. AJ0-8782, Phenomenex, Torrance, CA, USA) kept in a column oven at 40 °C.

The oxylipins are separated by a binary solvent gradient with 0.1% acetic acid as solvent A and 800/150/1 (v/v) acetonitrile/methanol/acetic acid as solvent B at a flow rate of 0.3 mL/min: 0-0.25 min isocratic 35% B, 0.25-3.00 min linear from 35% B to 53% B, 3.00-12.50 min linear from 53% B to 68% B, 12.50-17.50 min linear from 68% B to 95% B, 17.50-19.00 min isocratic 95 % B, 19.00-19.10 linear from 95% B to 35% followed by reconditioning for 2.40 min. Utilizing the 2-position-6-port valve build in the MS the eluent was directed to waste during the first 2.5 min and the last 3.5 min of each run to reduce contamination of the MS source.

The detection was carried out using a 6500 QTRAP instrument (AB Sciex, Darmstadt, Germany) following negative electrospray ionization. The oxylipins were detected in scheduled selected reaction monitoring mode (App. Table 9.1.2). The detection window was set to  $\pm 22.5$  s around the expected retention time and a maximum cycle time of 0.5 s allowing the detection of at least 18 data points per compound.

The optimized source settings are: Ion-spray voltage of -4500 V, 35 psi curtain gas, 60 psi nebulizer gas (gas 1) and 60 psi drying gas (gas 2) at a temperature of 475 °C. The vertical axis offset of the sprayer was 0.528 cm and the horizontal 0.540 cm. Nitrogen was used as collision gas at 12 psi ("high") and all transitions were monitored in unit resolution with an entrance potential of -10 V. Analyst Software (version 1.6.2., AB Sciex) was used for controlling the LC-ESI-MS system and data acquisition. Multiquant (version 2.1.1, AB Sciex) was used for integration and quantification. The analyte concentrations of the samples were calculated directly by comparison of the analyte peak area detected with that of the IS (App. Table 9.1.2). For calibration, the analyte to IS ratios were fitted in a linear way reciprocally weighted by concentration. Only those oxylipins were included in data analysis exceeding LOQ in >60% (e.g. 3 out of 5) of the samples.

**Table 9.1.2:** Parameters of the LC-ESI(-)-MS/MS method for the determination of the concentration of oxylipins in biological samples. Shown are all analytes covered, the mass transition used for quantification in scheduled SRM mode, the electronical MS parameters (Declustering Potential (DP), Collision Energy (CE), Collision Cell Exit Potential (CXP)), the internal standard (IS), the retention time and its standard deviation (SD), peak width (full width and full width at half maximum height (FWHM)), limit of detection and the calibration range. The actual dynamic range for the quantification in the sample matrix depends on the dilution or concentration steps (10 fold for 500  $\mu$ L plasma analysis) during sample preparation.

Analyte	Mass transition		MS			IS	Retention time		Peak width		LOD	Calibration	
	m/z (MS1)	m/z (MS3)	DP (V)	CE (V)	CXP (V)		(min)	SD <sup>1</sup> (sec)	Full (s)	FWHM (s)	LOD (nM)	lower conc <sup>2</sup> (nM)	upper conc <sup>3</sup> (nM)
6-keto-PGF <sub>1<math>\alpha</math></sub>	369.3	163.2	-70	-36	-6	<sup>2</sup> H <sub>4</sub> -6-keto-PGF <sub>1<math>\alpha</math></sub>	3.18	0.69	34	18	< 0.90	0.9	361
20-COOH-LTB <sub>4</sub>	365.2	347.2	-80	-25	-8	<sup>2</sup> H <sub>4</sub> -TxB <sub>2</sub>	3.22	1.5	17	3	0.5	1	200
ResolvinE <sub>1</sub>	349.3	195	-65	-22	-10	<sup>2</sup> H <sub>4</sub> -TxB <sub>2</sub>	3.25	0.34	13	3	0.6	1.2	480
20-OH-LTB <sub>4</sub>	351.2	195.2	-80	-25	-8	<sup>2</sup> H <sub>4</sub> -TxB <sub>2</sub>	3.37	0.3	14	3	0.1	0.25	200
TxB <sub>2</sub>	369.2	169.1	-60	-25	-7	<sup>2</sup> H <sub>4</sub> -TxB <sub>2</sub>	3.69	0.19	22	3	0.25	0.63	500
PGE <sub>3</sub>	349.3	269.2	-60	-22	-6	<sup>2</sup> H <sub>4</sub> -PGE <sub>2</sub>	4.01	0.2	7	3	0.15	0.3	120
PGD <sub>3</sub>	349.3	269.2	-60	-22	-6	<sup>2</sup> H <sub>4</sub> -PGD <sub>2</sub>	4.22	0.26	9	3	0.5	1	200
9,12,13-TriHOME	329.2	211.1	-80	-32	-10	<sup>2</sup> H <sub>4</sub> -PGE <sub>2</sub>	4.31	0.16	22	3	0.5	1.25	1000
9,10,13-TriHOME	329.2	171.1	-80	-32	-8	<sup>2</sup> H <sub>4</sub> -PGE <sub>2</sub>	4.38	0.17	16	2	0.2	0.5	400
PGF <sub>2<math>\alpha</math></sub>	353.2	309.2	-80	-26	-7	<sup>2</sup> H <sub>4</sub> -PGE <sub>2</sub>	4.39	0.34	13	3	0.35	0.7	281
PGE <sub>2</sub>	351.2	271.3	-60	-24	-6	<sup>2</sup> H <sub>4</sub> -PGE <sub>2</sub>	4.58	0.15	11	3	< 0.10	0.1	200
PGE <sub>1</sub>	353.3	317.2	-60	-20	-6	<sup>2</sup> H <sub>4</sub> -PGE <sub>2</sub>	4.71	0.17	9	2	0.13	0.33	260
PGD <sub>1</sub>	353.3	317.2	-60	-20	-6	<sup>2</sup> H <sub>4</sub> -PGD <sub>2</sub>	4.82	0.17	13	3	0.25	0.5	200
PGD <sub>2</sub>	351.2	271.3	-60	-24	-6	<sup>2</sup> H <sub>4</sub> -PGD <sub>2</sub>	4.85	0.29	12	3	0.5	1	200
LXA <sub>4</sub>	351.2	115.2	-60	-21	-8	<sup>2</sup> H <sub>4</sub> -PGE <sub>2</sub>	5.25	0.18	13	3	0.09	0.18	70
11,12,15-TriHETrE	353.2	167.1	-80	-28	-10	<sup>2</sup> H <sub>4</sub> -PGE <sub>2</sub>	5.23	0.1	10	3	0.5	1	100
LTB <sub>5</sub>	333.3	195.2	-65	-22	-8	<sup>2</sup> H <sub>4</sub> -LTB <sub>4</sub>	6.58	0.16	10	3	0.1	0.25	200
PGJ <sub>2</sub>	333.3	189.2	-60	-25	-8	<sup>2</sup> H <sub>4</sub> -PGE <sub>2</sub>	6.56	0.16	10	3	0.8	1.6	160
PGB <sub>2</sub>	333.3	175.1	-60	-28	-8	<sup>2</sup> H <sub>4</sub> -PGE <sub>2</sub>	6.67	0.11	16	3	< 0.40	0.4	800
THF diol	353.2	127.1	-80	-32	-8	<sup>2</sup> H <sub>4</sub> -LTB <sub>4</sub>	6.77	0.19	15	3	0.13	0.25	100
15,16-DiHODE	311.2	223.2	-80	-29	-10	<sup>2</sup> H <sub>4</sub> -9,10-DiHOME	7.36	0.16	12	3	0.2	0.5	400
8,15-DiHETE	335.2	235.2	-65	-22	-4	<sup>2</sup> H <sub>11</sub> -14,15-DiHETrE	7.39	0.14	13	3	0.4	0.8	80
9,10-DiHODE	311.2	201.2	-65	-27	-10	<sup>2</sup> H <sub>4</sub> -9,10-DiHOME	7.39	0.13	20	3	< 0.20	0.2	400
12,13-DiHODE	311.2	183.1	-80	-30	-8	<sup>2</sup> H <sub>4</sub> -9,10-DiHOME	7.47	0.16	14	4	1	2	400
6-trans-LTB <sub>4</sub>	335.2	195.1	-65	-23	-9	<sup>2</sup> H <sub>4</sub> -LTB <sub>4</sub>	7.75	0.15	15	4	0.25	0.5	200
5,15-DiHETE	335.3	173.2	-60	-21	-8	<sup>2</sup> H <sub>11</sub> -14,15-DiHETrE	7.77	0.14	17	4	0.13	0.25	100
17,18-DiHETE	335.3	247.2	-65	-24	-8	<sup>2</sup> H <sub>11</sub> -14,15-DiHETrE	7.91	0.16	18	4	0.13	0.25	100
LTB <sub>4</sub>	335.2	195.1	-65	-23	-9	<sup>2</sup> H <sub>4</sub> -LTB <sub>4</sub>	8.18	0.16	18	4	0.25	0.5	200
14,15-DiHETE	335.3	207.2	-65	-25	-10	<sup>2</sup> H <sub>11</sub> -14,15-DiHETrE	8.43	0.17	14	4	0.13	0.25	100
11,12-DiHETE	335.2	167.1	-65	-26	-5	<sup>2</sup> H <sub>11</sub> -14,15-DiHETrE	8.62	0.16	16	4	0.13	0.25	100
12,13-DiHOME	313.2	183.2	-80	-30	-8	<sup>2</sup> H <sub>4</sub> -9,10-DiHOME	8.82	0.2	28	4	0.5	1.25	1000
8,9-DiHETE	335.2	127.1	-65	-26	-5	<sup>2</sup> H <sub>4</sub> -9,10-DiHOME	8.98	0.19	15	4	0.25	0.5	100
9,10-DiHOME	313.2	201.2	-80	-29	-8	<sup>2</sup> H <sub>4</sub> -9,10-DiHOME	9.23	0.19	27	4	< 0.50	0.5	1000
19,20-DiHDPE	361.2	273.2	-65	-24	-6	<sup>2</sup> H <sub>11</sub> -14,15-DiHETrE	9.89	0.21	17	4	0.5	1	100
14,15-DiHETrE	337.2	207.1	-65	-25	-10	<sup>2</sup> H <sub>11</sub> -14,15-DiHETrE	9.86	0.23	18	4	0.1	0.25	200
LTB <sub>3</sub>	337.2	195.2	-65	-22	-8	<sup>2</sup> H <sub>4</sub> -LTB <sub>4</sub>	10.09	0.19	26	4	0.25	0.5	200
16,17-DiHDPE	361.2	233.2	-65	-24	-6	<sup>2</sup> H <sub>11</sub> -14,15-DiHETrE	10.45	0.19	16	4	0.25	0.5	100
11,12-DiHETrE	337.2	167.1	-65	-26	-8	<sup>2</sup> H <sub>11</sub> -14,15-DiHETrE	10.6	0.22	21	4	< 0.25	0.25	200
13,14-DiHDPE	361.2	193.2	-65	-24	-6	<sup>2</sup> H <sub>11</sub> -14,15-DiHETrE	10.71	0.23	19	4	0.13	0.25	100
9-HOTrE	293.2	171.2	-65	-22	-8	<sup>2</sup> H <sub>4</sub> -9-HODE	10.95	0.18	18	4	0.25	0.5	100
10,11-DiHDPE	361.2	153.2	-65	-24	-6	<sup>2</sup> H <sub>11</sub> -14,15-DiHETrE	11.07	0.25	18	4	0.25	0.5	100
8,9-DiHETrE	337.2	127.1	-70	-30	-8	<sup>2</sup> H <sub>11</sub> -14,15-DiHETrE	11.22	0.23	19	4	0.25	0.5	200

Table 9.1.2: Continued.

Analyte	Mass transition		MS			IS	Retention time		Peak width		LOD	Calibration	
	m/z (MS1)	m/z (MS3)	DP (V)	CE (V)	CXP (V)		(min)	SD <sup>1</sup> (sec)	Full (s)	FWHM (s)	LOD (nM)	lower conc <sup>2</sup> (nM)	upper conc <sup>3</sup> (nM)
EKODE	309.2	291.1	-65	-20	-6	<sup>2</sup> H <sub>4</sub> -9-HODE	11.26	0.23	16	4	0.25	0.5	100
13-HOTrE	293.2	195.1	-70	-24	-8	<sup>2</sup> H <sub>4</sub> -9-HODE	11.3	0.32	15	4	0.3	0.6	60
5,6-DiHETE	335.2	115.2	-60	-21	-8	<sup>2</sup> H <sub>11</sub> -14,15-DiHETrE	11.71	0.24	18	5	0.13	0.25	100
15-deoxy-PGJ <sub>2</sub>	315.2	271.2	-65	-20	-6	<sup>2</sup> H <sub>11</sub> -14,15-DiHETrE	11.76	0.24	25	5	0.5	1	400
7,8-DiHDPE	361.2	113.1	-65	-24	-6	<sup>2</sup> H <sub>11</sub> -14,15-DiHETrE	11.86	0.31	16	4	0.5	1	100
20-HETE	319.2	275.1	-80	-23	-6	<sup>2</sup> H <sub>8</sub> -20-HETE	12.04	0.25	18	5	1.3	2.6	260
15-HEPE	317.2	219.2	-60	-20	-10	<sup>2</sup> H <sub>8</sub> -12-HETE	12.04	0.25	17	5	0.63	1.25	500
5,6-DiHETrE	337.2	145.1	-70	-26	-10	<sup>2</sup> H <sub>11</sub> -14,15-DiHETrE	12.11	0.34	22	5	0.25	0.5	200
8-HEPE	317.2	155.2	-60	-20	-8	<sup>2</sup> H <sub>8</sub> -12-HETE	12.36	0.26	20	5	0.25	0.63	500
12-HEPE	317.2	179.2	-65	-20	-8	<sup>2</sup> H <sub>8</sub> -12-HETE	12.54	0.26	19	4	0.25	0.63	500
5-HEPE	317.2	115.1	-60	-20	-6	<sup>2</sup> H <sub>8</sub> -12-HETE	13.06	0.22	20	5	0.2	0.5	400
4,5-DiHDPE	361.2	229.3	-65	-24	-6	<sup>2</sup> H <sub>11</sub> -14,15-DiHETrE	13.09	0.29	16	5	1	2	100
13-HODE	295.2	195.2	-80	-26	-9	<sup>2</sup> H <sub>4</sub> -9-HODE	13.27	0.26	27	5	<1.00	1	2000
9-HODE	295.2	171.1	-80	-26	-7	<sup>2</sup> H <sub>4</sub> -9-HODE	13.38	0.27	27	5	<1.00	1	2000
15(16)-EpODE	293.3	235.2	-65	-20	-4	<sup>2</sup> H <sub>4</sub> -9(10)-EpOME	13.89	0.29	17	4	0.13	0.25	100
15-HETE	319.2	219.2	-60	-20	-8	<sup>2</sup> H <sub>8</sub> -12-HETE	13.97	0.26	22	4	0.5	1.25	1000
9(10)-EpODE	293.3	171.2	-65	-20	-8	<sup>2</sup> H <sub>4</sub> -9(10)-EpOME	14.04	0.19	18	4	0.1	0.2	80
17(18)-EpETE	317.2	215.2	-65	-20	-6	<sup>2</sup> H <sub>11</sub> -14(15)-EpETrE	14.11	0.28	16	4	0.25	0.5	100
11-HETE	319.2	167.2	-60	-23	-7	<sup>2</sup> H <sub>8</sub> -12-HETE	14.47	0.2	23	4	<0.50	0.5	1000
12(13)-EpODE	293.2	183.1	-65	-24	-8	<sup>2</sup> H <sub>4</sub> -9(10)-EpOME	14.44	0.24	16	4	0.13	0.25	100
13-oxo-ODE	293.2	195.1	-75	-20	-8	<sup>2</sup> H <sub>4</sub> -9-HODE	14.43	0.24	15	4	0.5	1	100
15-oxo-ETE	317.2	113.1	-65	-25	-8	<sup>2</sup> H <sub>8</sub> -5-HETE	14.66	0.24	11	4	0.25	0.5	100
9-oxo-ODE	293.2	185.1	-90	-28	-8	<sup>2</sup> H <sub>4</sub> -9-HODE	14.66	0.18	15	4	0.5	1	100
14(15)-EpETE	317.2	207.2	-65	-20	-6	<sup>2</sup> H <sub>11</sub> -14(15)-EpETrE	14.73	0.22	11	4	0.13	0.25	100
8-HETE	319.2	155.2	-60	-22	-6	<sup>2</sup> H <sub>8</sub> -12-HETE	14.81	0.17	16	4	1.25	2.5	1000
12-HETE	319.2	179.2	-60	-20	-8	<sup>2</sup> H <sub>8</sub> -12-HETE	14.83	0.17	16	4	<0.50	0.5	1000
11(12)-EpETE	317.2	167.2	-65	-20	-6	<sup>2</sup> H <sub>11</sub> -14(15)-EpETrE	14.87	0.15	10	4	0.25	0.5	100
8(9)-EpETE	317.2	127.2	-65	-20	-6	<sup>2</sup> H <sub>11</sub> -14(15)-EpETrE	15.01	0.23	13	3	0.5	1	100
9-HETE	319.2	167.2	-60	-23	-7	<sup>2</sup> H <sub>8</sub> -5-HETE	15.1	0.14	15	3	1.25	2.5	1000
15(S)-HETrE	321.2	221.2	-70	-23	-10	<sup>2</sup> H <sub>8</sub> -5-HETE	15.15	0.12	16	3	0.25	0.5	200
5-HETE	319.2	115.2	-60	-21	-7	<sup>2</sup> H <sub>8</sub> -5-HETE	15.33	0.11	17	3	0.5	1.25	1000
19(20)-EpDPE	343.2	241.2	-65	-20	-7	<sup>2</sup> H <sub>11</sub> -14(15)-EpETrE	15.8	0.11	10	3	0.13	0.25	100
12(13)-EpOME	295.3	195.2	-80	-23	-8	<sup>2</sup> H <sub>4</sub> -9(10)-EpOME	15.86	0.16	13	3	0.1	0.25	200
14(15)-EpETrE	319.2	219.3	-65	-20	-4	<sup>2</sup> H <sub>11</sub> -14(15)-EpETrE	15.99	0.14	15	3	0.25	0.5	100
9(10)-EpOME	295.3	171.1	-80	-23	-8	<sup>2</sup> H <sub>4</sub> -9(10)-EpOME	16.03	0.17	14	3	0.1	0.25	200
16(17)-EpDPE	343.2	233.2	-65	-20	-7	<sup>2</sup> H <sub>11</sub> -14(15)-EpETrE	16.18	0.15	19	3	0.13	0.25	100
13(14)-EpDPE	343.2	193.2	-65	-20	-7	<sup>2</sup> H <sub>11</sub> -14(15)-EpETrE	16.25	0.19	19	3	0.25	0.5	100
5-oxo-ETE	317.2	273.2	-65	-22	-6	<sup>2</sup> H <sub>4</sub> -9(10)-EpOME	16.3	0.1	10	3	1	2	100
10(11)-EpDPE	343.2	153.2	-65	-20	-7	<sup>2</sup> H <sub>11</sub> -14(15)-EpETrE	16.34	0.15	17	3	0.13	0.25	100
11(12)-EpETrE	319.3	167.2	-60	-20	-7	<sup>2</sup> H <sub>11</sub> -14(15)-EpETrE	16.44	0.1	12	3	0.25	0.5	200
8(9)-EpETrE	319.3	167.2	-60	-20	-7	<sup>2</sup> H <sub>11</sub> -14(15)-EpETrE	16.58	0.13	10	3	0.13	0.25	100
8(9)-EpETrE 2	319.2	155.2	-65	-20	-6	<sup>2</sup> H <sub>11</sub> -14(15)-EpETrE	16.58	0.2	10	3	1	2	100
5(6)-EpETrE	319.2	191.1	-60	-20	-7	<sup>2</sup> H <sub>11</sub> -14(15)-EpETrE	16.71	0.12	10	3	0.5	1	100

<sup>1</sup> Reported retention time variance within a batch of 20 injections. Following analysis on the machine with different mobile phases and another column a larger retention time drift ( $\leq 0.2$  min) was observed and the retention times in the method were adapted accordingly. <sup>2</sup> LLOQ was set to the lowest calibration standard injected within the sample set yielding a signal to noise ratio  $\leq 9$  and an accuracy in the calibration within  $\pm 20\%$ . ULOQ does not reflect the end of the linear range but the concentration of the highest calibrator.

**Table 9.1.3:** List of internal standards used and parameters of ESI(-)-MS/MS detection. Shown are the mass transition used for quantification in scheduled SRM mode and the electronical MS parameters (Declustering Potential (DP), Collision Energy (CE) and Collision Cell Exit Potential (CXP)).

Analyte	Retention time (min)	Mass transition		MS Parameters		
		m/z (MS1)	m/z (MS3)	DP (V)	CE (V)	CXP (V)
$^2\text{H}_4$ -6-keto-PGF <sub>1<math>\alpha</math></sub>	3.18	373.3	167.1	-80	-36	-8
$^2\text{H}_4$ -TxB <sub>2</sub>	3.95	373.3	173.2	-65	-24	-8
$^2\text{H}_4$ -PGE <sub>2</sub>	4.56	355.2	275.3	-60	-25	-6
$^2\text{H}_4$ -PGD <sub>2</sub>	4.84	355.2	275.3	-60	-25	-6
$^2\text{H}_4$ -LTB <sub>4</sub>	8.12	339.2	197.2	-65	-23	-9
$^2\text{H}_4$ -9,10-DiHOME	9.15	317.2	203.4	-80	-29	-8
$^2\text{H}_{11}$ -14,15-DiHETrE	9.72	348.2	207.1	-65	-25	-10
$^2\text{H}_6$ -20-HETE	11.97	325.2	281.2	-70	-23	-6
$^2\text{H}_4$ -9-HODE	13.27	299.2	172.3	-80	-26	-6
$^2\text{H}_8$ -12-HETE	14.68	327.2	184.2	-65	-22	-8
$^2\text{H}_8$ -5-HETE	15.21	327.2	116.1	-60	-21	-8
$^2\text{H}_4$ -9(10)-EpOME	15.95	299.2	172.2	-80	-23	-8
$^2\text{H}_{11}$ -14(15)-EpETrE	15.88	330.2	219.3	-65	-20	-4

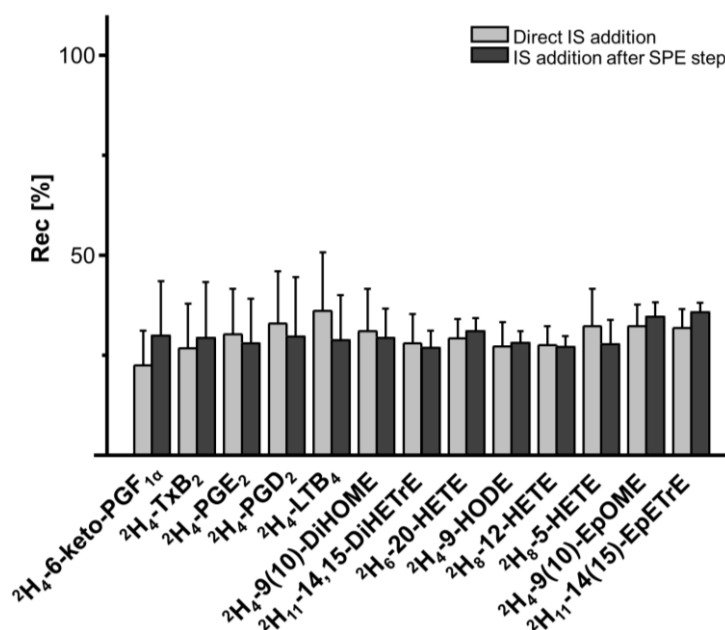


**Fig. 9.1.1:** Recoveries of internal standards (IS) for the LLE protocol with addition of IS before the SPE-step and after the SPE-step. Shown is the mean  $\pm$  SD (n=5).

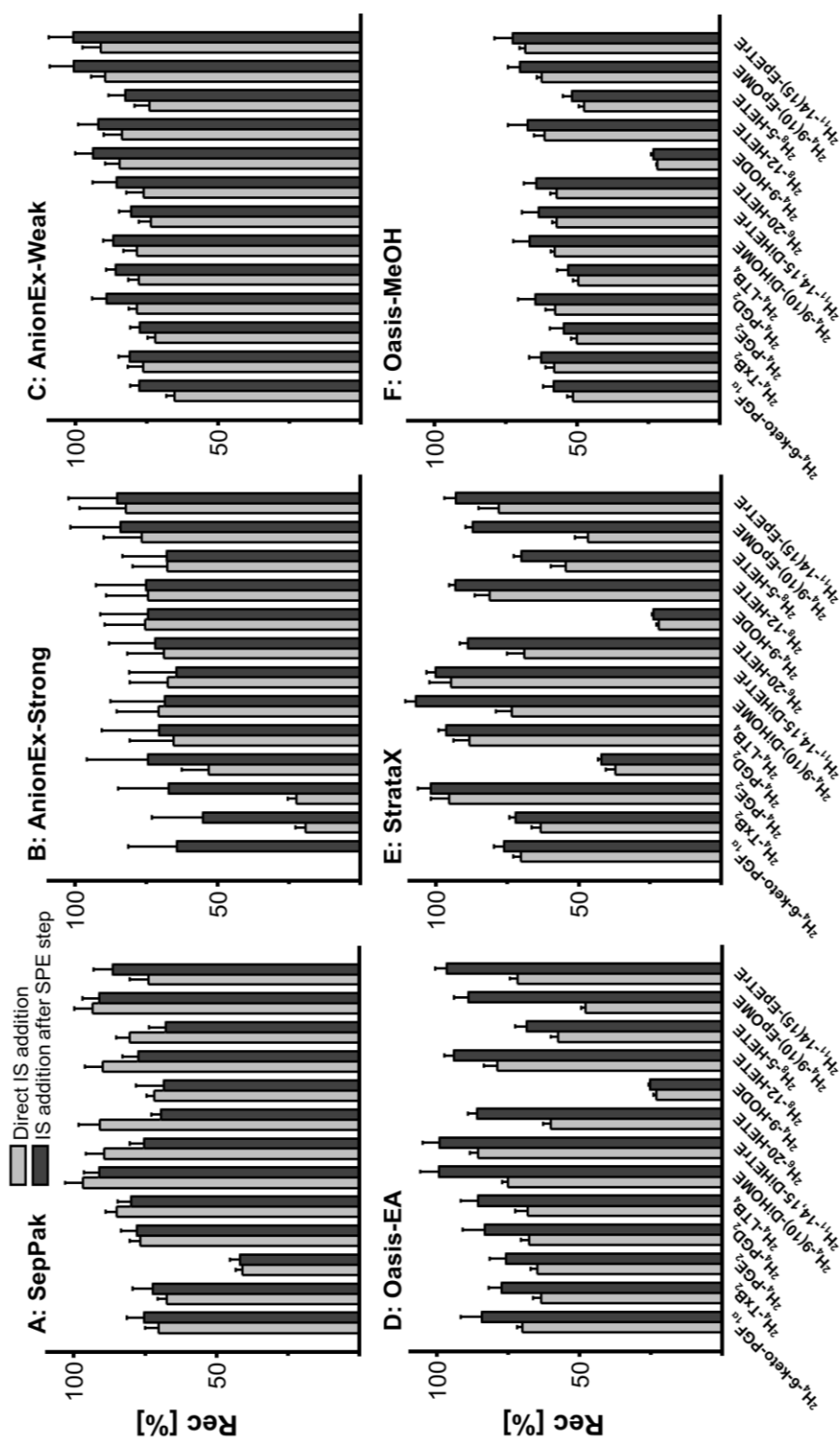


**Fig. 9.1.2:** Direct comparison of recoveries of internal standards (IS) with addition of IS at the beginning of the sample preparation (light grey bar) and after the SPE-step (dark grey bar) for (A) SepPak, (B) AnionEx-strong, (C) AnionEx-weak, (D) Oasis-EA, (E) StrataX and (F) Oasis-MeOH protocol. Shown is the mean  $\pm$  SD (n=5). The same data is presented in condensed fashion in Fig. 4.1.



**Table 9.1.4:** Recovery rates of internal standards (IS) for the SPE protocols with addition of IS before (A) the SPE-step and after (B) the SPE-step. Shown are the mean $\pm$ SD (n=5).

		<sup>2</sup> H <sub>4</sub> -6-keto-PGF <sub>1<math>\alpha</math></sub>	<sup>2</sup> H <sub>4</sub> -TxB <sub>2</sub>	<sup>2</sup> H <sub>4</sub> -PGE <sub>2</sub>	<sup>2</sup> H <sub>4</sub> -PGD <sub>2</sub>	<sup>2</sup> H <sub>4</sub> -LTB <sub>4</sub>	<sup>2</sup> H <sub>4</sub> -9,10-DiHOME
SepPak	A	70 $\pm$ 4.8	68 $\pm$ 3.1	41 $\pm$ 2.4	77 $\pm$ 3.8	85 $\pm$ 4	97 $\pm$ 6.2
	B	75 $\pm$ 6.1	72 $\pm$ 7.2	42 $\pm$ 3.6	78 $\pm$ 5.5	80 $\pm$ 4.7	91 $\pm$ 5.3
AnionEx-Strong	A		19 $\pm$ 3.4	22 $\pm$ 3.1	53 $\pm$ 9.3	66 $\pm$ 15	71 $\pm$ 15
	B	64 $\pm$ 17	55 $\pm$ 18	67 $\pm$ 18	75 $\pm$ 22	71 $\pm$ 20	69 $\pm$ 19
AnionEx-Weak	A	65 $\pm$ 2.8	76 $\pm$ 5.4	72 $\pm$ 2.7	79 $\pm$ 2.9	78 $\pm$ 3.7	78 $\pm$ 4.8
	B	78 $\pm$ 3.1	81 $\pm$ 3.9	78 $\pm$ 3.3	89 $\pm$ 5	86 $\pm$ 3.3	87 $\pm$ 3.5
Oasis-EA	A	70 $\pm$ 1.9	64 $\pm$ 3	65 $\pm$ 2.3	68 $\pm$ 2.9	68 $\pm$ 4.3	75 $\pm$ 2.1
	B	84 $\pm$ 7.3	77 $\pm$ 4.5	76 $\pm$ 5.7	83 $\pm$ 7.7	86 $\pm$ 6	99 $\pm$ 6.5
StrataX	A	70 $\pm$ 2.6	63 $\pm$ 3.2	96 $\pm$ 6.4	37 $\pm$ 3.3	88 $\pm$ 5.5	74 $\pm$ 5.6
	B	76 $\pm$ 3.6	72 $\pm$ 2.2	100 $\pm$ 4.6	42 $\pm$ 1.2	97 $\pm$ 2.6	110 $\pm$ 3.7
Oasis-MeOH	A	51 $\pm$ 2.1	58 $\pm$ 3	50 $\pm$ 1.9	58 $\pm$ 3.3	50 $\pm$ 1.8	58 $\pm$ 1.3
	B	58 $\pm$ 3.7	63 $\pm$ 4.4	55 $\pm$ 4.9	65 $\pm$ 6.1	53 $\pm$ 3.9	67 $\pm$ 5.8
LLE	A	23 $\pm$ 8.7	27 $\pm$ 11	30 $\pm$ 11	33 $\pm$ 13	36 $\pm$ 15	31 $\pm$ 11
	B	30 $\pm$ 14	29 $\pm$ 14	28 $\pm$ 11	30 $\pm$ 15	29 $\pm$ 11	29 $\pm$ 7.3

		<sup>2</sup> H <sub>11</sub> -14,15-DiHETrE	<sup>2</sup> H <sub>6</sub> -20-HETE	<sup>2</sup> H <sub>4</sub> -9-HODE	<sup>2</sup> H <sub>8</sub> -12-HETE	<sup>2</sup> H <sub>8</sub> -5-HETE	<sup>2</sup> H <sub>4</sub> -9(10)-EpOME	<sup>2</sup> H <sub>11</sub> -14(15)-EpETrE
SepPak	A	89 $\pm$ 6.3	91 $\pm$ 7.4	72 $\pm$ 2.8	90 $\pm$ 6.2	80 $\pm$ 4.8	93 $\pm$ 6.3	74 $\pm$ 6.6
	B	75 $\pm$ 5.2	70 $\pm$ 3.3	69 $\pm$ 9.8	77 $\pm$ 5.6	68 $\pm$ 5.8	91 $\pm$ 5.8	86 $\pm$ 6.7
AnionEx-Strong	A	68 $\pm$ 14	69 $\pm$ 13	75 $\pm$ 14	75 $\pm$ 15	68 $\pm$ 12	77 $\pm$ 13	82 $\pm$ 16
	B	64 $\pm$ 17	72 $\pm$ 16	75 $\pm$ 17	75 $\pm$ 18	68 $\pm$ 16	84 $\pm$ 18	85 $\pm$ 17
AnionEx-Weak	A	74 $\pm$ 4.2	76 $\pm$ 6.1	85 $\pm$ 5.3	84 $\pm$ 6.5	74 $\pm$ 5.3	90 $\pm$ 5	91 $\pm$ 6.5
	B	81 $\pm$ 4.2	86 $\pm$ 8.5	94 $\pm$ 6.2	92 $\pm$ 7.2	83 $\pm$ 6	100 $\pm$ 8.4	100 $\pm$ 8.7
Oasis-EA	A	86 $\pm$ 2.9	60 $\pm$ 2.7	23 $\pm$ 1	79 $\pm$ 4.9	58 $\pm$ 2.4	48 $\pm$ 1.7	72 $\pm$ 2.6
	B	99 $\pm$ 6.1	86 $\pm$ 3.2	25 $\pm$ 0.58	94 $\pm$ 3.4	69 $\pm$ 4.1	89 $\pm$ 5.1	97 $\pm$ 4.1
StrataX	A	95 $\pm$ 7.7	69 $\pm$ 6.2	22 $\pm$ 0.88	81 $\pm$ 5.2	55 $\pm$ 5.2	47 $\pm$ 4.5	78 $\pm$ 7.2
	B	100 $\pm$ 3.1	89 $\pm$ 2.8	24 $\pm$ 0.42	93 $\pm$ 2.1	70 $\pm$ 2.8	87 $\pm$ 2.6	93 $\pm$ 4
Oasis-MeOH	A	57 $\pm$ 1.6	57 $\pm$ 2.2	22 $\pm$ 0.21	62 $\pm$ 3.7	48 $\pm$ 1.7	62 $\pm$ 1.8	68 $\pm$ 2.1
	B	64 $\pm$ 5.7	64 $\pm$ 4.4	23 $\pm$ 0.79	67 $\pm$ 6.9	52 $\pm$ 3.1	70 $\pm$ 4.2	73 $\pm$ 6.5
LLE	A	28 $\pm$ 7.3	29 $\pm$ 4.8	27 $\pm$ 5.9	28 $\pm$ 4.7	32 $\pm$ 9.4	32 $\pm$ 5.4	32 $\pm$ 4.7
	B	27 $\pm$ 4.3	31 $\pm$ 3.2	28 $\pm$ 2.9	27 $\pm$ 2.7	28 $\pm$ 6.1	35 $\pm$ 3.6	36 $\pm$ 2.4

**Fig. 9.1.3:** Ion suppression analysis of the internal standards for the different SPE protocols tested: **(A)**  $^2\text{H}_4\text{-PGE}_2/{}^2\text{H}_4\text{-PGE}_2$ , **(B)**  $^2\text{H}_4\text{-TxB}_2$ , **(C)**  $^2\text{H}_4\text{-LTB}_4$ , **(D)**  $^2\text{H}_4\text{-9-HODE}$ , **(E)**  $^2\text{H}_8\text{-5-HETE}$ , **(F)**  $^2\text{H}_8\text{-12-HETE}$ , **(G)**  $^2\text{H}_6\text{-20-HETE}$ , **(H)**  $^2\text{H}_{11}\text{-14,15-DiHETrE}$ , **(I)**  $^2\text{H}_{11}\text{14(15)-EpETrE}$ , **(J)**  $^2\text{H}_4\text{-9,10-DiHOME}$ . The dark grey bar indicates the retention time of the IS and the light grey bar indicates the retention time range of all analytes quantified with the IS. Mean intensity in the ion suppression (5-10 min) chromatogram was set to 100% relative intensity.

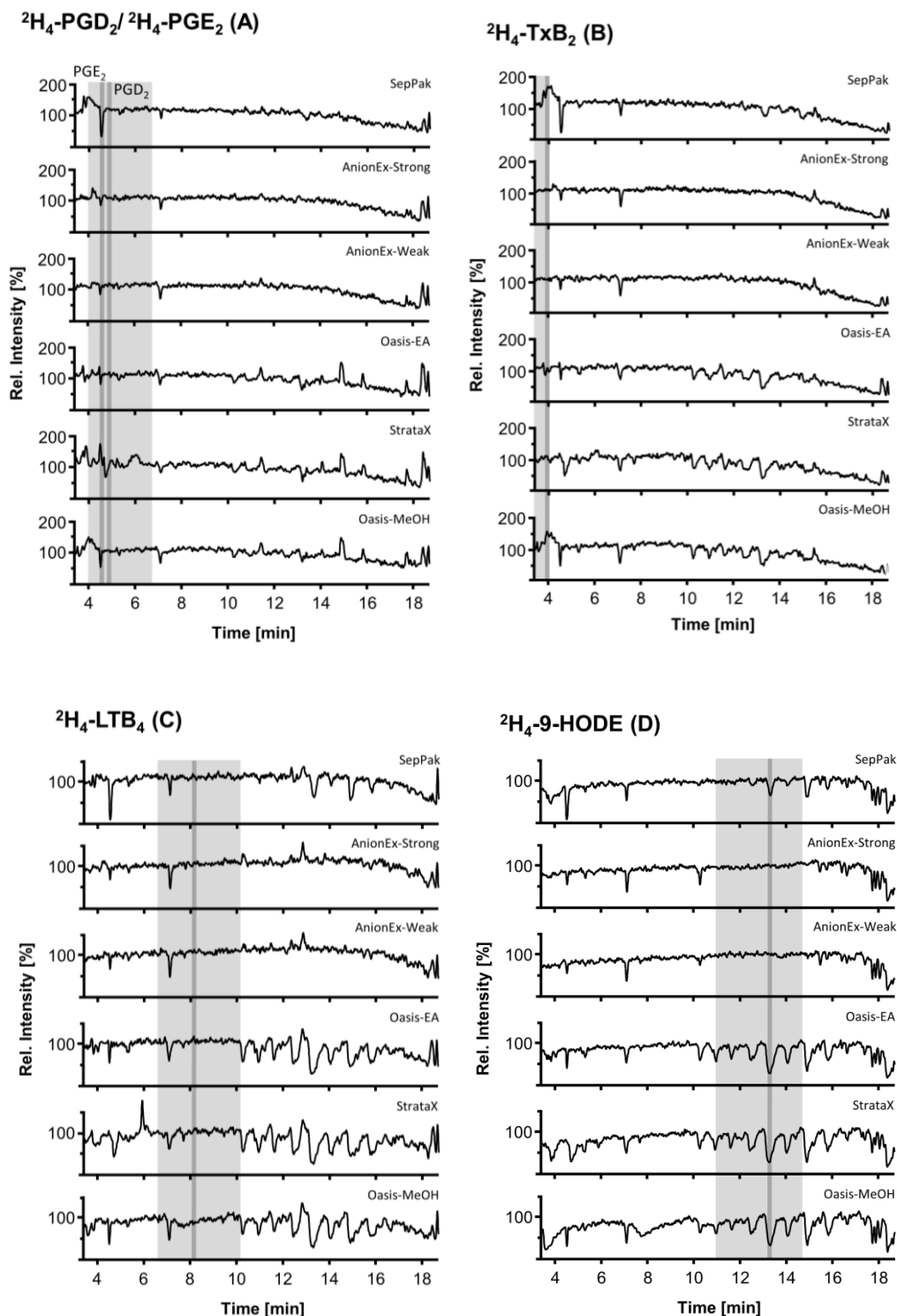


Fig. 9.1.3: Continued.

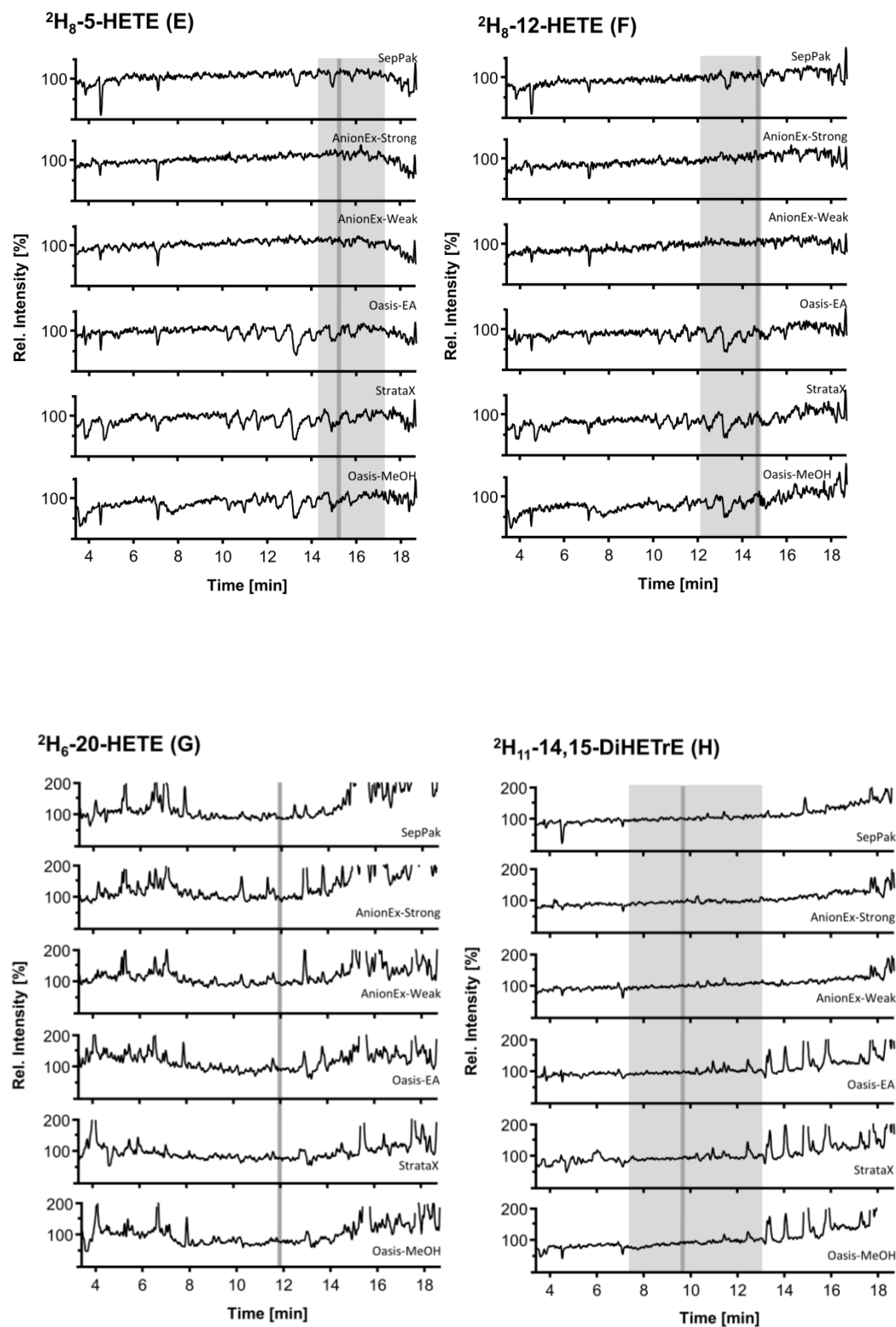
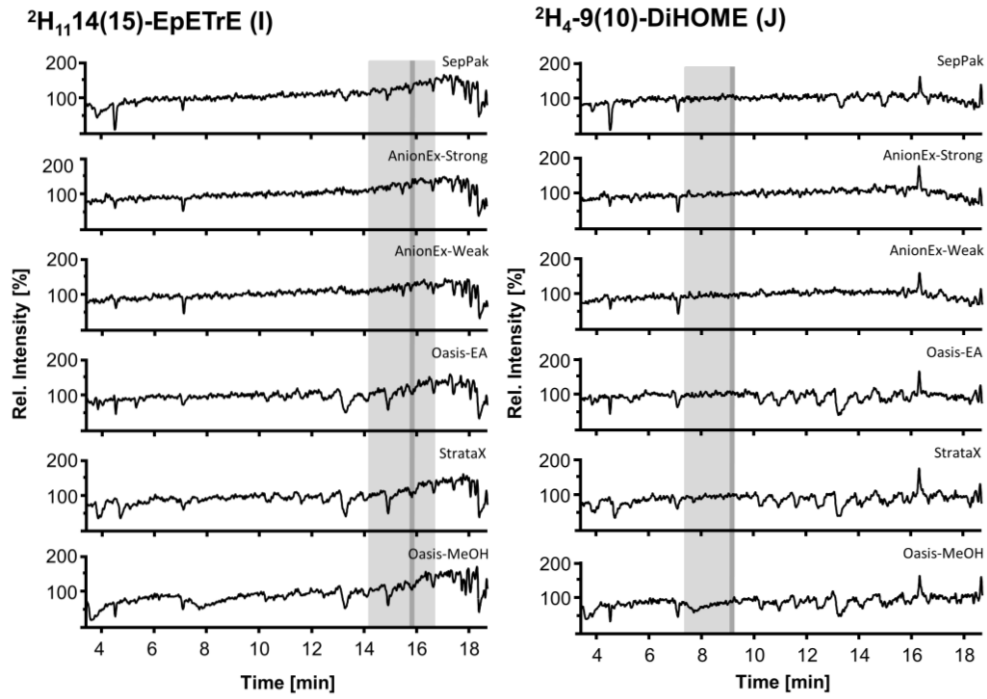


Fig. 9.1.3: Continued.



**Table 9.1.5:** Peak areas following extraction of 500 µL plasma of all oxylipins included in the LC-MS method with the different SPE-protocol tested. Shown is the mean ± SD (n=5).

[1000 counts]	SepPak		AnionEX-Strong		AnionEX-Weak		Oasis-EA		StrataX		Oasis-MeOH		LLE	
	Mean	SD	Mean	SD	Mean	SD	Mean	SD	Mean	SD	Mean	SD	Mean	SD
6-keto-PGF1a	<LOQ		<LOQ		<LOQ		29.6	11.0	<LOQ		<LOQ		<LOQ	
20-COOH-LTB4	<LOQ		<LOQ		<LOQ		<LOQ		<LOQ		<LOQ		<LOQ	
RvE1	<LOQ		<LOQ		<LOQ		<LOQ		<LOQ		<LOQ		<LOQ	
20-OH-LTB4	<LOQ		<LOQ		<LOQ		<LOQ		<LOQ		<LOQ		<LOQ	
TXB2	31.2	1.7	<LOQ		39.2	0.7	44.3	13.9	29.2	1.2	26.0	2.0	<LOQ	
PGE3	<LOQ		<LOQ		<LOQ		<LOQ		<LOQ		<LOQ		<LOQ	
PGD3	<LOQ		<LOQ		<LOQ		<LOQ		<LOQ		<LOQ		<LOQ	
9,12,13-TriHOME	858.0	48.3	256.3	35.0	642.7	160.5	622.7	115.0	423.7	11.3	435.0	25.6	180.3	129.9
9,10,13-TriHOME	275.0	8.2	78.5	15.5	145.8	16.3	183.8	34.7	120.5	5.7	126.0	8.4	62.9	54.0
PGF2a	8.8	0.9	<LOQ		11.4	1.4	9.9	1.5	9.7	0.5	8.0	1.3	<LOQ	
PGE2	21.4	2.2	14.9	2.0	36.4	1.9	40.7	4.4	62.1	6.7	26.4	1.9	<LOQ	
PGE1	<LOQ		<LOQ		<LOQ		<LOQ		<LOQ		<LOQ		<LOQ	
PGD1	<LOQ		<LOQ		<LOQ		<LOQ		<LOQ		<LOQ		<LOQ	
PGD2	30.4	1.7	21.8	5.0	27.2	2.1	18.4	1.6	4.9	0.9	16.3	2.2		
LXA4	8.8	0.8			4.0	0.8	3.5	0.8	4.9	0.3	2.6	0.3	1.8	1.2
11,12-,15-TriHETrE	<LOQ		<LOQ		<LOQ		<LOQ		<LOQ		<LOQ		<LOQ	
LTB5	<LOQ		<LOQ		<LOQ		<LOQ		<LOQ		<LOQ		<LOQ	
PGJ2	<LOQ		<LOQ		<LOQ		<LOQ		<LOQ		<LOQ		<LOQ	
PGB2	<LOQ		<LOQ		<LOQ		5.5	2.0	<LOQ		<LOQ		<LOQ	
THF diol	<LOQ		<LOQ		<LOQ		<LOQ		<LOQ		<LOQ		<LOQ	
15,16-DiHODE	4306.2	270.3	3570.4	760.3	3989.1	110.3	3580.3	68.9	4440.0	217.0	3090.0	89.5	1420.3	536.6
8,15-DiHETE	135.9	7.1	72.5	14.7	70.0	3.0	73.8	3.7	88.5	3.5	57.5	5.4	20.7	9.5
9,10-DiHODE	120.5	8.3	82.4	17.4	92.1	2.8	88.8	0.8	87.5	4.5	70.7	3.7	32.4	12.2
12,13-DiHODE	74.3	8.9	55.4	14.5	<LOQ		46.3	4.5	48.9	11.2	41.7	5.0	<LOQ	
6-trans-LTB4	23.8	1.3	12.2	2.8	11.4	0.4	46.0	9.3	17.0	1.1	13.6	2.5	<LOQ	
5,15-DiHETE	33.8	1.1	23.6	5.0	19.9	1.3	26.7	1.2	27.3	2.0	14.5	1.6	5.7	3.0
17,18-DiHETE	228.0	18.5	197.5	41.3	213.5	4.5	215.8	6.0	241.5	15.2	155.3	8.3	76.8	27.0
LTB4	<LOQ		<LOQ		<LOQ		<LOQ		<LOQ		<LOQ		<LOQ	
14,15-DiHETE	42.0	2.2	32.4	6.2	36.0	1.4	38.8	1.8	43.8	2.7	22.8	1.6	12.3	3.8
11,12-DiHETE	30.0	1.7	22.7	5.6	24.0	0.6	26.7	1.9	27.1	1.5	16.6	1.3	8.1	3.4
12,13-DiHOME	1958.0	132.2	1462.3	287.4	1573.3	47.1	1751.7	52.5	1918.0	111.8	1109.6	45.6	524.5	182.0
8,9-DiHETE	8.4	0.6	6.8	1.3	7.4	0.2	7.9	0.6	9.4	0.6	5.5	0.3	2.7	1.1
9,10-DiHOME	2183.4	138.7	1512.0	304.3	1660.8	52.5	1491.1	35.1	1360.7	82.6	1248.7	36.2	584.8	229.3
19,20-DiHDPE	234.6	15.8	196.8	38.5	210.3	6.8	200.4	6.9	232.9	11.2	172.1	7.9	77.9	26.8
14,15-DiHETrE	222.9	16.0	177.0	35.1	190.4	4.2	221.8	7.4	246.4	19.2	147.4	6.3	64.8	20.7
LTB3	<LOQ		<LOQ		<LOQ		<LOQ		<LOQ		<LOQ		<LOQ	
16,17-DiHDPE	51.1	4.3	37.6	7.1	41.3	0.4	45.6	2.7	49.8	3.0	32.1	1.0	14.2	4.4
11,12-DiHETrE	143.3	11.2	111.7	22.2	121.4	2.0	100.1	4.2	102.9	6.5	89.5	3.3	42.1	15.2

Table 9.1.5: Continued.

[1000 counts]	SepPak		AnionEX-Strong		AnionEX-Weak		Oasis-EA		StrataX		Oasis-MeOH		LLE	
	Mean	SD	Mean	SD	Mean	SD	Mean	SD	Mean	SD	Mean	SD	Mean	SD
13,14-DiHDPE	50.0	3.1	33.9	6.7	40.6	1.5	38.7	1.8	45.4	3.1	30.7	1.7	13.0	4.4
9-HOTrE	263.8	12.3	208.7	34.6	216.0	7.6	126.9	6.2	129.2	3.5	110.4	4.4	65.1	18.9
10,11-DiHDPE	28.7	1.2	21.9	4.4	24.0	0.5	24.6	1.4	27.0	1.3	17.1	0.8	8.9	3.2
8,9-DiHETrE	24.9	1.1	18.9	3.3	20.1	0.5	20.3	1.0	22.3	0.7	14.4	1.1	7.9	3.4
EKODE	664.0	56.8	290.3	80.1	223.9	36.1	651.2	54.7	252.3	35.8	327.1	17.7	45.3	22.3
13-HOTrE	205.7	30.7	157.4	25.7	159.8	5.3	137.9	4.3	147.0	7.3	113.4	3.3	48.5	11.9
5,6-DiHETE	<LOQ		<LOQ		<LOQ		<LOQ		<LOQ		<LOQ		<LOQ	
15-deoxy-PGJ2	<LOQ		<LOQ		<LOQ		23.1	15.9	<LOQ		<LOQ		<LOQ	
7,8-DiHDPE	4.5	0.6	3.5	0.9	3.8	0.4	4.7	0.6	4.2	0.4	2.6	0.5	1.5	0.7
20-HETE	29.0	5.2	21.9	3.8	27.4	2.1	23.8	1.7	24.1	1.7	22.7	2.9	9.9	3.0
15-HEPE	198.5	15.4	144.2	25.1	140.3	2.6	133.7	3.6	140.1	6.2	98.8	4.8	34.0	8.4
5,6-DiHETrE	36.7	3.0	25.7	5.2	27.1	1.0	38.0	3.1	29.4	2.4	22.1	0.5	12.6	5.2
8-HEPE	127.3	8.5	101.0	19.3	97.8	2.5	74.0	2.9	79.4	3.8	64.9	1.9	30.0	9.3
12-HEPE	223.3	13.7	426.7	87.5	350.4	14.5	128.4	3.3	118.0	5.5	107.7	4.1	43.9	11.0
5-HEPE	148.4	8.1	126.5	24.5	127.6	4.8	146.6	5.6	128.6	6.4	91.7	8.3	35.7	15.0
4,5-DiHDPE	13.4	1.0	10.4	2.2	11.0	0.2	12.3	0.4	14.0	1.0	8.9	0.9	5.2	2.1
13-HODE	5536.7	447.6	4916.2	867.9	5057.1	197.3	1508.1	56.9	1390.8	52.1	1614.9	53.0	1260.1	273.3
9-HODE	6523.8	278.1	6006.7	1092.1	6134.6	176.0	2401.6	103.5	2249.9	96.6	2463.2	109.4	1622.8	423.6
15(16)-EpODE	672.1	44.1	405.9	65.8	466.2	21.7	352.6	21.4	370.7	26.7	408.2	11.4	162.3	32.3
15-HETE	493.0	34.3	402.6	73.6	390.4	12.1	365.1	15.3	352.3	25.6	257.6	15.9	97.5	22.1
9(10)-EpODE	72.8	10.9	8.0	1.3	12.1	1.0	15.0	5.0	5.0	0.5	15.0	1.0	<LOQ	
17(18)-EpETE	20.6	3.0	6.1	1.3	7.2	0.6	7.6	0.8	6.7	0.5	6.5	0.9	<LOQ	
11-HETE	1369.1	91.0	1019.6	182.6	1044.7	26.8	921.6	43.5	945.4	42.6	744.4	54.3	290.1	81.4
12(13)-EpODE	88.8	11.3	25.1	5.7	29.7	2.7	26.0	3.9	17.7	1.8	34.1	2.3	12.2	2.4
13-oxo-ODE	45.9	3.4	18.2	4.1	20.4	7.2	22.2	4.7	12.6	1.4	29.3	1.2	8.0	3.9
15-oxo-ETE	97.8	8.8	116.7	20.9	128.1	6.8	151.2	8.0	149.5	16.7	108.1	8.4	34.1	7.3
9-oxo-ODE	605.4	53.2	358.1	59.4	431.3	33.3	531.4	21.0	464.5	41.9	512.4	17.5	126.0	38.2
14(15)-EpETE	27.0	6.5	<LOQ		4.9	0.6	7.4	1.5	5.8	1.0	6.4	0.7	<LOQ	
8-HETE	234.7	10.6	191.8	34.9	181.2	12.8	123.5	4.7	132.3	8.7	117.1	7.4	60.2	17.4
12-HETE	576.5	20.6	861.3	175.5	741.6	38.2	368.2	28.0	323.8	18.2	325.3	18.9	137.5	34.5
11(12)-EpETE	12.8	2.1	2.6	0.4	3.5	1.0	2.9	0.9	<LOQ		<LOQ		<LOQ	
8(9)-EpETE	2.6	0.3	<LOQ		<LOQ		1.5	0.8	<LOQ		1.1	0.1	<LOQ	
9-HETE	120.3	8.0	115.2	20.1	107.7	5.7	76.5	5.3	81.4	4.0	64.2	4.0	32.5	10.5
15(S)-HETrE	285.2	18.9	230.8	43.8	219.5	10.2	167.0	7.6	185.3	10.7	156.9	7.7	62.6	13.8
5-HETE	336.9	20.7	297.5	60.4	282.7	8.3	329.5	13.1	262.5	10.8	196.5	26.1	79.6	36.0
19(20)-EpDPE	56.2	8.6	14.1	2.7	16.3	0.6	17.4	2.3	12.2	0.6	18.2	0.5	4.7	1.0
12(13)-EpOME	1727.6	162.1	556.4	105.8	640.2	33.6	556.1	96.5	304.1	13.9	720.2	30.9	318.7	61.4
14(15)-EpETrE	48.3	9.3	8.8	2.0	10.2	0.9	22.8	5.8	11.0	0.6	14.8	1.5	3.8	1.0
9(10)-EpOME	1183.9	153.0	264.6	52.9	310.0	17.6	517.6	164.8	184.3	16.2	446.0	28.8	91.7	23.3
16(17)-EpDPE	37.0	8.8	3.1	0.8	4.0	0.8	7.5	2.8	4.3	0.7	8.5	0.6	<LOQ	
13(14)-EpDPE	31.5	6.1	<LOQ		<LOQ		6.8	3.2	<LOQ		7.0	0.8	<LOQ	
5-oxo-ETE	51.9	19.3	38.4	7.4	38.0	4.1	38.9	4.6	48.0	3.0	35.6	2.2	12.8	2.9
10(11)-EpDPE	63.1	11.1	10.7	2.4	14.2	1.1	21.5	7.8	13.2	1.2	20.2	1.2	3.8	0.8
11(12)-EpETrE	41.9	7.1	6.4	1.3	6.5	0.6	29.8	12.9	8.4	0.5	14.7	1.4	1.9	0.3
8(9)-EpETrE	11.6	2.2	2.9	0.6	3.4	0.5	9.1	3.8	3.2	0.4	4.4	0.7	1.2	0.1
5(6)-EpETrE	18.6	3.4	3.8	0.4	4.5	0.3	13.7	5.2	5.9	0.8	12.9	0.7	2.2	0.6

**Table 9.1.6:** Peak areas of all oxylipins included in the LC-MS method following extraction of 500  $\mu$ L plasma with the adjusted SepPak and AnionEx protocol, using 3 mL and 6 mL cartridges, respectively. Shown is the mean  $\pm$  SD (n=5).

[1000 counts]	SepPak - 3 mL		AnionEx-Weak - 6 mL		[1000 counts]	SepPak - 3 mL		AnionEx-Weak - 6 mL	
	Mean	SD	Mean	SD		Mean	SD	Mean	SD
6-keto-PGF1a	<LOQ		<LOQ		EKODE	505.8	156.3	358.2	120.2
20-COOH-LTB4	<LOQ		<LOQ		13-HOTrE	177.8	6.9	258.5	33.1
RvE1	<LOQ		<LOQ		5,6-DiHETE	<LOQ		<LOQ	
20-OH-LTB4	<LOQ		<LOQ		15-deoxy-PGJ2	<LOQ		<LOQ	
TXB2	35.8	3.2	39.7	6.9	7,8-DiHDPE	4.7	0.3	5.4	1.4
PGE3	10.8	1.4	6.7	1.7	20-HETE	29.2	5.7	27.9	8.7
PGD3	20.7	3.8	19.1	2.5	15-HEPE	203.4	16.4	164.7	25.6
9,12,13-TriHOME	845.9	85.0	860.0	127.5	5,6-DiHETrE	35.0	1.7	35.2	6.0
9,10,13-TriHOME	292.9	32.9	209.3	29.5	8-HEPE	113.3	7.3	112.5	14.3
PGF2a	6.3	1.1	11.5	2.3	12-HEPE	244.4	14.6	356.7	61.0
PGE2	10.2	0.9	23.7	4.3	5-HEPE	125.8	8.3	142.5	9.8
PGE1	<LOQ		<LOQ		4,5-DiHDPE	13.3	1.1	15.1	4.6
PGD1	<LOQ		<LOQ		13-HODE	5953.4	387.4	7394.6	1087.9
PGD2	22.8	5.7	24.3	4.7	9-HODE	7361.8	319.6	8174.8	827.6
LXA4	5.4	0.7	5.1	2.0	15(16)-EpODE	520.7	37.1	496.3	76.5
11,12-,15-TriHETrE	<LOQ		<LOQ		15-HETE	525.7	37.3	506.4	59.5
LTB5	<LOQ		<LOQ		9(10)-EpODE	39.6	3.3	11.5	3.0
PGJ2	<LOQ		<LOQ		17(18)-EpETE	8.6	0.8	7.7	1.2
PGB2	<LOQ		<LOQ		11-HETE	1387.2	50.8	1167.3	56.6
THF diol	<LOQ		<LOQ		12(13)-EpODE	56.3	4.7	31.4	3.1
15,16-DiHODE	4898.1	426.1	4590.9	744.7	13-oxo-ODE	27.5	2.1	23.2	4.0
8,15-DiHETE	119.3	8.2	80.0	11.2	15-oxo-ETE	52.0	23.0	135.0	12.4
9,10-DiHODE	101.2	5.1	103.4	16.4	9-oxo-ODE	557.4	19.4	443.6	54.3
12,13-DiHODE	57.9	4.9	53.8	9.7	14(15)-EpETE	9.3	0.6	4.5	0.5
6-trans-LTB4	18.1	1.9	12.2	4.8	8-HETE	248.8	13.3	185.0	31.7
5,15-DiHETE	24.6	2.8	18.5	2.9	12-HETE	659.3	47.4	677.0	91.8
17,18-DiHETE	264.2	30.2	254.2	48.9	11(12)-EpETE	6.8	0.8	<LOQ	
LTB4	<LOQ		<LOQ		8(9)-EpETE	1.5	0.6	<LOQ	
14,15-DiHETE	45.6	4.0	43.7	8.8	9-HETE	137.2	8.6	100.9	15.3
11,12-DiHETE	27.6	2.7	28.5	9.2	15(S)-HETrE	299.6	20.7	242.6	30.6
12,13-DiHOME	2065.6	176.6	1920.7	290.9	5-HETE	344.5	41.2	304.5	32.2
8,9-DiHETE	7.2	0.5	8.4	2.0	19(20)-EpDPE	32.2	2.0	19.3	3.6
9,10-DiHOME	2113.6	153.3	2035.2	333.9	12(13)-EpOME	1258.6	67.7	733.2	78.9
19,20-DiHDPE	310.5	30.6	283.4	60.0	14(15)-EpETrE	17.2	1.7	11.7	2.3
14,15-DiHETrE	268.1	30.4	239.0	47.9	9(10)-EpOME	682.9	45.9	284.2	39.2
LTB3	<LOQ		<LOQ		16(17)-EpDPE	20.0	1.4	5.5	1.4
16,17-DiHDPE	60.4	6.0	55.5	12.7	13(14)-EpDPE	19.6	2.5	<LOQ	
11,12-DiHETrE	171.2	18.1	158.6	32.6	5-oxo-ETE	57.5	4.8	47.4	5.5
13,14-DiHDPE	56.0	7.4	56.5	13.2	10(11)-EpDPE	50.0	5.1	16.2	3.3
9-HOTrE	238.8	8.6	273.9	24.6	11(12)-EpETrE	21.4	1.7	8.3	0.9
10,11-DiHDPE	33.3	4.3	31.5	6.2	8(9)-EpETrE	7.2	0.7	3.9	0.9
8,9-DiHETrE	25.8	2.2	25.4	6.0	5(6)-EpETrE	11.2	0.6	4.5	0.9

**Table 9.1.7:** Calculated concentrations for human plasma of all oxylipins included in the LC-MS method determined with the different SPE-protocols tested. Internal standards used for quantification can be found in Table 9.1.2. Shown is the mean  $\pm$  SD (n=5).

[nM]	SepPak		AnionEX-Strong		AnionEX-Weak		Oasis-EA		StrataX		Oasis-MeOH		LLE	
	Mean	SD	Mean	SD	Mean	SD	Mean	SD	Mean	SD	Mean	SD	Mean	SD
6-keto-PGF1a	<LOQ		<LOQ		<LOQ		<LOQ		<LOQ		<LOQ		<LOQ	
20-COOH-LTB4	<LOQ		<LOQ		<LOQ		<LOQ		<LOQ		<LOQ		<LOQ	
RvE1	<LOQ		<LOQ		<LOQ		<LOQ		<LOQ		<LOQ		<LOQ	
20-OH-LTB4	<LOQ		<LOQ		<LOQ		<LOQ		<LOQ		<LOQ		<LOQ	
TXB2	0.295	0.011	0.707	0.390	0.333	0.012	0.503	0.174	0.306	0.033	0.307	0.037	0.298	0.029
PGE3	<LOQ		<LOQ		<LOQ		<LOQ		<LOQ		<LOQ		<LOQ	
PGD3	<LOQ		<LOQ		<LOQ		<LOQ		<LOQ		<LOQ		<LOQ	
9,12,13-TriHOME	8.279	0.668	5.086	1.066	3.356	0.812	3.642	0.652	1.665	0.156	3.348	0.097	2.256	0.850
9,10,13-TriHOME	1.579	0.126	0.927	0.236	0.454	0.048	0.640	0.119	0.282	0.023	0.577	0.026	0.456	0.246
PGF2a	0.185	0.020	<LOQ		0.130	0.016	0.127	0.022	0.083	0.007	0.134	0.021	<LOQ	
PGE2	0.245	0.022	0.352	0.045	0.225	0.020	0.285	0.041	0.290	0.036	0.241	0.012	0.182	0.033
PGE1	<LOQ		<LOQ		<LOQ		<LOQ		<LOQ		<LOQ		<LOQ	
PGD1	<LOQ		<LOQ		<LOQ		<LOQ		<LOQ		<LOQ		<LOQ	
PGD2	0.523	0.025	0.549	0.071	0.455	0.043	0.358	0.049	0.174	0.034	0.374	0.052	<LOQ	
LXA4	0.438	0.035	<LOQ		0.107	0.023	0.104	0.021	0.099	0.005	0.104	0.006	0.118	0.036
11,12-,15-TriHETrE	<LOQ		<LOQ		<LOQ		<LOQ		<LOQ		<LOQ		<LOQ	
LTB5	<LOQ		<LOQ		<LOQ		<LOQ		<LOQ		<LOQ		<LOQ	
PGJ2	<LOQ		<LOQ		<LOQ		<LOQ		<LOQ		<LOQ		<LOQ	
PGB2	<LOQ		0.063	0.007	<LOQ		0.087	0.022	<LOQ		<LOQ		<LOQ	
THF diol	<LOQ		<LOQ		<LOQ		<LOQ		<LOQ		<LOQ		<LOQ	
15,16-DiHODE	9.118	0.296	10.555	0.334	10.584	0.580	9.911	0.380	12.629	0.951	11.318	0.237	10.566	0.371
8,15-DiHETE	2.027	0.104	1.460	0.114	1.285	0.126	1.147	0.045	1.245	0.102	1.377	0.116	1.076	0.233
9,10-DiHODE	0.227	0.009	0.217	0.009	0.218	0.010	0.219	0.005	0.222	0.013	0.230	0.008	0.215	0.010
12,13-DiHODE	<LOQ		0.227	0.018	<LOQ		<LOQ		<LOQ		<LOQ		<LOQ	
6-trans-LTB4	0.182	0.005	0.125	0.018	0.096	0.007	0.445	0.107	0.125	0.012	0.183	0.031	0.077	0.007
5,15-DiHETE	0.468	0.026	0.440	0.040	0.339	0.040	0.386	0.018	0.356	0.033	0.322	0.029	0.270	0.083
17,18-DiHETE	0.957	0.019	1.121	0.046	1.105	0.056	0.949	0.014	0.958	0.060	1.051	0.038	1.157	0.063
LTB4	<LOQ		<LOQ		<LOQ		<LOQ		<LOQ		<LOQ		<LOQ	
14,15-DiHETE	0.176	0.006	0.184	0.009	0.185	0.011	0.170	0.005	0.173	0.009	0.154	0.007	0.187	0.003
11,12-DiHETE	0.129	0.008	0.131	0.008	0.127	0.007	0.121	0.009	0.110	0.005	0.115	0.007	0.123	0.020
12,13-DiHOME	5.328	0.156	5.573	0.209	5.365	0.270	6.230	0.279	7.009	0.619	5.224	0.150	5.074	0.298
8,9-DiHETE	0.162	0.011	0.179	0.006	0.177	0.013	0.160	0.008	0.172	0.012	0.170	0.008	0.182	0.021
9,10-DiHOME	3.660	0.116	3.548	0.137	3.489	0.186	3.270	0.118	3.061	0.124	3.621	0.049	3.429	0.120
19,20-DiHDPE	2.764	0.083	3.140	0.146	3.052	0.132	2.471	0.063	2.594	0.197	3.266	0.074	3.302	0.142
14,15-DiHETrE	0.581	0.013	0.624	0.020	0.611	0.028	0.605	0.013	0.605	0.029	0.619	0.017	0.613	0.017
LTB3	<LOQ		<LOQ		<LOQ		<LOQ		<LOQ		<LOQ		<LOQ	
16,17-DiHDPE	0.378	0.013	0.378	0.019	0.377	0.021	0.353	0.013	0.348	0.017	0.384	0.013	0.383	0.029
11,12-DiHETrE	0.512	0.011	0.540	0.023	0.535	0.031	0.376	0.014	0.350	0.035	0.516	0.013	0.539	0.037



Table 9.1.7: Continued.

[nM]	SepPak		AnionEX-Strong		AnionEX-Weak		Oasis-EA		StrataX		Oasis-MeOH		LLE	
	Mean	SD	Mean	SD	Mean	SD	Mean	SD	Mean	SD	Mean	SD	Mean	SD
13,14-DiHDPE	0.280	0.009	0.257	0.012	0.279	0.011	0.226	0.008	0.239	0.015	0.276	0.015	0.263	0.009
9-HOTrE	1.803	0.115	1.360	0.065	1.243	0.077	3.127	0.079	3.408	0.217	2.896	0.101	1.299	0.086
10,11-DiHDPE	0.271	0.009	0.280	0.008	0.280	0.018	0.243	0.010	0.241	0.014	0.261	0.008	0.300	0.025
8,9-DiHETrE	0.345	0.015	0.355	0.022	0.343	0.027	0.295	0.009	0.292	0.022	0.322	0.022	0.385	0.066
EKODE	2.194	0.240	0.898	0.134	0.609	0.082	7.776	0.506	3.213	0.460	4.151	0.188	0.422	0.159
13-HOTrE	1.855	0.301	1.352	0.079	1.211	0.057	4.490	0.283	5.115	0.411	3.923	0.110	1.287	0.038
5,6-DiHETE	<LOQ		<LOQ		<LOQ		<LOQ		<LOQ		<LOQ		<LOQ	
15-deoxy-PGJ2	<LOQ		<LOQ		<LOQ		<LOQ		<LOQ		<LOQ		<LOQ	
7,8-DiHDPE	0.160	0.021	0.166	0.016	0.165	0.021	0.172	0.018	0.141	0.014	0.150	0.025	0.193	0.033
20-HETE	0.448	0.096	0.450	0.059	0.504	0.027	0.562	0.033	0.493	0.039	0.566	0.068	0.507	0.110
15-HEPE	1.650	0.054	1.465	0.090	1.266	0.104	1.281	0.079	1.298	0.074	1.224	0.047	0.990	0.057
5,6-DiHETrE	0.370	0.010	0.350	0.015	0.338	0.027	0.402	0.042	0.281	0.013	0.360	0.007	0.448	0.055
8-HEPE	1.158	0.043	1.117	0.060	0.964	0.065	0.778	0.037	0.806	0.027	0.881	0.046	0.940	0.122
12-HEPE	1.936	0.075	4.470	0.289	3.270	0.177	1.285	0.080	1.142	0.057	1.391	0.049	1.327	0.111
5-HEPE	1.749	0.037	1.814	0.149	1.629	0.168	1.984	0.121	1.683	0.097	1.603	0.107	1.422	0.351
4,5-DiHDPE	1.101	0.032	1.153	0.107	1.115	0.070	1.064	0.032	1.086	0.065	1.181	0.122	1.507	0.234
13-HODE	28.923	2.515	24.452	1.067	22.244	1.235	28.406	1.314	27.981	1.474	32.360	0.783	19.522	0.995
9-HODE	35.678	1.490	31.266	1.135	28.277	1.573	47.400	2.275	47.431	2.594	51.716	2.023	26.114	1.202
15(16)-EpODE	2.713	0.071	2.025	0.084	1.970	0.078	2.914	0.260	3.147	0.213	2.527	0.067	2.081	0.066
15-HETE	3.473	0.100	3.455	0.162	2.977	0.188	2.961	0.181	2.762	0.169	2.702	0.101	2.407	0.108
9(10)-EpODE	0.337	0.031	0.046	0.004	0.058	0.004	0.143	0.051	0.049	0.009	0.107	0.006	0.046	0.004
17(18)-EpETE	0.369	0.027	0.100	0.013	0.105	0.007	0.143	0.018	0.115	0.009	0.129	0.015	0.099	0.013
11-HETE	2.879	0.073	2.616	0.147	2.380	0.172	2.230	0.091	2.213	0.101	2.328	0.112	2.117	0.194
12(13)-EpODE	0.326	0.021	0.113	0.006	0.115	0.009	0.197	0.035	0.137	0.014	0.193	0.011	0.144	0.011
13-oxo-ODE	0.725	0.055	0.266	0.022	0.265	0.092	1.280	0.351	0.771	0.112	1.788	0.058	0.356	0.124
15-oxo-ETE	0.916	0.065	1.315	0.032	1.313	0.111	2.017	0.026	2.119	0.158	1.774	0.111	0.907	0.155
9-oxo-ODE	8.159	0.758	4.583	0.209	4.872	0.341	25.956	1.614	24.260	2.863	26.602	0.663	4.974	0.747
14(15)-EpETE	0.255	0.048	0.033	0.003	0.037	0.004	0.072	0.017	0.051	0.008	0.066	0.008	<LOQ	
8-HETE	1.754	0.086	1.744	0.096	1.465	0.108	1.069	0.045	1.107	0.059	1.306	0.084	1.556	0.166
12-HETE	3.485	0.153	6.291	0.343	4.824	0.282	2.557	0.187	2.178	0.096	2.919	0.097	2.889	0.209
11(12)-EpETE	0.142	0.018	<LOQ		<LOQ		<LOQ		<LOQ		<LOQ		<LOQ	
8(9)-EpETE	0.148	0.027	<LOQ		<LOQ		<LOQ		<LOQ		<LOQ		<LOQ	
9-HETE	2.255	0.097	2.601	0.154	2.205	0.116	2.045	0.098	2.326	0.215	2.111	0.100	1.677	0.094
15(S)-HETrE	1.113	0.034	1.084	0.061	0.937	0.041	0.932	0.038	1.100	0.074	1.075	0.043	0.695	0.105
5-HETE	3.781	0.133	4.018	0.371	3.476	0.286	5.271	0.146	4.485	0.386	3.862	0.436	2.363	0.316
19(20)-EpDPE	1.005	0.107	0.227	0.028	0.234	0.019	0.323	0.054	0.206	0.016	0.355	0.018	0.215	0.014
12(13)-EpOME	5.580	0.220	2.214	0.121	2.165	0.109	3.686	0.724	2.073	0.196	3.569	0.085	3.277	0.147
14(15)-EpETrE	0.602	0.080	0.095	0.011	0.100	0.010	0.294	0.081	0.128	0.010	0.200	0.014	0.119	0.014
9(10)-EpOME	3.359	0.226	0.923	0.054	0.920	0.039	3.023	1.021	1.102	0.112	1.943	0.086	0.820	0.077
16(17)-EpDPE	0.533	0.093	0.039	0.004	0.046	0.008	0.114	0.045	0.058	0.008	0.135	0.013	<LOQ	
13(14)-EpDPE	0.456	0.060	<LOQ		<LOQ		0.103	0.053	<LOQ		0.110	0.012	<LOQ	
5-oxo-ETE	0.895	0.349	0.809	0.111	0.673	0.052	1.363	0.146	1.748	0.217	0.930	0.043	0.689	0.071
10(11)-EpDPE	0.798	0.096	0.122	0.011	0.145	0.003	0.285	0.112	0.160	0.009	0.280	0.013	0.123	0.025
11(12)-EpETrE	0.572	0.069	0.081	0.016	0.072	0.005	0.426	0.190	0.110	0.010	0.220	0.017	0.070	0.015
8(9)-EpETrE	0.256	0.037	<LOQ		<LOQ		0.202	0.108	0.043	0.011	0.082	0.015	<LOQ	
5(6)-EpETrE	1.413	0.192	0.252	0.040	0.261	0.019	1.082	0.460	0.414	0.061	1.064	0.053	0.360	0.079

**Table 9.1.8:** Modified LC-MS quantification method using the SepPak protocol. Because of strong ion suppression occurring for  $^2\text{H}_4\text{-PGE}_2$  in this protocol, the quantification method (Tab S1) is modified and  $^2\text{H}_4\text{-PGD}_2$  is used for several analytes.

The calculated concentrations of  $\text{PGE}_3$ ,  $\text{PGD}_3$ , 9,12,13-TriHOME, 9,10,13-TriHOME,  $\text{PGF}_{2\alpha}$ ,  $\text{PGE}_2$ ,  $\text{PGE}_1$ ,  $\text{PGD}_1$ ,  $\text{PGD}_2$ ,  $\text{LXA}_4$ , 11,12-,15-TriHETrE,  $\text{PGJ}_2$ ,  $\text{PGB}_2$  with different internal standards is shown for the original (left) and modified method (right). Shown is the mean  $\pm$  SD (n=5).

	Original Quantification Method		Modified Method	
	IS	Mean [pM]	IS	Mean [pM]
$\text{PGE}_3$	$^2\text{H}_4\text{-PGE}_2$	<LOQ	$^2\text{H}_4\text{-PGD}_2$	<LOQ
$\text{PGD}_3$	$^2\text{H}_4\text{-PGD}_2$	<LOQ	$^2\text{H}_4\text{-PGD}_2$	<LOQ
9,12,13-TriHOME	$^2\text{H}_4\text{-PGE}_2$	8300 $\pm$ 670	$^2\text{H}_4\text{-PGD}_2$	4700 $\pm$ 360
9,10,13-TriHOME	$^2\text{H}_4\text{-PGE}_2$	1600 $\pm$ 130	$^2\text{H}_4\text{-PGD}_2$	890 $\pm$ 42
$\text{PGF}_{2\alpha}$	$^2\text{H}_4\text{-PGE}_2$	190 $\pm$ 20	$^2\text{H}_4\text{-PGD}_2$	100 $\pm$ 11
$\text{PGE}_2$	$^2\text{H}_4\text{-PGE}_2$	250 $\pm$ 22	$^2\text{H}_4\text{-PGE}_2$	250 $\pm$ 22
$\text{PGE}_1$	$^2\text{H}_4\text{-PGE}_2$	200 $\pm$ 28	$^2\text{H}_4\text{-PGD}_2$	110 $\pm$ 12
$\text{PGD}_1$	$^2\text{H}_4\text{-PGD}_2$	<LOQ	$^2\text{H}_4\text{-PGD}_2$	<LOQ
$\text{PGD}_2$	$^2\text{H}_4\text{-PGD}_2$	523 $\pm$ 25	$^2\text{H}_4\text{-PGD}_2$	520 $\pm$ 25
$\text{LXA}_4$	$^2\text{H}_4\text{-PGE}_2$	440 $\pm$ 35	$^2\text{H}_4\text{-PGD}_2$	250 $\pm$ 20
11,12-,15-TriHETrE	$^2\text{H}_4\text{-PGE}_2$	<LOQ	$^2\text{H}_4\text{-PGD}_2$	<LOQ
$\text{PGJ}_2$	$^2\text{H}_4\text{-PGE}_2$	<LOQ	$^2\text{H}_4\text{-PGD}_2$	<LOQ
$\text{PGB}_2$	$^2\text{H}_4\text{-PGE}_2$	<LOQ	$^2\text{H}_4\text{-PGD}_2$	<LOQ

## 9.2 Chapter 5

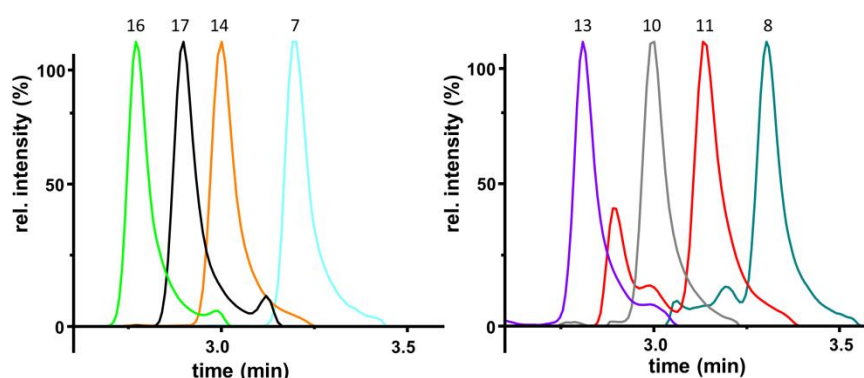


**Fig. 9.2.1:** Separation efficacy of the developed method. Shown are the SRM signals of DHA derived OH-FAs used for quantification following injection of a multianalyte standard (20 nM). The DHA derived HDHAs are shown in two panels allowing to assess the individual peaks of the OH-FAs.

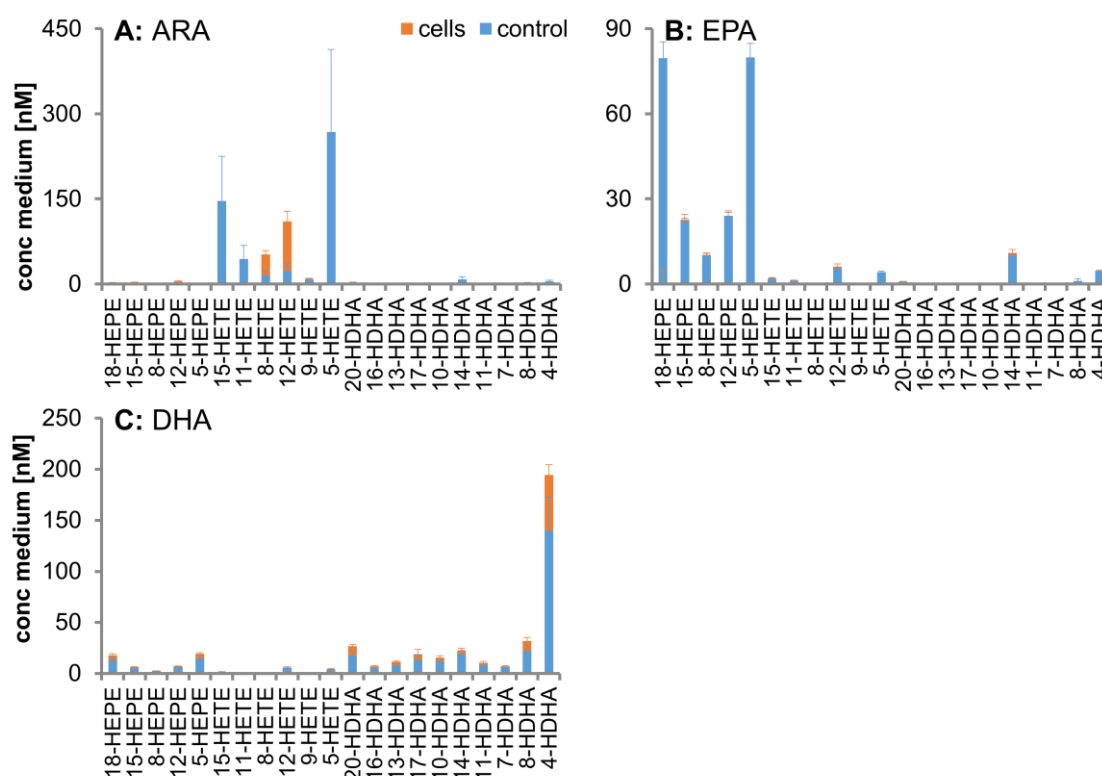


**Fig. 9.2.2A:** Formation of hydroxy-FAs in cell culture medium. **HCT-116 cells** were incubated with PUFA ethyl esters (50  $\mu$ M) for 24 hours. Shown is the concentration of an incubation with (orange) and without cells (blue) reflecting formation by hydrolysis and autoxidation. In panel **A** incubations were carried out with ARA ethyl ester, in panel **B** with EPA ethyl ester and in panel **C** with DHA ethyl ester. The concentration in the media before incubation and in incubations without added PUFA were below 10 nM (not shown). All results are given as mean $\pm$ SD (n=4).

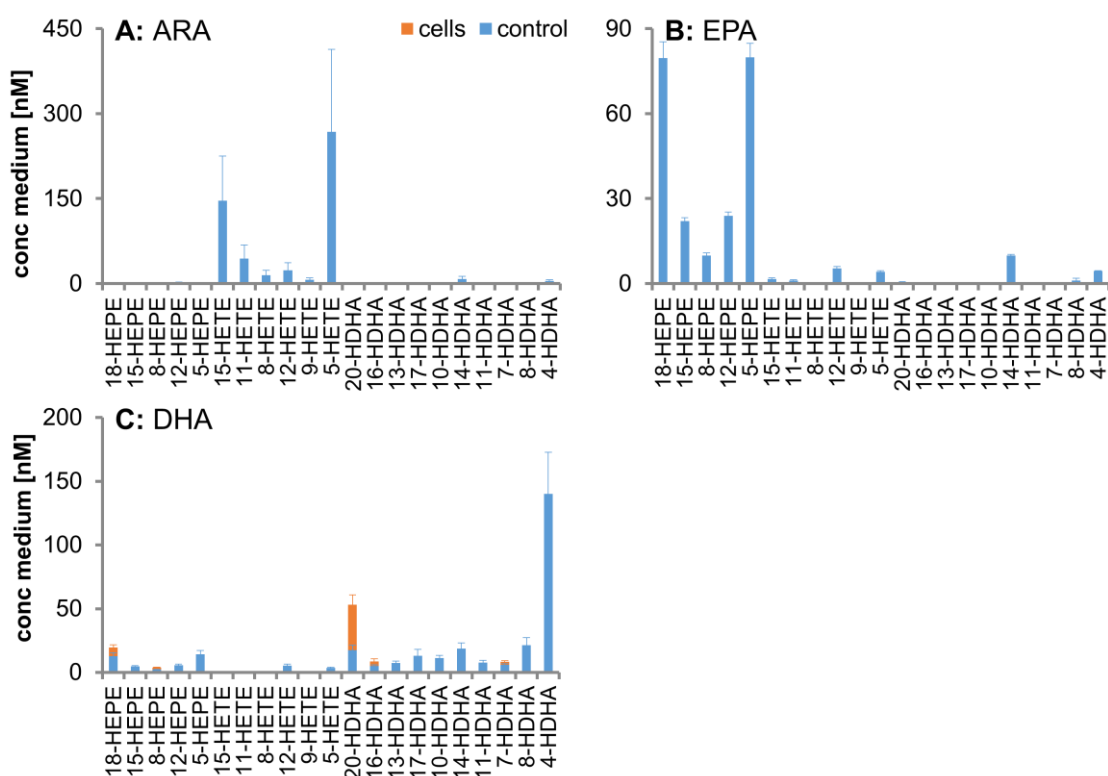


**Fig. 9.2.2B:** Formation of hydroxy-FAs in cell culture medium. **HT-29 cells** were incubated with PUFA ethyl esters (50  $\mu$ M) for 24 hours. Shown is the concentration of an incubation with (orange) and without cells (blue) reflecting formation by hydrolysis and autoxidation. In panel **A** incubations were carried out with ARA ethyl ester, in panel **B** with EPA ethyl ester and in panel **C** with DHA ethyl ester. The concentration in the media before incubation and in incubations without added PUFA were below 10 nM (not shown). All results are given as mean $\pm$ SD (n=4).

### 9.3 Chapter 6

**Table 9.3.1:** Determined fat content<sup>#</sup>, peroxide value<sup>+</sup> and fatty acid composition\* of the experimental diets. Diets were based on a standard experimental diet from ssniff Spezialdiäten GmbH (product number: E15051; with 17.6% crude protein, 5.0% crude fiber, 5.3% crude ash, 31.4% starch, 11.0% sugar and 10.1% fat as specified by the manufacturer). All results are shown as mean  $\pm$  deviation from the mean (n=2).

	STD	STD+n3
Determined <b>fat content</b> in the diet [g/100g]	9.7 $\pm$ 0.2	9.9 $\pm$ 0.2
<b>Peroxide value</b> [mEq O <sub>2</sub> /kg]	2.6 $\pm$ 0.1	3.6 $\pm$ 0.1
<b>[%] Fatty Acid</b> in lipid extract		
C14:0	0.15 $\pm$ 0.05	0.19 $\pm$ 0.04
C15:0	0.07 $\pm$ 0.02	-
C16:0	7.995 $\pm$ 0.008	6.61 $\pm$ 0.05
C16:1n7	0.217 $\pm$ 0.008	0.24 $\pm$ 0.03
C17:0	0.071 $\pm$ 0.007	0.058 $\pm$ 0.007
C18:0	3.288 $\pm$ 0.001	2.64 $\pm$ 0.03
C18:1n9	27.064 $\pm$ 0.004	21.65 $\pm$ 0.06
C18:1n7	1.26 $\pm$ 0.04	1.047 $\pm$ 0.003
C18:2n6	58.306 $\pm$ 0.003	46.5 $\pm$ 0.1
C18:3n3	0.335 $\pm$ 0.005	0.287 $\pm$ 0.003
C20:0	0.218 $\pm$ 0.003	0.184 $\pm$ 0.004
C20:1n9	0.167 $\pm$ 0.002	0.14 $\pm$ 0.01
C20:4n6	-	0.303 $\pm$ 0.003
C20:5n3	-	8.91 $\pm$ 0.07
C22:0	0.653 $\pm$ 0.008	0.95 $\pm$ 0.03
C22:5n3	-	1.18 $\pm$ 0.05
C24:0	0.204 $\pm$ 0.008	-
C22:6n3	-	8.91 $\pm$ 0.09
C24:1n9	-	0.17 $\pm$ 0.02

<sup>#</sup>For the determination of the fatty acid composition and the peroxide value, lipids were first extracted from the pellets according to the Weibull-Stoldt method, performed as rapid microextraction [1].

<sup>+</sup>Determination of the peroxide value was performed by iodometry as described [3]. Briefly, after dissolving the lipid extract in acetic acid/isooctane (3:2, v:v) and addition of potassium iodide the formed iodine titrated with sodium thiosulfate.

\*The fatty acid composition was determined after derivatization to fatty acid methyl esters by means of gas chromatography with flame ionization detection using response factors [2].

**Table 9.3.2:** Fatty acid composition of the standard mouse diet according to the manufacturer ssniff Spezialdiäten GmbH (product number: V1530; with 19.0% crude protein, 4.9% crude fiber, 6.4% crude ash, 36.5% starch, 4.7% sugar and 3.3% fat as specified by the manufacturer).

	[%] Fatty Acid in diet
C14:0	0.01
C16:0	0.47
C16:1	0.01
C18:0	0.08
C18:1	0.62
C18:2	1.80
C18:3	0.23
C20:0	0.01
C20:1	0.02
C20:5	-
C22:6	-

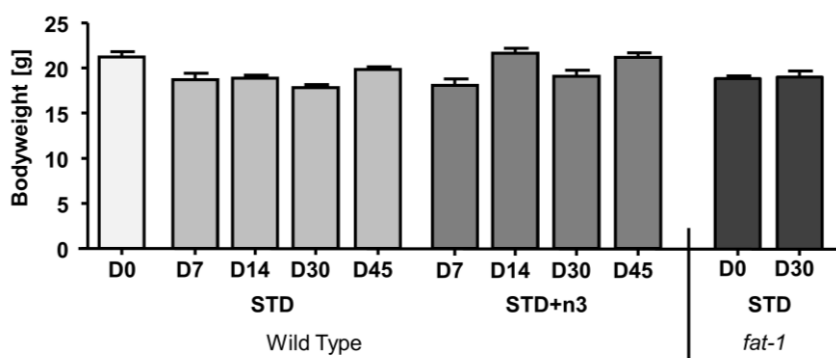


**Fig. 9.3.1:** Bodyweight of wild type C57BL/5 mice at baseline (days 0) and after 7-45 days on a standard sunflower based diet or the same diet enriched with EPA and DHA and of transgenic *fat-1* mice on a standard sunflower based diet (0 and 30 days).

**Table 9.3.3A:** Absolute concentrations of fatty acids in blood of wild type mice at the beginning of the experiment (Day 0) and during the course of the feeding experiment on a standard sunflower based diet (STD) or on the same diet enriched with n3-PUFA (1% EPA and 1% DHA as ethyl ester, STD+n3). Absolute concentrations in transgenic *fat-1* mice are shown at baseline (Day 0) and after 30 days on a standard sunflower based diet.

In case an analyte was below limit of quantification (<LOQ) in more than 50% of samples within one group, the LOQ is shown.

Table 9.3.3A: Whole Blood.

[µg/mL whole blood]	fat-1			Wild Type			STD			STD+n3				
	Day 0		Day 30		Day 0		Day 7		Day 14		Day 30		Day 45	
	Mean	SEM	Mean	SEM	Mean	SEM	Mean	SEM	Mean	SEM	Mean	SEM	Mean	SEM
C10:0	<1.0	<1.0	<1.0	<1.0	<1.0	<1.0	<1.0	<1.0	<1.0	<1.0	<1.0	<1.0	<1.0	<1.0
C11:0	<1.0	<1.0	<1.0	<1.0	<1.0	<1.0	<1.0	<1.0	<1.0	<1.0	<1.0	<1.0	<1.0	<1.0
C12:0	<1.0	<1.0	<1.0	<1.0	<1.0	<1.0	<1.0	<1.0	<1.0	<1.0	<1.0	<1.0	<1.0	<1.0
C13:0	<1.0	<1.0	<1.0	<1.0	<1.0	<1.0	<1.0	<1.0	<1.0	<1.0	<1.0	<1.0	<1.0	<1.0
C14:0	<1.0	<1.0	<1.0	<1.0	<1.0	<1.0	<1.0	<1.0	<1.0	<1.0	<1.0	<1.0	<1.0	<1.0
C15:0	<1.0	<1.0	<1.0	<1.0	<1.0	<1.0	<1.0	<1.0	<1.0	<1.0	<1.0	<1.0	<1.0	<1.0
<b>SFA</b>	513.34	57.15	287.22	30.44	468.72	37.62	512.40	26.36	387.29	26.78	429.78	25.15	387.61	37.08
C16:0	7.01	0.79	4.03	0.40	7.78	0.89	6.61	0.34	5.50	0.42	6.00	0.24	5.61	0.46
C17:0	241.44	18.46	200.52	23.93	249.78	18.80	298.16	13.13	254.28	16.09	290.43	16.36	264.28	19.52
C18:0	1.94	0.32	1.97	0.26	<1.0	<1.0	2.41	0.31	1.75	0.31	2.45	0.40	2.39	0.19
C20:0	<1.0	<1.0	<1.0	<1.0	<1.0	<1.0	<1.0	<1.0	<1.0	<1.0	<1.0	<1.0	<1.0	<1.0
C21:0	<1.0	<1.0	<1.0	<1.0	<1.0	<1.0	<1.0	<1.0	<1.0	<1.0	<1.0	<1.0	<1.0	<1.0
C22:0	11.38	0.68	10.26	1.30	9.48	0.31	13.19	0.80	10.46	0.64	14.23	0.71	12.71	0.38
C24:0	24.42	1.91	20.33	1.90	21.13	0.98	25.07	1.74	18.89	0.73	21.92	0.83	22.57	1.00
C14:1n5	<1.0	<1.0	<1.0	<1.0	<1.0	<1.0	<1.0	<1.0	<1.0	<1.0	<1.0	<1.0	<1.0	<1.0
C15:1n5	<1.0	<1.0	<1.0	<1.0	<1.0	<1.0	<1.0	<1.0	<1.0	<1.0	<1.0	<1.0	<1.0	<1.0
C16:1n7	31.52	7.77	7.69	1.16	28.90	4.29	24.29	1.86	16.45	1.18	18.51	3.40	12.07	0.72
C17:1n7	<1.0	<1.0	<1.0	<1.0	<1.0	<1.0	<1.0	<1.0	<1.0	<1.0	<1.0	<1.0	<1.0	<1.0
C18:1n7	50.43	11.65	23.19	3.13	48.79	5.82	44.24	1.86	31.02	2.49	38.99	3.40	33.33	2.34
C18:1n9	351.10	74.73	188.49	22.58	285.12	32.63	301.57	16.16	219.44	13.11	254.49	22.71	239.71	17.73
C20:1n9	7.81	1.29	4.16	0.53	6.35	0.71	6.64	0.69	5.12	0.37	5.71	0.46	5.28	0.56
C22:1n9	<1.0	<1.0	<1.0	<1.0	2.23	0.54	3.39	0.88	6.53	2.03	2.32	0.64	<1.0	<1.0
C24:1n9	11.52	1.77	20.17	1.14	15.15	0.62	9.35	1.94	11.08	1.13	17.51	0.72	25.21	1.26
C18:2n6	408.06	58.63	258.59	26.16	311.43	29.75	494.68	37.30	369.51	21.13	407.85	27.22	338.66	42.14
C18:3n6	3.28	0.45	2.01	0.23	2.84	0.65	4.06	0.67	3.64	0.37	4.65	0.46	4.15	0.67
C20:2n6	5.76	0.90	3.91	0.39	4.10	0.55	6.72	0.64	4.49	0.19	6.03	0.71	5.45	0.59
C20:3n6	24.93	2.47	14.22	1.58	18.68	2.15	20.80	0.82	16.01	1.22	19.98	1.59	16.19	1.26
<b>n6-PUFA</b>	249.99	20.36	270.32	28.60	372.88	41.31	461.84	10.20	386.61	17.85	506.67	34.44	455.77	40.25
C22:2n6	<1.0	<1.0	<1.0	<1.0	<1.0	<1.0	<1.0	<1.0	<1.0	<1.0	<1.0	<1.0	<1.0	<1.0
C22:4n6	8.99	1.30	13.31	1.17	24.52	2.03	31.36	0.77	26.85	1.29	38.09	1.67	35.07	2.30
C18:3n3	10.81	2.77	1.38	0.14	4.69	0.61	<1.0	<1.0	<1.0	<1.0	<1.0	<1.0	<1.0	<1.0
C20:3n3	<1.0	<1.0	<1.0	<1.0	<1.0	<1.0	<1.0	<1.0	<1.0	<1.0	<1.0	<1.0	<1.0	<1.0
C20:5n3	28.41	4.08	23.79	1.43	7.24	1.90	<1.0	<1.0	<1.0	<1.0	8.96	2.58	14.29	1.80
C22:5n3	33.30	2.45	15.59	1.58	8.10	0.93	8.02	1.59	4.02	0.14	4.33	0.33	2.41	0.82
C22:6n3	147.63	14.35	85.81	9.59	103.03	12.15	103.24	3.98	74.13	3.10	65.92	1.90	56.41	4.97
<b>SFA</b>	799.19	77.06	524.16	57.59	760.80	59.20	857.67	38.65	677.84	43.35	764.65	41.98	695.17	57.10
<b>MUFA</b>	453.38	95.84	245.36	28.58	386.14	43.47	388.99	17.70	289.63	17.56	337.19	30.39	315.60	20.68
<b>n6-PUFA</b>	701.01	82.39	562.36	57.29	734.24	74.98	1019.30	40.99	807.12	39.11	983.27	57.73	855.29	85.41
<b>n3-PUFA</b>	220.15	20.76	126.24	11.68	122.86	14.01	113.88	5.64	79.31	3.58	78.88	2.52	72.62	3.36
<b>AllFA</b>	2173.73	270.41	1458.11	152.10	2004.05	188.99	2379.85	98.35	1853.90	99.62	2163.99	128.95	1938.67	161.34
							1785.78	130.29	1558.16	94.22	1831.39	115.73	1828.08	123.94
							701.23	40.68	628.98	49.60	705.32	48.90	718.48	92.94
							272.36	31.54	226.27	10.09	275.24	17.34	272.02	18.83
							551.71	53.72	442.45	28.32	489.05	32.37	473.56	19.27
							260.48	15.15	260.46	16.73	361.79	21.56	364.01	16.88
							141.49	6.73	142.33	1.86	190.31	9.88	197.04	8.64

Table 9.3.3A: Blood Cells.

[µg/mL whole blood]	fat-1			Wild Type			STD			STD+n3				
	Day 0		Day 30		Day 0		Day 7		Day 14		Day 30		Day 45	
	Mean	SEM	Mean	SEM	Mean	SEM	Mean	SEM	Mean	SEM	Mean	SEM	Mean	SEM
C10-0	<0.25		<0.25		<0.25		<0.25		<0.25		<0.25		<0.25	
C11-0	<0.25		<0.25		<0.25		<0.25		<0.25		<0.25		<0.25	
C12-0	<0.25		<0.25		<0.25		<0.25		<0.25		<0.25		<0.25	
C13-0	<0.25		<0.25		<0.25		<0.25		<0.25		<0.25		<0.25	
C14-0	2.96	0.29	2.10	0.40	2.92	0.18	2.68	0.18	5.40	0.33	2.27	0.24	2.65	0.29
C15-0	2.06	0.19	1.14	0.29	1.93	0.16	1.87	0.07	3.78	0.18	1.19	0.13	1.35	0.24
C16-0	324.33	10.54	282.80	11.47	314.89	8.66	290.36	9.58	255.95	5.36	262.59	13.06	267.59	21.39
C17-0	3.60	0.14	2.89	0.14	3.81	0.20	3.28	0.08	2.71	0.12	2.88	0.10	2.88	0.22
C18-0	147.90	4.24	164.20	6.88	155.45	5.76	163.58	3.03	149.81	2.94	158.36	5.57	156.52	14.78
C20-0	3.78	0.18	3.59	0.26	2.96	0.10	4.05	0.21	3.27	0.18	3.70	0.25	3.24	0.22
C21-0	<0.25		<0.25		<0.25		<0.25		<0.25		<0.25		<0.25	
C22-0	13.08	0.37	11.32	0.52	11.68	0.37	12.28	0.15	11.08	0.19	11.84	0.39	11.20	0.92
C24-0	26.86	0.81	22.95	0.83	22.76	0.54	22.88	0.35	20.24	0.46	21.55	0.57	19.96	1.64
C14:1n6	<0.25		<0.25		<0.25		<0.25		<0.25		<0.25		<0.25	
C15:1n6	<0.25		<0.25		<0.25		<0.25		<0.25		<0.25		<0.25	
C16:1n7	6.69	0.39	3.74	0.24	6.60	0.33	4.32	0.23	5.05	0.22	4.09	0.31	4.85	0.60
C17:1n7	<0.25		<0.25		<0.25		<0.25		<0.25		<0.25		<0.25	
C18:1n7	23.87	1.44	17.73	1.00	27.23	0.51	20.68	0.50	18.52	0.63	17.77	0.52	20.02	2.22
C18:1n9	146.33	3.66	136.17	5.41	133.42	3.67	126.51	2.37	119.22	2.06	124.23	3.95	133.26	11.83
C20:1n9	3.11	0.15	2.83	0.15	3.66	0.12	3.18	0.08	2.97	0.15	2.86	0.10	2.80	0.33
C22:1n9	1.09	0.05	1.13	0.15	1.42	0.09	1.05	0.07	2.06	1.02	1.01	0.07	1.25	0.05
C24:1n9	14.34	0.51	12.87	0.66	16.54	0.47	13.11	0.33	11.79	0.47	12.47	0.30	12.47	1.86
C18:2n6	148.79	4.48	140.68	6.71	118.37	2.70	138.97	3.40	126.20	2.62	134.16	2.63	128.91	10.05
C18:3n6	1.14	0.19	1.13	0.28	0.96	0.24	1.45	0.06	3.45	0.11	1.36	0.07	1.47	0.20
C20:2n6	3.56	0.20	3.58	0.22	3.01	0.12	3.65	0.12	3.09	0.16	3.52	0.12	3.68	0.36
C20:3n6	15.76	0.40	13.92	0.73	14.34	0.57	13.58	0.18	11.85	0.25	12.83	0.37	12.58	1.20
n6-PUFA	165.87	4.02	206.47	8.02	253.84	6.43	245.32	2.46	231.55	4.27	242.87	7.90	246.55	22.53
C22:2n6	<0.25		<0.25		<0.25		<0.25		<0.25		<0.25		<0.25	
C22:4n6	9.98	0.65	17.18	0.67	28.32	0.63	28.43	0.48	27.96	0.52	32.46	1.04	32.80	3.19
C18:3n3	2.67	0.11	0.53	0.13	1.30	0.13	<0.25		<0.25		<0.25		<0.25	
C20:3n3	<0.25		<0.25		<0.25		<0.25		<0.25		<0.25		<0.25	
C20:5n3	24.14	1.01	10.65	0.76	2.66	0.22	1.33	0.09	0.58	0.05	<0.25		<0.25	
C22:5n3	30.17	0.90	18.15	1.27	7.96	0.31	6.99	0.24	5.56	0.37	2.53	1.07	1.41	0.15
C22:6n3	101.24	2.37	74.98	3.83	79.62	2.20	69.44	0.90	55.71	1.42	43.04	1.19	38.18	3.39
SFA	524.58	14.06	490.96	19.77	516.39	14.26	500.98	12.57	452.22	7.88	464.38	18.30	465.39	38.72
MUFA	195.44	5.74	174.47	7.35	188.86	4.27	168.86	2.71	159.61	3.62	162.43	4.89	174.65	16.68
n6-PUFA	345.08	7.76	382.96	15.80	418.84	8.75	431.40	5.89	404.10	6.61	427.20	11.06	426.00	37.01
n3-PUFA	158.22	3.51	104.20	5.79	91.54	2.46	77.76	0.97	61.85	1.60	45.77	1.17	39.59	3.53
AllFA	1223.32	28.75	1152.59	47.65	1215.63	28.35	1179.00	19.88	1077.78	17.09	1099.78	33.52	1105.63	95.63





**Table 9.3.3B:** Relative distribution of fatty acids in blood and tissues of wild type mice at the beginning of the experiment (Day 0) and during the course of the feeding experiment on a standard sunflower based diet (STD) or on the same diet enriched with n3-PUFA (1% EPA and 1% DHA as ethyl ester, STD+n3). Fatty acid pattern in transgenic *fat-1* mice are shown at baseline (Day 0) and after 30 days on a standard sunflower based diet. The relative amount of an analyte was not calculated if it was below the limit of quantification (<LOQ, S/N<9) in more than 50% of the samples within one group.

\* the analyte could not be quantified in the samples due to chromatographic interferences.

Table 9.3.3B: Whole Blood.

[% of total IFA]	fat-1				Wild Type				STD				STD+n3									
	Day 0		Day 30		Day 0		Day 14		Day 30		Day 14		Day 30		Day 14		Day 30					
	Mean	SEM	Mean	SEM	Mean	SEM	Mean	SEM	Mean	SEM	Mean	SEM	Mean	SEM	Mean	SEM	Mean	SEM				
C10:0																						
C11:0																						
C12:0																						
C13:0																						
C14:0																						
C15:0																						
<b>SFA</b>	23.76	0.45	19.75	0.56	23.55	0.45	21.49	0.34	20.79	0.47	19.88	0.27	19.96	0.80	23.86	0.50	23.71	0.76	23.43	0.37	22.86	0.76
C16:0	0.33	0.03	0.28	0.01	0.39	0.03	0.28	0.01	0.30	0.01	0.28	0.01	0.29	0.01	0.34	0.03	0.32	0.03	0.28	0.01	0.29	0.02
C17:0	11.39	0.57	13.62	0.34	12.59	0.38	12.53	0.17	13.70	0.35	13.44	0.20	13.67	0.24	13.15	0.35	14.06	0.69	12.61	0.24	13.43	1.50
C18:0	0.11	0.01	0.14	0.01	0.11	0.01	0.11	0.00	0.11	0.01	0.12	0.01	0.13	0.01	0.14	0.00	0.17	0.03	0.13	0.01	0.18	0.04
C20:0	0.54	0.03	0.69	0.02	0.49	0.04	0.56	0.05	0.57	0.02	0.66	0.03	0.67	0.04	0.70	0.04	0.79	0.07	0.66	0.06	0.58	0.03
C21:0	1.17	0.10	1.41	0.03	1.08	0.09	1.07	0.10	1.03	0.05	1.02	0.03	1.18	0.05	1.36	0.09	1.17	0.05	1.34	0.06	1.29	0.05
C22:0																						
C24:0																						
<b>MUFA</b>	1.38	0.14	0.51	0.03	1.43	0.12	1.02	0.06	0.90	0.07	0.83	0.11	0.64	0.08	0.98	0.06	0.96	0.07	0.74	0.08	0.52	0.11
C14:1n5																						
C15:1n5																						
C16:1n7																						
C17:1n7																						
C18:1n7	2.21	0.18	1.56	0.07	2.43	0.12	1.86	0.06	1.67	0.09	1.79	0.05	1.73	0.09	1.42	0.05	1.35	0.05	1.32	0.05	1.24	0.05
C18:1n9	15.56	1.10	12.81	0.31	14.11	0.40	12.64	0.20	11.83	0.23	11.68	0.42	12.42	0.45	11.41	0.70	11.37	0.28	11.58	0.32	11.62	0.72
C20:1n9	0.35	0.03	0.29	0.02	0.32	0.02	0.28	0.02	0.28	0.02	0.26	0.01	0.27	0.02	0.26	0.03	0.27	0.03	0.24	0.02	0.23	0.01
C22:1n9	0.17	0.04	0.14	0.01	0.14	0.01	0.20	0.03	0.35	0.11	0.13	0.03	0.13	0.03	0.18	0.02	0.30	0.07	0.25	0.14	0.29	0.14
C24:1n9	0.54	0.07	1.43	0.09	0.79	0.11	0.48	0.07	0.59	0.04	0.81	0.02	1.32	0.11	0.79	0.07	0.56	0.14	1.00	0.09	1.22	0.08
C18:2n6	18.66	0.55	17.78	0.15	15.52	0.19	20.67	0.83	19.95	0.47	18.84	0.44	17.29	0.80	17.21	1.52	16.38	0.60	17.73	0.30	18.06	0.63
C18:3n6	0.15	0.02	0.14	0.00	0.17	0.02	0.20	0.01	0.19	0.01	0.21	0.01	0.22	0.03	0.18	0.02	0.15	0.01	0.18	0.01	0.20	0.01
C20:2n6	0.26	0.02	0.27	0.02	0.20	0.02	0.28	0.03	0.24	0.01	0.28	0.02	0.28	0.02	0.18	0.02	0.28	0.02	0.28	0.02	0.20	0.01
C20:3n6	1.16	0.03	0.97	0.03	0.92	0.03	0.88	0.04	0.86	0.04	0.92	0.03	0.84	0.03	0.73	0.04	0.74	0.03	0.75	0.03	0.77	0.04
C20:4n6	11.75	0.53	18.56	0.42	18.48	0.54	19.53	0.70	20.92	0.40	23.45	0.82	23.49	0.34	11.62	0.65	10.49	0.71	7.61	0.27	6.92	0.32
C22:2n6																						
C22:4n6	0.41	0.03	0.93	0.04	1.23	0.04	1.33	0.05	1.45	0.02	1.77	0.03	1.82	0.07	0.95	0.04	0.74	0.07	0.38	0.02	0.23	0.02
C18:3n3	0.47	0.05	0.11	0.01	0.23	0.01																
C20:3n3	1.34	0.18	1.74	0.24	0.44	0.03																
C20:5n3	1.58	0.09	1.07	0.02	0.40	0.03	0.34	0.07	0.22	0.02	0.20	0.01	0.19	0.01	1.03	0.06	1.10	0.05	1.55	0.05	1.61	0.07
C22:5n3	6.88	0.19	5.90	0.25	5.09	0.27	4.37	0.22	4.02	0.11	3.07	0.10	2.91	0.08	8.03	0.39	9.14	0.35	10.45	0.28	10.90	0.41
C22:6n3																						
<b>n3-PUFA</b>	37.25	1.09	35.87	0.70	38.27	0.81	36.02	0.36	36.46	0.61	35.38	0.21	35.89	0.90	39.49	0.84	40.21	1.32	38.44	0.41	38.64	2.19
SFA	20.09	1.38	16.71	0.37	19.16	0.59	16.33	0.18	15.82	0.41	15.46	0.52	16.39	0.64	15.05	0.62	14.61	0.35	15.06	0.47	15.03	0.86
MUFA	32.39	0.71	38.64	0.39	36.50	0.56	42.85	0.29	43.63	0.50	45.46	0.47	43.93	0.84	30.69	0.90	28.47	0.98	26.67	0.16	26.20	0.85
n6-PUFA	10.27	0.31	8.78	0.39	6.07	0.26	4.80	0.23	4.30	0.13	3.69	0.19	3.79	0.17	14.77	0.81	16.71	0.27	19.82	0.57	20.14	0.79
n3-PUFA																						



Table 9.3.3B: Plasma.

[% of total FA]	fat-1			Wild Type			STD						STD+n3								
	Day 0		Day 30	Day 0		Day 7	Day 14		Day 30		Day 45		Day 7		Day 14		Day 30		Day 45		
	Mean	SEM	Mean	SEM	Mean	SEM	Mean	SEM	Mean	SEM	Mean	SEM	Mean	SEM	Mean	SEM	Mean	SEM	Mean	SEM	
	0.20	0.02			0.32	0.01															
	0.11	0.02			0.15	0.01															
	0.43	0.06	0.04	0.01	0.62	0.03															
	0.10	0.02			0.19	0.02															
	0.46	0.02	0.27	0.04	0.52	0.03															
	0.16	0.00	0.08	0.02	0.15	0.01															
	19.97	0.24	16.80	0.39	18.93	0.14															
	0.30	0.01	0.17	0.01	0.30	0.02															
	9.88	0.55	12.28	0.51	11.06	0.43															
			0.08	0.01																	
	0.32	0.05	0.28	0.03	0.29	0.07															
	0.09	0.02	0.26	0.01	0.09	0.01															
	0.07	0.02			0.07	0.01															
	1.96	0.15	1.05	0.08	1.93	0.20															
	2.04	0.24	1.25	0.16	2.18	0.22															
	18.52	1.43	12.74	1.01	16.00	1.03															
	0.35	0.03	0.19	0.02	0.30	0.03															
	0.29	0.14	0.41	0.15	0.19	0.08															
	0.63	0.06	0.50	0.02	0.68	0.06															
	25.79	0.41	25.09	0.34	22.39	0.48															
	0.32	0.02	0.41	0.03	0.34	0.03															
	0.23	0.02	0.14	0.02	0.19	0.02															
	1.17	0.03	0.94	0.03	1.05	0.06															
	8.53	0.72	20.04	0.43	15.97	0.71															
	0.07	0.02	0.15	0.02	0.15	0.02															
	0.86	0.07	0.14	0.02	0.45	0.04															
	1.24	0.08	0.59	0.10	0.45	0.02															
	0.53	0.01	0.14	0.03	0.23	0.03															
	5.47	0.19	6.08	0.52	5.12	0.27															
	31.98	0.73	30.24	0.48	32.42	0.67															
	23.84	1.75	16.05	1.23	21.35	1.40															
	36.08	0.95	46.76	0.57	40.09	0.86															
	8.11	0.20	6.95	0.63	6.14	0.30															





Table 9.3.3B: Spleen.

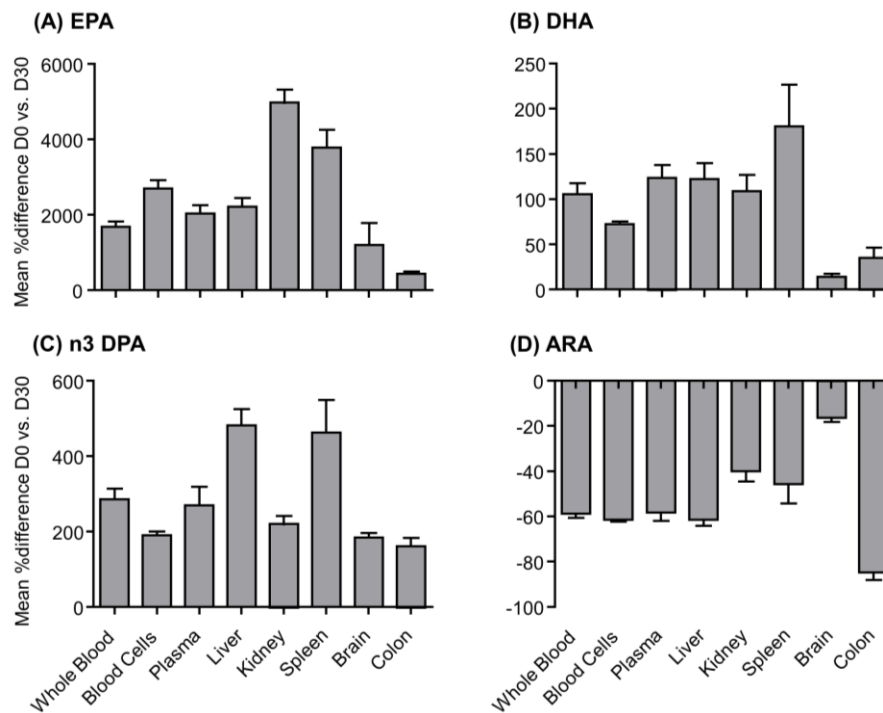
[% of total FA]	fat-1			Wild Type			STD			STD+n3							
	Day 0		Day 30	Day 0		Day 14	Day 30	Day 45	Day 7		Day 14	Day 30	Day 45				
	Mean	SEM	Mean	SEM	Mean	SEM	Mean	SEM	Mean	SEM	Mean	SEM	Mean	SEM			
<b>SFA</b>	C10:0	0.07	0.01	0.07	0.00	0.07	0.00	0.10	0.01	0.06	0.00	0.06	0.01	0.07	0.01	0.06	0.00
	C11:0	0.05	0.01	0.04	0.01	0.05	0.00	0.07	0.01	0.04	0.00	0.04	0.01	0.04	0.01	0.04	0.00
	C13:0	0.69	0.09	0.65	0.08	0.67	0.07	0.57	0.02	0.59	0.06	0.58	0.04	0.66	0.04	0.63	0.03
	C14:0	0.18	0.01	0.14	0.01	0.15	0.01	0.13	0.00	0.15	0.00	0.18	0.00	0.14	0.00	0.17	0.01
	C15:0	24.95	0.18	23.11	0.33	22.84	0.20	23.05	0.07	23.44	0.31	23.79	0.18	24.61	0.18	24.61	0.17
	C17:0	0.24	0.01	0.17	0.01	0.21	0.01	0.21	0.01	0.19	0.01	0.23	0.00	0.18	0.00	0.19	0.00
	C18:0	14.79	0.74	15.36	0.90	15.18	0.84	16.77	0.28	16.34	0.45	16.37	0.34	15.56	0.27	16.03	0.36
	C20:0	0.25	0.01	0.25	0.02	0.29	0.01	0.29	0.01	0.29	0.01	0.29	0.01	0.24	0.01	0.26	0.01
	C21:0	0.04	0.01	0.03	0.01	0.06	0.01	0.06	0.01	0.04	0.00	0.06	0.00	0.04	0.01	0.04	0.00
	C22:0	0.53	0.04	0.67	0.05	0.75	0.05	0.80	0.02	0.83	0.03	0.73	0.02	0.67	0.02	0.71	0.03
C24:0	0.67	0.06	0.71	0.07	0.73	0.06	0.79	0.02	0.78	0.04	0.85	0.02	0.78	0.03	0.84	0.04	
<b>MUFA</b>	C14:1n5	0.05	0.00	0.02	0.00	0.02	0.00	0.02	0.00	0.02	0.00	0.02	0.00	0.02	0.00	0.02	0.00
	C15:1n5	1.79	0.32	1.31	0.24	1.65	0.34	0.96	0.09	1.35	0.29	1.05	0.16	1.37	0.14	1.22	0.14
	C16:1n7	2.72	0.10	2.05	0.09	2.16	0.05	2.08	0.05	2.13	0.03	1.87	0.04	1.81	0.03	1.80	0.04
	C18:1n7	13.32	2.63	13.15	2.50	12.76	2.02	9.07	0.59	10.37	1.30	8.44	0.79	9.96	0.71	8.28	0.63
	C18:1n9	0.39	0.02	0.39	0.01	0.40	0.01	0.38	0.01	0.38	0.00	0.30	0.00	0.28	0.01	0.27	0.00
	C22:1n9	0.09	0.01	0.12	0.02	0.09	0.01	0.14	0.01	0.10	0.01	0.09	0.00	0.09	0.01	0.10	0.01
	C24:1n9	1.46	0.16	1.25	0.15	1.27	0.12	1.46	0.06	1.38	0.06	1.53	0.06	1.33	0.06	1.44	0.05
	C18:2n6	12.00	0.44	13.50	1.54	12.96	0.99	11.53	0.42	11.82	0.59	12.36	0.34	12.71	0.42	12.91	0.29
	C18:3n6	0.07	0.02	0.06	0.01	0.06	0.01	0.07	0.00	0.06	0.00	0.03	0.00	0.04	0.00	0.03	0.00
	C20:2n6	0.86	0.09	1.01	0.07	1.11	0.08	1.20	0.03	1.14	0.05	0.92	0.03	0.77	0.02	0.88	0.03
<b>n6-PUFA</b>	C20:3n6	1.14	0.12	0.98	0.08	0.93	0.08	1.03	0.01	1.02	0.05	1.05	0.04	1.15	0.04	1.25	0.02
	C20:4n6	10.18	0.94	13.52	1.31	17.32	1.49	20.70	0.45	20.38	0.83	10.53	0.48	8.29	0.40	7.69	0.19
	C22:2n6	0.05	0.01	0.06	0.01	0.07	0.01	0.08	0.00	0.07	0.00	0.06	0.00	0.05	0.00	0.05	0.00
	C22:4n6	1.09	0.10	2.08	0.18	3.58	0.30	4.39	0.10	4.88	0.17	0.80	0.04	0.44	0.02	0.38	0.01
<b>n3-PUFA</b>	C18:3n3	0.35	0.07	0.11	0.03	0.09	0.02	0.02	0.00	0.02	0.00	0.05	0.01	0.03	0.00	0.02	0.00
	C20:3n3	0.11	0.02	0.04	0.01	0.04	0.01	0.04	0.00	0.04	0.01	3.58	0.07	3.98	0.12	4.29	0.14
	C20:5n3	2.04	0.26	1.58	0.22	0.51	0.05	0.35	0.02	0.28	0.01	4.36	0.09	4.38	0.10	4.63	0.13
	C22:5n3	3.86	0.52	2.69	0.31	3.94	0.40	3.71	0.14	2.63	0.10	9.80	0.26	10.31	0.21	11.17	0.22
<b>Sums</b>	C22:6n3	6.04	0.62	4.89	0.61	4.62	0.43	4.12	0.15	2.97	0.10	17.79	0.37	18.72	0.37	20.11	0.47
	SFA	35.37	7.09	41.22	1.30	41.00	0.78	42.83	0.30	42.76	0.53	43.19	0.22	42.99	0.32	43.59	0.30
	MUFA	16.48	3.96	18.28	2.54	18.34	2.19	14.07	0.62	15.72	1.51	13.28	0.88	14.84	0.72	13.11	0.73
	n6-PUFA	21.15	4.28	31.22	0.25	36.04	1.02	38.99	0.25	38.55	1.08	25.75	0.35	23.45	0.42	23.19	0.17
n3-PUFA	10.33	2.33	9.29	1.15	4.62	0.43	4.12	0.15	2.97	0.10	17.79	0.37	18.72	0.37	20.11	0.47	



Table 9.3.3B: Brain.

[% of total FA]	fat-1			Wild Type			STD			STD+n3			Day45				
	Day0		Day30	Day7		Day14	Day30		Day45	Day7		Day14	Day30		Day45		
	Mean	SEM	Mean	SEM	Mean	SEM	Mean	SEM	Mean	SEM	Mean	SEM	Mean	SEM	Mean	SEM	
C10:0																	
C11:0																	
C12:0	0.01	0.00			0.01	0.00			0.01	0.00							
C13:0					0.01	0.00			0.01	0.00							
C14:0	0.13	0.01	0.06	0.01	0.13	0.01	0.04	0.01	0.12	0.03	0.04	0.01	0.06	0.01	0.15	0.01	0.01
C15:0	0.04	0.00			0.03	0.01			0.03	0.02							
C16:0	22.38	0.28	20.89	1.17	21.42	0.38	22.44	0.37	22.92	0.27	24.06	0.59	21.49	0.53	22.42	0.37	22.30
C17:0	0.14	0.01	0.14	0.01	0.16	0.01	0.13	0.00	0.14	0.00	0.14	0.00	0.14	0.00	0.13	0.00	0.14
C18:0	22.39	0.17	21.60	0.45	22.41	0.03	22.56	0.14	22.29	0.12	22.81	0.07	22.40	0.27	22.56	0.07	22.13
C20:0	0.24	0.05	0.44	0.09	0.24	0.04	0.32	0.02	0.34	0.03	0.32	0.03	0.34	0.04	0.35	0.03	0.34
C21:0	0.03	0.00	0.03	0.01	0.03	0.00	0.03	0.00	0.02	0.00	0.03	0.00	0.03	0.00	0.03	0.00	0.02
C22:0	0.37	0.03	0.56	0.13	0.38	0.02	0.55	0.04	0.40	0.04	0.39	0.04	0.49	0.07	0.38	0.03	0.40
C24:0	0.62	0.05	1.07	0.30	0.65	0.05	1.00	0.07	0.70	0.08	0.68	0.08	0.87	0.13	0.65	0.08	0.67
C14:1n5																	
C15:1n5																	
C16:1n7	0.55	0.01	0.47	0.02	0.52	0.01	0.49	0.01	0.49	0.02	0.47	0.01	0.50	0.01	0.52	0.01	0.56
C17:1n7																	
C18:1n7	3.58	0.05	3.83	0.25	3.60	0.06	3.77	0.06	3.47	0.07	3.60	0.04	3.61	0.09	3.34	0.10	3.41
C18:1n9	14.31	0.24	15.98	1.28	14.77	0.30	15.31	0.34	14.46	0.37	14.18	0.32	15.31	0.49	14.64	0.35	14.90
C20:1n9	1.01	0.07	1.97	0.58	1.09	0.09	1.34	0.14	1.08	0.12	0.96	0.09	1.28	0.20	1.03	0.12	1.03
C22:1n9	0.07	0.02			0.10	0.02	0.13	0.01					0.11	0.02			
C24:1n9	1.35	0.12	2.36	0.66	1.50	0.13	1.92	0.14	1.44	0.18	1.28	0.18	1.76	0.26	1.36	0.18	1.31
C18:2n6	0.73	0.02	0.86	0.03	0.52	0.02	0.70	0.02	0.72	0.03	0.81	0.02	0.64	0.02	0.68	0.01	0.77
C18:3n6																	
C20:2n6	0.13	0.00	0.22	0.03	0.10	0.00	0.16	0.01	0.14	0.01	0.17	0.01	0.12	0.01	0.11	0.00	0.13
C20:3n6	0.56	0.02	0.47	0.02	0.35	0.01	0.38	0.01	0.38	0.01	0.35	0.01	0.41	0.01	0.48	0.01	0.58
C20:4n6	10.50	0.30	9.81	0.82	11.26	0.16	10.45	0.16	11.65	0.39	11.29	0.21	10.32	0.33	10.63	0.23	9.46
C22:2n6																	
C22:4n6	2.48	0.12	2.62	0.21	3.13	0.12	2.74	0.16	2.95	0.13	2.84	0.09	2.82	0.14	2.74	0.13	2.24
C18:3n3																	
C20:3n3																	
C20:5n3	0.08	0.01	0.07	0.00	0.01	0.01							0.15	0.02	0.14	0.01	0.18
C22:5n3	0.29	0.01	0.22	0.01	0.15	0.00	0.14	0.01	0.13	0.00	0.12	0.01	0.26	0.00	0.33	0.00	0.42
C22:6n3	18.04	0.41	16.26	0.87	16.61	0.41	16.66	0.41	16.47	0.54	17.11	0.27	16.72	0.41	17.41	0.32	18.97
SFA	46.32	0.69	44.79	1.06	46.30	0.56	45.83	0.74	46.64	0.29	46.80	0.22	45.97	0.43	46.58	0.31	46.03
MUFA	20.88	1.04	24.67	2.78	21.58	1.36	22.96	1.66	20.92	0.72	20.51	0.61	22.58	1.03	20.90	0.73	21.22
n6-PUFA	14.39	0.82	14.00	0.88	15.35	0.47	14.42	0.59	15.84	0.45	15.45	0.26	14.31	0.40	14.65	0.34	13.18
n3-PUFA	18.42	0.92	16.54	0.87	16.77	0.99	16.80	0.99	16.60	0.54	17.23	0.26	17.14	0.41	17.87	0.31	19.57
Sums																	





**Fig. 9.3.2:** Mean% difference of relative levels of EPA (A), DHA (B), n3 DPA (C) and ARA (D) in WT animals after 30 days on a sunflower diet enriched with EPA and DHA in comparison to baseline (WT mice, D0). Shown is the mean %difference in all investigated tissues and blood fractions. It was calculated using the formula  $[\%difference = (conc_{D30} - conc_{D0})/conc_{D0} * 100]$ .

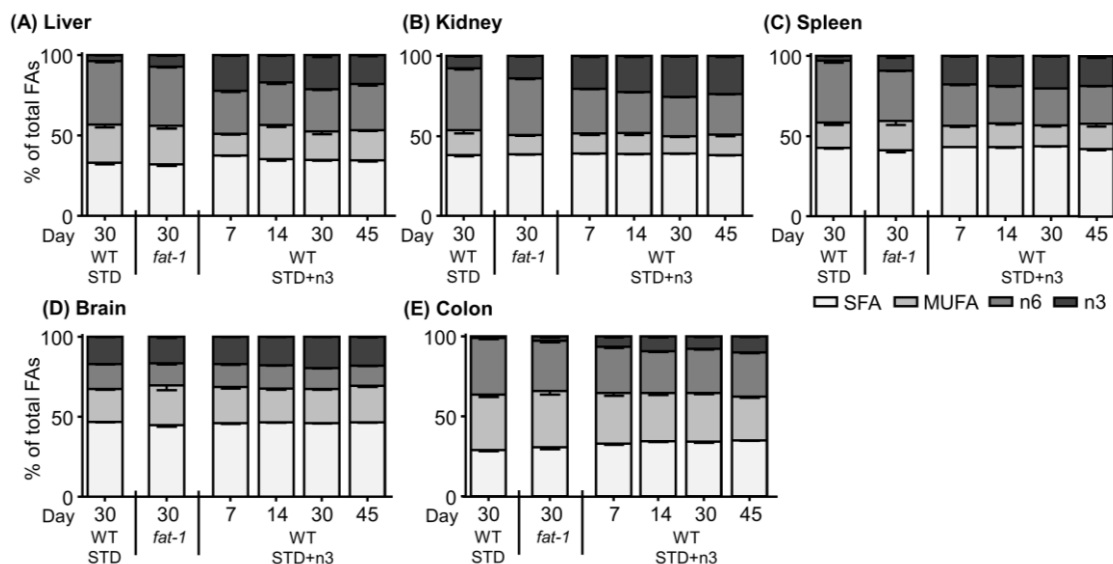


**Fig. 9.3.3:** Relative distribution of n3-polyunsaturated fatty acids (PUFA), n6-PUFA, monounsaturated fatty acids (MUFA) and saturated fatty acids (SFA) in transgenic *fat-1* mice and wild type animals (WT-STD) after 30 days on a sunflower based diet, as well as in wild type mice on the same diet enriched with EPA and DHA (WT-STD+n3) during the course of the feeding period (45 days) in tissues. (A): liver, (B): kidney, (C): spleen, (D): brain and (E): colon.

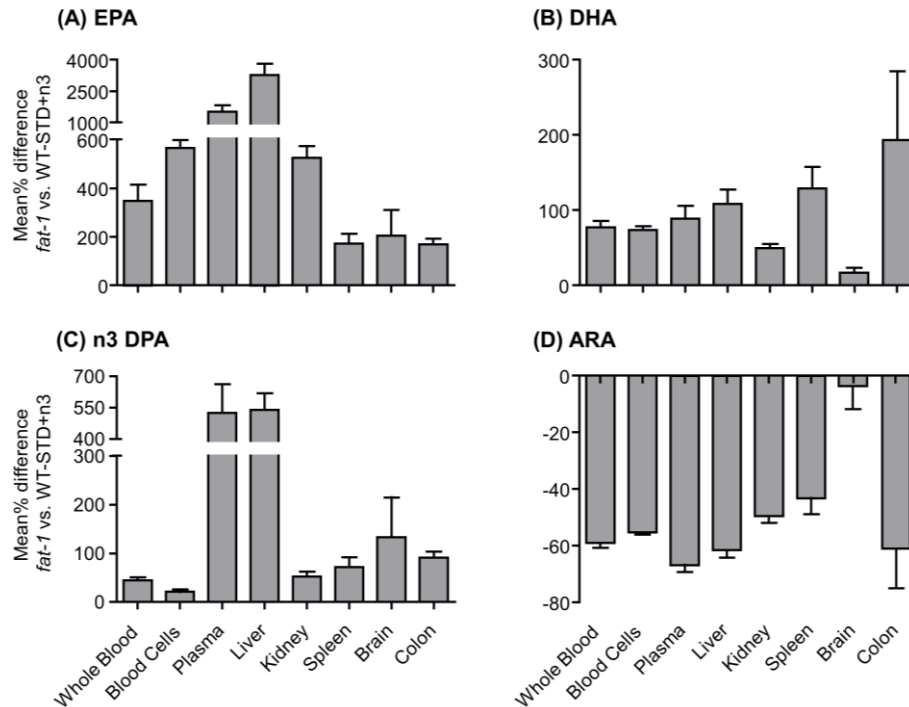


**Fig. 9.3.4:** Mean% difference of relative levels of EPA (A), DHA (B), n3 DPA (C) and ARA (D) in WT animals after 30 days on a sunflower diet enriched with EPA and DHA in comparison to *fat-1* mice after 30 days on standard sunflower diet. Shown is the mean %difference in all investigated tissues and blood fractions. It was calculated using the formula [%difference =  $(\text{conc}_{D30} - \text{conc}_{Fat-1}) / \text{conc}_{Fat-1} * 100$ ].

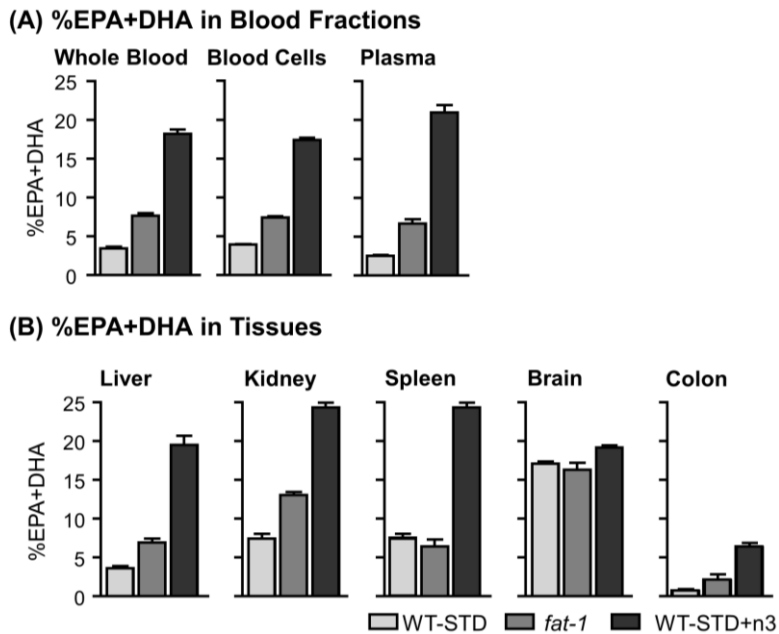


**Fig. 9.3.5:** %EPA+DHA in blood fractions (A) and in tissues (B) in transgenic *fat-1* mice and wild type animals (WT-STD) on a sunflower based diet, as well as in wild type mice on the same diet enriched with EPA and DHA (WT-STD+n3) after 30 days of supplementation.

**Table 9.3.4:** n6/n3 ratio and %EPA+DHA in blood and tissues of wild type mice at the beginning of the experiment (Day 0) and during the course of the feeding experiment on a standard sunflower based diet (STD) or on the same diet enriched with n3-PUFA (1% EPA and 1% DHA as ethyl ester, STD+n3). Ratios in transgenic *fat-1* mice are shown at baseline (Day 0) and after 30 days on a standard sunflower based diet. The n6/n3 ratio was calculated as  $\Sigma\%(18:2\ n6, 18:3\ n6, 20:3\ n6, 20:4\ n6, C22:4n6) / \Sigma\%(18:3\ n3, 20:5\ n3, 22:5\ n3, 22:6\ n3)$ .

		n6/n3 ratio								%EPA+DHA [%]							
		Whole Blood	Blood Cells	Plasma	Liver	Kidney	Spleen	Colon	Brain	Whole Blood	Blood Cells	Plasma	Liver	Kidney	Spleen	Colon	Brain
<b><i>fat-1</i></b>																	
Day 0	Mean	3.14	2.16	4.42	3.37	2.35	2.07	4.48	0.78	8.22	10.26	6.71	8.37	11.49	8.08	4.26	18.12
	SEM	0.12	0.03	0.06	0.09	0.11	0.19	0.54	0.03	0.27	0.13	0.26	0.25	0.73	0.86	0.88	0.41
Day 30	Mean	4.41	3.66	6.91	5.12	2.52	3.58	16.40	0.83	7.64	7.42	6.67	6.93	13.06	6.46	2.17	16.32
	SEM	0.19	0.11	0.73	0.34	0.11	0.54	5.33	0.02	0.37	0.19	0.60	0.52	0.41	0.83	0.65	0.87
<b>Wild Type</b>																	
Day 0	Mean	6.02	4.55	6.57	4.53	3.40	5.66	6.70	0.91	5.44	6.77	5.49	6.58	8.74	4.10	3.66	16.62
	SEM	0.22	0.04	0.32	0.13	0.18	0.36	0.20	0.03	0.23	0.07	0.30	0.38	0.71	0.67	0.16	0.41
<b>STD</b>																	
Day 7	Mean	8.97	5.50	14.13	6.86	3.73	7.78	19.78	0.85	4.42	6.01	3.40	5.65	9.66	4.03	1.42	16.66
	SEM	0.45	0.09	1.06	0.24	0.13	0.50	3.32	0.03	0.20	0.12	0.28	0.28	0.39	0.40	0.31	0.41
Day 14	Mean	10.13	6.49	16.44	9.83	4.09	9.20	28.38	0.95	4.08	5.22	3.06	3.91	8.92	3.75	1.06	16.47
	SEM	0.27	0.07	0.40	0.40	0.17	0.28	3.80	0.05	0.12	0.07	0.08	0.16	0.40	0.14	0.15	0.54
Day 30	Mean	12.42	9.28	20.32	10.54	5.09	12.60	41.63	0.89	3.49	3.93	2.53	3.66	7.45	2.67	0.78	17.11
	SEM	0.72	0.31	0.80	0.61	0.39	0.14	6.70	0.02	0.19	0.08	0.13	0.24	0.62	0.10	0.14	0.27
Day 45	Mean	11.62	10.69	21.15	15.66	4.90	14.63	34.61	0.99	3.69	3.45	2.42	2.33	7.65	2.36	0.94	15.63
	SEM	0.70	0.20	1.05	0.80	0.35	0.99	7.53	0.02	0.20	0.08	0.11	0.23	0.57	0.21	0.17	0.56
<b>STD+n3</b>																	
Day 7	Mean	2.12	2.15	1.38	1.20	1.34	1.39	4.50	0.83	13.75	12.16	22.08	20.76	19.52	13.38	5.38	16.87
	SEM	0.20	0.03	0.08	0.06	0.05	0.01	0.46	0.03	0.75	0.17	0.72	0.60	0.76	0.30	0.67	0.41
Day 14	Mean	1.70	1.58	1.61	1.57	1.12	1.21	2.91	0.81	15.61	14.50	20.16	15.49	21.49	14.30	7.77	17.54
	SEM	0.05	0.04	0.05	0.08	0.04	0.03	0.29	0.02	0.25	0.27	0.42	0.58	0.76	0.28	0.77	0.31
Day 30	Mean	1.34	1.16	1.54	1.25	0.95	1.11	3.64	0.67	18.23	17.40	21.02	19.50	24.28	15.46	6.44	19.15
	SEM	0.04	0.02	0.08	0.09	0.03	0.03	0.28	0.02	0.53	0.27	0.94	1.18	0.62	0.34	0.47	0.32
Day 45	Mean	1.29	1.08	1.65	1.60	1.04	1.25	2.72	0.69	18.45	17.86	19.99	16.69	22.76	14.34	8.68	17.60
	SEM	0.02	0.01	0.08	0.12	0.05	0.09	0.15	0.03	0.73	0.10	0.69	0.87	0.87	0.78	0.56	0.49

**Table 9.3.5:** Absolute concentrations of oxylipins in plasma, colon and brain of wild type mice at the beginning of experiment (Day 0) and during the course of the feeding experiment on a standard sunflower based diet (STD) or on the same diet enriched with n3-PUFA (1% EPA and 1% DHA as ethyl ester, STD+n3). Absolute concentrations in transgenic *fat-1* mice are shown at baseline (Day 0) and after 30 days on a standard sunflower based diet.

In case an analyte was below limit of quantification (<LOQ) in more than 50% of samples within one group, the LOQ is shown.

Table 9.3.5: Plasma.

ARA	[nM]	fat -1		Wild Type		STD		STD+n3		Day 45														
		Day 0 mean SEM	Day 30 mean SEM	Day 0 mean SEM	Day 30 mean SEM	Day 7 mean SEM	Day 14 mean SEM	Day 30 mean SEM	Day 45 mean SEM	Day 7 mean SEM	Day 14 mean SEM	Day 30 mean SEM	Day 45 mean SEM											
Prostanoids	6-keto-PGF1a	0.39	0.08	0.67	0.10	0.53	0.06	0.47	0.11	1.36	0.62	1.18	0.31	1.42	0.27	1.36	0.04	0.57	0.10	0.44	0.03	0.59	0.13	
	PGF2a	<0.18	<0.18	<0.18	<0.18	<0.18	<0.18	<0.18	<0.18	<0.18	<0.18	<0.18	<0.18	<0.18	<0.18	<0.18	<0.18	<0.18	<0.18	<0.18	<0.18	<0.18	<0.18	<0.18
	PGE2	0.05	0.01	0.11	0.01	0.05	0.01	0.08	0.01	0.10	0.03	0.18	0.03	0.12	0.02	0.06	0.02	0.04	0.00	0.06	0.01	0.05	0.01	0.05
	PGD2	<0.25	<0.25	<0.25	<0.25	<0.25	<0.25	<0.25	<0.25	<0.25	<0.25	<0.25	<0.25	<0.25	<0.25	<0.25	<0.25	<0.25	<0.25	<0.25	<0.25	<0.25	<0.25	<0.25
	PGI2	<0.4	<0.4	<0.4	<0.4	<0.4	<0.4	<0.4	<0.4	<0.4	<0.4	<0.4	<0.4	<0.4	<0.4	<0.4	<0.4	<0.4	<0.4	<0.4	<0.4	<0.4	<0.4	<0.4
	PGB2	<0.1	<0.1	<0.1	<0.1	<0.1	<0.1	<0.1	<0.1	<0.1	<0.1	<0.1	<0.1	<0.1	<0.1	<0.1	<0.1	<0.1	<0.1	<0.1	<0.1	<0.1	<0.1	<0.1
	15-deoxy-PGJ2	<0.25	<0.25	<0.25	<0.25	<0.25	<0.25	<0.25	<0.25	<0.25	<0.25	<0.25	<0.25	<0.25	<0.25	<0.25	<0.25	<0.25	<0.25	<0.25	<0.25	<0.25	<0.25	<0.25
	11b-PGF2a	<0.03	<0.03	<0.03	<0.03	<0.03	<0.03	<0.03	<0.03	<0.03	<0.03	<0.03	<0.03	<0.03	<0.03	<0.03	<0.03	<0.03	<0.03	<0.03	<0.03	<0.03	<0.03	<0.03
	bic PGE2	<0.25	<0.25	<0.25	<0.25	<0.25	<0.25	<0.25	<0.25	<0.25	<0.25	<0.25	<0.25	<0.25	<0.25	<0.25	<0.25	<0.25	<0.25	<0.25	<0.25	<0.25	<0.25	<0.25
	13,14dih-15k-PGF2a	0.25	0.05	0.26	0.07	0.33	0.04	0.67	0.35	0.49	0.22	0.52	0.14	0.34	0.03	0.18	0.02	0.19	0.03	0.14	0.04	0.14	0.14	0.04
Epoxy-FA	TxB2	<0.16	<0.16	<0.16	<0.16	<0.16	<0.16	<0.16	<0.16	<0.16	<0.16	<0.16	<0.16	<0.16	<0.16	<0.16	<0.16	<0.16	<0.16	<0.16	<0.16	<0.16	<0.16	<0.16
	5(6)-EpETE	3.31	0.23	4.92	0.44	6.95	0.63	5.46	0.47	5.10	0.51	6.34	0.88	6.17	0.95	1.93	0.17	1.82	0.24	2.18	0.33	1.63	0.16	
	8(9)-EpETE alt	0.80	0.05	1.24	0.16	1.35	0.08	1.36	0.22	1.48	0.15	1.32	0.19	1.57	0.28	0.62	0.07	0.59	0.04	0.61	0.07	<0.5	<0.5	
	11(12)-EpETE	1.00	0.08	1.58	0.16	2.04	0.10	2.42	0.11	2.19	0.10	1.91	0.14	2.60	0.29	0.81	0.06	0.74	0.07	0.54	0.05	0.57	0.07	
	14(15)-EpETE	0.92	0.06	1.35	0.14	1.68	0.06	2.10	0.06	1.90	0.12	1.58	0.13	2.26	0.19	0.70	0.05	0.64	0.04	0.52	0.03	0.51	0.06	
Dihydroxy-FA	5,6-DHETE	0.61	0.03	0.65	0.07	0.98	0.05	0.89	0.07	0.62	0.05	0.97	0.14	0.85	0.09	0.39	0.04	0.32	0.02	0.33	0.05	0.27	0.02	
	8,9-DHETE	1.59	0.10	1.31	0.14	2.06	0.13	1.37	0.08	1.07	0.07	1.59	0.23	1.42	0.16	0.59	0.05	0.50	0.09	0.52	0.06	0.46	0.07	
Hydroxy-FA	11,12-DHETE	1.73	0.40	1.07	0.12	2.15	0.38	0.94	0.11	1.09	0.15	1.17	0.26	1.12	0.25	0.43	0.08	0.61	0.15	0.43	0.09	0.54	0.15	
	14,15-DHETE	3.89	0.95	2.55	0.36	4.43	0.76	2.48	0.31	2.69	0.38	2.64	0.60	2.93	0.70	1.19	0.20	1.94	0.49	1.19	0.27	1.59	0.40	
	5-HETE	1.70	0.13	1.79	0.12	2.75	0.20	2.34	0.26	2.39	0.37	2.70	0.56	2.12	0.20	1.20	0.14	0.92	0.08	1.05	0.15	0.74	0.08	
	8-HETE	1.39	0.16	1.83	0.16	1.91	0.20	1.16	0.11	1.77	0.31	1.56	0.15	2.22	0.36	1.50	0.41	0.87	0.10	0.94	0.10	1.00	0.21	
	9-HETE	<0.63	<0.63	<0.63	<0.63	<0.63	<0.63	<0.63	<0.63	<0.63	<0.63	<0.63	<0.63	<0.63	<0.63	<0.63	<0.63	<0.63	<0.63	<0.63	<0.63	<0.63	<0.63	<0.63
	12-HETE	0.60	0.04	0.66	0.02	0.85	0.06	0.73	0.07	1.12	0.19	1.03	0.14	1.03	0.14	0.54	0.06	0.53	0.01	0.48	0.03	0.42	0.03	
Multiple Hydroxylated FA	6-trans-LTB4	13	2.91	20	2.71	16	2.79	26	8.01	38	13	41	12	59	12	127	54	39	6.77	39	9.46	39	13	
	20-OH-LTB4	0.87	0.04	1.13	0.03	1.24	0.07	1.10	0.07	1.72	0.25	1.51	0.17	1.90	0.25	1.08	0.14	0.91	0.04	0.82	0.09	0.80	0.05	
	LXA4	<0.44	<0.44	<0.44	<0.44	<0.44	<0.44	<0.44	<0.44	<0.44	<0.44	<0.44	<0.44	<0.44	<0.44	<0.44	<0.44	<0.44	<0.44	<0.44	<0.44	<0.44	<0.44	
	5,15-DHETE	<0.63	<0.63	<0.63	<0.63	<0.63	<0.63	<0.63	<0.63	<0.63	<0.63	<0.63	<0.63	<0.63	<0.63	<0.63	<0.63	<0.63	<0.63	<0.63	<0.63	<0.63	<0.63	
	8,15-DHETE	<0.2	<0.2	<0.2	<0.2	<0.2	<0.2	<0.2	<0.2	<0.2	<0.2	<0.2	<0.2	<0.2	<0.2	<0.2	<0.2	<0.2	<0.2	<0.2	<0.2	<0.2	<0.2	
Isoprostanes	5-IPF2a	<0.25	<0.25	<0.25	<0.25	<0.25	<0.25	0.31	0.03	0.29	0.04	0.33	0.06	<0.25	<0.25	<0.25	<0.25	<0.25	<0.25	<0.25	<0.25	<0.25	<0.25	
	8-HPGF2a	<0.025	<0.025	<0.025	<0.025	<0.025	<0.025	<0.025	<0.025	<0.025	<0.025	<0.025	<0.025	<0.025	<0.025	<0.025	<0.025	<0.025	<0.025	<0.025	<0.025	<0.025	<0.025	
Others	5-oxo-ETE	<0.5	<0.5	<0.5	<0.5	<0.5	<0.5	<0.5	<0.5	<0.5	<0.5	<0.5	<0.5	<0.5	<0.5	<0.5	<0.5	<0.5	<0.5	<0.5	<0.5	<0.5	<0.5	
	15-oxo-ETE	<0.125	<0.125	0.23	0.03	0.17	0.01	0.29	0.02	0.31	0.05	0.28	0.03	0.39	0.04	0.14	0.01	0.15	0.01	<0.125	<0.125	<0.125	<0.125	
	11,12-,15-TriHETE	<0.25	<0.25	<0.25	<0.25	<0.25	<0.25	<0.25	<0.25	<0.25	<0.25	<0.25	<0.25	<0.25	<0.25	<0.25	<0.25	<0.25	<0.25	<0.25	<0.25	<0.25	<0.25	
	THF diol	<0.63	<0.63	<0.63	<0.63	<0.63	<0.63	<0.63	<0.63	<0.63	<0.63	<0.63	<0.63	<0.63	<0.63	<0.63	<0.63	<0.63	<0.63	<0.63	<0.63	<0.63	<0.63	
Prostanoids	PGE3	<0.075	<0.075	<0.075	<0.075	<0.075	<0.075	<0.075	<0.075	<0.075	<0.075	<0.075	<0.075	<0.075	<0.075	<0.075	<0.075	<0.075	<0.075	<0.075	<0.075	<0.075	<0.075	
	PGD3	<0.25	<0.25	<0.25	<0.25	<0.25	<0.25	<0.25	<0.25	<0.25	<0.25	<0.25	<0.25	<0.25	<0.25	<0.25	<0.25	<0.25	<0.25	<0.25	<0.25	<0.25	<0.25	
	d17-8k-PGF1a	<0.25	<0.25	<0.25	<0.25	<0.25	<0.25	<0.25	<0.25	<0.25	<0.25	<0.25	<0.25	<0.25	<0.25	<0.25	<0.25	<0.25	<0.25	<0.25	<0.25	<0.25	<0.25	
Epoxy-FA	TxB3	<0.125	<0.125	<0.125	<0.125	<0.125	<0.125	<0.125	<0.125	<0.125	<0.125	<0.125	<0.125	<0.125	<0.125	<0.125	<0.125	<0.125	<0.125	<0.125	<0.125	<0.125	<0.125	
	8(9)-EpETE	<0.25	<0.25	<0.25	<0.25	<0.25	<0.25	<0.25	<0.25	<0.25	<0.25	<0.25	<0.25	<0.25	<0.25	<0.25	<0.25	<0.25	<0.25	<0.25	<0.25	<0.25	<0.25	
	11(12)-EpETE	0.17	0.02	<0.125	0.01	<0.125	<0.125	<0.125	<0.125	<0.125	<0.125	<0.125	<0.125	<0.125	<0.125	0.97	0.15	0.95	0.13	1.07	0.10	0.94	0.14	
	14(15)-EpETE	0.20	0.02	0.09	0.01	0.08	0.01	<0.063	<0.063	<0.063	<0.063	<0.063	<0.063	<0.063	<0.063	1.20	0.17	1.25	0.10	1.06	0.18	1.16	0.12	
	17(18)-EpETE	1.90	0.07	0.99	0.14	0.44	0.04	<0.125	<0.125	<0.125	<0.125	<0.125	<0.125	<0.125	<0.125	5.48	0.89	5.60	0.59	5.12	0.93	5.06	0.74	

Table 9.3.5: Plasma Continued.

EPA	[nM]	fat-1			Wild Type			STD			STD+n3				
		Day 0 mean SEM	Day 30 mean SEM	Day 0 mean SEM	Day 7 mean SEM	Day 14 mean SEM	Day 30 mean SEM	Day 45 mean SEM	Day 7 mean SEM	Day 14 mean SEM	Day 30 mean SEM	Day 45 mean SEM			
Dihydroxy-FA	5,6-DiHETE	<0.063	<0.063	<0.063	<0.063	<0.063	<0.063	<0.063	<0.063	<0.063	<0.063	<0.063			
	8,9-DiHETE	0.43	0.09	<0.125	0.15	0.02	<0.125	0.24	0.02	<0.125	1.82	0.20	1.92	0.35	
	11,12-DiHETE	0.45	0.14	0.13	0.18	0.04	<0.063	0.18	0.04	<0.063	0.26	1.35	0.20	1.47	0.30
	14,15-DiHETE	1.19	0.36	0.44	0.53	0.09	<0.063	0.18	0.04	<0.063	0.56	3.48	0.76	3.02	0.64
	17,18-DiHETE	9.20	1.79	5.27	2.92	0.43	<0.063	1.42	0.24	<0.063	2.18	16.55	3.90	14.09	2.92
Hydroxy-FA	8-HEPE	0.73	0.08	0.48	0.24	0.02	<0.125	0.57	0.17	<0.125	1.63	4.29	0.59	9.71	1.60
	9-HEPE	0.61	0.09	0.34	0.05	0.04	<0.125	0.93	0.09	<0.125	3.20	4.40	6.80	1.62	2.55
	12-HEPE	6.26	1.44	3.29	0.96	0.21	<0.125	0.30	0.06	<0.125	178.59	53.06	236.73	77.49	201.10
	15-HEPE	<0.313	<0.313	<0.313	<0.313	<0.313	<0.313	<0.313	<0.313	<0.313	7.30	2.01	3.49	0.42	6.26
	18-HEPE	7.63	0.62	2.85	0.34	0.22	<0.025	0.57	0.17	<0.025	16.42	2.67	7.07	0.56	14.49
19-HEPE	2.96	0.46	1.62	1.44	0.22	<0.025	0.93	0.09	<0.025	10.97	2.26	11.32	1.99	15.48	
20-HEPE	2.91	0.38	1.59	1.84	0.24	<0.025	0.93	0.09	<0.025	18.87	3.26	19.73	3.23	25.38	
Multiple Hydroxylated FA	LTB5	<0.063	<0.063	<0.063	<0.063	<0.063	<0.063	<0.063	<0.063	<0.063	<0.063	<0.063	<0.063	<0.063	<0.063
	Resolvin E1	<0.3	<0.3	<0.3	<0.3	<0.3	<0.3	<0.3	<0.3	<0.3	<0.3	<0.3	<0.3	<0.3	<0.3
	RVE2	<0.25	<0.25	<0.25	<0.25	<0.25	<0.25	<0.25	<0.25	<0.25	<0.25	<0.25	<0.25	<0.25	<0.25
	18(S)-RVE3	<0.125	<0.125	<0.125	<0.125	<0.125	<0.125	<0.125	<0.125	<0.125	<0.125	<0.125	<0.125	<0.125	<0.125
	18(S)-RVE3 alt	<0.25	<0.25	<0.25	<0.25	<0.25	<0.25	<0.25	<0.25	<0.25	<0.25	<0.25	<0.25	<0.25	<0.25
Others	18(R)-RVE3	<0.25	<0.25	<0.25	<0.25	<0.25	<0.25	<0.25	<0.25	<0.25	<0.25	<0.25	<0.25	<0.25	<0.25
	18(R)-RVE3 alt	<0.125	<0.125	<0.125	<0.125	<0.125	<0.125	<0.125	<0.125	<0.125	<0.125	<0.125	<0.125	<0.125	<0.125
	12-OH-17(18)-EpETE	<0.063	<0.063	<0.063	<0.063	<0.063	<0.063	<0.063	<0.063	<0.063	<0.063	<0.063	<0.063	<0.063	<0.063
	12-OH-17(18)-EpETE alt	<0.25	<0.25	<0.25	<0.25	<0.25	<0.25	<0.25	<0.25	<0.25	<0.25	<0.25	<0.25	<0.25	<0.25
	10(11)-EpDPE	1.00	0.07	0.74	0.10	0.10	0.06	0.53	0.06	0.40	0.02	0.26	0.03	0.27	0.02
DHA	13(14)-EpDPE	0.71	0.05	0.54	0.06	0.06	0.40	0.04	0.35	0.03	0.19	0.03	0.22	0.02	0.22
	16(17)-EpDPE	0.80	0.05	0.63	0.09	0.09	0.43	0.04	0.37	0.04	0.20	0.02	0.25	0.02	0.25
	19(20)-EpDPE	7.91	0.49	6.23	0.63	0.63	3.30	0.34	3.04	0.19	1.99	0.38	1.50	0.12	2.3
	4,5-DiHDPE	4.72	0.12	4.15	0.47	0.47	1.87	0.40	1.70	0.36	1.92	0.38	1.16	0.14	16
	7,8-DiHDPE	0.81	0.03	0.60	0.10	0.10	0.44	0.03	<0.25	0.35	0.03	0.28	0.02	1.58	0.24
Hydroxy-FA	10,11-DiHDPE	0.78	0.09	0.45	0.07	0.07	0.34	0.02	0.26	0.02	0.25	0.04	0.19	0.04	1.52
	13,14-DiHDPE	0.93	0.17	0.43	0.07	0.07	0.65	0.11	0.25	0.02	0.22	0.02	0.19	0.03	1.34
	16,17-DiHDPE	2.45	0.61	1.10	0.22	0.22	1.64	0.30	0.56	0.07	0.53	0.05	0.39	0.08	3.15
	19,20-DiHDPE	17	3.02	9.41	1.42	1.42	5.85	0.36	4.56	0.26	3.29	0.64	3.39	0.72	25
	4-HDHA	1.07	0.04	0.68	0.07	0.07	0.89	0.05	0.49	0.03	0.44	0.06	0.29	0.05	4.39
Multiple Hydroxylated FA	7-HDHA	0.37	0.02	0.26	0.02	0.02	0.31	0.02	0.17	0.04	0.13	0.03	0.10	0.02	2.52
	8-HDHA	2.47	0.10	1.73	0.12	0.12	2.09	0.20	1.08	0.14	0.96	0.16	0.71	0.11	32
	10-HDHA	1.19	0.11	0.75	0.05	0.05	0.67	0.07	0.31	0.05	0.42	0.08	0.21	0.04	18
	11-HDHA	0.36	0.03	0.24	0.02	0.02	0.26	0.03	0.12	0.01	0.12	0.05	0.10	0.02	4.02
	13-HDHA	0.52	0.04	0.27	0.02	0.02	0.37	0.04	0.15	0.02	0.17	0.05	0.11	0.02	5.75
Multiple Hydroxylated FA	14-HDHA	9.92	2.51	6.47	1.68	1.68	4.46	0.95	3.05	1.36	3.68	1.26	2.51	0.51	346
	16-HDHA	0.54	0.05	0.33	0.03	0.03	0.48	0.05	0.21	0.03	0.23	0.03	0.13	0.01	3.46
	17-HDHA	1.34	0.10	1.40	0.31	0.31	0.84	0.12	0.30	0.09	0.47	0.12	0.31	0.08	26
	20-HDHA	2.76	0.19	1.99	0.29	0.29	0.89	0.08	0.40	0.06	0.45	0.04	0.32	0.05	12
	21-HDHA	13.24	0.86	8.18	1.25	1.25	12.05	1.63	4.15	0.44	3.46	0.12	2.86	0.37	28
22-HDHA	2.98	0.17	2.76	0.23	0.23	2.63	0.16	1.89	0.18	2.10	0.11	1.78	0.13	63	
RvD1	<0.025	<0.025	<0.025	<0.025	<0.025	<0.025	<0.025	<0.025	<0.025	<0.025	<0.025	<0.025	<0.025	<0.025	<0.025

Table 9.3.5: Plasma Continued.

[nM]	<i>fat-1</i>		Wild Type		STD		STD+n3		Day 45 mean SEM												
	Day 0 mean SEM	Day 30 mean SEM	Day 0 mean SEM	Day 7 mean SEM	Day 14 mean SEM	Day 30 mean SEM	Day 45 mean SEM	Day 7 mean SEM		Day 14 mean SEM	Day 30 mean SEM										
LA	Epoxy-FA	8.86	0.31	7.51	0.53	6.68	0.42	6.24	0.65	10	0.32	6.13	0.86	5.44	0.77	6.71	0.72	5.93	1.01	7.49	1.14
	12(13)-EpOME	15	1.32	8.98	0.67	11	0.92	7.61	0.60	12	0.27	7.66	0.97	6.93	0.87	8.71	0.82	7.57	1.06	9.37	1.20
	Dihydroxy-FA	22	3.60	8.60	0.81	16	1.99	6.50	1.14	11	1.96	11	2.04	5.03	0.94	6.87	1.33	6.31	1.88	7.57	1.74
Hydroxy-FA	9-HODE	73	11	27	3.23	48	6.55	9.29	3.54	26	6.94	23	8.51	10	4.55	18	4.86	16	6.48	20	5.54
	13-HODE	64	13	30	11	36	4.27	53	7.16	32	6.79	64	11	17	1.35	35	6.30	27	3.67	36	6.11
	Others	125	33	43	15	81	13	62	6.77	37	7.24	99	17	19	2.29	52	12	33	4.20	55	11
ALA	EKODE	8.22	0.67	5.70	0.34	5.98	0.35	6.82	1.19	7.10	0.81	5.54	0.48	5.33	0.23	4.66	0.35	6.44	1.05	4.69	0.54
	9-oxo-ODE	14	0.43	8.50	1.11	11	1.15	15	2.57	13	1.68	13	1.74	8.52	0.15	7.74	0.52	9.78	1.71	7.94	0.93
	13-oxo-ODE	1.95	0.18	0.58	0.05	1.25	0.13	0.63	0.10	0.69	0.10	0.51	0.06	0.52	0.02	0.41	0.05	0.55	0.08	0.42	0.04
	9,12,13-TrHOME	5.27	0.54	4.20	0.69	4.92	0.72	9.34	1.10	7.62	0.48	5.37	0.47	5.65	0.63	6.01	0.11	6.58	0.66	3.97	0.33
	9,10,13-TrHOME	1.02	0.09	0.81	0.12	1.00	0.09	2.12	0.23	1.66	0.07	0.99	0.09	1.36	0.15	1.38	0.07	1.53	0.12	0.84	0.07
	9(10)-EpODE	0.77	0.06	0.12	0.01	0.48	0.04	0.08	0.01	0.13	0.01	0.10	0.01	0.07	0.01	0.08	0.01	0.12	0.01	0.11	0.02
DGLA	12(13)-EpODE	0.84	0.13	0.09	0.01	0.53	0.07	<0.063	0.08	0.01	<0.063	0.08	0.01	<0.063	<0.063	1.18	0.28	1.49	0.30	1.07	0.30
	15(16)-EpODE	38	6.57	0.81	0.07	28	3.50	0.76	0.19	1.26	0.17	1.17	0.21	0.29	0.05	0.68	0.11	0.81	0.15	0.68	0.15
	15,16-DiHODE	20	4.81	0.62	0.06	11	0.84	0.64	0.12	0.74	0.12	0.89	0.12	0.28	0.03	0.68	0.11	0.81	0.15	0.68	0.15
	9,10-DiHODE	2.56	0.63	0.14	0.00	1.45	0.16	0.13	0.01	0.15	0.02	0.23	0.03	0.08	0.01	0.15	0.02	0.17	0.02	0.19	0.03
	12,13-DiHODE	2.29	0.55	<0.5		1.20	0.16	<0.5		<0.5		<0.5		<0.5		<0.5		<0.5		<0.5	
	9-HOTrE	4.60	1.42	0.57	0.15	2.67	0.37	0.64	0.15	0.67	0.17	0.80	0.09	0.40	0.01	0.37	0.03	0.64	0.21	0.52	0.06
Prostanoids	13-HOTrE	7.31	2.64	0.79	0.16	3.43	0.62	0.85	0.23	0.66	0.18	1.29	0.17	0.43	0.01	0.63	0.10	1.03	0.51	0.91	0.13
	PGE1	<0.081	<0.081	<0.081		<0.081		<0.081		<0.081		<0.081		<0.081		<0.081		<0.081		<0.081	
	PGD1	<0.125	<0.125	<0.125		<0.125		<0.125		<0.125		<0.125		<0.125		<0.125		<0.125		<0.125	
	PGF1a	<0.025	<0.025	<0.025		<0.025		<0.025		<0.025		<0.025		<0.025		<0.025		<0.025		<0.025	
	15-k-PGF1a	<0.063	<0.063	<0.063		<0.063		<0.063		<0.063		<0.063		<0.063		<0.063		<0.063		<0.063	
	13,14-dih-15-k-PGE1	<0.025	<0.025	<0.025		<0.025		<0.025		<0.025		<0.025		<0.025		<0.025		<0.025		<0.025	
Oleic Acid	TXB1	<0.125	<0.125	<0.125		<0.125		<0.125		<0.125		<0.125		<0.125		<0.125		<0.125		<0.125	
	15(S)-HETE	0.61	0.07	0.43	0.02	0.57	0.05	0.38	0.06	0.53	0.08	0.46	0.07	0.46	0.06	0.63	0.11	0.52	0.05	0.54	0.10
	Epoxy-18-1	24	2.07	20	0.46	24	1.02	23	2.72	26	2.01	20	1.32	21	1.44	17	0.61	21	2.15	18	1.50
C20:3n9	t-dOH-18-1	3.21	0.32	1.78	0.28	2.85	0.38	3.15	0.36	2.33	0.12	2.98	0.44	2.05	0.07	2.23	0.09	2.37	0.19	2.15	0.31
	LTB3	<0.125	<0.125	<0.125		<0.125		<0.125		<0.125		<0.125		<0.125		<0.125		<0.125		<0.125	
C22:4n6	dihomo-PGF2a	<0.025	<0.025	<0.025		<0.025		<0.025		<0.025		<0.025		<0.025		<0.025		<0.025		<0.025	
		<0.025	<0.025	<0.025		<0.025		<0.025		<0.025		<0.025		<0.025		<0.025		<0.025		<0.025	



Table 9.3.5: Brain.

ARA	[ng/kg tissue wet weight]	fat-1		Wild Type		STD				STD+n3														
		Day 0 mean SEM	Day 30 mean SEM	Day 0 mean SEM	Day 30 mean SEM	Day 7 mean SEM	Day 14 mean SEM	Day 30 mean SEM	Day 45 mean SEM	Day 7 mean SEM	Day 14 mean SEM	Day 30 mean SEM	Day 45 mean SEM											
<b>Prostanoids</b>	6-keto-PGF1a	30	4.3	28	3.0	41	6.8	50	9.5	41	5.8	44	5.1	37	5.7	31	2.9	39	8.2	21	2.1	21	2.4	
	PGF2a	226	17	119	8.6	259	19	105	8.3	145	14	284	35	257	15	103	13	126	20	99	8.0	111	19	
	PGE2	37	3.0	21	1.0	43	3.4	22	2.0	33	2.3	50	5.3	52	4.0	17	1.9	24	5.0	18	1.8	20	2.3	
	PGD2	532	50	342	51	529	54	435	45	593	43	748	41	664	81	406	34	466	62	373	41	392	44	
	PGJ2	3.7	0.4	4.7	0.6	5.7	0.7	4.2	0.4	6.1	0.4	4.9	0.2	5.4	1.1	3.8	0.5	4.3	0.4	4.3	0.2	4.7	0.6	
	PGB2	<0.4	<0.4	<0.4	<0.4	<0.4	<0.4	<0.4	<0.4	<0.4	<0.4	<0.4	<0.4	<0.4	<0.4	<0.4	<0.4	<0.4	<0.4	<0.4	<0.4	<0.4	<0.4	<0.4
	15-deoxy-PGJ2	<1	<1	<1	<1	<1	<1	<1	<1	<1	<1	<1	<1	<1	<1	<1	<1	<1	<1	<1	<1	<1	<1	<1
	11b-PGF2a	<1	<1	<1	<1	<1	<1	<1	<1	<1	<1	<1	<1	<1	<1	<1	<1	<1	<1	<1	<1	<1	<1	<1
	bic PGE2	<1	<1	<1	<1	<1	<1	<1	<1	<1	<1	<1	<1	<1	<1	<1	<1	<1	<1	<1	<1	<1	<1	<1
	13,14dih-15k-PGF2a	38	1.8	15	0.4	30	2.7	16	1.7	24	2.0	34	3.5	36	2.8	15	1.7	19	2.8	14	0.9	17	1.6	
TXB2	91	6.9	54	2.1	99	5.6	56	6.3	80	8.0	145	17	125	14	51	6.7	62	8.7	45	3.9	52	6.1		
<b>Epoxy-FA</b>	5(6)-EpETE	99	14	41	6.0	100	5.5	53	18	40	22	81	14	107	8.4	51	8.2	70	12	47	10.0	41	8.1	
	8(9)-EpETE alt	27	3.3	10	1.3	31	1.6	13	4.0	9.0	5.4	22	4.3	26	3.4	13	2.1	23	4.0	16	3.3	11	2.1	
	11(12)-EpETE	76	7.8	29	3.8	92	4.7	35	8.9	27	12	64	11	71	10	38	4.7	61	10	48	11	32	4.7	
<b>Dihydroxy-FA</b>	14(15)-EpETE	46	4.9	20	3.0	57	3.1	23	6.5	21	8.5	39	6.1	45	6.2	27	3.7	64	12	33	6.9	26	4.7	
	5,6-DiHETE	<0.5	<0.5	<0.5	<0.5	<0.5	<0.5	<0.5	<0.5	<0.5	<0.5	<0.5	<0.5	<0.5	<0.5	<0.5	<0.5	<0.5	<0.5	<0.5	<0.5	<0.5	<0.5	
	8,9-DiHETE	<0.5	<0.5	<0.5	<0.5	0.7	0.03	<0.5	<0.5	<0.5	<0.5	<0.5	<0.5	0.7	0.05	<0.5	<0.5	<0.5	<0.5	<0.5	<0.5	<0.5	<0.5	
<b>Hydroxy-FA</b>	11,12-DiHETE	0.9	0.2	0.5	0.1	0.9	0.05	0.5	0.04	0.6	0.1	0.7	0.1	0.8	0.05	0.6	0.04	0.5	0.1	0.6	0.04	0.6	0.05	
	14,15-DiHETE	1.5	0.2	0.9	0.1	1.5	0.04	1.0	0.1	1.2	0.1	1.3	0.1	1.5	0.1	1.1	0.1	1.1	0.1	1.0	0.04	1.2	0.05	
	5-HETE	21	3.8	16	3.0	29	1.8	19	3.1	14	1.1	21	1.3	23	3.2	17	1.6	17	2	26	3.5	21	2.5	
<b>Multiple Hydroxylated FA</b>	8-HETE	26	12	9.7	1.8	17	1.8	8.8	2.4	6.1	0.7	10	0.8	11	0.9	8.8	1.1	8.5	1.6	13	2.5	14	2.6	
	9-HETE	14	2.3	8.8	1.7	16	1.4	14	1.8	13	1.3	14	1.3	16	2.1	11	1.1	10	1.0	18	1.6	15	2.1	
	11-HETE	86	6.8	43	3.1	80	4.4	48	5.9	59	4.6	93	7.5	93	6.1	44	4.0	54	7.6	47	4.0	52	4.1	
	12-HETE	63	13	154	55	105	16	82	9.4	93	13	102	32	122	32	45	4.6	68	8.2	59	8.4	60	6.6	
	15-HETE	104	11	68	4.5	101	5.5	80	8.6	98	2.6	129	10	121	12	70	4.5	81	5.9	83	5.8	84	5.5	
	20-HETE	<2.6	<2.6	<2.6	<2.6	3.0	0.2	<2.6	<2.6	<2.6	<2.6	2.9	0.2	3.4	0.4	3.3	0.2	<2.6	<2.6	<2.6	<2.6	<2.6	<2.6	<2.6
	LTB4	<0.5	<0.5	<0.5	<0.5	<0.5	<0.5	<0.5	<0.5	<0.5	<0.5	<0.5	<0.5	<0.5	<0.5	<0.5	<0.5	<0.5	<0.5	<0.5	<0.5	<0.5	<0.5	
	6-trans-LTB4	<0.5	<0.5	<0.5	<0.5	<0.5	<0.5	<0.5	<0.5	<0.5	<0.5	<0.5	<0.5	<0.5	<0.5	<0.5	<0.5	<0.5	<0.5	<0.5	<0.5	<0.5	<0.5	
	20-COOH-LTB4	<1	<1	<1	<1	<1	<1	<1	<1	<1	<1	<1	<1	<1	<1	<1	<1	<1	<1	<1	<1	<1	<1	
	20-OH-LTB4	<0.25	<0.25	<0.25	<0.25	<0.25	<0.25	<0.25	<0.25	<0.25	<0.25	<0.25	<0.25	<0.25	<0.25	<0.25	<0.25	<0.25	<0.25	<0.25	<0.25	<0.25	<0.25	
<b>Isoprostanes</b>	LX44	<0.175	<0.175	<0.175	<0.175	<0.175	<0.175	<0.175	<0.175	<0.175	<0.175	<0.175	<0.175	<0.175	<0.175	<0.175	<0.175	<0.175	<0.175	<0.175	<0.175	<0.175	<0.175	
	5,15-DiHETE	1.0	0.1	0.7	0.1	0.7	0.03	0.9	0.1	1.1	0.1	1.2	0.1	1.5	0.1	0.9	0.02	1.0	0.1	1.0	0.1	1.3	0.1	
	8,15-DiHETE	3.4	0.9	1.0	0.1	1.7	0.4	1.8	0.2	2.0	0.2	2.4	0.2	3.0	0.1	1.6	0.1	1.8	0.1	1.8	0.1	2.6	0.5	
<b>Others</b>	5-iPF2a	<1	<1	<1	<1	<1	<1	<1	<1	<1	<1	<1	<1	<1	<1	<1	<1	<1	<1	<1	<1	<1	<1	
	8-i-PGF2a	<0.1	<0.1	<0.1	<0.1	<0.1	<0.1	<0.1	<0.1	<0.1	<0.1	<0.1	<0.1	<0.1	<0.1	<0.1	<0.1	<0.1	<0.1	<0.1	<0.1	<0.1	<0.1	
<b>Others</b>	5-oxo-ETE	4.0	0.6	4.0	0.8	4.6	0.3	<2	<2	5.2	0.3	4.3	0.6	4.3	0.6	4.4	1.3	3.1	0.6	<2	5.3	1.6	5.3	1.6
	15-oxo-ETE	4.6	0.2	6.0	0.6	5.9	0.5	7.3	1.1	7.6	0.9	6.0	0.6	5.6	0.5	6.7	1.1	5.6	0.7	8.9	1.6	8.2	1.4	
	11,12-,15-TriHETE	2.2	0.5	<1	<1	1.7	0.2	<1	<1	<1	0.0	1.5	0.2	<1	<1	<1	<1	<1	<1	<1	<1	<1	<1	
	THF diol	<0.25	<0.25	<0.25	<0.25	<0.25	<0.25	<0.25	<0.25	<0.25	<0.25	<0.25	<0.25	<0.25	<0.25	<0.25	<0.25	<0.25	<0.25	<0.25	<0.25	<0.25	<0.25	

Table 9.3.5: Brain Continued.

EPA	[ng/kg tissue wet weight]	fat -1		Wild Type			STD						STD+n3					
		Day 0	Day 30	Day 0	Day 7	Day 14	Day 30	Day 45	Day 7	Day 14	Day 30	Day 45	Day 7	Day 14	Day 30	Day 45		
		mean SEM	mean SEM	mean SEM	mean SEM	mean SEM	mean SEM	mean SEM	mean SEM	mean SEM	mean SEM	mean SEM	mean SEM	mean SEM	mean SEM	mean SEM	mean SEM	
<b>Prostanoids</b>	PGE3	<0.3	<0.3	<0.3	<0.3	<0.3	<0.3	<0.3	<0.3	<0.3	<0.3	<0.3	<0.3	<0.3	<0.3	<0.3	<0.3	
	PGD3	<1	<1	<1	<1	<1	<1	<1	<1	<1	<1	<1	<1	<1	<1	<1	<1	
	d17-6k-PGF1a	<1	<1	<1	<1	<1	<1	<1	<1	<1	<1	<1	<1	<1	<1	<1	<1	
	TXB3	0.5	0.03	<0.5	<0.5	<0.5	<0.5	<0.5	<0.5	<0.5	<0.5	<0.5	<0.5	<0.5	<0.5	<0.5	<0.5	
<b>Epoxy-FA</b>	8(9)-EpETE	<1	<1	<1	<1	<1	<1	<1	<1	<1	<1	<1	<1	<1	<1	<1	<1	
	11(12)-EpETE	0.6	0.1	<0.5	<0.5	<0.5	<0.5	<0.5	<0.5	<0.5	<0.5	<0.5	<0.5	<0.5	<0.5	<0.5	<0.5	
	14(15)-EpETE	0.4	0.05	<0.25	<0.25	<0.25	<0.25	<0.25	<0.25	<0.25	<0.25	<0.25	<0.25	<0.25	<0.25	<0.25	<0.25	
	17(18)-EpETE	<0.5	<0.5	<0.5	<0.5	<0.5	<0.5	<0.5	<0.5	<0.5	<0.5	<0.5	<0.5	<0.5	<0.5	<0.5	<0.5	
<b>Dihydroxy-FA</b>	5,6-DiHETE	<0.25	<0.25	<0.25	<0.25	<0.25	<0.25	<0.25	<0.25	<0.25	<0.25	<0.25	<0.25	<0.25	<0.25	<0.25	<0.25	
	8,9-DiHETE	<0.5	<0.5	<0.5	<0.5	<0.5	<0.5	<0.5	<0.5	<0.5	<0.5	<0.5	<0.5	<0.5	<0.5	<0.5	<0.5	
	11,12-DiHETE	<0.25	<0.25	<0.25	<0.25	<0.25	<0.25	<0.25	<0.25	<0.25	<0.25	<0.25	<0.25	<0.25	<0.25	<0.25	<0.25	
	14,15-DiHETE	<0.25	<0.25	<0.25	<0.25	<0.25	<0.25	<0.25	<0.25	<0.25	<0.25	<0.25	<0.25	<0.25	<0.25	<0.25	<0.25	
	17,18-DiHETE	0.8	0.1	0.5	0.04	0.3	0.03	<0.25	<0.25	<0.25	<0.25	<0.25	<0.25	<0.25	<0.25	<0.25	<0.25	
<b>Hydroxy-FA</b>	5-HEPE	0.7	0.1	<0.5	<0.5	<0.5	<0.5	<0.5	<0.5	<0.5	<0.5	<0.5	<0.5	<0.5	<0.5	<0.5	<0.5	
	8-HEPE	<0.625	<0.625	<0.625	<0.625	<0.625	<0.625	<0.625	<0.625	<0.625	<0.625	<0.625	<0.625	<0.625	<0.625	<0.625	<0.625	
	12-HEPE	4.2	1.0	12	6.3	1.2	0.2	1.0	0.1	1.2	0.3	0.8	0.1	1.5	0.5	1.5	0.5	
	15-HEPE	<1.25	<1.25	<1.25	<1.25	<1.25	<1.25	<1.25	<1.25	<1.25	<1.25	<1.25	<1.25	<1.25	<1.25	<1.25	<1.25	<1.25
	18-HEPE	1.2	0.2	0.5	0.1	<0.1	<0.1	<0.1	<0.1	<0.1	<0.1	<0.1	<0.1	<0.1	<0.1	<0.1	<0.1	
	19-HEPE	<0.25	<0.25	<0.25	<0.25	<0.25	<0.25	<0.25	<0.25	<0.25	<0.25	<0.25	<0.25	<0.25	<0.25	<0.25	<0.25	
	20-HEPE	<1	<1	<1	<1	<1	<1	<1	<1	<1	<1	<1	<1	<1	<1	<1	<1	
<b>Multiple Hydroxylated FA</b>	LTB5	<0.25	<0.25	<0.25	<0.25	<0.25	<0.25	<0.25	<0.25	<0.25	<0.25	<0.25	<0.25	<0.25	<0.25	<0.25	<0.25	
	Resolvin E1	<1.2	<1.2	<1.2	<1.2	<1.2	<1.2	<1.2	<1.2	<1.2	<1.2	<1.2	<1.2	<1.2	<1.2	<1.2	<1.2	
	RvE2	<1	<1	<1	<1	<1	<1	<1	<1	<1	<1	<1	<1	<1	<1	<1	<1	
	18(S)-RvE3	<0.5	<0.5	<0.5	<0.5	<0.5	<0.5	<0.5	<0.5	<0.5	<0.5	<0.5	<0.5	<0.5	<0.5	<0.5	<0.5	
<b>Others</b>	18(S)-RvE3 alt	<1	<1	<1	<1	<1	<1	<1	<1	<1	<1	<1	<1	<1	<1	<1	<1	
	18(R)-RvE3	<1	<1	<1	<1	<1	<1	<1	<1	<1	<1	<1	<1	<1	<1	<1	<1	
	18(R)-RvE3 alt	<0.5	<0.5	<0.5	<0.5	<0.5	<0.5	<0.5	<0.5	<0.5	<0.5	<0.5	<0.5	<0.5	<0.5	<0.5	<0.5	
	12-OH-17(18)-EpETE	<0.25	<0.25	<0.25	<0.25	<0.25	<0.25	<0.25	<0.25	<0.25	<0.25	<0.25	<0.25	<0.25	<0.25	<0.25	<0.25	
<b>DHA</b>	12-OH-17(18)-EpETE alt	<1	<1	<1	<1	<1	<1	<1	<1	<1	<1	<1	<1	<1	<1	<1	<1	
	10(11)-EpDPE	8.1	1.0	4.4	0.5	10	0.9	3.7	1.2	2.9	1.4	5.3	1.1	7.3	0.6	6.2	0.9	
	13(14)-EpDPE	7.1	0.8	3.6	0.4	9.3	0.9	3.2	1.0	2.9	1.2	4.3	0.8	6.2	0.7	5.3	0.8	
	16(17)-EpDPE	6.6	0.6	3.6	0.5	8.4	0.8	2.9	0.8	2.2	1.1	4.1	0.7	5.6	0.5	4.9	0.7	
	19(20)-EpDPE	9.7	1.2	6.9	0.8	13	0.8	4.9	1.5	4.3	1.7	6.3	0.9	8.5	0.6	9.8	1.3	
	4,5-DiHDPE	<2	<2	<2	<2	<2	<2	<2	<2	<2	<2	<2	<2	<2	<2	<2	<2	
	7,8-DiHDPE	<1	<1	<1	<1	<1	<1	<1	<1	<1	<1	<1	<1	<1	<1	<1	<1	
	10,11-DiHDPE	<0.5	<0.5	<0.5	<0.5	<0.5	<0.5	<0.5	<0.5	<0.5	<0.5	<0.5	<0.5	<0.5	<0.5	<0.5	<0.5	
	13,14-DiHDPE	0.3	0.03	<0.25	<0.25	0.3	0.01	<0.25	<0.25	<0.25	<0.25	<0.25	<0.25	0.3	0.02	<0.25	<0.25	
	16,17-DiHDPE	<0.5	<0.5	<0.5	<0.5	<0.5	<0.5	<0.5	<0.5	<0.5	<0.5	<0.5	<0.5	<0.5	<0.5	<0.5	<0.5	
<b>Hydroxy-FA</b>	19,20-DiHDPE	2.3	0.2	1.9	0.2	2.8	0.2	1.2	0.1	1.1	0.1	1.6	0.2	1.8	0.2	3.0	0.3	
	4-HDHA	5.5	0.6	5.6	1.3	7.8	0.7	4.0	0.6	3.0	0.4	4.1	0.3	5.3	0.6	7.3	0.7	
	7-HDHA	2.3	0.4	1.2	0.4	2.4	0.2	<0.25	<0.25	<0.25	<0.25	1.5	0.2	1.7	0.4	1.2	0.4	
	8-HDHA	9.4	1.1	12	1.9	13	0.8	7.7	0.9	7.1	1.1	7.3	0.4	9.1	0.8	14	0.7	
	10-HDHA	8.6	4.5	2.4	0.6	3.6	0.4	1.3	0.3	0.6	0.2	1.2	0.2	2.1	0.2	2.5	0.5	
	11-HDHA	3.8	0.7	5.1	1.2	4.1	0.4	3.4	0.4	2.9	0.3	2.4	0.1	3.4	0.4	5.1	0.8	

Table 9.3.5: Brain Continued.

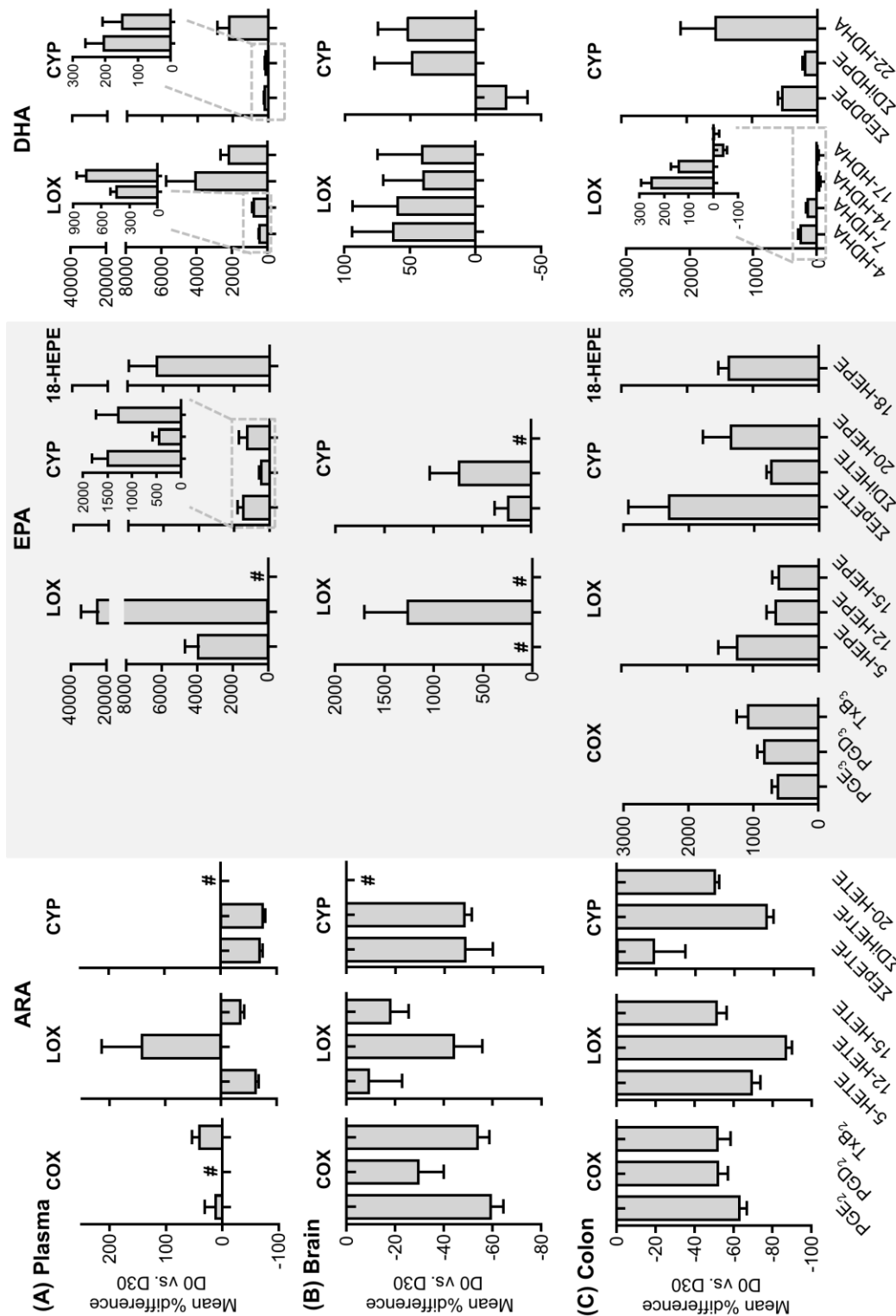
[ng/kg tissue wet weight]	fat-1		Wild Type		STD		STD+n3																
	Day 0	Day 30	Day 0	mean SEM	Day 7	Day 14	Day 30	Day 45	Day 7	Day 14	Day 30	Day 45											
<b>DHA</b>																							
Hydroxy-FA	9.2	1.5	6.6	1.2	9.1	0.5	4.8	1.0	3.9	0.5	8.0	0.8	8.7	0.6	8.4	1.7	8.3	1.5	11	3.1	7.7	1.1	
13-HDHA	16	5.5	11	2.2	11	1.0	5.9	0.7	5.3	0.5	5.7	0.7	11	2.0	9.4	2.1	12	1.6	15	3.0	12	1.5	
14-HDHA	5.6	1.3	6.3	1.1	5.2	0.2	4.1	0.7	3.5	0.2	4.1	0.3	5.5	0.3	8.3	1.8	7.6	1.0	12	3.3	8.3	1.0	
16-HDHA	20	4.6	15	2.1	17	0.9	8.8	0.8	11	0.9	14	1.2	18	1.5	17	3.6	19	2.1	24	5.8	20	2.0	
17-HDHA	10	1.8	11	1.9	12	0.8	6.3	0.6	6.8	0.7	9.5	0.6	13	0.4	11	1.2	13	1.7	18	3.8	15	1.5	
20-HDHA	4.3	0.5	4.0	0.4	4.7	0.2	3.3	0.3	3.3	0.3	3.3	0.1	4.4	0.3	4.9	0.4	5.7	0.3	6.8	0.7	6.1	0.4	
21-HDHA	2.9	0.3	2.1	0.3	2.9	0.2	<1.4		<1.4		2.3	0.4	3.8	0.4	4.6	0.5	5.7	1.9	4.3	0.6	5.0	0.5	
22-HDHA																							
<b>Multiple</b>																							
<b>Hydroxylated FA</b>																							
RvD1	<0.1	<0.1	<0.1		<0.1		<0.1		<0.1		<0.1		<0.1		<0.1		<0.1		<0.1		<0.1		<0.1
<b>LA</b>																							
Epoxy-FA	7.8	1.2	5.6	1.5	3.2	0.1	8.3	1.7	10	2.7	8.0	1.3	6.3	1.4	4.3	0.8	5.5	1.1	6.3	1.2	4.1	0.7	
9(10)-EpOME	8.8	1.8	5.8	1.5	3.6	0.1	9.0	2.0	13	3.8	8.8	1.5	6.6	1.3	5.2	0.8	6.3	1.4	7.1	1.3	4.5	0.7	
12(13)-EpOME																							
Dihydroxy-FA	2.4	0.2	1.3	0.1	2.0	0.2	1.2	0.1	1.8	0.1	1.9	0.2	2.2	0.8	1.1	0.1	1.4	0.1	1.3	0.1	1.3	0.1	
9,10-DiHOME	6.3	0.5	2.6	0.2	4.3	0.7	2.0	0.2	2.6	0.3	3.5	0.2	4.4	1.4	1.9	0.3	1.9	0.1	2.2	0.2	2.1	0.2	
12,13-DiHOME																							
Hydroxy-FA	67	5.6	53	5.1	35	2.0	63	11	121	48	72	5.2	73	9.0	48	5.8	47	5.0	42	3.3	41	2.6	
9-HODE	69	6.0	44	5.7	38	3.0	57	11	166	81	71	5.2	73	8.9	43	5.9	48	7.1	37	2.7	38	2.9	
13-HODE																							
<b>Others</b>																							
EKODE	21	2.8	8.1	1.1	9.3	1.7	12	2.4	13	2.3	15	1.7	21	6.4	11	2.7	6.5	1.1	8.7	1.0	8.1	1.0	
9-oxo-ODE	30	3.2	17	1.7	9.3	0.7	22	4.1	31	12	25	2.5	28	6.4	18	2.2	14	1.5	15	1.7	14	1.3	
13-oxo-ODE	1.7	0.2	<1		<1		<1		1.9	0.7	2.0	0.1	2.4	0.7	<1		<1		<1		<1		
9,12,13-TriHOME	13	1.0	11	2.3	9.2	0.7	13	3.2	12	1.2	21	4.2	14	2.2	10	1.8	11	1.6	9.9	1.7	8.2	0.6	
9,10,13-TriHOME	2.5	0.1	2.3	0.4	1.8	0.2	2.5	0.5	2.5	0.2	3.5	0.7	3.0	0.6	2.4	0.4	2.4	0.2	2.2	0.4	2.0	0.2	
<b>ALA</b>																							
Epoxy-FA	0.5	0.1	<0.2		<0.2		0.6	0.1	0.6	0.2	0.4	0.1	0.3	0.1	<0.2		<0.2		<0.2		<0.2		
9(10)-EpODE	0.5	0.1	<0.25		<0.25		<0.25		<0.25		<0.25		<0.25		<0.25		<0.25		<0.25		<0.25		
12(13)-EpODE	2.6	0.7	<0.25		0.9	0.1	<0.25		<0.25		1.0	0.2	0.8	0.2	<0.25		<0.25		<0.25		<0.25		
15(16)-EpODE																							
Dihydroxy-FA	2.2	0.2	<0.5		1.8	0.3	<0.5		<0.5		<0.5		<0.5		<0.5		<0.5		<0.5		<0.5		
9,10-DiHODE	0.3	0.0	<0.2		0.2	0.02	<0.2		<0.2		0.2	0.02	<0.2		<0.2		<0.2		<0.2		<0.2		
12,13-DiHODE	<2		<2		<2		<2		<2		<2		<2		<2		<2		<2		<2		
<b>DGLA</b>																							
9-HOTfE	3.1	0.4	2.0	0.3	1.0	0.1	2.6	0.5	3.6	1.7	2.8	0.4	2.5	0.5	1.9	0.3	1.4	0.2	1.4	0.2	1.1	0.1	
13-HOTfE	3.2	0.4	1.9	0.4	1.9	0.3	2.7	0.7	8.2	4.6	3.9	0.8	2.3	0.4	1.8	0.3	2.3	0.5	1.8	0.2	1.4	0.2	
PGE1	0.5	0.0	<0.325		0.5	0.0	<0.325		<0.325		0.4	0.0	0.5	0.0	<0.325		<0.325		<0.325		<0.325		
PGD1	8.5	0.8	5.3	0.6	7.5	0.8	5.9	0.7	8.1	0.7	9.7	0.5	8.9	1.2	5.7	0.5	7.4	1.0	5.8	0.6	6.3	0.7	
PGF1a	4.2	0.3	1.7	0.2	3.3	0.3	1.1	0.1	1.7	0.1	3.8	0.5	3.3	0.4	1.3	0.2	2.0	0.4	1.6	0.1	2.0	0.3	
15-k-PGF1a	<0.25		<0.25		<0.25		<0.25		<0.25		<0.25		<0.25		<0.25		<0.25		<0.25		<0.25		
13,14-dih-15-k-PGE1	<0.1		<0.1		<0.1		<0.1		<0.1		<0.1		<0.1		<0.1		<0.1		<0.1		<0.1		
TXB1	<0.5		<0.5		<0.5		<0.5		<0.5		<0.5		<0.5		<0.5		<0.5		<0.5		<0.5		
<b>Oleic Acid</b>																							
15(S)-HETfE	3.9	0.3	4.4	1.3	2.7	0.2	5.0	1.1	6.7	1.2	4.4	0.6	3.5	0.7	4.0	0.9	5.0	1.1	6.4	0.7	6.3	1.3	
Epoxy-18-1	171	28	122	43	51	3	226	73	129	16	205	59	184	51	103	27	76	17	95	21	66	12	
t-GlOH-18-1	9.4	1.1	7.0	0.9	9.0	1.1	6.3	0.3	17	0.6	12	1.1	13	2.3	7.8	1.1	18	1.2	25	9.0	19	4.7	
<b>C20:3n9</b>	<0.5		<0.5		<0.5		<0.5		<0.5		<0.5		<0.5		<0.5		<0.5		<0.5		<0.5		
LTB3																							
dihomo-PGF2a	2.3	0.2	0.8	0.3	3.2	0.3	0.5	0.1	1.1	0.3	4.0	0.7	3.4	0.2	0.5	0.2	0.6	0.2	<0.1		0.3	0.2	

Table 9.3.5: Colon.

ARA	fat-1		Wild Type		STD		STD+n3				
	Day 0 mean SEM	Day 30 mean SEM	Day 0 mean SEM	Day 30 mean SEM	Day 7 mean SEM	Day 14 mean SEM	Day 30 mean SEM	Day 45 mean SEM			
Prostanoids	6-keto-PGF1a	6139 220 9035 414	11511 758	10736 398	8772 440	12642 570	8611 493	8327 494	6094 646	6563 472	4953 411
	PGF2a	1225 155 1578 187	2431 300	1796 362	1752 155	2386 193	1193 344	1692 82	792 115	852 105	709 80
	PGE2	2705 237 3719 231	5405 306	4956 353	3965 366	5549 235	3524 452	2726 182	1889 142	1995 162	1543 133
	PGD2	4321 273 6744 468	8164 631	7923 560	7347 477	9373 552	6487 1201	5673 271	4021 331	3932 296	3477 281
	PGJ2	232 1.3 49.3 3.1	54.6 6.5	57.8 9.2	42.3 6.0	78.8 5.9	47.9 11.1	38.6 4.0	23.9 3.0	29.4 2.6	25.6 2.5
	PGB2	<0.4	<0.4	<0.4	<0.4	<0.4	<0.4	<0.4	<0.4	<0.4	<0.4
	15-deoxy-PGJ2	<1	1.0 0.0	<1	<1	1.1 0.0	1.2 0.1	<1	<1	<1	<1
	11b-PGF2a	<1	<1	<1	<1	<1	<1	<1	<1	<1	<1
	bic PGE2	<1	<1	<1	<1	<1	<1	<1	<1	<1	<1
	13,14dih-15k-PGF2a	<0.1	<0.1	<0.1	<0.1	<0.1	<0.1	<0.1	<0.1	<0.1	<0.1
TXB2	339.8 27.0 591.0 55.0	600.8 40.0	595.7 27.6	630.5 90.1	730.8 19.7	563.0 59.8	354.2 12.9	293.3 43.3	290.5 35.8	195.6 16.9	
Epoxy-FA	5(6)-EpETE	33 3.7 169 23	99 15	60 6.7	153 13	260 21	103 5.7	51 9.8	91 18	73 8.8	33 2.1
	8(9)-EpETE alt	10 0.9 49 7.0	26 3.4	16 2.2	44 3.7	78 8.0	31 3.1	15 3.2	26 4.9	21 2.8	12 1.2
	11(12)-EpETE	33 4.1 150 23	80 11	46 8.7	136 11	241 28	99 14	47 9.7	81 14	65 10	45 4.5
	14(15)-EpETE	22 2.4 104 15	50 6.3	33 6.3	98 6.5	165 18	75 8.9	33 7.5	55 8.6	47 6.9	33 3.1
	5,6-DiHETE	<0.5	0.8 0.1	1.0 0.1	0.6 0.1	0.8 0.04	1.2 0.1	0.7 0.04	<0.5	0.6 0.04	<0.5
Dihydroxy-FA	8,9-DiHETE	2.4 0.3 4.1 0.6	5.7 0.8	2.9 0.3	3.1 0.2	4.3 0.1	3.0 0.2	1.5 0.1	1.7 0.1	1.8 0.1	1.0 0.1
	11,12-DiHETE	3.4 0.6 5.1 1.0	10.0 1.7	4.2 0.4	4.0 0.5	5.7 0.2	3.6 0.3	1.7 0.1	1.8 0.2	1.9 0.1	1.2 0.1
	14,15-DiHETE	5.7 0.7 8.3 0.9	16 1.4	9.9 1.0	7.0 0.6	11 0.4	7.4 0.1	3.6 0.2	3.3 0.2	3.8 0.2	2.0 0.1
	5-HETE	83 13 77 8.5	121 12	113 21	78 8.4	142 8.1	75 15	66 5.4	36 4.7	37 3.5	24 2.3
	8-HETE	34 5.3 58 13	92 16	78 12	73 15	116 19	49 9.0	35 4.2	14 2.1	11 1.2	10 1.7
Hydroxy-FA	9-HETE	13 1.3 29 3.3	33 6.3	26 1.4	27 3.5	47 6.1	23 2.2	16 1.4	13 1.0	12 0.7	8.8 0.7
	11-HETE	1293 119 1756 50	2224 115	2000 104	1698 106	2492 234	1531 261	1367 72	1011 106	1116 88	875 78
	12-HETE	690 81 1437 284	1986 332	2078 249	1636 355	3239 639	1255 307	801 100	290 55	264 40	297 56
	15-HETE	1027 85 1614 74	1960 105	1915 91	1529 127	2539 256	1354 205	1184 70	898 105	957 78	709 63
	20-HETE	<2.6	4.2 0.7	<2.6	6.3 2.7	11 3.2	5.0 1.2	3.9 0.8	<2.6	<2.6	<2.6
	LTB4	0.8 0.1 1.5 0.3	1.3 0.2	3.0 0.5	2.7 0.6	4.1 0.3	1.2 0.2	1.2 0.2	1.4 0.1	0.9 0.2	0.9 0.2
	6-trans-LTB4	1.9 0.2 4.0 0.8	4.4 0.9	2.7 0.3	4.4 1.0	7.8 1.2	4.1 1.8	1.6 0.1	1.0 0.2	1.0 0.1	0.7 0.1
	20-COOH-LTB4	<1	3.4 0.9	<1	<1	2.6 0.5	1.9 0.4	2.2 0.5	4.7 2.1	<1	<1
	20-OH-LTB4	<0.25	<0.25	<0.25	<0.25	<0.25	<0.25	<0.25	<0.25	<0.25	<0.25
	LXA4	<0.175	<0.175	<0.175	<0.175	<0.175	<0.175	<0.175	<0.175	<0.175	<0.175
Isoprostanes	5,15-DiHETE	2.3 0.2 3.4 0.6	5.6 1.4	4.2 0.6	3.4 0.6	6.9 1.1	2.9 0.5	2.2 0.3	1.1 0.2	1.2 0.1	0.8 0.1
	8,15-DiHETE	6.8 1.0 12 3.1	20 4.7	16 2.9	16 3.8	26 4.9	12 2.4	7.8 1.0	3.4 0.5	3.0 0.2	2.7 0.4
	5-IPF2a	1.3 0.1 1.8 0.2	3.8 0.3	2.4 0.3	2.1 0.2	4.1 0.4	2.1 0.2	1.7 0.2	1.6 0.2	1.1 0.1	<1
	8-IPF2a	52 5.9 75 4.5	119 8.5	95 13	82 3.5	125 8.8	67 9.1	65 2.6	40 3.8	42 3.8	39 3.7
	5-oxo-EETE	7.3 0.7 16 1.0	13 1.2	12 1.3	15 1.1	18 0.8	12 1.4	8.8 0.9	12 1.6	13 1.0	6.8 0.6
Others	15-oxo-EETE	12 1.2 22 1.5	31 3.3	28 2.9	21 3.0	43 4.3	19 2.4	15 0.9	12 1.5	12 1.0	10 1.2
	11,12-,15-TriHETE	15 1.9 33 3.5	41 4.1	28 5.1	26 4.1	49 4.9	22 4.2	17 1.4	18 2.2	17 1.7	13 1.9
	THF diol	<0.25	<0.25	<0.25	<0.25	<0.25	<0.25	<0.25	<0.25	<0.25	<0.25
	PGE3	399 49 225 27	76 9.1	17 2.2	8.4 1.3	8.2 0.6	5.5 0.8	635 41	490 44	549 35	502 50
	PGD3	219 18 231 22	49 3.4	14 2.5	8.5 0.9	8.4 0.9	5.6 1.5	511 34	381 49	457 46	395 45
Epoxy-FA	d17-6k-PGF1a	393 36 320 15	62 4.4	19 2.1	14 1.6	16 1.1	238 76	671 48	607 86	826 65	533 117
	TXB3	94 14 60 7.5	12 1.7	3.2 0.3	2.3 0.3	2.0 0.1	56 19	125 4.7	128 18	144 8.5	98 20
	8(9)-EpETE	3.7 0.7 9.1 1.0	<1	<1	<1	<1	<1	10 2.0	25 4.5	31 3.1	15 1.6
	11(12)-EpETE	6.4 1.2 14 1.9	1.4 0.3	<0.5	1.0 0.1	2.0 0.2	<0.5	15 3.1	36 6.4	46 4.4	25 2.4
	14(15)-EpETE	6.0 1.1 14 1.7	1.3 0.3	<0.25	0.4 0.02	0.5 0.1	<0.25	15 3.0	37 6.7	47 4.4	23 2.2
17(18)-EpETE	26 4.6 87 56	6.1 1.5	1.4 0.2	1.0 0.1	1.2 0.1	<0.5	35 3.2	71 9.7	99 6.4	45 3.3	







**Fig. 9.3.6:** Mean% difference of selected oxylipin concentrations in **(A)** plasma **(B)** brain and **(C)** colon in WT animals after 30 days on a sunflower diet enriched with EPA and DHA in comparison to baseline (WT mice, D0). It was calculated using the formula [%difference =  $(\text{conc}_{\text{D30}} - \text{conc}_{\text{D0}}) / \text{conc}_{\text{D0}} * 100$ ]. # mean %difference was not calculated because more than 50% of samples of one group (D30 or D0) were <LOQ.

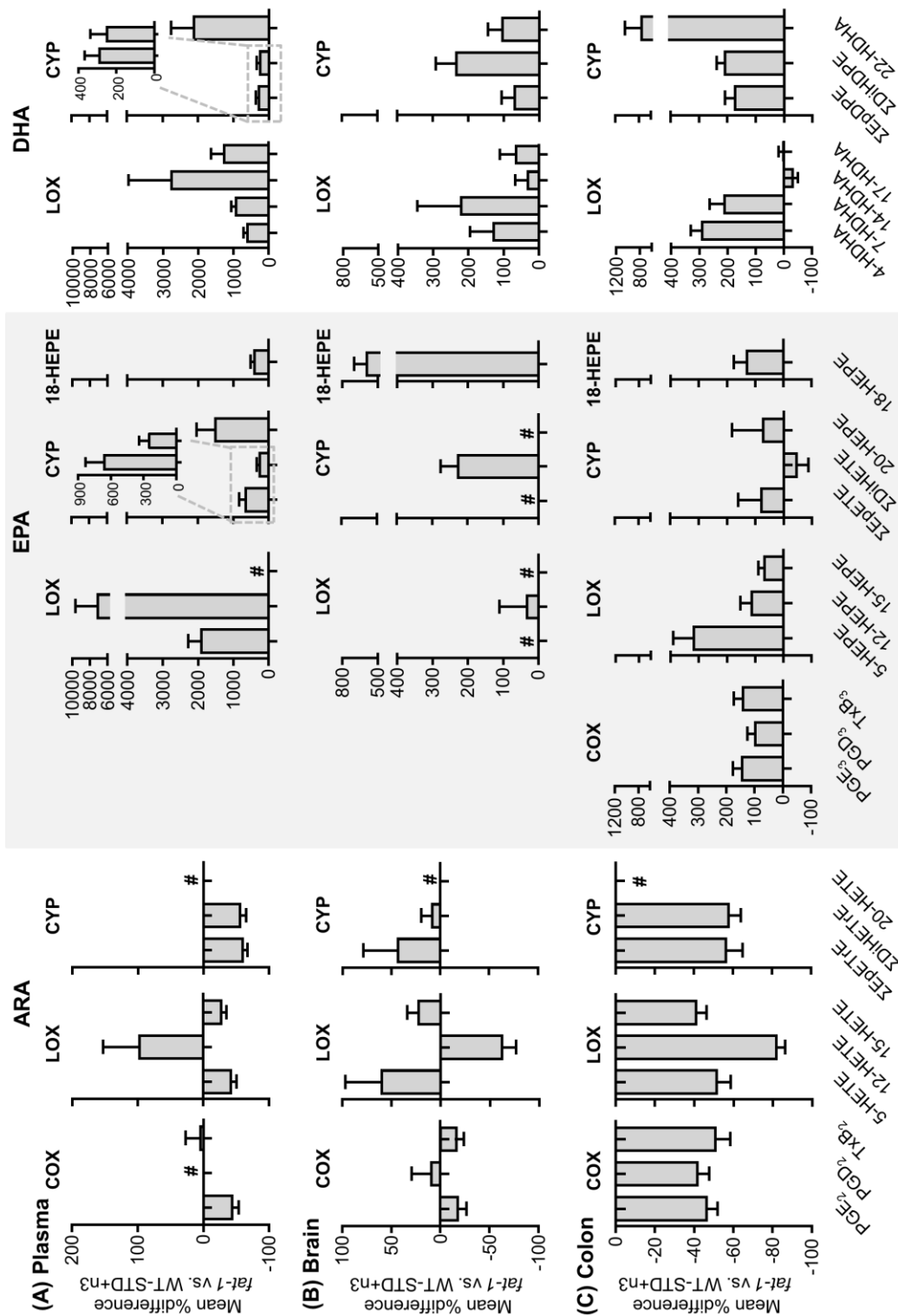


**Fig. 9.3.7:** Mean%difference of selected oxylipin concentrations in **(A)** plasma **(B)** brain and **(C)** colon in WT animals after 30 days on a sunflower diet enriched with EPA and DHA (WT-STD+n3) in comparison to *fat-1* mice after 30 days on standard sunflower diet. It was calculated using the formula  $[\% \text{ difference} = (\text{conc}_{\text{WT-STD+n3}} - \text{conc}_{\text{fat-1}}) / \text{conc}_{\text{fat-1}} * 100]$ . # mean %difference was not calculated because more than 50% of samples of one group (D30 or D0) were <LOQ.



## References Appendix Chapter 6

1. Schulte E. Vereinfachte Mikromethode zur gravimetrischen Bestimmung des Fettgehaltes von Lebensmittels nach Säureaufschluss (Kurzmitteilung). Deutsche Lebensmittelrundschau. 2004;100(5):188-9.
2. Ostermann AI, Muller M, Willenberg I, Schebb NH. Determining the fatty acid composition in plasma and tissues as fatty acid methyl esters using gas chromatography - a comparison of different derivatization and extraction procedures. Prostaglandins Leukot Essent Fatty Acids. 2014;91(6):235-41.
3. Untersuchung von Lebensmitteln, Bestimmung der Peroxidzahl in tierischen und pflanzlichen Fetten und Ölen, Iodometrische (visuelle) Endpunktbestimmung (13.00-37). In Amtliche Sammlung von Untersuchungsverfahren nach § 64 LFBG, 2012; BVL.

## 9.4 Chapter 7

**Table 9.4.1:** Absolute concentrations of fatty acids in brain tissue of C57BL/6 and NMRI mice in after 30 days of feeding a standard sunflower oil based diet (STD) or the same diet enriched with n3-PUFA (1% EPA and 1% DHA as ethyl ester in the diet, STD+n3). Shown are mean  $\pm$  SEM.

[ $\mu\text{g}/\text{mg}$ tissue]	FA	C57BL/6		NMRI	
		STD	STD+n3	STD	STD+n3
<b>SFA</b>	C10:0	< 0.0017	< 0.0017	< 0.0017	< 0.0017
	C11:0	< 0.0017	< 0.0017	< 0.0017	< 0.0017
	C12:0	0.0023 $\pm$ 0.0003	0.0027 $\pm$ 0.0005	< 0.0017	< 0.0017
	C13:0	< 0.0017	< 0.0017	< 0.0017	< 0.0017
	C14:0	0.069 $\pm$ 0.004	0.08 $\pm$ 0.01	0.033 $\pm$ 0.001	0.032 $\pm$ 0.001
	C15:0	0.019 $\pm$ 0.002	0.022 $\pm$ 0.003	0.0148 $\pm$ 0.0002	0.013 $\pm$ 0.002
	C16:0	8.2 $\pm$ 0.6	8.2 $\pm$ 0.6	7.09 $\pm$ 0.06	7.1 $\pm$ 0.2
	C17:0	0.06 $\pm$ 0.003	0.062 $\pm$ 0.004	0.0461 $\pm$ 0.0004	0.047 $\pm$ 0.002
	C18:0	9 $\pm$ 0.6	9.2 $\pm$ 0.4	7.45 $\pm$ 0.05	7.5 $\pm$ 0.2
	C19:0	0.017 $\pm$ 0.001	0.019 $\pm$ 0.001	0.0129 $\pm$ 0.0004	0.013 $\pm$ 0.001
	C20:0	0.23 $\pm$ 0.03	0.28 $\pm$ 0.03	0.123 $\pm$ 0.003	0.12 $\pm$ 0.01
	C21:0	< 0.0017	< 0.0017	0.01 $\pm$ 0.001	0.009 $\pm$ 0.001
	C22:0	0.26 $\pm$ 0.02	0.3 $\pm$ 0.02	0.145 $\pm$ 0.003	0.14 $\pm$ 0.01
	C23:0	0.08 $\pm$ 0.01	0.09 $\pm$ 0.01	0.04 $\pm$ 0.002	0.041 $\pm$ 0.004
C24:0	0.37 $\pm$ 0.03	0.44 $\pm$ 0.04	0.26 $\pm$ 0.01	0.24 $\pm$ 0.02	
	sum SFA	18 $\pm$ 1	19 $\pm$ 1	15.2 $\pm$ 0.1	15.2 $\pm$ 0.4
<b>MUFA</b>	C14:1n5	< 0.0017	< 0.0017	< 0.0017	< 0.0017
	C15:1n5	< 0.0017	< 0.0017	< 0.0017	< 0.0017
	C16:1n7	0.2 $\pm$ 0.01	0.22 $\pm$ 0.01	0.151 $\pm$ 0.004	0.151 $\pm$ 0.004
	C17:1n7	< 0.0017	< 0.0017	< 0.0017	< 0.0017
	C18:1n7	1.5 $\pm$ 0.1	1.59 $\pm$ 0.06	5.2 $\pm$ 0.1	5.2 $\pm$ 0.1
	C18:1n9	6.7 $\pm$ 0.4	7.5 $\pm$ 0.3	1.22 $\pm$ 0.02	1.16 $\pm$ 0.03
	C20:1n9	0.77 $\pm$ 0.08	0.95 $\pm$ 0.07	0.54 $\pm$ 0.02	0.53 $\pm$ 0.04
	C22:1n9	0.083 $\pm$ 0.003	0.11 $\pm$ 0.01	0.082 $\pm$ 0.003	0.08 $\pm$ 0.01
	C24:1n9	0.93 $\pm$ 0.07	1.14 $\pm$ 0.08	0.74 $\pm$ 0.02	0.75 $\pm$ 0.06
	sum MUFA	10.2 $\pm$ 0.6	11.5 $\pm$ 0.5	7.9 $\pm$ 0.1	7.8 $\pm$ 0.3
<b>n3 PUFA</b>	C18:3n3	< 0.0017	< 0.0017	0.0075 $\pm$ 0.0002	0.008 $\pm$ 0.001
	C20:3n3	< 0.0017	< 0.0017	< 0.0017	< 0.0017
	C20:4n3	< 0.0017	< 0.0017	< 0.0017	< 0.0017
	C20:5n3	< 0.0017	0.084 $\pm$ 0.005	< 0.0017	0.032 $\pm$ 0.002
	C22:5n3	0.037 $\pm$ 0.003	0.18 $\pm$ 0.01	0.036 $\pm$ 0.002	0.112 $\pm$ 0.003
	C22:6n3	6.1 $\pm$ 0.5	6.9 $\pm$ 0.4	5.4 $\pm$ 0.07	6.1 $\pm$ 0.2
	sum n3 PUFA	6.2 $\pm$ 0.5	7.2 $\pm$ 0.4	5.4 $\pm$ 0.1	6.3 $\pm$ 0.2
<b>n6 PUFA</b>	C18:2n6	0.33 $\pm$ 0.02	0.31 $\pm$ 0.02	0.25 $\pm$ 0.01	0.273 $\pm$ 0.005
	C18:3n6	< 0.0017	< 0.0017	< 0.0017	< 0.0017
	C20:2n6	0.1 $\pm$ 0.01	0.09 $\pm$ 0.01	0.057 $\pm$ 0.002	0.061 $\pm$ 0.003
	C20:3n6	0.17 $\pm$ 0.01	0.25 $\pm$ 0.01	0.118 $\pm$ 0.004	0.2 $\pm$ 0.01
	C20:4n6	4.6 $\pm$ 0.4	3.9 $\pm$ 0.3	3.5 $\pm$ 0.03	3.04 $\pm$ 0.08
	C22:2n6	< 0.0017	< 0.0017	0.007 $\pm$ 0.001	0.007 $\pm$ 0.001
	C22:4n6	1.18 $\pm$ 0.09	0.88 $\pm$ 0.04	1.12 $\pm$ 0.02	0.88 $\pm$ 0.02
C22:5n6	0.35 $\pm$ 0.02	0.09 $\pm$ 0.01	0.32 $\pm$ 0.02	0.079 $\pm$ 0.004	
	sum n6 PUFA	6.7 $\pm$ 0.5	5.5 $\pm$ 0.3	5.4 $\pm$ 0.1	4.5 $\pm$ 0.1
<b>n9 PUFA</b>	C20:3 n9	0.06 $\pm$ 0.01	0.07 $\pm$ 0.02	0.023 $\pm$ 0.002	0.025 $\pm$ 0.001
	sum all PUFA	13 $\pm$ 1	12.8 $\pm$ 0.8	10.5 $\pm$ 0.1	10.8 $\pm$ 0.3
	sum ALL FA	41 $\pm$ 3	43 $\pm$ 2	33.9 $\pm$ 0.3	33.9 $\pm$ 0.8

**Table 9.4.2:** Relative distribution of fatty acids in brain tissue of C57BL/6 and NMRI mice after 30 days of feeding a standard sunflower oil based diet (STD) or the same diet enriched with n3-PUFA (1% EPA and 1% DHA as ethyl ester in the diet, STD+n3). Wt%n3 and wt%n6 in HUFA were calculated as follows: %n3 in HUFA =  $100 \times (\text{C20:5 n3} + \text{C22:5 n3} + \text{C22:6 n3}) / (\text{C20:3 n6} + \text{C20:4 n6} + \text{C22:4 n6} + \text{C22:5n6} + \text{C20:3 n9} + \text{C20:5 n3} + \text{C22:5 n3} + \text{C22:6 n3})$ ; %n6 in HUFA =  $100 \times (\text{C20:3 n6} + \text{C20:4 n6} + \text{C22:4 n6} + \text{C22:5n6}) / (\text{C20:3 n6} + \text{C20:4 n6} + \text{C22:4 n6} + \text{C22:5 n6} + \text{C20:3 n9} + \text{C20:5 n3} + \text{C22:5 n3} + \text{C22:6 n3})$ . Shown are mean  $\pm$  SEM.

[% FA of all FA]		C57BL/6		NMRI	
		STD	STD+n3	STD	STD+n3
<b>SFA</b>	C10:0	< LOQ	< LOQ	<LOQ	<LOQ
	C11:0	< LOQ	< LOQ	<LOQ	<LOQ
	C12:0	0.007 $\pm$ 0.001	0.007 $\pm$ 0.001	<LOQ	<LOQ
	C13:0	< LOQ	< LOQ	<LOQ	<LOQ
	C14:0	0.166 $\pm$ 0.004	0.173 $\pm$ 0.007	0.098 $\pm$ 0.001	0.096 $\pm$ 0.003
	C15:0	0.045 $\pm$ 0.001	0.05 $\pm$ 0.005	0.044 $\pm$ 0.001	0.043 $\pm$ 0.002
	C16:0	19.8 $\pm$ 0.4	19.1 $\pm$ 0.4	20.89 $\pm$ 0.09	20.8 $\pm$ 0.2
	C17:0	0.145 $\pm$ 0.002	0.144 $\pm$ 0.003	0.136 $\pm$ 0.001	0.14 $\pm$ 0.003
	C18:0	21.7 $\pm$ 0.1	21.4 $\pm$ 0.2	22 $\pm$ 0.1	22.1 $\pm$ 0.1
	C19:0	0.041 $\pm$ 0.003	0.045 $\pm$ 0.002	0.038 $\pm$ 0.001	0.038 $\pm$ 0.001
	C20:0	0.56 $\pm$ 0.07	0.65 $\pm$ 0.05	0.362 $\pm$ 0.007	0.35 $\pm$ 0.02
	C21:0	< LOQ	< LOQ	0.028 $\pm$ 0.003	0.025 $\pm$ 0.003
	C22:0	0.63 $\pm$ 0.05	0.7 $\pm$ 0.03	0.428 $\pm$ 0.009	0.42 $\pm$ 0.03
	C23:0	0.2 $\pm$ 0.02	0.22 $\pm$ 0.01	0.119 $\pm$ 0.005	0.12 $\pm$ 0.01
C24:0	0.9 $\pm$ 0.07	1.02 $\pm$ 0.09	0.77 $\pm$ 0.02	0.71 $\pm$ 0.06	
	sum SFA	44.2 $\pm$ 0.3	43.4 $\pm$ 0.4	44.9 $\pm$ 0.1	44.9 $\pm$ 0.2
<b>MUFA</b>	C14:1n5	< LOQ	< LOQ	<LOQ	<LOQ
	C15:1n5	< LOQ	< LOQ	<LOQ	<LOQ
	C16:1n7	0.475 $\pm$ 0.008	0.51 $\pm$ 0.06	0.446 $\pm$ 0.008	0.446 $\pm$ 0.006
	C17:1n7	< LOQ	< LOQ	<LOQ	<LOQ
	C18:1n7	3.71 $\pm$ 0.06	3.7 $\pm$ 0.1	3.59 $\pm$ 0.05	3.43 $\pm$ 0.05
	C18:1n9	16.1 $\pm$ 0.4	17.6 $\pm$ 0.5	15.2 $\pm$ 0.2	15.2 $\pm$ 0.2
	C20:1n9	1.9 $\pm$ 0.2	2.2 $\pm$ 0.1	1.58 $\pm$ 0.04	1.6 $\pm$ 0.1
	C22:1n9	0.2 $\pm$ 0.01	0.25 $\pm$ 0.02	0.24 $\pm$ 0.01	0.25 $\pm$ 0.02
	C24:1n9	2.3 $\pm$ 0.2	2.7 $\pm$ 0.2	2.17 $\pm$ 0.06	2.2 $\pm$ 0.2
	sum MUFA	24.6 $\pm$ 0.7	26.9 $\pm$ 0.9	23.2 $\pm$ 0.3	23.1 $\pm$ 0.5
<b>n3 PUFA</b>	C18:3n3	< LOQ	< LOQ	0.022 $\pm$ 0.001	0.023 $\pm$ 0.002
	C20:3n3	< LOQ	< LOQ	<LOQ	<LOQ
	C20:4n3	< LOQ	< LOQ	< LOQ	< LOQ
	C20:5n3	< LOQ	0.2 $\pm$ 0.01	<LOQ	0.094 $\pm$ 0.007
	C22:5n3	0.09 $\pm$ 0.002	0.41 $\pm$ 0.01	0.107 $\pm$ 0.005	0.329 $\pm$ 0.006
	C22:6n3	14.8 $\pm$ 0.5	16.1 $\pm$ 0.4	15.9 $\pm$ 0.2	18.1 $\pm$ 0.2
	sum n3 PUFA	14.9 $\pm$ 0.5	16.7 $\pm$ 0.4	16 $\pm$ 0.2	18.5 $\pm$ 0.2
<b>n6 PUFA</b>	C18:2n6	0.8 $\pm$ 0.01	0.72 $\pm$ 0.02	0.72 $\pm$ 0.03	0.81 $\pm$ 0.02
	C18:3n6	< LOQ	< LOQ	<LOQ	<LOQ
	C20:2n6	0.25 $\pm$ 0.03	0.2 $\pm$ 0.02	0.168 $\pm$ 0.007	0.18 $\pm$ 0.008
	C20:3n6	0.4 $\pm$ 0.02	0.588 $\pm$ 0.007	0.35 $\pm$ 0.01	0.58 $\pm$ 0.02
	C20:4n6	11 $\pm$ 0.2	9 $\pm$ 0.2	10.31 $\pm$ 0.08	9 $\pm$ 0.1
	C22:2n6	< LOQ	< LOQ	0.021 $\pm$ 0.001	0.021 $\pm$ 0.002
	C22:4n6	2.84 $\pm$ 0.09	2.06 $\pm$ 0.06	3.3 $\pm$ 0.05	2.61 $\pm$ 0.03
C22:5n6	0.84 $\pm$ 0.03	0.2 $\pm$ 0.02	0.94 $\pm$ 0.04	0.23 $\pm$ 0.01	
	sum n6 PUFA	16.3 $\pm$ 0.3	13 $\pm$ 0.2	15.9 $\pm$ 0.1	13.5 $\pm$ 0.1
<b>n9 PUFA</b>	C20:3 n9	0.14 $\pm$ 0.03	0.16 $\pm$ 0.03	0.068 $\pm$ 0.005	0.072 $\pm$ 0.003
	sum all PUFA	31.2 $\pm$ 0.5	29.7 $\pm$ 0.5	31.9 $\pm$ 0.3	32 $\pm$ 0.3
	<b>wt % n3 in HUFA</b>	49 $\pm$ 1	58.1 $\pm$ 0.5	51.7 $\pm$ 0.3	59.7 $\pm$ 0.3
	<b>wt % n6 in HUFA</b>	50.3 $\pm$ 0.9	41.4 $\pm$ 0.5	48.1 $\pm$ 0.3	40 $\pm$ 0.3

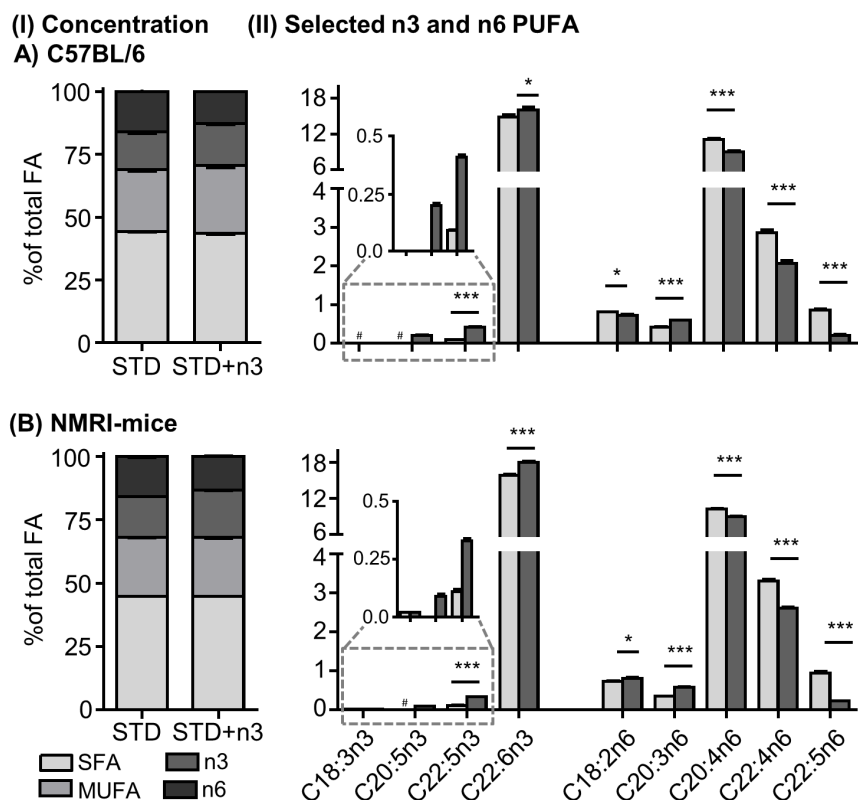


**Fig. 9.4.1:** Fatty acid (FA) pattern in brain tissue of C57BL/6 (A) and NMRI-mice (B) fed with a standard sunflower diet (STD) or the same diet enriched with n3-PUFA (STD+n3). Shown are (I) relative amounts of saturated (SFA), monounsaturated (MUFA), n3 and n6 polyunsaturated fatty acids (PUFA) as well as (II) selected n3- and n6-PUFA. n9-PUFA not shown in (I) due to relative amounts below 0.2 % of total FA. # Analyte was below LOQ. Statistical differences were determined with a two-tailed t-test for unpaired samples (\*  $p < 0.05$ , \*\*  $p < 0.01$ , \*\*\*  $p \leq 0.0001$ ). No t-test was performed for C18:3 n3 and C20:5 n3. Results are shown as mean  $\pm$  SEM.

# Abbreviations

ARA	arachidonic acid
ACN	acetonitrile
ARA	arachidonic acid
BF <sub>3</sub>	boron trifluoride
BMI	body mass index
CAD	collision activated dissociation
CE	cholesterol ester
CE	collision energy
CID	collision-induced dissociation
CNS	central nervous system
COX	cyclooxygenase
CXP	collision cell exit potential
CYP	cytochrom P450
D5D / D6D	delta-5/delta-6 desaturase
DGLA	dihomo gamma-linolenic acid
DHA	docosahexaenoic acid
DiHDPE	dihydroxy docosapentaenoic acid
DIHETE	dihydroxy eicosatetraenoic acid
DIHETrE	dihydroxy eicosatrienoic acid
DiH-FA	dihydroxy fatty acid
DiHODE	dihydroxy octadecadienoic acid
DiHOME	dihydroxy octadecenoic acid
DMEM	Dulbecco's modified Eagle's medium
DP	declustering potential
DPA	docosapentaenoic acid
EA	ethyl acetate
EDTA	ethylenediaminetetraacetic acid

EKODE	epoxyketoctadecenoic acid
EPA	eicosapentaenoic acid
EpDPE	epoxy docosapentaenoic acid
EpETE	epoxy eicosatetraenoic acid
EpETrE	epoxy eicosatrienoic acid
Ep-FA	epoxy fatty acid
EpODE	epoxy octadecadienoic acid
EpOME	epoxy octadecenoic acid
ESI	electrospray ionization
FA	fatty acid
FAME	fatty acid methyl ester
FCS	fetal calf serum
FFA	free fatty acid (non-esterified FA, non-amide-bound FA)
FWHM	full width at half maximal height
GC-FID	gas chromatography flame ionization detection
GLA	gamma-linolenic acid
HAc	acetic acid
HDHA	hydroxy docosahexaenoic acid
HEPE	hydroxy eicosapentaenoic acid
HETE	hydroxy eicosatetraenoic acid
HETrE	hydroxyl eicosatrienoic acid
HODE	hydroxy octadecadienoic acid
HOTrE	hydroxy octadecatrienoic acid
HpETE	hydroperoxyeicosatetraenoic acid
IS	internal standard
LA	linoleic acid
LC-MS	liquid chromatography mass spectrometry
LLE	liquid-liquid extraction
LLOQ	lower limit of quantification
LOD	limit of detection
LOQ	limit of quantification
LOX	lipoxygenase
LT	leukotriene
LTB	leukotriene

---

LXA	lipoxin
MeOH	methanol
mRNA	messenger ribonucleic acid
MTBE	<i>tert</i> -butyl methyl ether
MUFA	monounsaturated fatty acid
n3-DPA	n3 docosapentaenoic acid
NaOH	sodium hydroxide
NMRI	Naval Medical Research Institute
OH-FA	hydroxy fatty acid
oxo-ETE oxo	eicosatetraenoic acid
oxo-ODE oxo	octadecadienoic acid
PC	phosphatidylcholine
PG	prostaglandin
PL	phospholipid
PUFA	polyunsaturated fatty acid
qRT-PCR	quantitative real-time polymerase chain reaction
RBC	red blood cells
RP	reversed phase
RSD	relative standard deviation
Rv	resolvin
SD	standard deviation
sEH	soluble epoxide hydrolyse
SEM	standard error of the mean
SFA	saturated fatty acids
SPE	solid phase extraction
SPM	specialized pro-resolving lipid mediator
SRM	selected reaction monitoring
TG	triacylglycerols
THF diol	tetrahydrofurandiol
TMSH	trimethylsulfonium hydroxide
TriHETrE	trihydroxy-eicosatrienoic acid
TriHOME	trihydroxy-ocadecenoic acid
Tx	thromboxane
WT	wild type





# Acknowledgement

This work was carried out from February 2013 to March 2017 at the Institute for Food Toxicology (University of Veterinary Medicine Hannover) in the research group of Prof. Dr. Nils Helge Schebb.

I would like to thank my supervisor Prof. Dr. Nils Helge Schebb for the opportunity to work in his group on an interesting topic that combined the work with analytical techniques and relevant biological questions. I thank him for his continuous support and encouragement and I am grateful for the opportunity to participate and present my work at numerous national and international conferences.

I thank Prof. Dr. Pablo Steinberg not only for being a board member of the PhD committee, but also for his kind support and scientific advice during the years of my thesis.

This thesis is based on cooperations with many researchers. I would like to gratefully acknowledge the help and support from all colleagues working with me on different chapters of this thesis.

I would like to thank Prof. Dr. Dr. Karsten H. Weylandt for the successful cooperation in the feeding/*fat-1* experiments and the cell incubations from Chapter 5. Moreover, I thank the members of K. H. Weylandts working group, especially Cheng-Ying Chiu for the collaboration in the animal experiments and Nadine Rohwer for her support and kind collaboration.

Furthermore, I would like to thank Prof. Dr. Gunter P. Eckert and the members of his group for the collaboration in Chapter 7.

I thank Maïke Müller and Moritz Schmidt for working with me during their master thesis and internship and for their valuable contributions to this work.

For the pleasant atmosphere, workwise and beyond, I want to thank all members of the Institute of Food Toxicology of the University of Veterinary Medicine Hannover.

I would like to thank all my colleagues from the AG Schebb in particular: Katharina Rund, Laura Kutzner, Nicole Hartung and Patrick Waindok. I hope our next "*Stammtisch*" will come soon.

I want to thank Michael Empl for endless discussions, "*Döner Dates*", and a continuous supply with jokes and advices. I would like to thank Ina Willenberg, my friend and former colleague for a wonderful time and the fun we had working together.

Ich möchte mich bei meiner Familie und bei meinen Freunden für die Unterstützung in den letzten Jahren bedanken. Insbesondere bei Christian möchte ich mich für seine Geduld und seinen Zuspruch bedanken und dafür, dass er in den letzten Jahren immer für mich da war. Meinen Eltern möchte ich einen tiefen Dank aussprechen, dass sie mir alles ermöglicht, immer an mich geglaubt und mich in jeglicher Hinsicht unterstützt haben.

# Curriculum Vitae

Der Lebenslauf inklusive Publikationsliste ist in der Online-Version aus Gründen des Datenschutzes nicht enthalten.



# List of Publications

Der Lebenslauf inklusive Publikationsliste ist in der Online-Version aus Gründen des Datenschutzes nicht enthalten.

Der Lebenslauf inklusive Publikationsliste ist in der Online-Version aus Gründen des Datenschutzes nicht enthalten.

Der Lebenslauf inklusive Publikationsliste ist in der Online-Version aus Gründen des Datenschutzes nicht enthalten.

Der Lebenslauf inklusive Publikationsliste ist in der Online-Version aus Gründen des Datenschutzes nicht enthalten.



Der Lebenslauf inklusive Publikationsliste ist in der Online-Version aus Gründen des Datenschutzes nicht enthalten.

Der Lebenslauf inklusive Publikationsliste ist in der Online-Version aus Gründen des Datenschutzes nicht enthalten.

Der Lebenslauf inklusive Publikationsliste ist in der Online-Version aus Gründen des Datenschutzes nicht enthalten.

Der Lebenslauf inklusive Publikationsliste ist in der Online-Version aus Gründen des Datenschutzes nicht enthalten

